

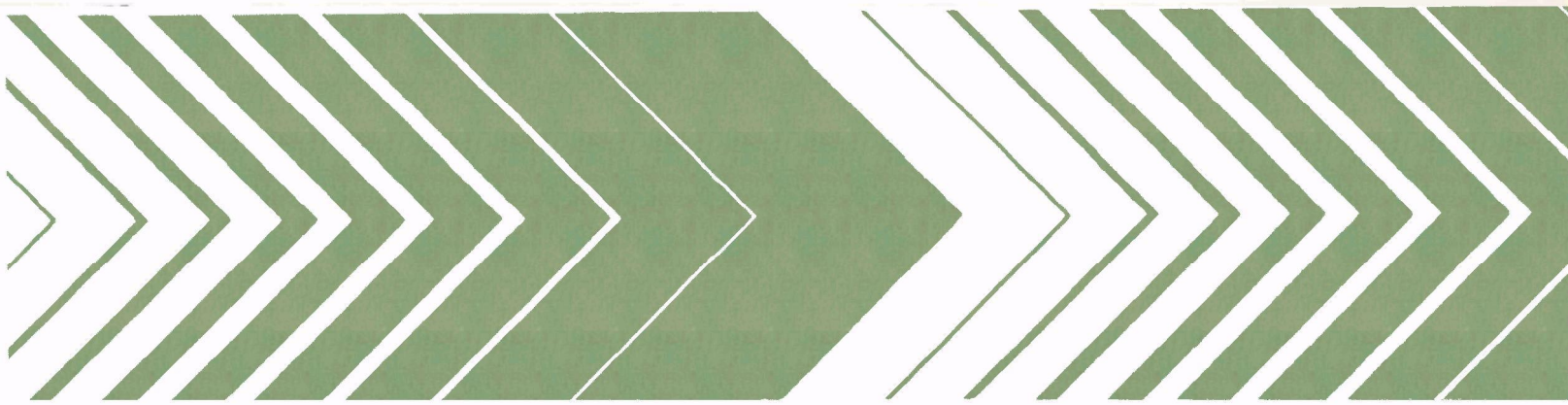
Research and Development



Impacts of Coal-Fired Power Plants on Local Ground-Water Systems

Wisconsin Power Plant Impact Study

Environmental
Protection Agency
Region 5



RESEARCH REPORTING SERIES

Research reports of the Office of Research and Development, U.S. Environmental Protection Agency, have been grouped into nine series. These nine broad categories were established to facilitate further development and application of environmental technology. Elimination of traditional grouping was consciously planned to foster technology transfer and a maximum interface in related fields. The nine series are:

1. Environmental Health Effects Research
2. Environmental Protection Technology
3. Ecological Research
4. Environmental Monitoring
5. Socioeconomic Environmental Studies
6. Scientific and Technical Assessment Reports (STAR)
7. Interagency Energy-Environment Research and Development
8. "Special" Reports
9. Miscellaneous Reports

This report has been assigned to the ECOLOGICAL RESEARCH series. This series describes research on the effects of pollution on humans, plant and animal species, and materials. Problems are assessed for their long- and short-term influences. Investigations include formation, transport, and pathway studies to determine the fate of pollutants and their effects. This work provides the technical basis for setting standards to minimize undesirable changes in living organisms in the aquatic, terrestrial, and atmospheric environments.

EPA-600/3-80-079

August 1980

IMPACTS OF COAL-FIRED POWER PLANTS
ON LOCAL GROUND-WATER SYSTEMS

Wisconsin Power Plant Impact Study

by

Charles B. Andrews
Mary P. Anderson
Institute for Environmental Studies
University of Wisconsin-Madison
Madison, Wisconsin 53706

Grant No. R803971

Project Officer
Gary E. Glass
Environmental Research Laboratory-Duluth
Duluth, Minnesota

This study was conducted in cooperation with

Wisconsin Power and Light Company,
Madison Gas and Electric Company,
Wisconsin Public Service Corporation,
Wisconsin Public Service Commission,
and Wisconsin Department of Natural Resources

ENVIRONMENTAL RESEARCH LABORATORY-DULUTH
OFFICE OF RESEARCH AND DEVELOPMENT
U.S. ENVIRONMENTAL PROTECTION AGENCY
DULUTH, MINNESOTA 55804

DISCLAIMER

This report has been reviewed by the Environmental Research Laboratory - Duluth, U.S. Environmental Protection Agency, and approved for publication. Approval does not signify that the contents necessarily reflect the views and policies of the U.S. Environmental Protection Agency, nor does mention of trade names or commercial products constitute endorsement or recommendation of use.

FOREWORD

The U.S. Environmental Protection Agency was established to coordinate our country's efforts toward protecting and improving the environment. Research projects in a multitude of scientific and technical areas are necessary to monitor changes in the environment, to discover relationships within that environment, to determine health standards, and to eliminate potential hazards.

One such project, which the EPA is supporting through its Environmental Research Laboratory in Duluth, Minnesota, is the study "The Impacts of Coal-Fired Power Plants on the Environment." This interdisciplinary study, based at the Columbia Generating Station, near Portage, Wis., and involving investigators and experiments from many academic departments at the University of Wisconsin, is being carried out by the Environmental Monitoring and Data Acquisition Group of the Institute for Environmental Studies at the University of Wisconsin-Madison. Several utilities and state agencies are cooperating in the study: Wisconsin Power and Light Company, Madison Gas and Electric Company, Wisconsin Public Service Corporation, Wisconsin Public Service Commission, and Wisconsin Department of Natural Resources.

Reports from this study will be published as a series within the EPA Ecological Research Series. These reports will include topics related to chemical constituents, chemical transport mechanisms, biological effects, social and economic effects, and integration and synthesis.

This report describes the research undertaken by the Hydrogeology Subproject of the Columbia project. This research includes monitoring of ground-water flows and temperatures at the Columbia site, development of mathematical models for predicting such flows, and applications of the models to several problems.

Norbert A. Jaworski
Director
Environmental Research Laboratory
Duluth, Minnesota

ABSTRACT

Quantitative techniques for simulating the impacts of a coal-fired power plant on the ground-water system of river flood-plain wetland in central Wisconsin were developed and tested by using field data collected at the site of the 500-MW Columbia Generating Station. The most important effects were those related to the construction and operation of the 200-ha cooling lake and the 28-ha ashpit.

Several two-dimensional vertically oriented steady-state models of the ground-water flow system were used to simulate ground-water flows before and after the filling of the cooling lake and ashpit. The simulations and supporting field evidence indicated that the creation of the cooling lake greatly altered the configuration of the local flow systems and increased the discharge of ground water to the wetland west of the site by a factor of 6.

Chemical changes in the ground-water system were minor. The plume of contaminated ground water originating from the ashpit was confined to a relatively small area near the ashpit. Thermal changes in the ground-water system are a major impact of the operation of the cooling lake inasmuch as the lake loses water to the ground-water system at a rate of $2 \times 10^4 \text{ m}^3$ per day. The wetland, which is a major ground-water discharge area, has undergone a rapid and dramatic change in vegetation as a result of changes in both water temperature and water levels.

Ground-water temperatures in the vicinity of the cooling lake were monitored in detail for 1 1/2 yr. The response of subsurface temperatures temperature was simulated by means of a mathematical model, and predictions were made of the long-term changes expected in substrate temperatures in the wetland adjacent to the power plant. In addition, the use of ground-water estimate ground-water flow rates away from the cooling lake was investigated.

The model, which couples equations describing ground-water flow with those describing heat transport in the subsurface, was used to simulate the seasonal temperature fluctuation within seven cross sections oriented parallel to the direction of ground-water flow and downgradient from the cooling lake. Simulated temperature patterns agreed well with field data, but were very sensitive to the distribution of subsurface lithologies. The predictive simulations suggest that by 1987 temperatures at a depth of 0.6 m will not fall below 8°C within 200 m of the dike, and that peak temperatures near the dike will be 10-15°C above normal and will occur in October and November rather than in August. The increase in ground-water temperatures by 1987 will also result in a 24% increase in ground-water flow. The

subsurface stratigraphy of the site is such that major changes in near-surface temperatures will only occur within 340 m of the dikes, but, if the different, impacts could extend to much greater distances from the cooling-lake dikes.

This report was prepared with the cooperation of faculty and graduate students in the Department of Geology at the University of Wisconsin-Madison.

Most of the funding for the research reported here was provided by the U.S. Environmental Protection Agency, but funds were also granted by the University of Wisconsin-Madison, Wisconsin Power and Light Company, Madison Gas and Electric Company, Wisconsin Public Service Corporation, and Wisconsin Public Service Commission. This report was submitted in fulfillment of Grant No. R803971 by the Environmental Monitoring and Data Acquisition Group, Institute for Environmental Studies, University of Wisconsin-Madison under the partial sponsorship of the U.S. Environmental Protection Agency.

CONTENTS

Foreword	iii
Abstract	iv
Figures	viii
Tables	xii
1. Introduction	1
2. Conclusions and Recommendations	4
Recommendations for siting future power plants	6
Recommendations for future research	6
3. The Site of the Columbia Generating Station	8
4. The Impact of a Power Plant on the Ground-Water System of a Wetland	19
Configuration of the ground-water flow system	19
Wetland water levels	23
Ground-water temperature	24
Relationship between ground-water temperatures and flow rates	26
Changes in water chemistry	26
5. Thermal Alteration of Ground Water Caused by Seepage from the Cooling Lake	30
Mathematical model	30
Results	35
6. Long-Term Temperature Changes in the Ground Water of the Wetland	41
Simulation studies	41
Results and discussion	43
References	51
Appendices	
A. Data specifications for the water-flow model	57
B. Techniques for determining boundary conditions and parameters in the heat-flow model	61
C. A finite element program to simulate single-phase heat flow and conservative mass transport in a aquifer	73
D. Estimation of aquifer parameters by using subsurface temperature data	195

FIGURES

<u>Number</u>	<u>Page</u>
1 The site of the Columbia Generating Station during construction of the first unit (24 May 1971)	9
2 The site of the Columbia Generating Station after construction of both units (12 August 1977)	10
3 Main features of the site of the Columbia Generating Station . . .	11
4 Water flows and energy flows at the site of the Columbia Generating Station	12
5 Potentiometric surface contours in the area of the Columbia Generating Station	13
6 Representative stratigraphic cross sections of the subsurface at the site of the Columbia Generating Station	14
7 Topographic map of the site of the Columbia Generating Station . .	16
8 Peat thicknesses in the subsurface at the site of the Columbia Generating Station	18
9 Simulated head distribution in cross-section A-A' of Figure 6 before filling of the Columbia cooling lake	20
10 Simulated head distribution in cross-section A-A' of Figure 6 after filling of the Columbia cooling lake	22
11 Water levels in the wetland west of the Columbia cooling lake before and after filling of the lake	24
12 Ground-water temperature variations in wells west of the Columbia cooling lake	25
13 Stiff diagrams of water in the cooling lake and ground water . . .	27
14 Stiff diagrams of water in the ashpit and in a well cased to 1.5 m below the surface and located 2 m west of the ashpit	28
15 Location of seven cross sections of the Columbia site for which ground-water temperature distributions were simulated	31

16	Observed temperatures in the subsurface west of the Columbia cooling lake and temperatures simulated by the mathematical model	36
17	Observed (solid line) and simulated (dashed line) ground-water temperature distributions in cross-section A-A' of Figure 15 . .	37
18	Observed (solid line) and simulated (dashed line) ground-water temperature distributions in cross-section B-B' of Figure 15 . .	38
19	Seasonal fluctuations of ground-water temperature in cross-section A-A' of Figure 15 at a depth of 4.5 m at distances of 2 m, 15 m, 50 m, and 84 m west of the cooling-lake dike	39
20	Simulated temperatures (solid lines) and observed temperatures (open circles) in cross-section A-A' of Figure 15 at a depth of 3.28 m at various distances west of the cooling lake	40
21	Cooling lake inlet temperatures for 1975-87 used in the simulations of long-term temperature change in the ground-water system	42
22	Predicted ground-water temperatures from 1975 to 1987 at a distance of 2 m west of the cooling-lake dike in cross-section A-A' of Figure 15 at a depth of 0.6 m	44
23	Pre-lake temperatures and simulated temperatures 2 m west of the cooling-lake dike in cross-section A-A' of Figure 15 at a depth of 0.6 m	45
24	Temperatures 150 m west of the cooling-lake dike in cross-section A-A' of Figure 15 at depths of 0.6 m and 3 m for the simulated period 1975-87	46
25	Temperatures 150 m west of the cooling-lake dike in cross-section A-A' of Figure 15 at a depth of 0.6 m	47
26	Temperatures in cross-section B-B' of Figure 15 at a depth of 0.6 m and at (a) 2 m west of the dike, (b) 50 m west of the dike, and (c) 200 m west of the cooling-lake dike	48-50
A-1	Location of monitoring wells at the Columbia site	58
B-1	Location of temperature sampling points at the Columbia Generating Station site	62
B-2	A simple circuit for measuring temperature	65
B-3	Temperature-resistance characteristics of Yellow Springs Series 400 thermistors and the change in resistance with a 0.1° change in temperature	67

B-4	Potted thermistor assembly showing the details of the thermistor mounts	67
B-5	Schematic of thermistor placement in subsurface wells at the Columbia Generating Station site	69
B-6	Schematic of digital bridge circuit used as a portable field meter for measuring ground-water temperatures	71
B-7	Details of (a) the needle probe and (b) the experimental arrangement to measure thermal conductivities of unconsolidated materials	72
B-8	Thermal conductivities of three ground-water samples from the Columbia Generating Station site which were analyzed with the needle probe	72
C-1	The basic procedure for linking the ground-water flow and the transport equations of the model	73
C-2	Examples of refinement of a finite element grid	81
C-3	Examples of numbering of nodes in a structure	93
C-4	Cartesian orientation of finite element grid	94
C-5	Typical elements of finite element grid and correct method of numbering the elements	95
C-6	Numbering of nodes and elements in rectangular grid	95
C-7	Two variants of the rectangular grid that can be generated	96
C-8	Numbering of sides of an element	97
C-9	Finite element grids used to discretize a linear heat transport problem	104
C-10	Input data used to model one-dimensional heat transport with all linear elements	105
C-11	Program output for one-dimensional heat transport problem with linear elements	107
C-12	Data deck used to model one-dimensional heat transport with mixed elements	111
C-13	Program output for the one-dimensional heat transport problem with mixed elements	113

C-14	Analytical solutions (solid lines) and numerical solutions (dots) for the linear heat transport problem for $t = 25, 50,$ and 75 days	118
C-12	Areal view of the Mohawk River Valley showing location of the Schenectady and Rotterdam well fields	121
C-16	Cross-sectional view of the Mohawk River alluvial aquifer along section A-A' of Figure C-15	121
C-17	Grid used to discretize the Mohawk River problem	122
C-18	Data deck used to model heat flow in the Mohawk River alluvial aquifer	123
C-19	Program output for Mohawk River problem	125
C-20	Schematic cross section of the Columbia Generating Station site along an east-west line	131
C-21	The grid used to discretize the cross section simulated at the Columbia Generating Station site	131
C-22	Data deck used to model heat flow at the Columbia Generating Station site	132
C-23	Program output for Columbia Generating Station problem	134
C-24	Grid used to discretize the aquifer simulated in the heat pump problem	138
C-25	Data deck used to model the heat pump simulation with no regional ground-water flow	139
C-26	Program output for the heat pump problem	141
C-27	Program flow chart	147
D-1	Temperatures ($^{\circ}\text{C}$) in a section of the marsh adjacent to the cooling lake at the Columbia Generating Station site on 7 October 1977	200
D-2	Temperatures in a 60-m portion of cross-section B-B' of Figure 6 adjacent to the drainage ditch east of the cooling lake on 9 June 1977 and 24 October 1977	201

TABLES

<u>Number</u>	<u>Page</u>
1 Horizontal Hydraulic Conductivities for the Lithologies in the Subsurface of the Columbia Generating Station	15
2 Selected Chemical Concentrations in Ground Water Near the Ashpit of the Columbia Generating Station	29
3 Parameters Used in the Simulations for the Model Describing Thermal Alteration of Ground-water	35
B-1 Temperature Sampling Points: Locations, Depths, Methods, and Frequency of Readings	63
B-2 Heat Capacities of the Common Components of Unconsolidated Glacial Materials	72
C-1 Parameters for Both Mass and Heat Transport Problems	76
C-2 Parameters, Initial Conditions, and Boundary Conditions Used for the Heat-Flow Equation in the Linear Heat Transport Problem . .	106
C-3 Analytical Solution at $t = 50$ Days for the Problem Posed in Figure C-9 and Finite Element Numerical Solutions at $t = 50$ Days for Two Grid Configurations and Two Types of Boundary Conditions	117
C-4 Parameters, Initial Conditions, and Boundary Conditions Used for the Simulation of Temperatures in the Mohawk River Alluvial Aquifer	120
C-5 Parameters, Initial Conditions, and Boundary Conditions Used in the Columbia Generating Station Problem	130

SECTION 1

INTRODUCTION

Large industrial facilities are common features of the American landscape, but knowledge of the mechanisms by which they change natural systems is inadequate. The Hydrogeology Subproject of the interdisciplinary research project "The Impacts of Coal-Fired Power Plants on the Environment" quantified the effects of construction and operation of the Columbia Generating Station on the hydrogeologic system of an adjacent wetland. The investigators developed techniques for simulating the observed changes and for predicting potential impacts at other sites. Impacts on the ground-water system of the wetland resulted from the construction of a 200-ha cooling lake and a 28-ha ashpit. Specifically, this study assesses the alteration of three characteristics of the ground-water system: (1) the quantity of ground-water flow from the cooling lake and the ashpit into the wetland and surface-water levels in the wetland, (2) the quality of ground water and surface water as expressed by concentrations of the common cations and anions, and (3) the temperatures of ground water and surface water at the site.

Data on ground-water temperatures were collected from 1971, 4 yr before the operation of the Columbia Generating Station, through 1977. The basic monitoring network consisted of 100 small-diameter wells and a subsurface network of 64 temperature monitoring points.

During the initial phase of the study the ground-water flow systems in the vicinity of the generating station were delineated and the way in which the flow systems were altered by the construction and operation of a cooling lake and ashpit were documented. A finite difference model was used to simulate the alterations in the configuration of the ground-water flow system. Analyses of changes in the chemical quality and temperature of ground water were descriptive during this phase of the study.

The second phase of the study dealt with the monitoring and simulation of the transfer of one byproduct of the generating process, specifically heat, away from the site via the ground-water system. The study of the transfer of heat was chosen rather than the transfer of chemical byproducts because: (1) temperatures can be monitored inexpensively and rapidly at a large number of points, (2) the processes of heat transfer are well understood, and (3) the initial phase of the study had shown that alterations in the temperature of ground water were large, whereas alterations in the chemical characteristics of ground water were small. The development of the capability to simulate the transfer of heat is a prerequisite to studying the flow of a chemical away from the site. The processes determining the chemical composition of ground

water are poorly understood, and it is difficult to obtain representative ground-water samples.

Data on ground-water temperatures were collected for an 18-mo period during 1976-77, in the vicinity of the cooling lake of the Columbia Generating Station. The finite element method, using isoparametric quadrilateral elements, was used to solve the partial differential equations describing ground-water flow and heat transport in the subsurface. The model was tested by comparing the observed ground-water temperatures in the vicinity of the cooling lake with predicted temperatures. The simulated temperatures were in close agreement with the observed temperatures.

The model was then used to simulate the long-term (12-yr) effects of seepage from the cooling lake on ground-water temperatures near the lake. The temperature data collected at the Columbia Generating Station site and the model were also used to refine estimates of ground-water flow from the cooling lake calculated by using potentiometric data. A third application of the model was the simulation of the impacts on ground-water temperatures on the use of heat pumps for residential heating and cooling (Andrews 1978).

Although ground-water systems have been explored for possible energy storage or as a source of energy, the published literature contains no previous work documenting the effects of a power plant on a ground-water system. The possibility of temporary storage of energy in the form of heated water in aquifers has been explored by Meyer and Todd (1973), Hausz and Meyer (1975), Kley and Nieskens (1975), Molz et al. (1976), Tsang et al. (1976), and Werner and Kley (1977). Gass and Lehr (1977) advocated the use of ground water itself as an energy source. Gringarten and Sauty (1975), Intercomp Resource Development and Engineering (1976), and Tsang et al. (1976) developed models of the transport of heat in ground-water systems to study the feasibility of temporary storage of heated water in aquifers. Mercer et al. (1975) modeled the movement of heat and water in a hydrothermal system.

Alterations in the ground-water system induced by activities at a power-plant site can bring about significant changes in nearby flora, fauna, and surface waters. For example, in a wetland environment, here defined as an area where the water table is at or near the surface at all times, alterations in ground-water quality and ground-water discharge rates have been shown to alter wetland ecosystems (Bay 1967, Dix and Smeins 1967, Walker and Coupland 1968, Millar 1973). In addition, Vadas et al. (1976) and Gibbons (1976) found that changes in wetland water temperatures led to changes in wetland ecosystems.

Boulter (1972) studied the extent of water-table drawdown after a wetland is ditched. But no one has investigated the changes that occur in water levels, water quality, or water and substrate temperatures in a wetland when a ground-water system discharging into a wetland is altered. In the wetland adjacent to the Columbia Generating Station, wetland vegetation changed quickly and markedly following changes in water temperatures, water levels, and water flows caused by the presence of the cooling lake (Bedford 1977). During the first 2 yr of operation of the Columbia Generating Station, a

community previously dominated by sedge meadow species was replaced by emergent aquatic species and annuals (Bedford 1978).

This report deals with the hydrogeologic environment of the site of the Columbia Generating Station and the major effects of power-plant construction and operation; the impacts of the generating station on the ground-water system; the simulation of heat flow in the subsurface near the site; the expected long-term changes in ground water at the site; and the major conclusions and recommendations of the study. The appendices contain a description of the field methods used in the study (appendix A and appendix B), the computer program for solving the model of heat and water flow in shallow ground-water systems (appendix C), and a discussion of the use of the heat- and water-flow model to refine estimates of flow using temperature data (appendix D). An additional application of the model is reported by Andrews (1978).

SECTION 2

CONCLUSIONS AND RECOMMENDATIONS

The cooling lake at the Columbia Generating Station has dramatically altered the water supply to the marsh west of the lake. Before the filling of the lake, ground water, the major source of water to this area, discharged at a rate of less than $0.03 \text{ m}^3/\text{s}$ annually. The discharge rate increased by a factor of 6 after the filling of the cooling lake. The increased water supply to the marsh has raised surface-water levels in the sedge meadow approximately 10 cm above pre-lake levels, and the water levels now have much less seasonal variability.

The changes in ground-water patterns have been confined to the area between the station's cooling lake and ashpit and the Wisconsin River. To the east of the cooling lake, a drainage ditch limits the effects of the lake on the ground-water system to a narrow band east of the lake, except in the northeast corner of the lake where there is no ditch. In this area the water table has risen several feet, but flow in this area is small.

Thermal patterns in the marsh have been significantly altered by the cooling lake. Temperatures of the ground water that discharges in the marsh now average several degrees above prior average ground-water temperatures, and temperatures in the marsh are out of phase with seasonal air-temperature patterns. Much of the sedge meadow no longer freezes over in winter, and temperatures just below the surface are as high as 25°C prolong the growing season. Winter temperatures as high as 21°C and summer temperatures as low as 8°C were observed. In some areas the peak ground-water temperature occurred during the winter months. Changes in vegetation within the thermally altered zone were documented by Willard et al. (1976) and are thought to occur in response to changes in ground-water temperatures.

As with changes in ground-water flows, the thermal alteration of ground water was confined to the area west of the cooling lake. Moreover, significant changes in temperatures extended only to about 100 m west from the dike. The seasonal maximum ground-water temperature at any depth is a function of distance from the cooling lake and the distribution of subsurface lithologies.

The movement of heat in the subsurface was simulated by using the finite element method to approximate the differential equations for water and heat flow. The simulated temperature patterns agreed well with field data, but were very sensitive to the distribution of subsurface lithologies. Detailed stratigraphic information was necessary to obtain reliable results. The problem of simulating heat flow in the subsurface is further complicated by a

poor understanding of how to estimate dispersivity. Results presented in this study show that the amplitude of the seasonal temperature wave is best simulated when small dispersivities are used.

Long-term simulations of thermal alterations in the ground-water system of the marsh indicate that the cooling lake will significantly alter substrate temperatures but only within 350 m of the cooling lake dike. By 1987 peak temperatures near the dike were elevated 10-15° C above normal levels and lagged behind seasonal temperature changes by 1-2 months. At 150 m from the dike, peak temperatures at a depth of 0.6 m were only elevated 2.3° C above normal levels in the summer, but winter temperatures were elevated 6-10° C above normal levels. Temperatures within the wetland varied spatially, but trends were expected to be similar to those simulated in the two cross sections modeled. Seepage rates will increase 20% as the result of the increase in temperature of seepage waters.

The simulations indicate that winter temperatures will be warm enough to prevent formation of an ice cover in almost the entire marsh between the cooling lake and the Wisconsin River. Near the dikes a relatively warm microclimate will exist during most of the winter, since the temperature of the discharging water will be above 20° C during the early winter.

The potential for significant thermal alteration of surface-water bodies located in ground-water discharge zones is great. The temperature of the ground water may rise considerably near a cooling lake, even though the total heat flux is small. At the site of the Columbia Generating Station 40% of the water pumped into the cooling lake seeps into the ground-water system, yet less than 2% of the waste heat load is discharged to the ground-water reservoir. The discharge rate of water from the generating station to the cooling lake is $1 \times 10^6 \text{ m}^3$ per day, and the temperature of the surface water is increased 10-15° C. However, because the seepage rate is only $2 \times 10^4 \text{ m}^3$ per day, much of the heat load is dissipated through evaporation. The percentage of the heat load that leaves a cooling lake via seepage to the ground-water system is unlikely to be greater at other power-plant sites.

Seepage from the ashpit averages 0.3-0.6 m³/s. Surface water in the wetland within 50 m of the ashpit has been contaminated by seepage through the ashpit dikes, and total dissolved solids in the surface waters have increased over fivefold above background levels in this area. However, significant chemical degradation of ground water, judged by the concentration of the common cations and anions, has not occurred in the vicinity of the ashpit.

A plume of contaminated ground water is slowly moving eastward from the coal pile. Three years after coal was piled in the area, a plume of water with a sulfate concentration greater than 1,000 mg/liter extended to a depth of greater than 30 m and outward from the limits of the coal pile more than 100 m.

RECOMMENDATIONS FOR SITING FUTURE POWER PLANTS

All new power plants should be required to gauge accurately (within 1%) all water flows into and out of the plant and the plant site. In addition, precipitation into and evapotranspiration from all bodies of open water, such as ashpits and cooling lakes, should be monitored. Seepage from ashpits and cooling lakes cannot be determined accurately by direct methods; instead, seepage should be calculated indirectly by a mass balance approach. Data on water flows, precipitation, and evapotranspiration are required for calculating a mass balance. Control rooms of power plants are now designed to measure accurately mass flows within the generating station, and therefore water flows between the environment and the plant can also be carefully monitored.

Coal-storage areas should be designed so that water infiltrating the coal pile cannot reach the water table. Since crushed coal is highly permeable and leachable, an open coal pile allows most of the annual precipitation to pass through the pile, which creates water similar to acid mine drainage. Unless infiltration is controlled or the infiltrating water is captured and treated, a volume of contaminated water equal to the product of the annual precipitation and the area of the coal pile will flow into the subsurface.

Estimations of impacts of generating stations should recognize that significant thermal alterations of nearby surface waters can occur even when a closed-cycle cooling lake is used.

Dikes of all ashpits and cooling lakes should be lined with several inches of a relatively impermeable clay material. Seepage can be controlled, and sloppy designs should not be tolerated. More seepage can usually be allowed from a cooling lake than from an ashpit, since cooling-lake water is usually less threatening to the environment.

Simulation techniques should be used to evaluate potential seepage from ashpits, cooling lakes, and coal-storage areas in the design stage of these structures. Designs should minimize ground water seepage and contamination. Competent geologic consulting firms should be retained to conduct these studies.

Although seepage from a cooling lake may contribute to alterations in an adjacent wetland ecosystem, the high leakage rates are not undesirable from a lake-management standpoint. Seepage to the ground-water system prevents an increase in total dissolved solids in the lake. Such an increase would necessitate periodic flushing of the lake and the consequent release of saline water.

RECOMMENDATIONS FOR FUTURE RESEARCH

More field data are needed on the distribution of temperature or conservative chemical characteristics, or both, in small ground-water systems subjected to stresses that are altering these characteristics from background levels. The flow of mass and energy in ground-water systems is much more difficult to quantify than the flow of water, mainly because the former is

sensitive to the hydraulic conductivity distribution. The development of quantitative techniques to date has been hampered by the lack of field data to verify the models. As demonstrated in this study, it may be more fruitful to monitor temperature changes than chemical changes in a ground-water system if the goal is to determine the system's capability to transport mass and energy. Temperature can be inexpensively and rapidly monitored at a large number of points, which is not the case for chemical characteristics.

Existing ground-water models will be adequate in most cases for quantifying impacts of power plants on hydrogeologic systems. The best existing models for these purposes are those devised by the U.S. Geological Survey. Future research should not be directed towards developing new models for these purposes, unless the investigator can show clearly that existing models are deficient.

More study is needed of the factors controlling dispersivity, and the appropriateness of the concept should be evaluated.

An evaluation is needed of the prediction ability of models used when historical data are not available. The magnitude of error associated with predictions should be quantified. It may be that transport models should not be used for predictions if historical data are not available for calibration.

A theoretical evaluation of the validity of using either chemical or energy distribution in the subsurface to determine hydraulic conductivity distributions is needed. The question to be asked is whether or not the inverse approach can produce useful approximations in a problem that is more complex than those investigated by Bredehoeft and Papadopoulos (1965).

SECTION 3

THE SITE OF THE COLUMBIA GENERATING STATION

The Columbia Generating Station is a 1,000-MW coal-fired electric-power-generating complex located on the flood plain of the Wisconsin River 5 miles south of Portage, Wis. Construction began in 1971, and the two 500-MW units began operation in May 1975 and May 1978. The 1,620-ha site on which the facility was constructed consisted of an extensive marsh, mainly sedge meadows, and wetland forests with sandy upland knolls (Figure 1). Construction activities have dramatically altered the site. A 200-ha cooling lake, a 28-ha ashpit, a 16-ha coal pile, and the generating station itself are now the dominate features of the site (Figure 2, Figure 3).

The power plant dynamically interacts with the environment. On an average day the first unit alone burns 2,000 tons of coal, producing 385 MW of electricity, 1,000 MW of waste heat, and 552 tons of coal residue. This rate of coal burning is approximately 38 kg/s, which represents over 1,000 MW of power of which only about 360 MW are converted to electricity. The cooling lake and the ashpit are the direct recipients of most of the byproducts. The thermal and chemical characteristics of the byproducts differ markedly from the thermal and chemical characteristics of water in the adjacent wetland environments (Figure 4).

The site of the Columbia Generating Station is located in a regional discharge area (Figure 5). The discharge area includes the wetlands on the site of the power plant, the wetlands to the east of the site, which are used for mint farming, and extensive wetlands along the lower reaches of Rocky Run Creek. The marsh on which the site is located occupies a former river channel.

The geology beneath the site of the Columbia Generating Station consists of irregularly eroded Upper Cambrian quartz sandstone overlain by sediments from glacial lake bottoms and drift deposits of the Green Bay lobe of the Wisconsin ice sheet. The bedrock is composed of Upper Cambrian sandstones and Precambrian granites which occur 125 m below the surface. The surface is covered by a layer of peat 1.5 m thick, which overlies a thin layer of organic clay and silt. The peat and clay are in turn underlain by alluvial sands with clay lenses. Representative stratigraphic cross sections are shown in Figure 6. The hydraulic conductivity of the clay is an order of magnitude less than the peat and thus controls the rate of ground-water discharge (Table 1). Vertical hydraulic conductivities were estimated to be 5 to 20 times less than horizontal hydraulic conductivities.

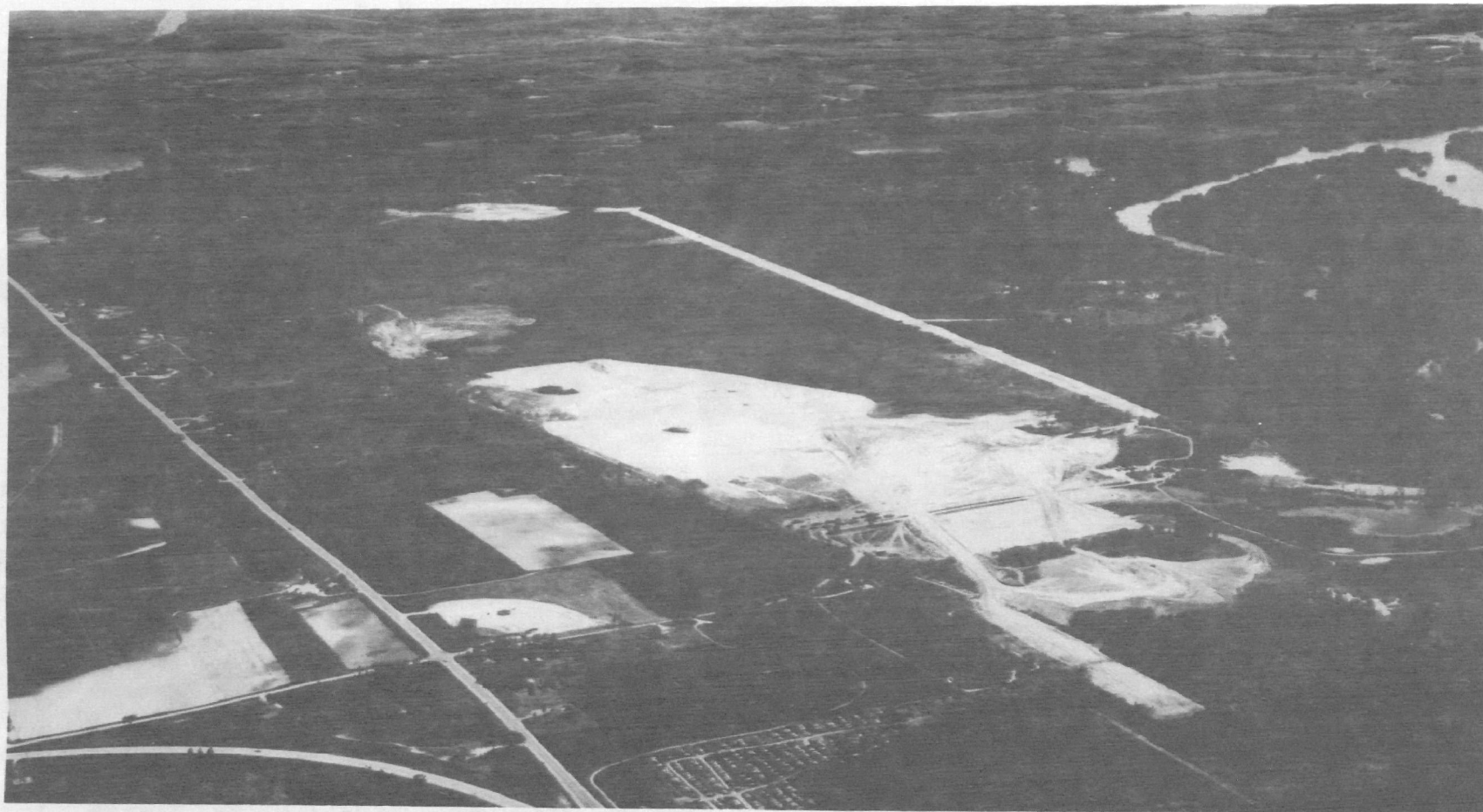


Figure 1. The site of the Columbia Generating Station during construction of the first unit (24 May 1971).

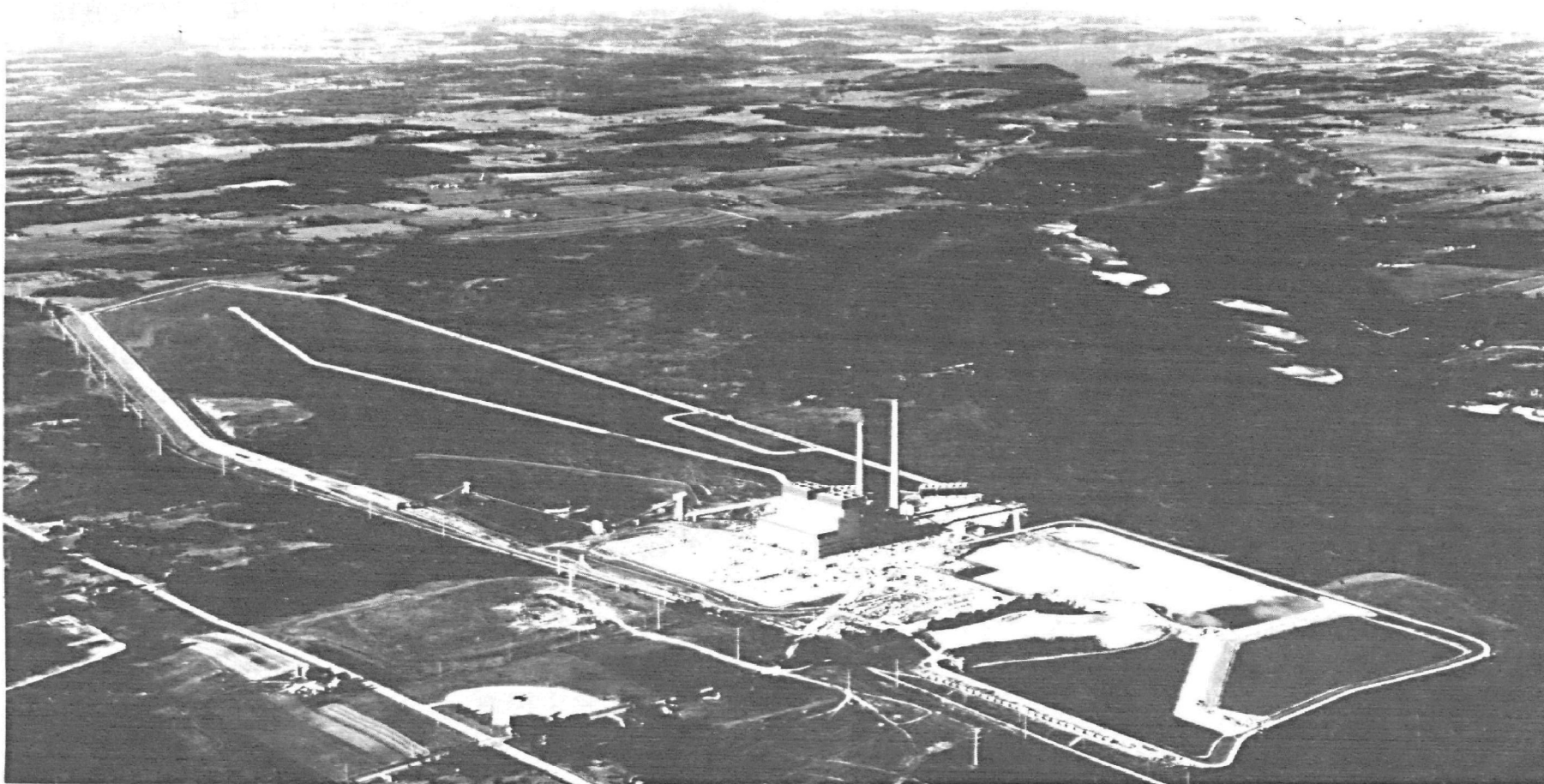


Figure 2. The site of the Columbia Generating STation after construction of both units (12 August 1977).

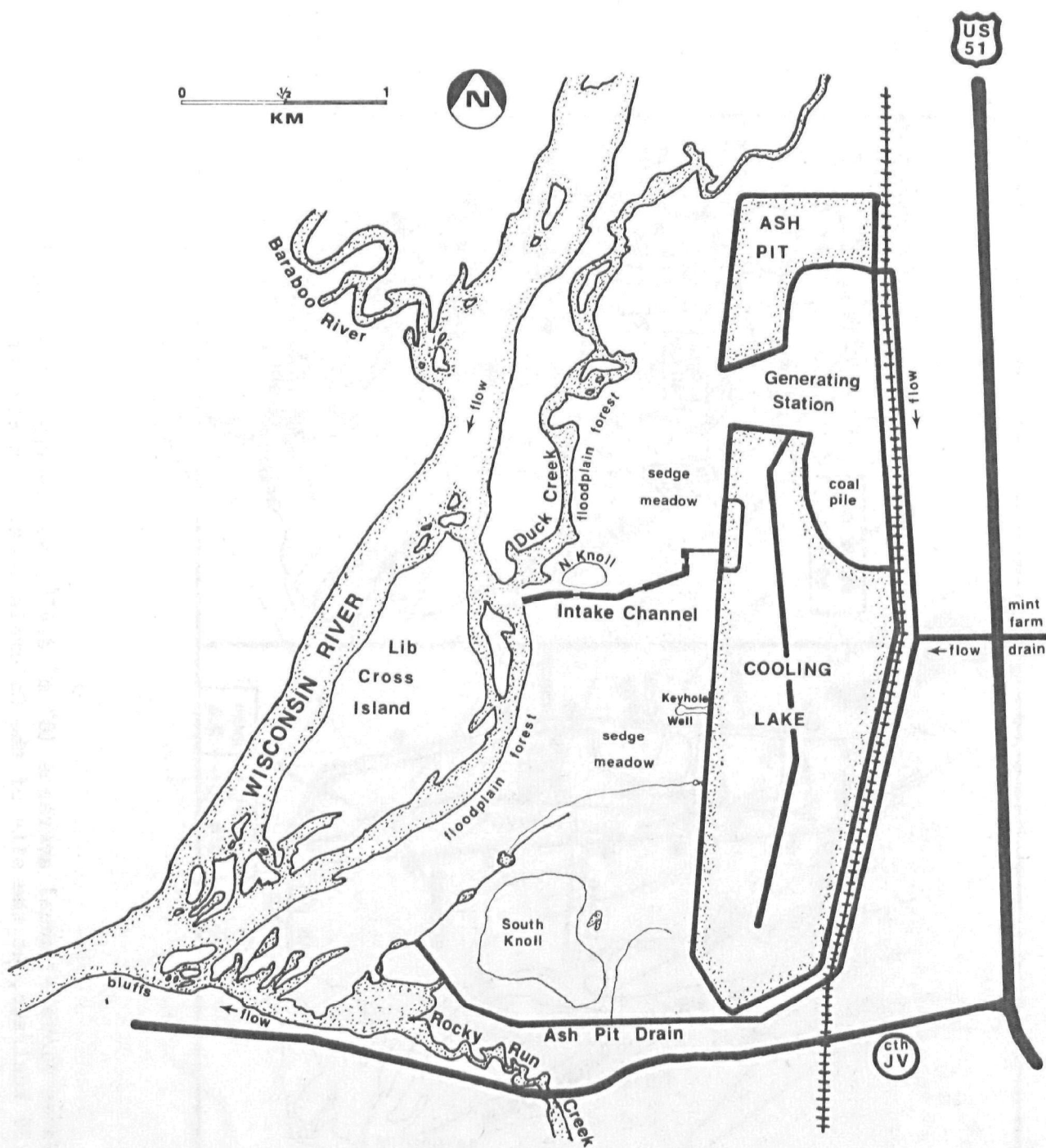


Figure 3. Main features of the site of the Columbia Generating Station.

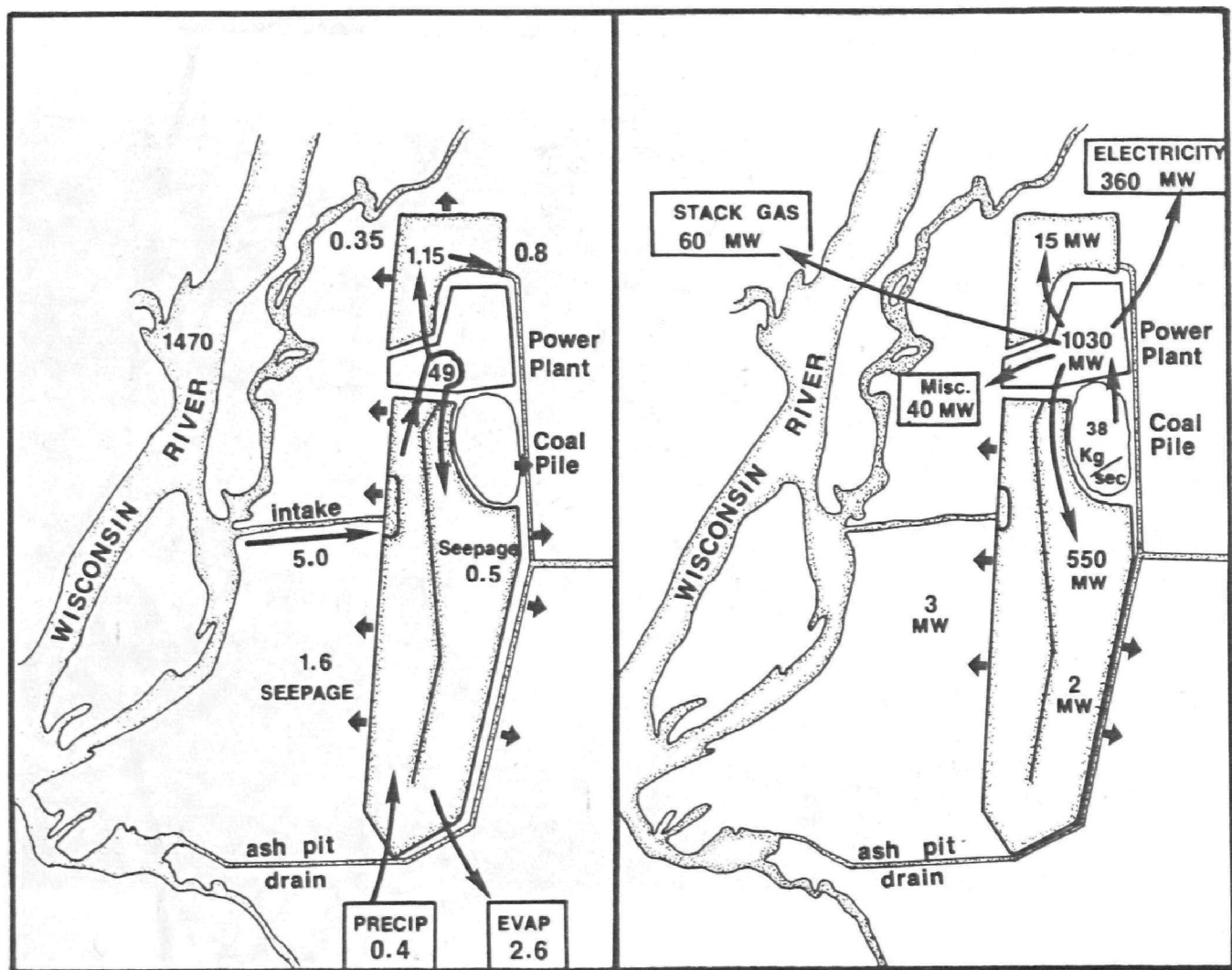


Figure 4. Water flows - annual averages $10^4 \text{ m}^3 \text{ day}^{-1}$, and energy flows - approximate values $1 \text{ MW} = 239 \text{ kcal/sec}$, at the site of the Columbia Generating Station.

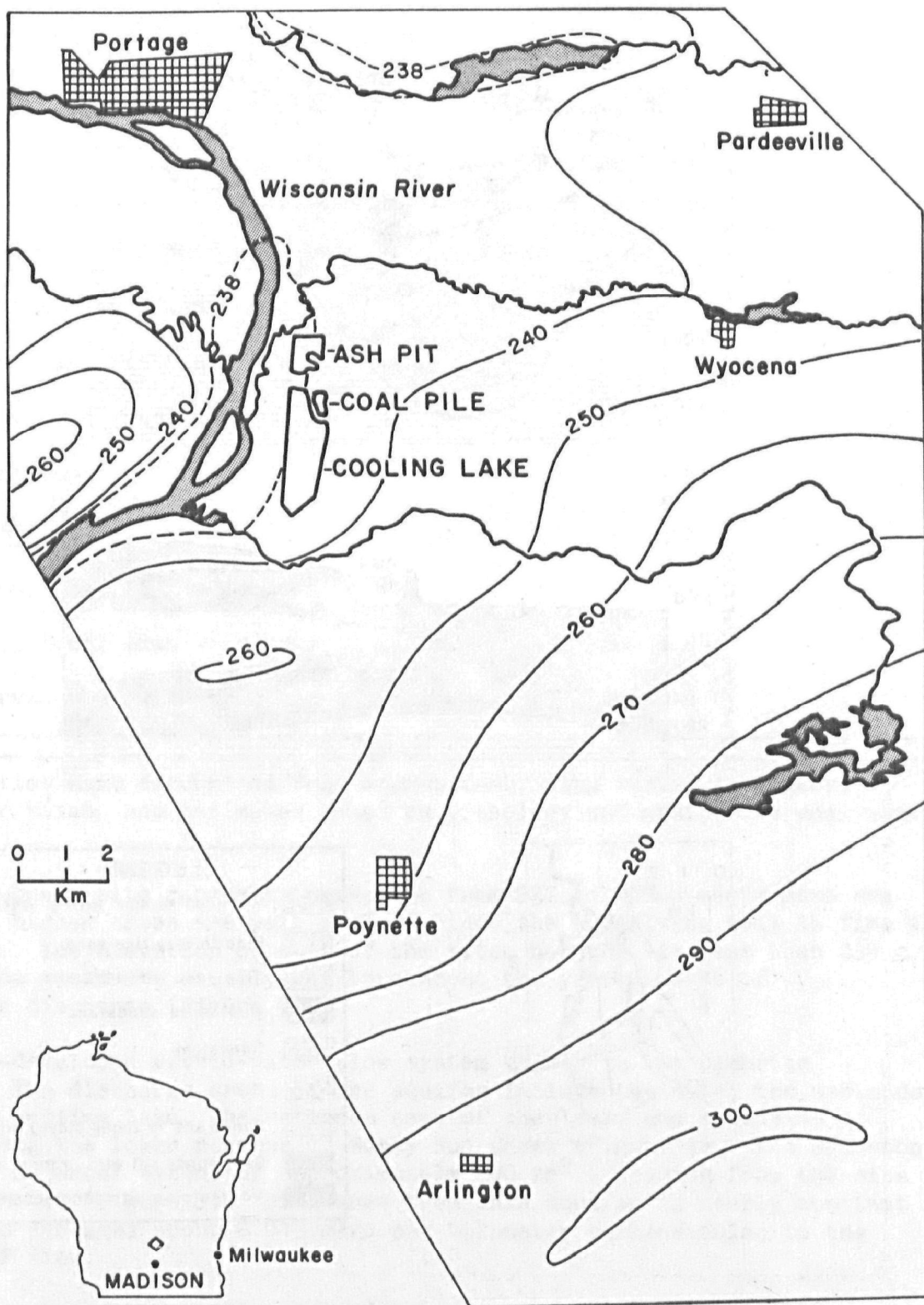


Figure 5. Potentiometric surface contours in the Cambrian sandstone (meters above mean sea level) in the area of the Columbia Generating Station. Location is shown by diamond on insert map of the State of Wisconsin.

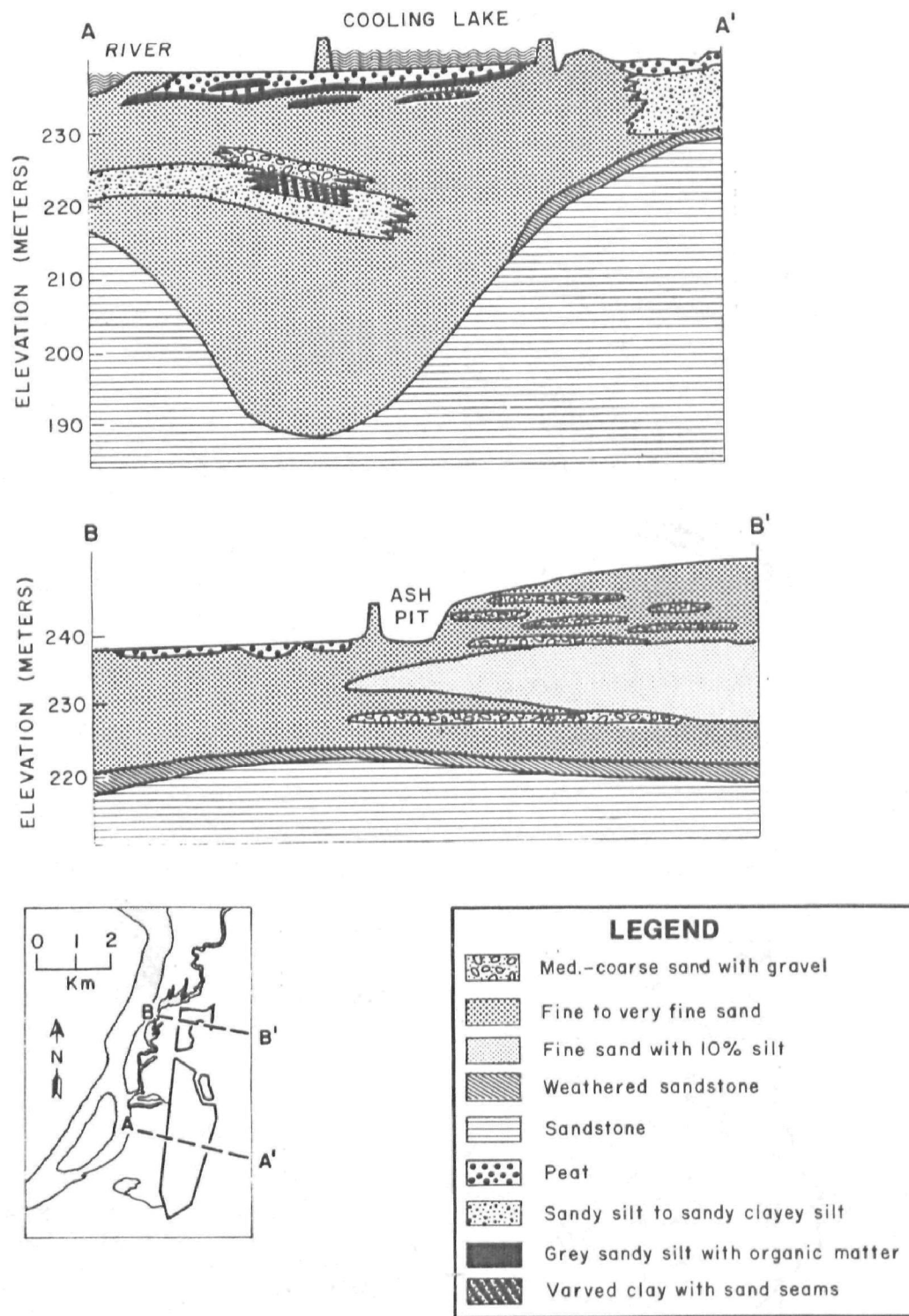


Figure 6. Representative stratigraphic cross sections of the subsurface at the site of the Columbia Generating Station. Insert shows locations of sections at the site.

TABLE 1. HORIZONTAL HYDRAULIC CONDUCTIVITIES FOR THE LITHOLOGIES
IN THE SUBSURFACE OF THE COLUMBIA GENERATING STATION

Lithology	Horizontal hydraulic conductivity (m/day) ^a
Medium-coarse sand with gravel	30
Fine to very fine sand	10
Fine sand with 10% silt	6
Weathered sandstone	8
Sandstone	3--4
Peat	0.4--3
Sandy silt to sandy clayey silt	0.4
Gray sandy silt with organic matter	0.04
Varved clay with sand seams	0.02--0.04

^aConductivities were determined from a pump test, slug tests, laboratory permeameter tests, and estimates based on lithology and grain-size analyses.

The 1,900-ha site ranges in elevation from 237 to 248 m above mean sea level. The higher areas are well drained since the underlying soil is fine to medium sand. The elevation of most of the site, however, is less than 239 m, and these low areas are usually wet throughout the year because of ground-water discharge (Figure 7).

A well-developed ground-water flow system exists in the Cambrian sandstone. The discharge areas of the aquifer include the site, the wetlands west of the cooling lake, the wetlands east of the lake, and extensive wetlands along the lower reaches of Rocky Run Creek (Figure 3). The sandstone aquifer has an areal extent of approximately 200 km² extending from the site to the southeast (Figure 5). Discharge from this aquifer is nearly constant all year and averages about 0.013 m³/s per kilometer perpendicular to the direction of flow.

The low areas also receive ground-water recharge from the upland areas located on the site and adjacent to the site. These upland areas act as recharge areas during precipitation events, when the infiltrating water flows toward the low areas. Travel time for water from the upland areas to the low

areas is usually less than 3 months, but flow rates are seasonally variable. Before construction of the cooling lake, approximately 50% of the ground water discharging in the low areas in the spring originated from the upland areas on and near the site; during the summer the percentage dropped to less than 5%.

The ground-water inflow rates to the low areas are greatest where the peat deposits are thinnest (Figure 8), namely in areas recently reworked by fluvial processes. The peat deposits are generally less than 2 m thick west of the railroad track; east of the railroad track, kettles in the outwash and ice-contact drift have been filled in by organic deposits as thick as 10 m. North of the ashpit alluvial deposits are more complex than in other parts of the site; sediments range from coarse to very fine, indicating that depositional processes characteristic of both the Wisconsin River and Duck Creek have formed these deposits.

The cooling lake was designed to dissipate the waste heat, which is discharged from the plant after steam has been used to generate the electricity. The 200-ha lake has an effective length of 5,500 m. The lake and the ashpit were formed by dikes 5 m high constructed entirely of local silty sand. The western dikes around the cooling lake were lined with bentonite. Water is pumped into the cooling lake from the Wisconsin River at an average rate of 50,000 m³/day. Of this water 20% discharges into the ashpit, 40% is lost by ground-water seepage, and 40% is lost by evaporation.

Hot water is discharged at a rate of 1×10^6 m³ into the north end of the lake east of the central divide (Figure 3). Water circulates in a clockwise direction and is withdrawn from the north end of the lake west of the central divide. Average residence time of a water particle in the lake is 5 days. Water temperatures at the discharge point average 10-15° C higher than temperatures at the intake and decrease exponentially with distance from the discharge point. The average annual range of lake temperature is 0-45° C. Temperatures in the lake vary only slightly with depth.

Cooling towers have been built to dissipate some of the additional waste heat that is being generated by the second unit. However, the cooling lake is projected to receive 80% of the annual heat load. The discharge of the additional waste heat into the cooling lake is estimated to increase lake temperature by approximately 8° C when the cooling towers are not operating (Wisconsin Public Service Commission 1974).

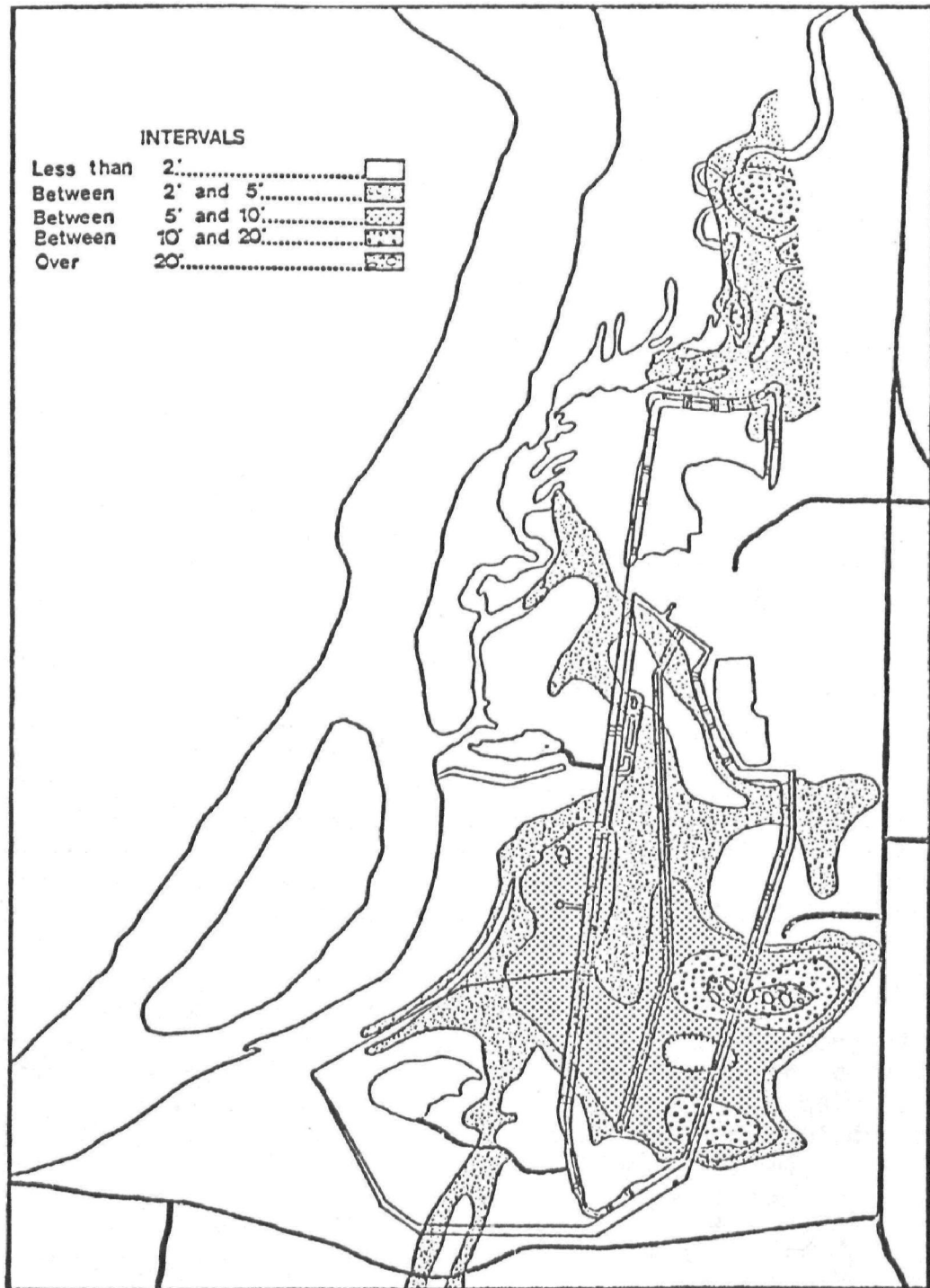


Figure 8. Peat thicknesses in the subsurface at the site of the Columbia Generating Station.

SECTION 4

THE IMPACT OF A POWER PLANT ON THE GROUND-WATER SYSTEM OF A WETLAND

CONFIGURATION OF THE GROUND-WATER FLOW SYSTEM

The first goal of the hydrogeologic investigation at the site of the Columbia Generating Station was to determine the impact of the station on ground-water flows, temperature, and chemistry in the adjacent wetland (Anderson and Andrews 1977, Andrews and Anderson 1978). To determine the physical setting in the ground-water system of the wetland before operation of the plant, data were collected beginning in the summer of 1971. The position of the water table was monitored in 80 small-diameter observation wells, and vertical head gradients were measured in 19 nested observation wells.

Two-dimensional steady-state models of several representative vertical cross sections oriented perpendicular to the western dike of the cooling lake were generated. (Figure 6 illustrates two of these cross sections.) These models were then combined to construct a quasi-three-dimensional model of the flow system. This model was used to simulate the head distribution before and after filling of the lake and to compute the total ground-water discharge to the wetland in the area affected by the lake. The vertically oriented cross section models were patterned after the regional ground-water model of Freeze and Witherspoon (1966). The finite difference equations were solved by using the method of successive over-relaxation. A 25-by-50 node grid was used for all simulations. Horizontal nodal spacing ranged from 15 m near the dike to 120 m farther from the dike, and vertical spacing ranged from 0.6 m near the surface to 30 m at depth. Details of the modeling procedure can be found in Andrews (1976).

Field data were used to check the validity of the model, and the model then computed ground-water discharge to the wetland. The simulated head distribution in cross-section A-A' of Figure 6 before filling of the cooling lake is shown in Figure 9. The ground-water flow system was modeled to a depth of 150 m, but for clarity only the upper 30 m are shown. Horizontal flows ranged from 0 to 4.1 cm/day. Vertical flows were mostly toward the surface at rates of 0-0.16 cm/day. Approximately 300 m west of what is now the western dike, vertical flows were as high as 0.53 cm/day. Total discharge to the wetland in the cross section shown in Figure 9 was 1.00 m³/day per meter dike length, of which 0.43 m³/day per meter discharged in the area of high vertical flows shown in the figure.

A steady-state model was used to simulate pre-lake conditions, although the water table fluctuated about 0.5 m/yr in the lowlands and as much as

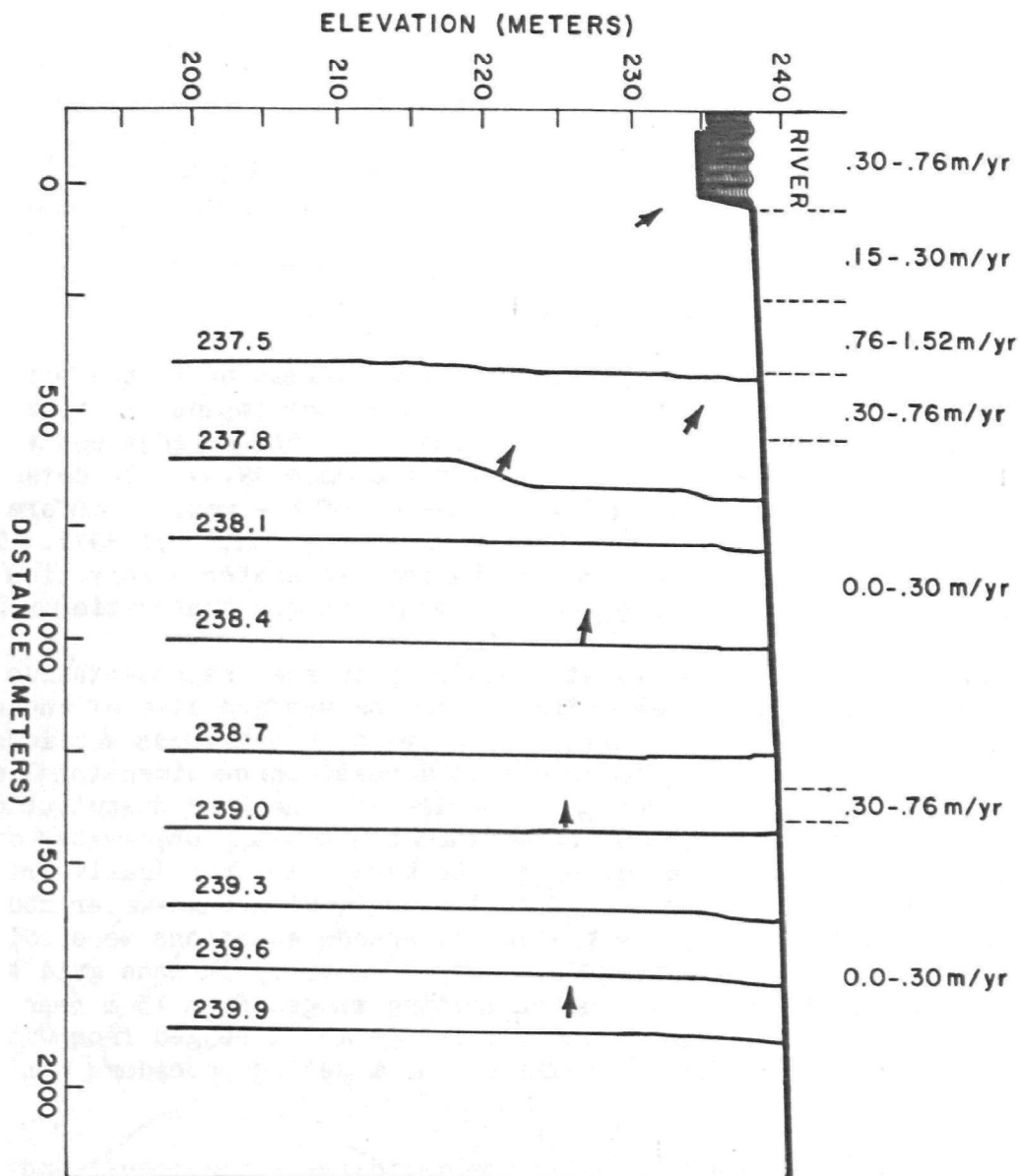


Figure 9. Simulated head distribution in cross-section A-A' of Figure 6 before filling of the Columbia cooling lake. Equipotential lines are labeled in meters. Vertical discharge rates are given across the top of the figure.

2 m/yr in the uplands. However, the water-table gradient remained nearly constant throughout the year, except in the upland areas where the gradient increased markedly during periods of recharge. The head distribution presented in Figure 9 approximates the average annual head distribution.

The initial filling of the cooling lake began 13 June 1974 with water pumped from the Wisconsin River. Pumping stopped on 17 July, when the level was 0.5 m below the fill line. By 1 September the lake was almost empty, and on 4 November 1974 pumping resumed. The water level reached the fill line on 2 January 1975. Water levels in observation wells monitored during the filling of the lake showed increases in vertical gradients in the area west of the cooling lake (Andrews 1976).

The filling of the lake greatly altered the head distribution in the ground-water system (Figure 10). What had been one ground-water system became three systems. Ground water that formerly discharged to the wetland began to discharge near the drainage ditch east of the cooling lake. The lake became the only source of water for the discharge area west of the lake. For the cross section in Figure 10, the simulation predicted that the ground-water discharge to the wetland west of the dike was $3.5 \text{ m}^3/\text{day}$ per meter and that the flow into the drainage ditch was $3.7 \text{ m}^3/\text{day}$ per meter. As in the pre-lake simulation, vertical discharge rates were highest approximately 240-300 m west of the dike. In this main discharge area vertical flow rates varied from 1.02 to 1.34 cm/day. Elsewhere, vertical flows ranged from 0.24 to 0.94 cm/day. The position of the main discharge area varied with the cross section modeled. A comparison of total discharge rates to the wetland for Figure 9 and Figure 10 shows that discharge to the wetland in that cross section after filling of the lake was 3 1/2 times greater than discharge before filling.

The effect of the cooling lake on the head distribution in several other cross sections was also simulated. In all simulations the horizontal component of flow was assumed to be perpendicular to the dike. Changes in configuration of the flow system in other cross sections modeled were similar to the changes shown in Figure 9 and Figure 10. In some cross sections, however, the discharge to the wetland was 15 times greater after the filling of the cooling lake. Total discharge to the area of the wetland affected by the lake was estimated to be six times greater after filling.

The assumption of steady-state conditions after filling of the cooling lake is acceptable in view of the stabilization of ground-water levels within a month of the filling of the lake. However, since the water in the cooling lake is warmer than the ground water in the system before the lake was filled, the ground-water system is not yet in equilibrium with the altered thermal regime. The model allows for variation in hydraulic conductivity as a result of differences in ground-water temperatures. For the simulation presented in Figure 10, the temperatures in the ground-water system were assumed to vary from 26°C directly beneath the cooling lake to 10°C at a depth of 20 m below the lake. The relationship between ground-water temperature and ground-water flows is discussed in section 5.

From the simulations and the supporting field evidence, the following observations can be made. On the east and south sides of the cooling lake,

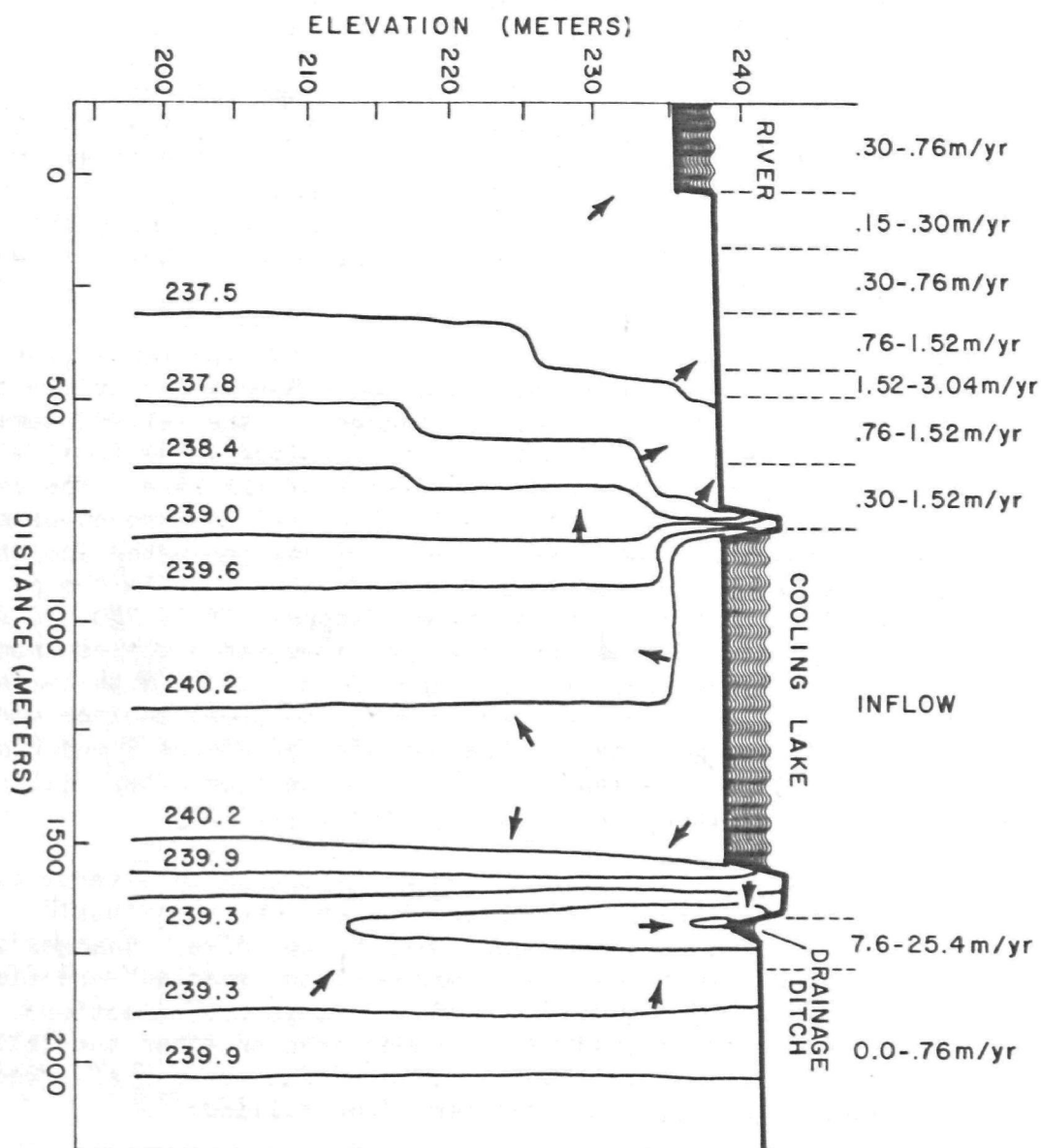


Figure 10. Simulated head distribution in cross section A-A' of Figure 6 after filling of the Columbia cooling lake. Equipotential lines are labeled in meters. Vertical discharge rates are given across the top of the figure.

the drainage ditch effectively limited the impact of the lake on the ground-water system to a relatively narrow zone. On the north and northeast sides of the lake where there is no drainage ditch, the filling of the cooling lake resulted in a rise of ground-water levels of almost 1 m. This rise reversed flow in this area such that water now flows from the lake eastward beneath the coal pile and discharges in the wetland area east of the site. The average annual seepage from the cooling lake is estimated to be 0.18 to 0.27 m³/s. Flow rates fluctuate about 20% during the year as a result of changing ground-water temperatures.

The average annual seepage from the cooling lake will increase by approximately 20% with both generating units in operation. The discharge rates will also increase because of the formation of springs in the wetland west of the cooling lake. Springs have formed since the filling of the cooling lake, because vertical hydraulic gradients in many areas near the dike exceeded 1 m/m, which approximates the critical gradient for the onset of heaving in unconsolidated materials. In addition, increased temperatures in the marsh have speeded up the process of peat decomposition, and deeper water levels in the marsh have resulted in the floating of parts of the peat mat. The result of both these processes is a decrease in the total load on the confining silt-clay layer, a decrease that enhances the onset of heaving. Heaving is not predictable, and therefore accurate estimates of its rapidity and of its impact on flow rates are impossible. Potentiometric data from observation wells in the marsh indicate that the springs that have formed during the first 2 yr since the cooling lake was filled have not significantly altered flow rates. Increases in flow rates caused by these processes will probably not exceed 8% during the next 10 yr.

WETLAND WATER LEVELS

The wetland west of the cooling lake lies in two distinct drainage basins, each of which is connected by distinct channels to tributaries of the Wisconsin River. The wetland area adjacent to the cooling lake and north of a line 350 m south of the intake channel drains to Duck Creek, and the area south of this line drains to Rocky Run Creek via a small channel (Figure 3). Ground-water inflow to the northern basin averages approximately 0.09±0.03 m³/s, and inflow to the southern basin averages approximately 0.10±0.03 m³/s.

The water level in the wetland is a function of the ground-water inflow rate, the rate of water leaving the wetland via surface outflow, the rate of precipitation and evapotranspiration, and the wetland basin shape. The rate at which water leaves the wetland is a function of the water level and the shape of the channels draining the wetlands. On a daily basis evapotranspiration from each wetland basin seldom exceeds 0.04 m³/s. Because of the shape of the channels that drain the basins, a change in outflow from 0.04 to 0.20 m³/s raises water levels less than 5 cm.

Water levels in the wetland have been almost constant since the cooling lake was filled. The level averages about 10 cm higher than previous levels (Figure 11). Wetland water levels do fluctuate during the winter when ice clogs the drainage channels and during floods on the Wisconsin River.

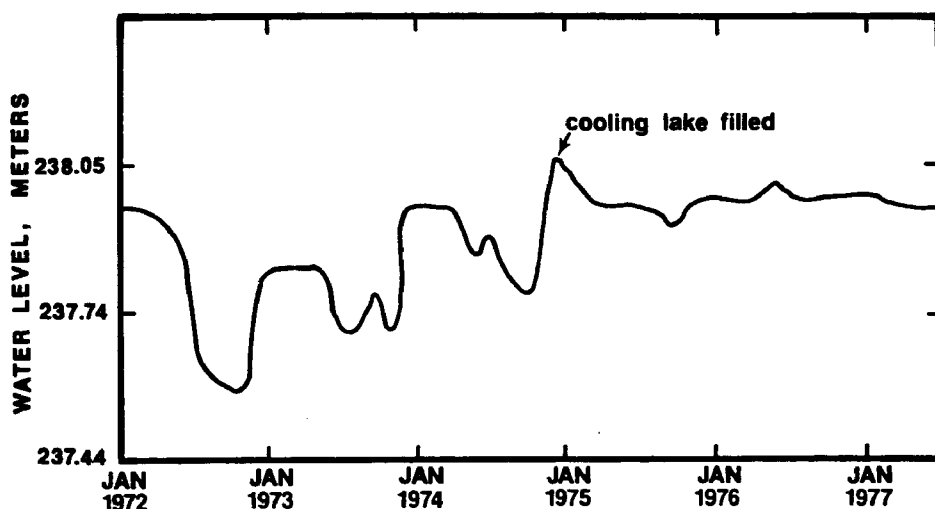


Figure 11. Water levels in the wetland west of the Columbia cooling lake before and after filling of the lake.

Before the cooling lake was filled, ground-water inflow rates in the summer to each of the wetland basins were only 0.2 to 0.3 m³/s. Evapotranspiration often exceeded inflow, and there was no outflow from the wetlands via the channels. During the late summer water levels were lowered as much as 0.6 m.

The peat substrate in the wetland has been altered by the increased flow rates within the wetland, the increased water temperatures, and the increased water levels. Some peat has been eroded, and new channels have been cut in the wetland as the internal drainage system adjusts to the increased flow. Other parts of the peat mat have floated to the surface and been broken down by various physical and biological processes. Peat decomposition rates have increased because of the increased water temperatures and increased oxygen content of discharging ground water. The plant community is rapidly responding to the new environment as evidenced by the replacement of formerly dominant sedges, Carex lacustris and Carex stricta, by plants more tolerant of deeper water, primarily Sagittaria latifolia and Rumex orbiculata (Willard et al. 1976).

GROUND-WATER TEMPERATURE

Before the cooling lake was filled, the temperature of ground water discharging to the wetland was approximately equal to the average annual air temperature (10° C). The cooling lake, now the source of water discharging to the wetland, has an average annual temperature between 10° C and 17° C, depending on location in the lake.

In areas with a layer of relatively high permeability near the dike, discharge rates are high and seepage from the lake has a travel time of less than 1 yr before discharging to the wetland. Consequently, the range of ground-water temperatures is similar to that of the lake water, although the extremes are somewhat attenuated. The temperature of water in the western

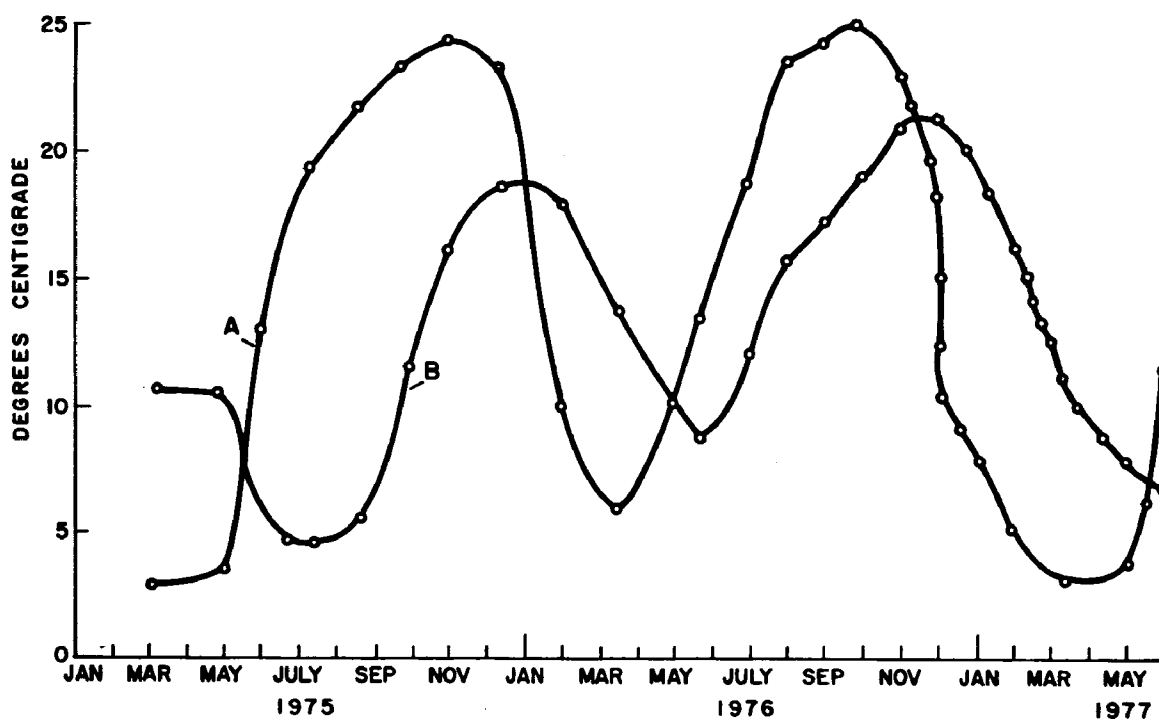


Figure 12. Ground-water temperature variations in wells west of the Columbia cooling lake. Curve A: data from a well cased to 4 m below the surface and located 3 m west of the dike. Curve B: data from a well cased to 2.5 m below the surface and located 60 m west of the dike.

portion of the lake from May 1975 to May 1976 ranged from 1° C to over 30° C. Ground-water temperature in a well 3 m west of the dike varied from 2° C to 25° C (Figure 12, curve A), and in areas west of this well, attenuation of extremes was even greater (Figure 12, curve B).

To measure the heat discharge into the ground-water system, 47 thermistors were installed in the summer of 1976 to depths of 10 m below the surface along cross-section A-A' of Figure 6. Temperature data were collected twice a week to document seasonal trends in the variation of ground-water temperature. The temperature changes observed in the ground-water system are described in detail in section 5. Preliminary calculations based on these thermistors suggest that approximately 16 MW, less than 5% of the heat released to the cooling lake, is discharged to the ground-water system. Ground-water temperatures increased as much as 20° C, however, in some areas west of the cooling lake.

Normally, the species of sedges present in the marsh emerge early and die back late in the growing season. During the winter of 1975, however, sedges in some areas of the marsh turned green in December because of the warm water. In the spring these sedges were dead, possibly because they had used up their stored food reserves. In 1976 these vegetation changes occurred over a considerably larger area (Willard et al. 1977).

RELATIONSHIP BETWEEN GROUND-WATER TEMPERATURES AND FLOW RATES

The ground-water system was not yet in equilibrium with the altered thermal regime. Because ground-water flow rates depend on temperature of the ground water, leakage is greatest in late summer when the water is the warmest. Furthermore, as ground-water temperatures rise in response to heat input from the cooling lake, the flow rates will increase. The ground-water flow model predicted that flows in the cross section shown in Figure 10 will increase by 24% when the system reaches equilibrium. A model which couples ground-water flow with heat flow is discussed in section 5.

CHANGES IN WATER CHEMISTRY

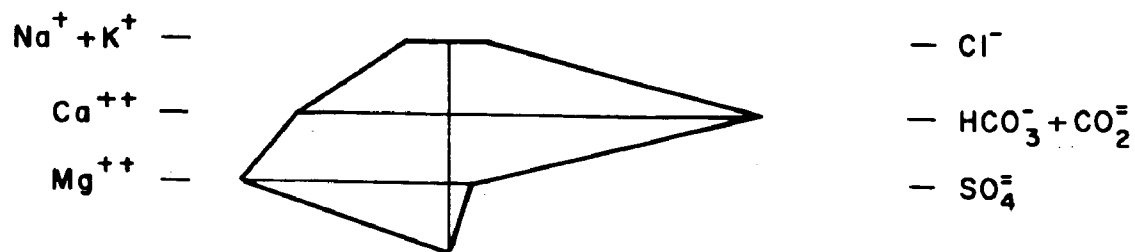
During the preoperational period (August 1972 to September 1974) 144 water samples were taken from observation wells on the site. During the first 7 months of operation 134 samples were collected from 57 wells. Some of the types of water on the site are illustrated by Stiff diagrams in Figure 13 and Figure 14.

Significant changes in the ionic composition of ground water and surface waters in the wetland since the generating station began operation were observed only near the ashpit. Because of the similarity in the chemical composition of cooling-lake water and ground water, no significant changes are likely to be observed in ground-water quality near the cooling lake. If changes do occur, they are likely to be in sodium concentrations caused by changes in ion-exchange processes associated with higher flow rates.

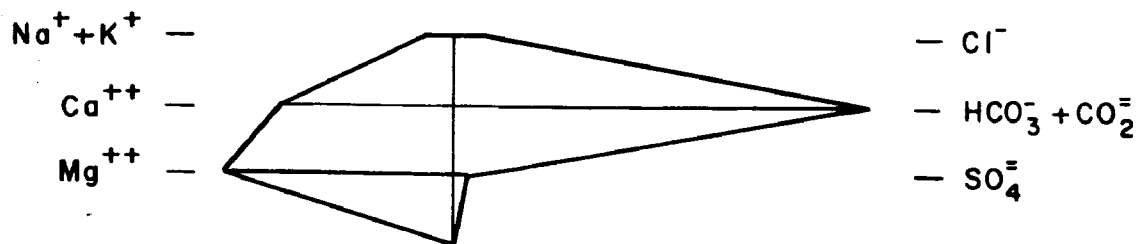
Major changes are likely to occur in ground-water quality near the ashpit because ground water and water in the ashpit differ in quality. Prediction of these changes is not yet possible because water levels in the ashpit have fluctuated widely during the first 2 yr of operation and because the chemical composition of ashpit waters has varied widely. Ground-water flow rates from the ashpit have consistently ranged from 0.3 to 0.6 m³/s. The filling of the pit with ash has reduced seepage through the bottom, but this reduction has been offset by increased flow through the dikes caused by elevated water levels. Most ground-water flow from the ashpit now occurs through the dikes, and most of the seepage water discharges near the dikes.

Some change has been observed in ground-water quality near the ashpit. Calcium and sulfate concentrations have increased significantly in two wells close to the ashpit dike (Table 2). Changes in water quality have been noted in other wells farther from the dike, but these changes have not been as great (Table 2). The plume of contaminated ground water appears to be confined to a relatively small area near the dikes. However, pronounced increases in specific conductivity in surface waters in the marsh have been measured up to 50 m from the dike, which suggests that water is leaking from the ashpit through the ground-water system and is discharging to the wetland where the water then spreads outward. Head gradients in observation wells support this hypothesis.

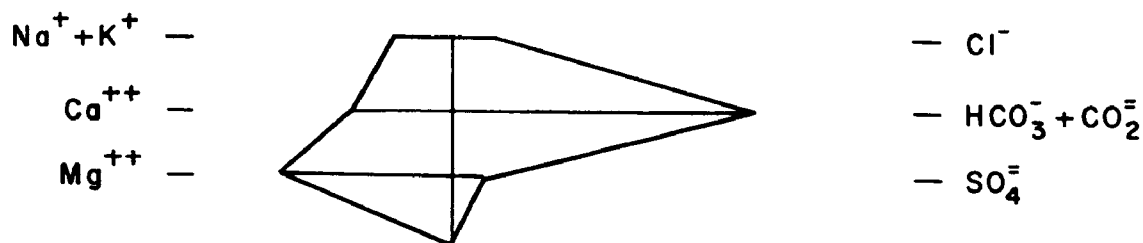
The most significant degradation of ground-water quality has occurred in the vicinity of the 17-ha coal pile. Although background sulfate



(a) COOLING LAKE



(b) SHALLOW GROUNDWATER



(c) DEEP GROUNDWATER

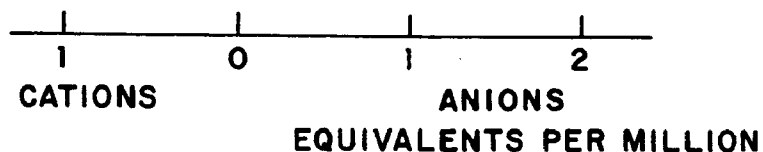


Figure 13. Stiff diagrams of water in the cooling lake (a) and ground water (b and c). Data were collected in fall 1975. Ground water (b) is from a well cased to 2 m below the surface and located 50 m west of the north end of the cooling lake; ground water (c) is from a well cased to 6 m below the surface and located 60 m west of the south end of the cooling lake.

concentrations are less than 20 mg/liter, a plume of contaminated ground water has been created with a sulfate concentration of greater than 1,000 mg/liter. This concentration exists to a depth of more than 30 m near the coal pile and extends more than 100 m to the east of the pile. The plume is gradually spreading east, toward the wetland discharge area (Andrews 1976).

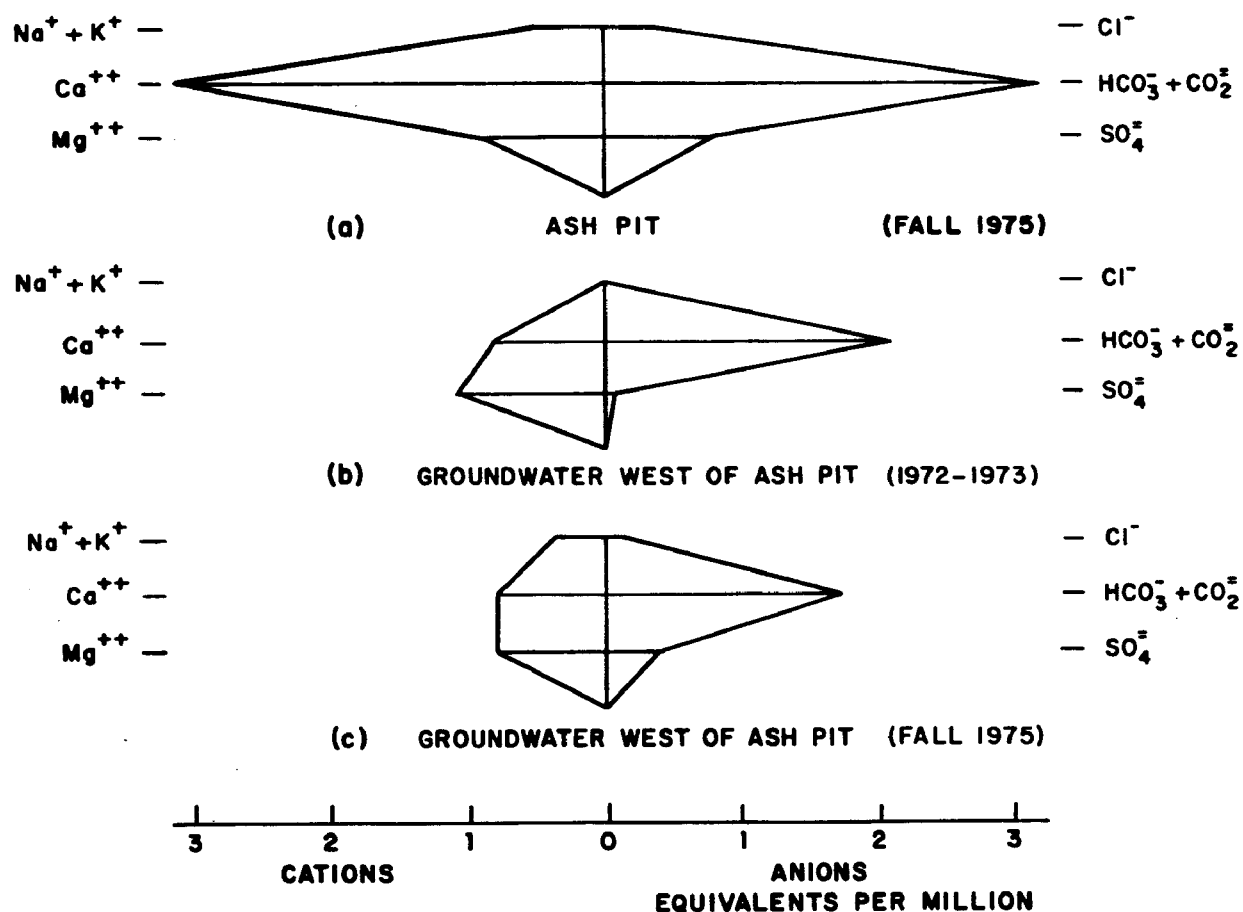


Figure 14. Stiff diagrams of water in the ashpit (a) and in a well cased to 1.5 m below the surface and located 2 m west of the ashpit (b and c). Comparison of (b) and (c) shows the change in water quality after the partial filling of the ashpit.

TABLE 2. SELECTED CHEMICAL CONCENTRATIONS IN GROUND WATER NEAR
THE ASHPIT OF THE COLUMBIA GENERATING STATION

A. West of the dike							
(m/l)	Ashpit water	1 m west			75 m west		
		1972-73	1975-76	1977	1972-73	1975-76	1977
K ⁺	2.3	1.2	9.2	6.9	1.2	0.75	0.5
Na ⁺	10.2	2.2	8.5	13.2	3.6	3.5	4.0
Ca ⁺⁺	77.8	13.9	16.9	21.6	31.6	28.8	24.3
Mg ⁺⁺	10.6	11.1	9.8	14.7	20.3	22.0	16.9
SO ₄	44.6	5.4	18.5	10.5	0.8	0.2	0.1
Cl ⁻	10.6	3.4	4.5	6.5	4.49	2.64	5.0
B. North of the dike							
(m/l)	Ashpit water	1 m north			25 m north		
		1972-73	1975-76	1977	1972-73	1975-76	1977
K ⁺	2.4	1.7	0.75	1.5	2.0	0.75	0.5
Na ⁺	10.3	4.3	2.6	5.1	5.2	3.1	3.7
Ca ⁺⁺	54.7	18.8	23.3	37.0	22.0	22.6	21.5
Mg ⁺⁺	4.3	17.3	22.5	33.8	18.0	18.8	25.8
SO ₄	36.0	7.7	9.6	22.0	9.7	9.3	14.0
Cl ⁻	10.5	2.8	4.2	8.5	7.2	3.2	3.5

SECTION 5

THERMAL ALTERATION OF GROUND WATER CAUSED BY SEEPAGE FROM THE COOLING LAKE

In addition to monitoring and modeling ground-water flow rates near the Columbia Generating Station, we investigated the effect of the station's cooling lake on ground-water temperatures (Andrews and Anderson 1979). Ground-water temperatures in the vicinity of the cooling lake were monitored in detail in the field for 1.5 yr. The presence of the cooling lake, which loses water to the ground-water system at a rate of $2 \times 10^4 \text{ m}^3$ per day, has created a zone of thermally altered ground water, but the zone is confined to a relatively small area hydraulically downgradient from the cooling lake.

A mathematical model was developed to simulate the response of subsurface temperatures to seasonal changes in lake and air temperatures. To create the model, equations describing ground-water flow were coupled with equations for heat flow in the subsurface. An equation describing the rate of heat loss from the marsh surface was used as one of the boundary conditions for the heat-flow model. The model was solved numerically by using the finite element technique. The model assumed that the flow of heat and water from the cooling lake occurred in planes normal to the plane of the dike. The flux of water and heat was modeled in seven of these planes (Figure 15), which represent two-dimensional vertical cross sections of the ground-water system. Results from each of the cross sections were combined to obtain the total flow of heat and water outward from the west dike of the cooling lake.

Simulated temperature patterns agreed well with field data, but were very sensitive to the distribution of subsurface lithologies. Results from a predictive simulation suggest that operation of the second 500-MW unit will increase ground-water temperatures less than 5°C at distances greater than 15 m from the cooling lake. The results of this study suggest that the potential for significant thermal alteration of surface water bodies located in ground-water discharge areas is slight.

MATHEMATICAL MODEL

Governing Equations

The equation describing the two-dimensional flow of water through a nonhomogeneous aquifer may be written

$$\frac{\partial}{\partial x_i} (K_{ij} \frac{\partial \phi}{\partial x_j}) = 0, \quad i, j = 1, 2, \quad (1)$$

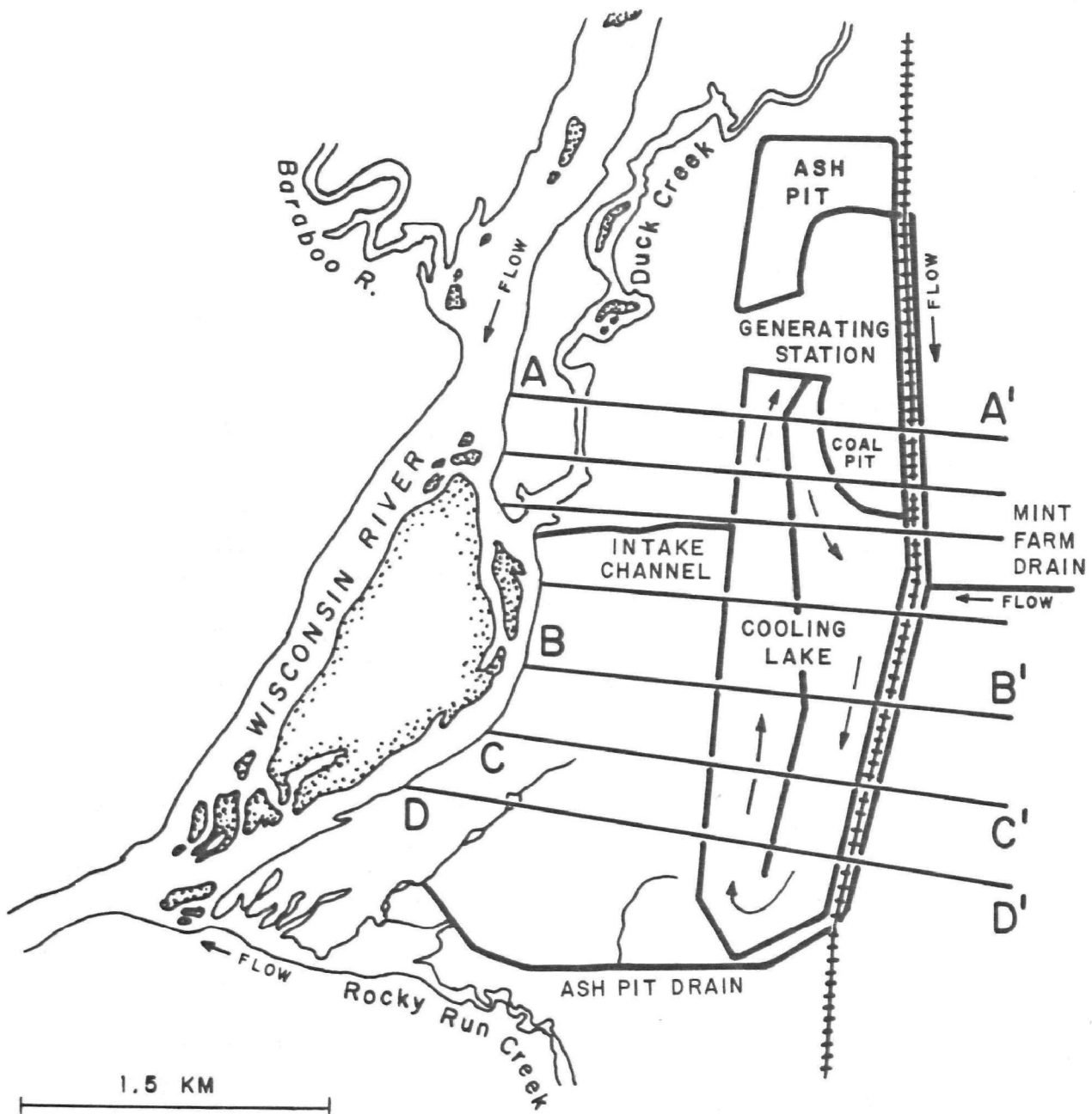


Figure 15. Location of seven cross sections of the Columbia site for which ground-water temperature distributions were simulated.

where K_{ij} = hydraulic conductivity, L/t; ϕ = head, L; and x_1, x_2 = cartesian coordinates, L. The ground-water velocity or specific discharge can then be determined from

$$q_i = -K_{ij} \frac{\partial \phi}{\partial x_j} \quad (2)$$

The movement of heat in a ground-water system can be described mathematically assuming that: (1) Thermal equilibrium between the liquid and the soil particles is achieved instantaneously, (2) the density of the soil particles is constant, (3) the heat capacity is constant, and (4) the chemical system is inert. Under these assumptions the heat transport equation is

$$\frac{\partial}{\partial x_i} \left(D_{ij} \frac{\partial T}{\partial x_j} \right) - \rho C_w \frac{\partial (q_i T)}{\partial x_i} - \rho C_s \frac{\partial T}{\partial t} = 0, \quad i, j = 1, 2 \quad (3)$$

where T = temperature, T; D_{ij} = coefficient of dispersion, H/TtL ; ρC_w = heat capacity of the saturated media, H/L^3T ; ρC_s = heat capacity of water, H/L^3T ; and q_i = specific discharge in direction x_i , L/t.

If the medium is isotropic, the coefficient of dispersion is a second-rank tensor (Scheidegger 1961) composed of two parts: (1) The thermal conductivity of the medium and (2) the coefficient of mechanical dispersion, which represents the mixing caused by the heterogeneity of the velocity field. In this analysis the coefficient of dispersion was assumed to have the following form (Reddel and Sunada 1970):

$$\begin{aligned} D_{22} &= K_{22}^t + \alpha_L \frac{q_2 q_2}{q} + \alpha_T \frac{q_1 q_1}{q} \\ D_{11} &= K_{11}^t + \alpha_L \frac{q_1 q_1}{q} + \alpha_T \frac{q_2 q_2}{q} \\ D_{21} &= D_{12} = K_{12}^t + (\alpha_L - \alpha_T) \frac{q_1 q_2}{q} \end{aligned} \quad (4)$$

where $q = (q_1^2 + q_2^2)^{1/2}$; $K_{11} = K_{22}$ = thermal conductivity, H/TtL (thermal conductivity is assumed to be independent of direction); α_L = longitudinal (horizontal) dispersivity, L; and α_T = transverse (vertical) dispersivity, L.

Boundary Conditions

For the ground-water flow model, heads were specified at the water table and along the vertical boundary east of the cooling lake. The model can be modified to consider the time-dependent case of a moving water table, but for the problem considered here fluctuations of the water table were negligible. No-flow boundaries were specified along the lower boundary and at the Wisconsin River.

For the heat-flow model, a heat flux was specified along the upper boundary and along the vertical boundary east of the cooling lake. The fluxes of heat across these boundaries were specified to be proportional to the water

flow across the boundaries. Along that part of the upper boundary representing the marsh, a heat flux resulting from atmospheric exchanges was specified. The other two boundaries were specified as no-flow boundaries.

The process of heat exchange between the marsh surface and the atmosphere is complex, and mathematical representations are necessarily rough approximations. For this study the boundary between the marsh and the atmosphere was assumed to occur in the vegetation at the height where transfer of heat and water vapor by turbulent exchange becomes effective. This level, known as the zero-displacement plane, was assumed equal to 0.63 of the vegetation height. Heat flow from the ground surface to the zero-displacement plane was assumed to occur by conduction and free convection. The heat flow at this boundary can be expressed as

$$q_s = h_\gamma (T_m - T_a) + h_m (e_m - e_a)/\gamma + (1-a)\epsilon\sigma(T_m^4 - T_{sky}^4) - (1-a)\alpha_s q_{sun}, \quad (5)$$

where T_{sky} = effective sky temperature, T ; T_m = temperature at the marsh surface, T ; T_a = air temperature above the plane of zero displacement, T ; q_s = heat flux from the marsh boundary, H/tL^2 ; h_m = mass transfer coefficient, H/L^2Tt ; h_γ = heat transfer coefficient, H/L^2Tt ; γ = psychrometer constant, assumed equal to $0.66 \text{ mbar}/T$, M/t^2L ; e_m = saturation vapor pressure at the marsh boundary temperature, M/t^2L ; e_a = partial vapor pressure of water in air, M/t^2L ; ϵ = marsh boundary long-wave emissivity, dimensionless; σ = Stefan-Blotzmann constant, H/T^4tL^2 ; α_s = marsh boundary solar absorptivity dimensionless; q_{sun} = solar flux incident on the marsh boundary, H/tL^2 ; and a = percentage of open water in the marsh, dimensionless.

In addition to areas of dense vegetation, the marsh also contains some areas of open water. For the latter it was assumed that radiative exchange and solar absorption occur at the surface.

The heat and mass transfer coefficients (h_v and h_m) are equal if the roughness height is the same for both. According to Mitchell et al. (1975) these coefficients are given by an equation of the form

$$h_m = h_v = k^2 \rho C_p u / \ln(Z_a - d/Z_o + 1), \quad (6)$$

where k = Karman coefficient, dimensionless; ρC_p = heat capacity of air, H/L^3T ; u = air velocity, L/t ; Z_a = reference height, L ; Z_o = surface roughness height, L ; and d = height of the zero-displacement plane, L . The surface roughness height can be estimated from vegetation height by using the relationship given by Tanner and Pelton (1960), $\log Z_o = 0.997 - \log 0.833$, where \bar{z} is the average height of the vegetation.

Following the method of Jobson (1972), we used daily average values for air temperature (T_a) and vapor pressure (e_a) in Eq. (6). Moreover, Eq. (6) can be simplified when temperature data at the marsh surface are available, and the terms involving higher order dependence on T_m are approximated by linear relations. Then, the heat transfer from the marsh surface is proportional to the temperature difference between the marsh surface and the

air temperature at 2 m above the surface. The constants of proportionality were determined for a cross section for which data had been collected, and these values were used when simulating heat flow in the other cross sections. The heat-flow rates calculated by this method agreed well with values calculated by using Eq. (6).

Solution Procedure

The finite element method (Zienkiewicz 1977, Pinder and Gray 1977) was used to solve Eq. (1) and Eq. (3) subject to the boundary conditions described in the previous section. Each cross section modeled was divided into 100-150 quadrilateral elements. The procedure used to link the equations was: (a) Eq. (1) was solved for head at each node and Eq. (2) was solved for velocity; (b) Eq. (3) was solved for temperature at each node; (c) the solution to Eq. (3) was stepped forward in time by the Crank-Nicolson approximation for the time derivative for a specified number of time steps; (d) the hydraulic conductivity distribution, which is a function of temperature, was adjusted for the new temperature distribution; and (e) steps (a)-(d) were repeated.

Required Parameters

The physical properties required as input parameters are thermal conductivity, specific heat capacity, hydraulic conductivity, and porosity for each material type in the subsurface and dispersivity.

The values of the parameters for each of the subsurface materials used in the simulations are listed in Table 3. Thermal conductivities were determined by the needle probe technique (Von Herzen and Maxwell 1959). Heat capacities were determined by standard additive techniques (Van Wijk and deVries 1963). Horizontal hydraulic conductivities were estimated from aquifer test data, slug tests, and grain-size analyses. Vertical hydraulic conductivity in each element was assumed to be one-tenth of the horizontal hydraulic conductivity. Porosities, which were needed to estimate pC_s , were approximated from grain-size analyses.

Longitudinal dispersivity was assumed constant for all elements and was estimated by a trial-and-error adjustment procedure. Lateral dispersivity is usually assumed to be one-quarter to one-tenth of longitudinal dispersivity (Cherry et al. 1975). For the simulations reported here, the ratio of longitudinal to transverse dispersivity was assumed to be 4. The field data were best simulated by using a longitudinal dispersivity of 10 cm. When higher values were used the amplitude of the annual temperature wave observed in the field could not be reproduced. In Figure 16 the observed temperatures 2 m west of the dike at a depth of 3 m are plotted along with the simulated temperatures obtained by using various values for longitudinal dispersivity.

Values for longitudinal dispersivity reported in the literature range from 0.1 cm for laboratory studies with homogeneous sands (Hoopes and Harleman 1967) to over 100 m for field studies (Bredehoeft et al. 1976). The value of dispersivity is known to be related to media inhomogeneities and the scale of the problem, but the exact relationship is unknown. For the problem described

TABLE 3. PARAMETERS USED IN THE SIMULATIONS FOR THE MODEL
DESCRIBING THERMAL ALTERATION OF GROUND-WATER

Lithology	Horizontal hydraulic conductivity (m/day)	Thermal conductivity (10^{-1} cal/m sec $^{\circ}$ C)	Heat capacity (cal/cm 3 $^{\circ}$ C)	Porosity
Medium coarse sand with gravel	30	0.45	0.64	0.33
Fine to very fine sand	10	0.51	0.67	0.39
Weathered sandstone	8	0.51	0.67	0.39
Sandstone	3.5	0.64	0.60	0.26
Peat	3.0	0.12	0.91	0.75
Sandy silt to sandy clayey silt	0.4	0.42	0.72	0.48
Gray sandy silt with organic matter	0.04	0.42	0.72	0.48
Varbed clay with sand seams	0.03	0.40	0.74	0.52

RESULTS

Field Data

Temperatures were monitored twice a week at 48 points in cross-section A-A' in Figure 15 for 13 months and at 18 points in cross-section B-B' in Figure 15 for 6 months. Temperatures were recorded at the surface and at depths to 10 m below the surface. In situ thermistors, hardwired to a central control box, were used to obtain ground-water temperatures in cross-section A-A'. Temperatures in cross-section B-B' were measured by lowering a thermistor probe into three 3.175-cm wells. The thermistors were calibrated to $\pm 0.1^{\circ}$ C. A high-resolution digital ohmmeter was used to measure the resistance of the thermistors. Surface-water temperatures at two sites along cross-section A-A' were monitored continuously with liquid expansion thermographs.

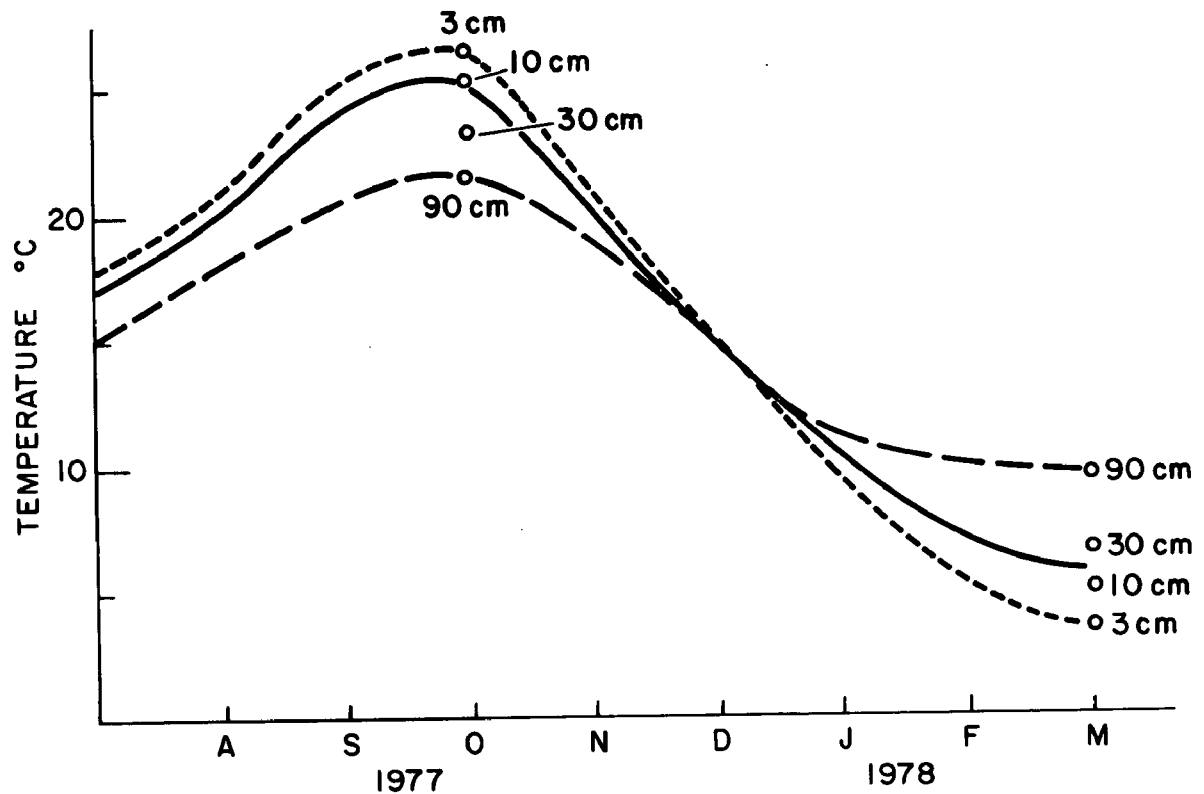


Figure 16. Observed temperatures in the subsurface west of the Columbia cooling lake and temperatures simulated by the mathematical model. The ratio of longitudinal dispersivity (α_L) to transverse dispersivity (α_T) is set at 4. (—) is observed temperatures with $\alpha_L = 3$ cm. (---) is simulated temperatures with $\alpha_L = 90$ cm. (o) indicate maximum and minimum simulated temperatures for $\alpha_L/\alpha_T = 4$ with L equal to 3, 10, 30, and 90 cm.

The temperature distributions recorded in cross-sections A-A' and B-B' at 3-month intervals are shown in Figure 17 and Figure 18. Dissimilarities in the temperature distributions recorded in the two cross sections are attributed to differences in the subsurface materials, which result in different distributions of ground-water velocity. Average ground-water velocity is slower in cross-section B-B' by a factor of 2. The fluctuations in average lake temperature and the seasonal fluctuations of ground-water temperature at several distances from the dike along cross-section A-A' at a depth of 4.5 m are illustrated in Figure 19. The lag time between the occurrence of the maximum temperature in the ground water and the maximum cooling-lake temperature gradually increases, and the amplitude of the fluctuation decreases with distance from the dike.

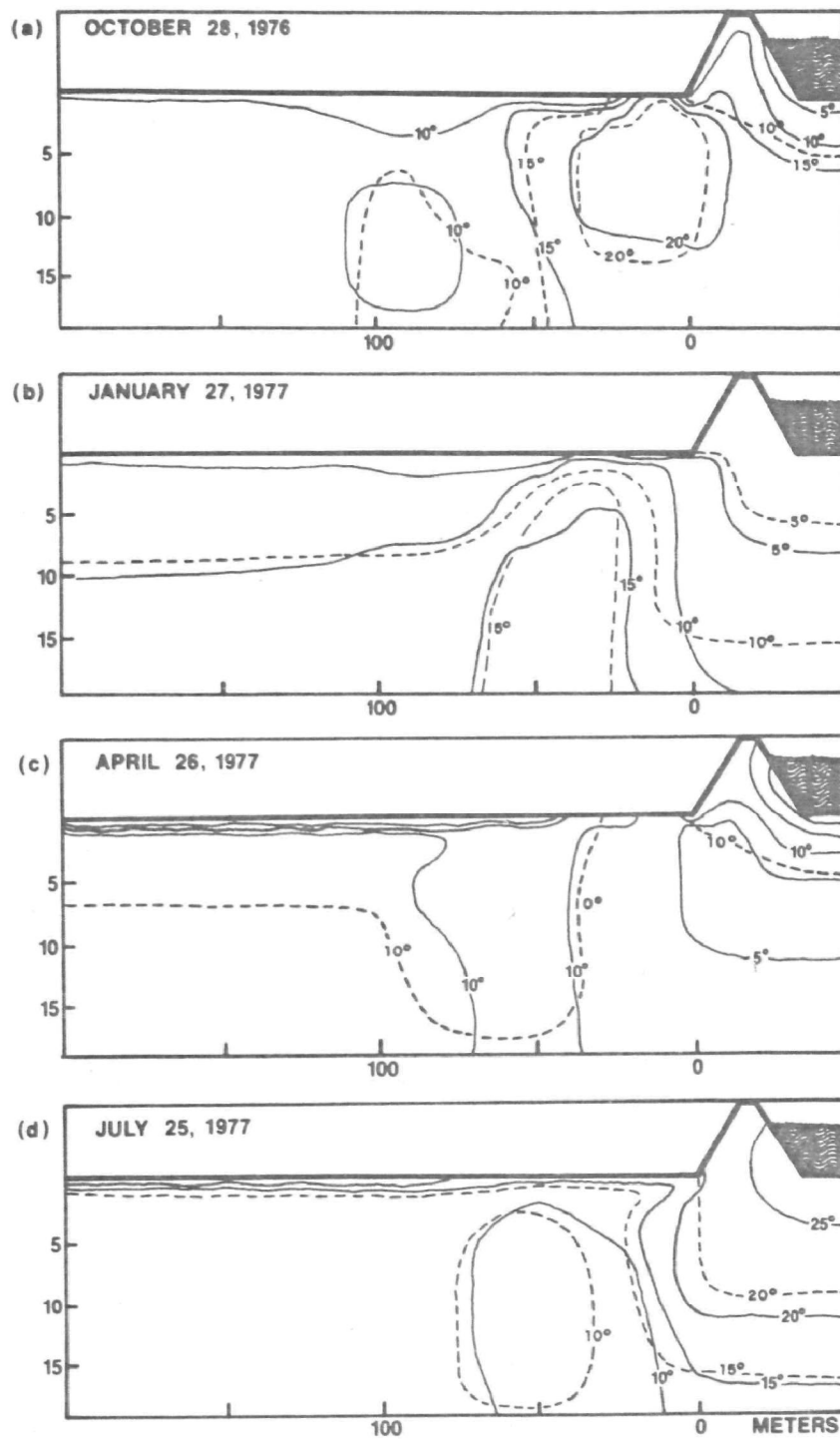


Figure 17. Observed (—) and simulated (----) ground-water temperature distributions in cross-section A-A' of Figure 15.

Simulations

Good agreement between simulated and actual temperatures was obtained when the model was used to simulate temperatures in cross-sections A-A' and B-B' (Figure 17, Figure 18, Figure 20), but only because detailed data on the subsurface distribution of materials had been obtained. The temperature patterns observed in the subsurface were very sensitive to the distribution of layers with low hydraulic conductivity. The model was most sensitive to the extent and depth of the clay layer under the peat (Figure 8) and to a clay layer that is present in some areas at a depth of 6-8 m. Over 70 borings were made in the marsh to determine the subsurface lithology.

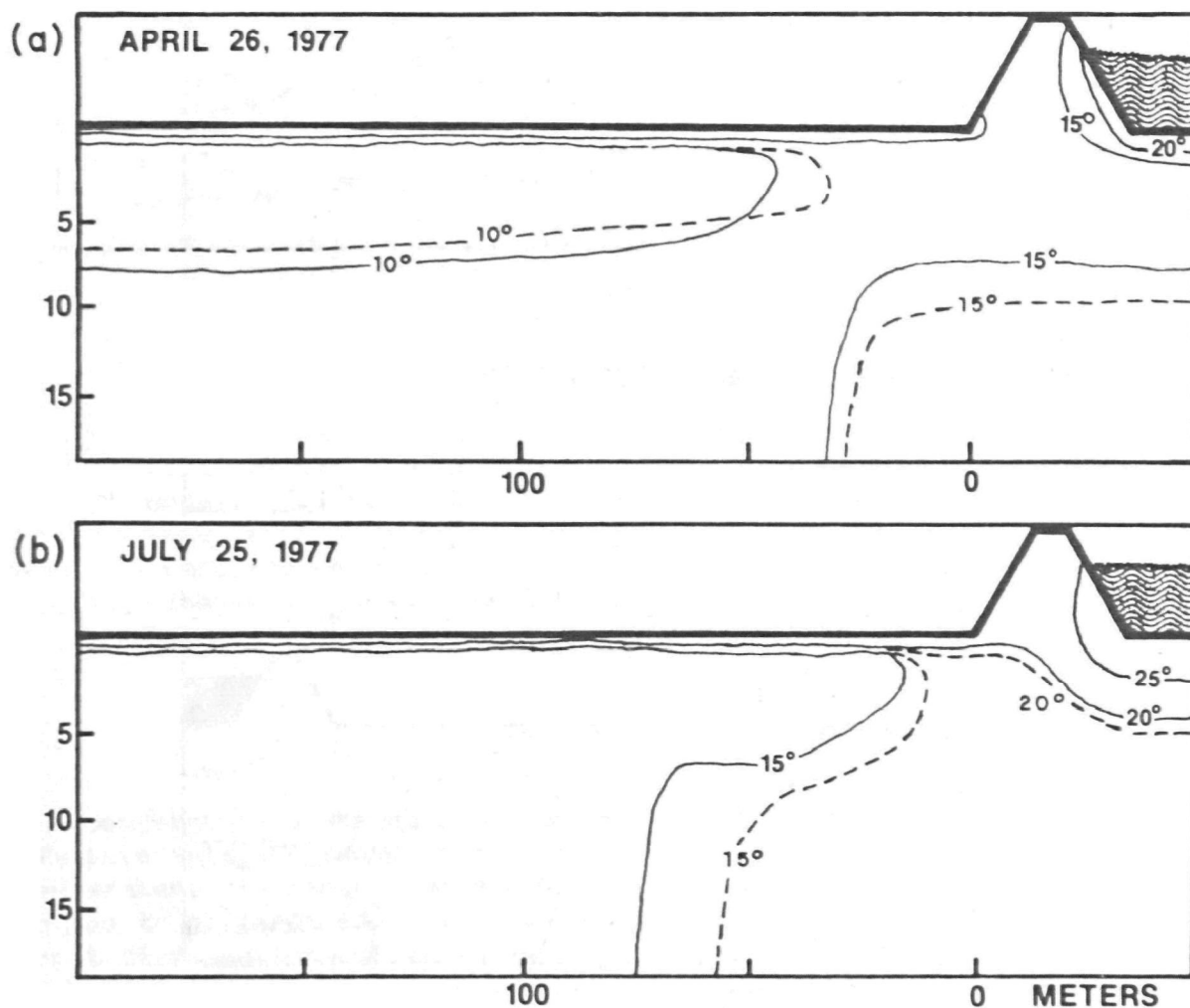


Figure 18. Observed (—) and simulated (---) ground-water temperature distributions in cross-section B-B' of Figure 15.

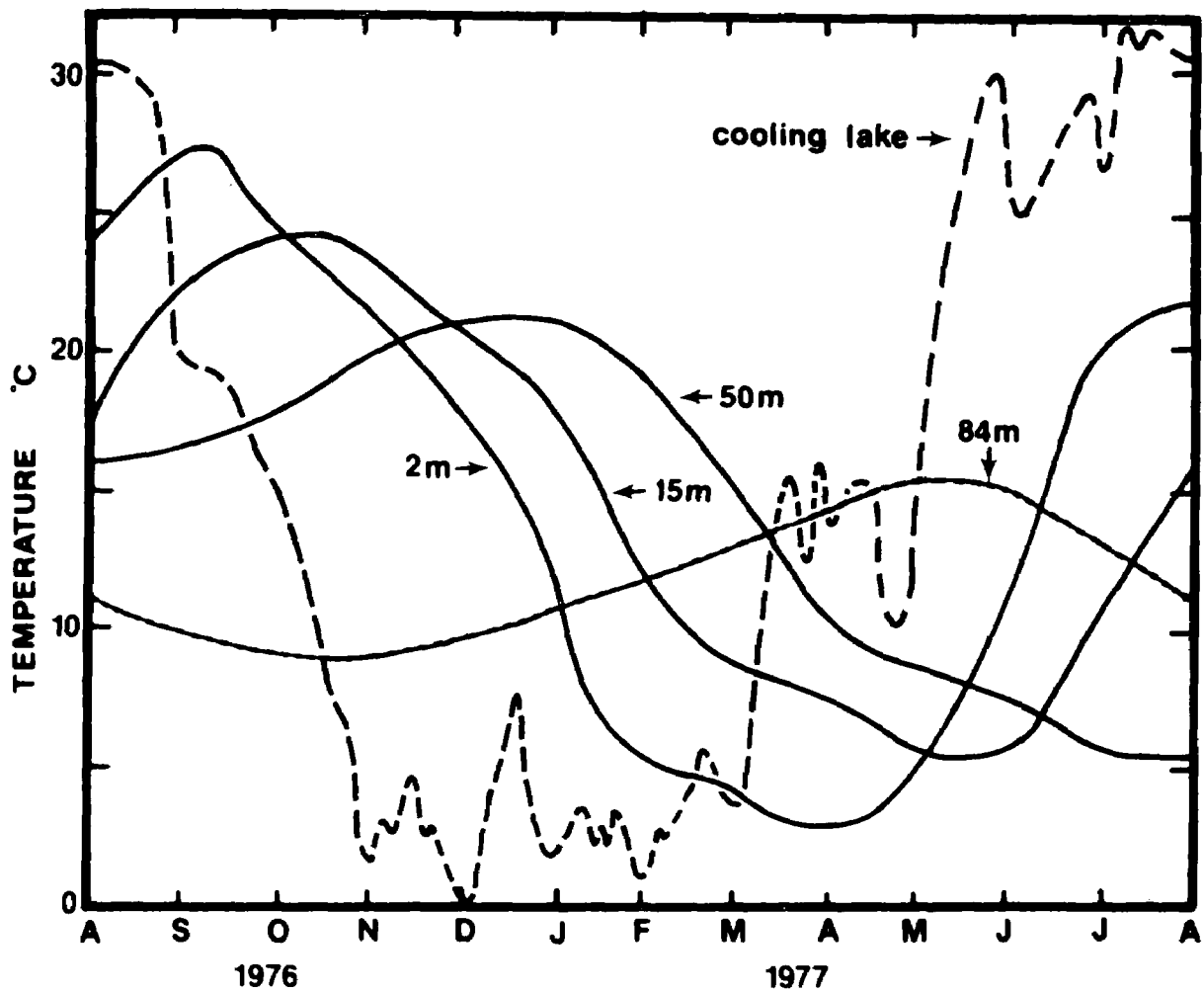


Figure 19. Seasonal fluctuations of ground-water temperature in cross-section A-A' of Figure 15 at a depth of 4.5 m at distances of 2, 15, 50, and 84 m west of the cooling lake dike. The fluctuations of average lake temperature are also shown (----).

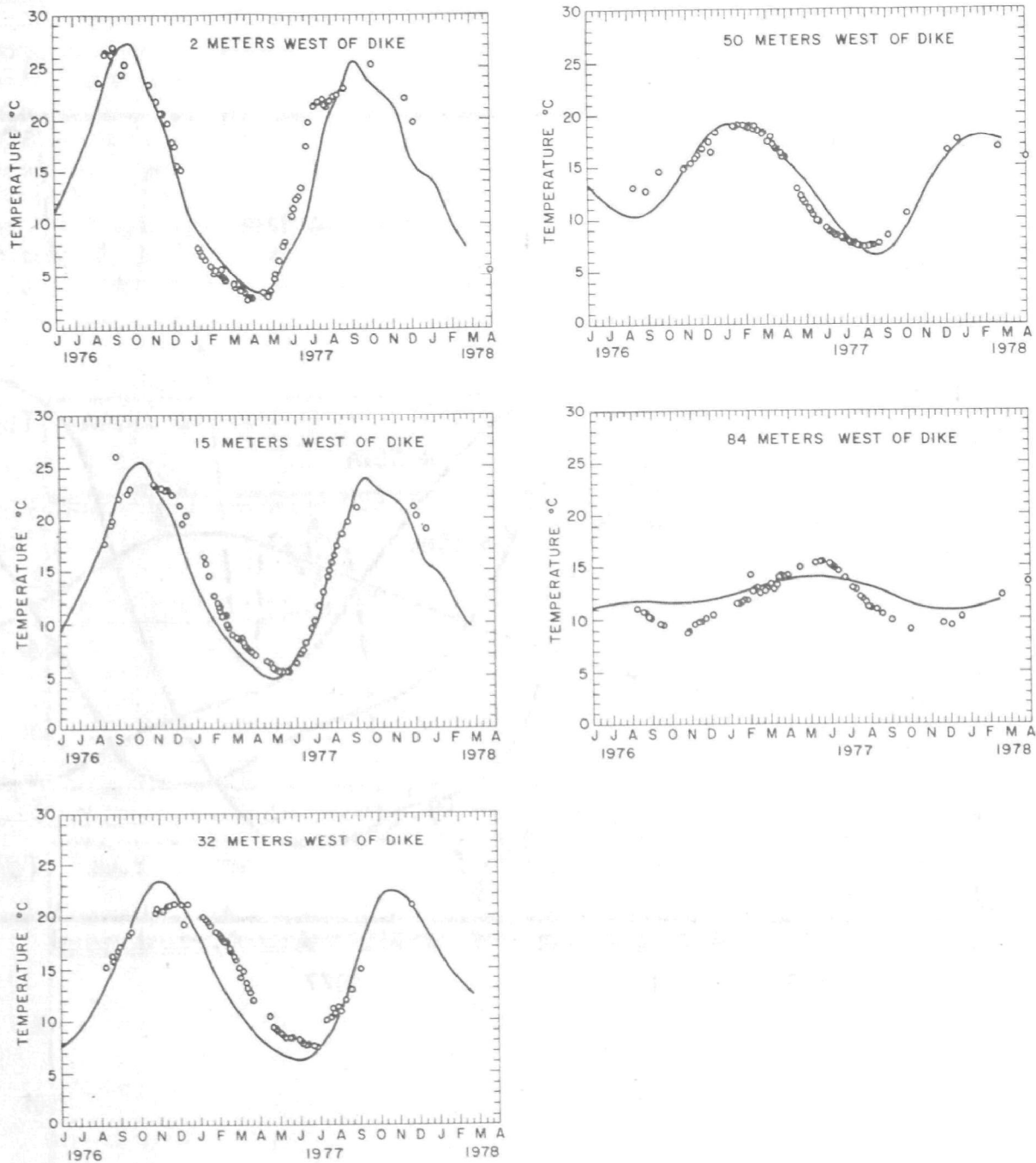


Figure 20. Simulated temperatures (—) and observed temperatures (o) in cross-section A-A' of Figure 15 at a depth of 3.28 m at 2, 15, 32, 50, and 84 m west of the cooling lake dike.

SECTION 6

LONG-TERM TEMPERATURE CHANGES IN THE GROUND WATER OF THE WETLAND

SIMULATION STUDIES

Simulations were used to predict the long-term changes in substrate temperature that may occur in the wetland adjacent to the Columbia Generating Station. Wetland water levels and ground-water flow rates into the wetland had stabilized during the first 2 yr of operation of the generating station, but neither ground-water temperatures nor wetland vegetation (Bedford 1977) had yet reached equilibrium. Prediction of the nature and magnitude of change in vegetation was not possible without an understanding of the probable changes in substrate temperatures.

The model that was described in section 5 to simulate the response of subsurface temperatures to changes in the temperatures of the cooling lake and the air was used to simulate seasonal temperature patterns for the 12-yr period from November 1974 to January 1987. The governing equations, boundary conditions, microclimatic model, and parameters remained the same in the long-term simulation. Changes in temperature for the 12 yr were modeled in the same two planes, which represent two-dimensional vertical cross sections of the ground-water system (A-A' and B-B' in Figure 15).

Cooling-lake temperatures and air temperatures for the 10-yr period 1978-87 were synthesized by repeating five times the actual temperatures recorded from January 1976 to January 1978. For the period after April 1978 when two generating units were assumed to be operating, the temperatures were adjusted to account for the added heat load. When the temperature at the generating station outlet rose above 40° C, it was assumed that the entire heat load from the second generating unit was dissipated in the cooling towers. The cooling-lake temperatures at the generating station inlet for the period 1975-87 are shown in Figure 21.

The simulations predict that temperatures at a depth of 0.6 m will not fall below 8° C within 200 m of the dike by 1987 and that peak temperatures near the dike will be 10-15° C above normal and will occur in October and November rather than in August. The subsurface stratigraphy of the site is such that major changes in near-surface temperatures will only occur within 350 m of the dikes, but if the stratigraphy were different the effects could extend to much greater distances from the cooling-lake dikes.

The temperature changes simulated in the ground-water system for the period 1975-87 are only an approximation of the actual temperatures that may exist in the ground-water system during this period. Lake and air

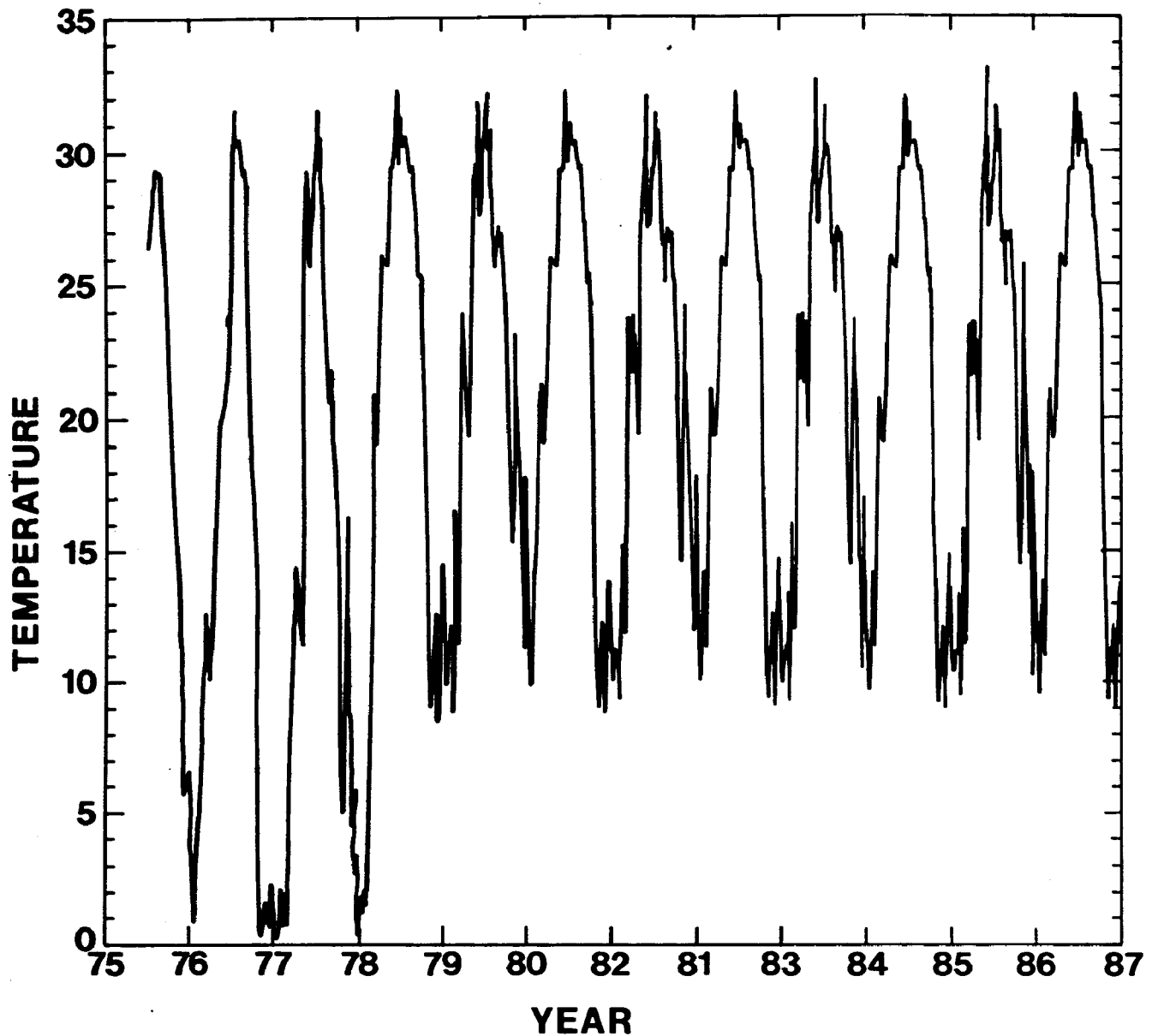


Figure 21. Cooling-lake inlet temperatures for 1975-87 used in the simulations of long-term temperature change in the ground-water system. Actual temperatures are shown from May 1975 to March 1978. Temperatures from March 1978 to January 1987 were synthesized from the 1976-78 temperature record.

temperatures may deviate widely from those assumed in this report, and processes not accounted for in the model, such as substrate decomposition and flood-induced erosion, may alter ground-water flow rates. These simulations are, however, a reasonable approximation of the changes to be expected in ground-water and substrate temperatures in the vicinity of the cooling-lake.

RESULTS AND DISCUSSION

The simulation of temperatures in the ground-water system near the cooling-lake shows that temperatures in the vegetation rooting zone in the wetland will reach a new steady-state condition that is much different from the prevailing condition before the filling of the cooling-lake. The annual temperature patterns near the dike will stabilize by 1980, but at 150 m from the dike temperatures will not reach equilibrium by 1987.

Simulated temperatures in cross-section A-A' (Figure 15) 2 m from the dike from 1975 to 1987 at a depth of 3 m deviated from those at 0.6 m by less than 1.0° C (Figure 22). When pre-lake temperatures are compared with simulated temperatures at 0.6 m depth and 2 m west of the dike in cross-section A-A' for the periods 1978-86 and 1984-86, the change in annual temperature patterns is pronounced. In the period 1984-86 the temperature does not fall below 14° C, whereas before the cooling lake was filled, substrate temperatures at this depth approached freezing and in the 1976-78 period the temperature fell below 5° C (Figure 23). The peak temperatures occur approximately 45 days later in the period 1976-78 than in the pre-lake period and approximately 30 days later in the 1984-86 period than in the pre-lake period. The lag decreases as the ground-water temperature rises because the hydraulic conductivity of the subsurface material increases with temperature, which increases the ground-water flow velocity.

The simulated temperatures in cross section A-A' 150 m from the dike for the period 1975-87 are shown in Figure 24. Pre-lake temperatures at a depth of 0.6 m and temperatures simulated for the periods 1976-78 and 1985-87 are shown in Figure 25. The attenuation in the annual temperature patterns between the pre-lake period and the 1976-78 period is a result of the increased ground-water flow rate in the latter period. At a distance of 150 m from the dikes, several years are required before the impact of the temperature variations in the lake become pronounced at a depth of 0.6 m. By 1986 the change in temperatures is pronounced with maximum and minimum annual temperatures elevated several degrees centigrade above pre-lake temperatures.

In cross-section A-A' (Figure 15) most of the ground-water discharge occurs within 200 m of the dike. Consequently, the atmospheric heat flux beyond this distance is much larger than the ground-water heat flux, and thus substrate temperatures in 1987 at a depth of 0.6 m are only slightly altered from pre-lake conditions. Ground-water temperatures at greater depths do show increases, but the rate of increase at a depth of several meters is much slower than shown in Figure 24 for a point at a depth of 0.6 m and a distance of 150 m from the dike. (Text continues on p. 48.)

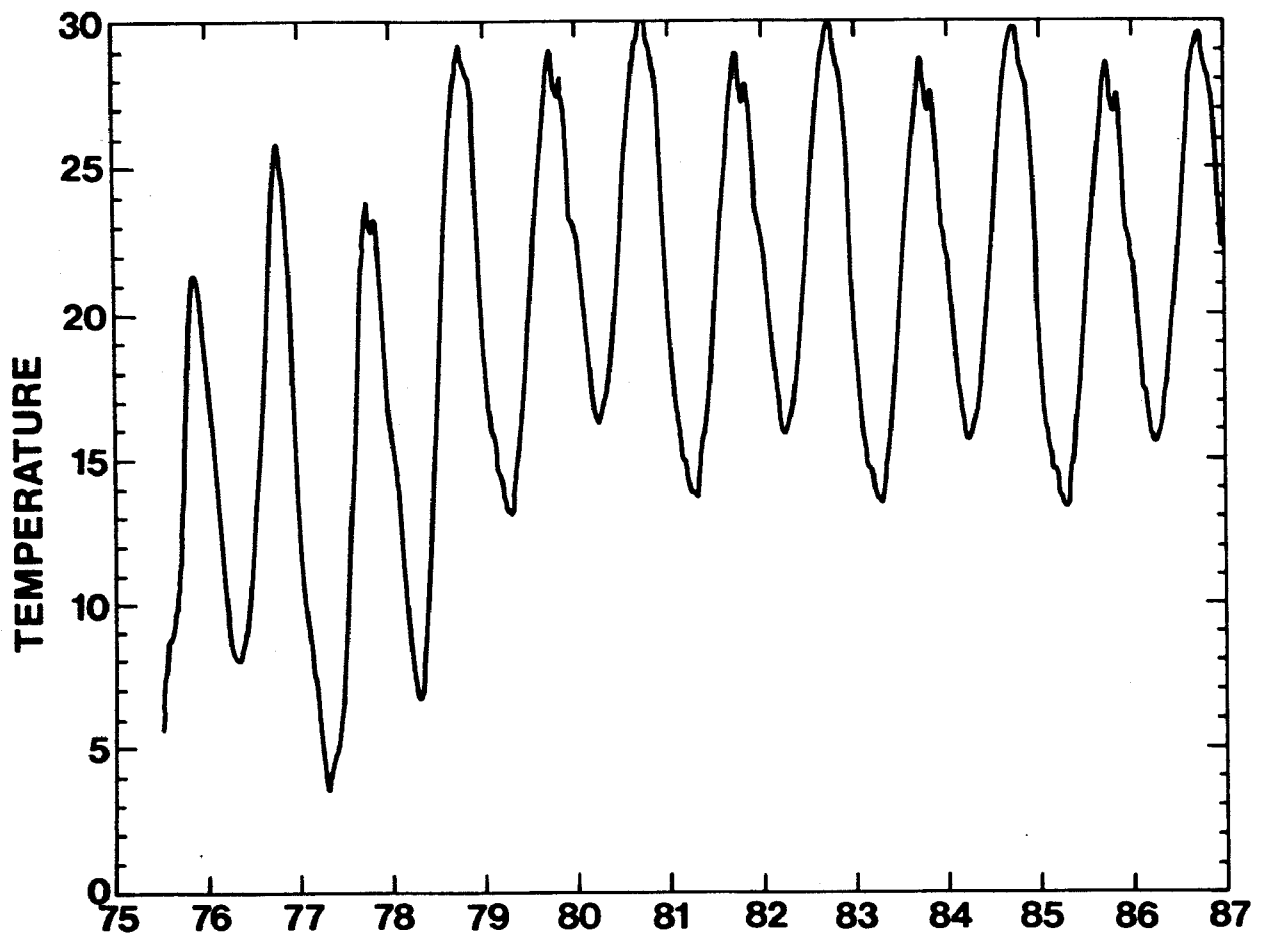


Figure 22. Predicted ground-water temperatures from 1975-87 at a distance of 2 m west of the cooling-lake dike in cross-section A-A' of Figure 15 at a depth of 0.6 m.

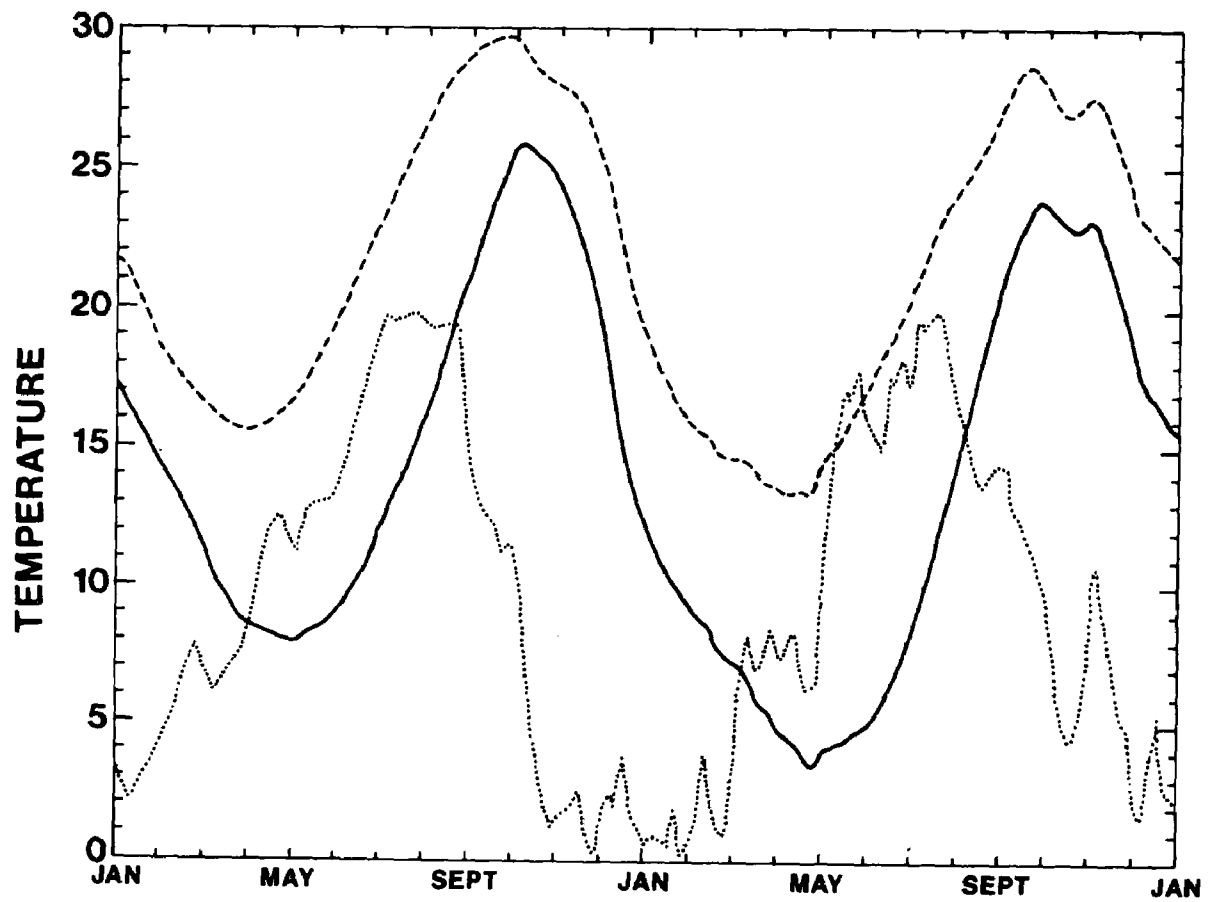


Figure 23. Pre-lake temperatures and simulated temperatures 2 m west of the cooling-lake dike in cross-section A-A' of Figure 15 at a depth of 0.6 m. (---) = simulated temperatures from 1984 to 1986; (—) = actual temperatures from 1976 to 1978; (···) = simulated temperatures from 1976 to 1978 assuming that the cooling lake had not been present.

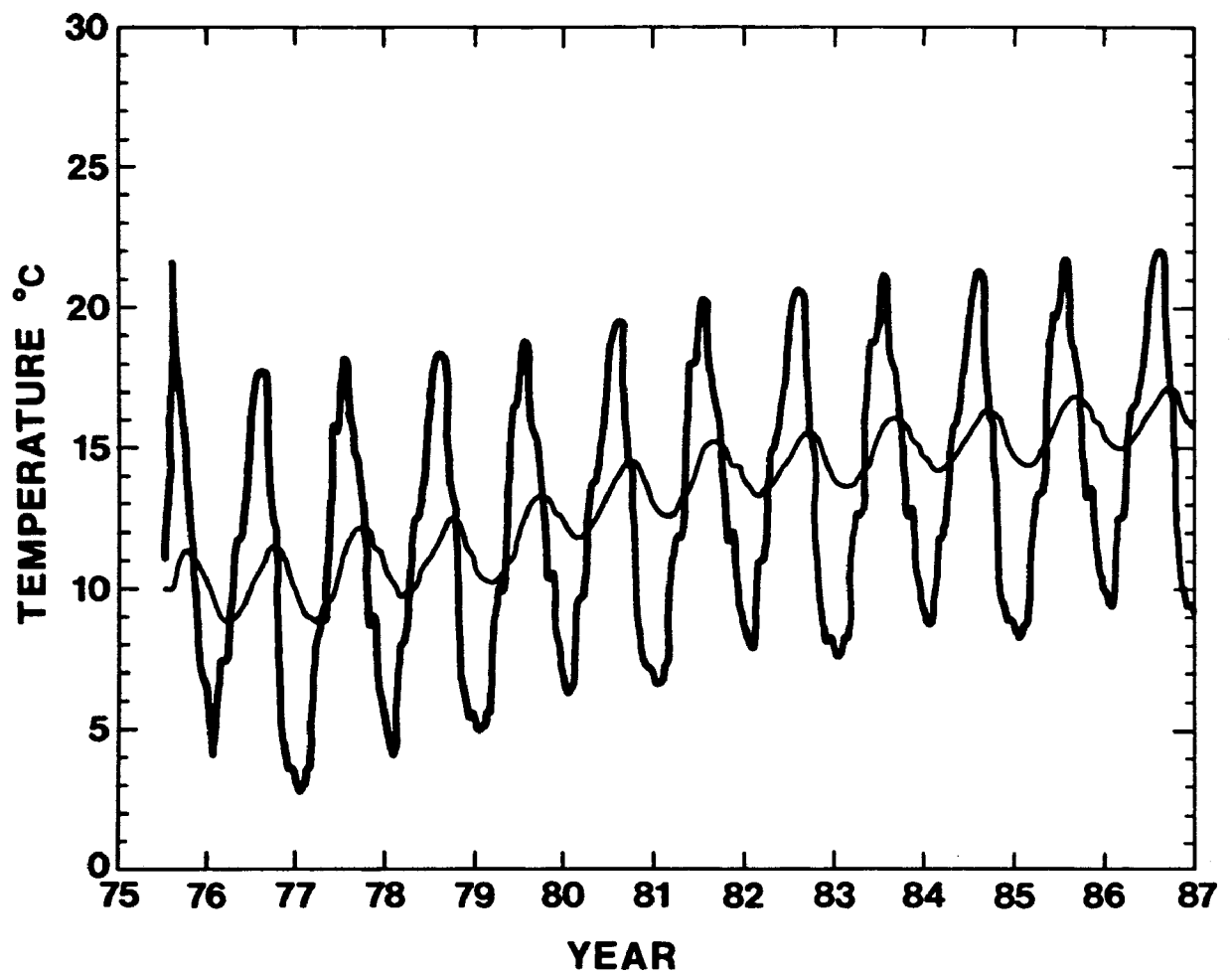


Figure 24. Temperatures 150 m west of the cooling-lake dike in cross-section A-A' of Figure 15 at depths of 0.6 m and 3 m for the simulated period 1975-87. (—), 0.6 m level; (—), 3 m level.

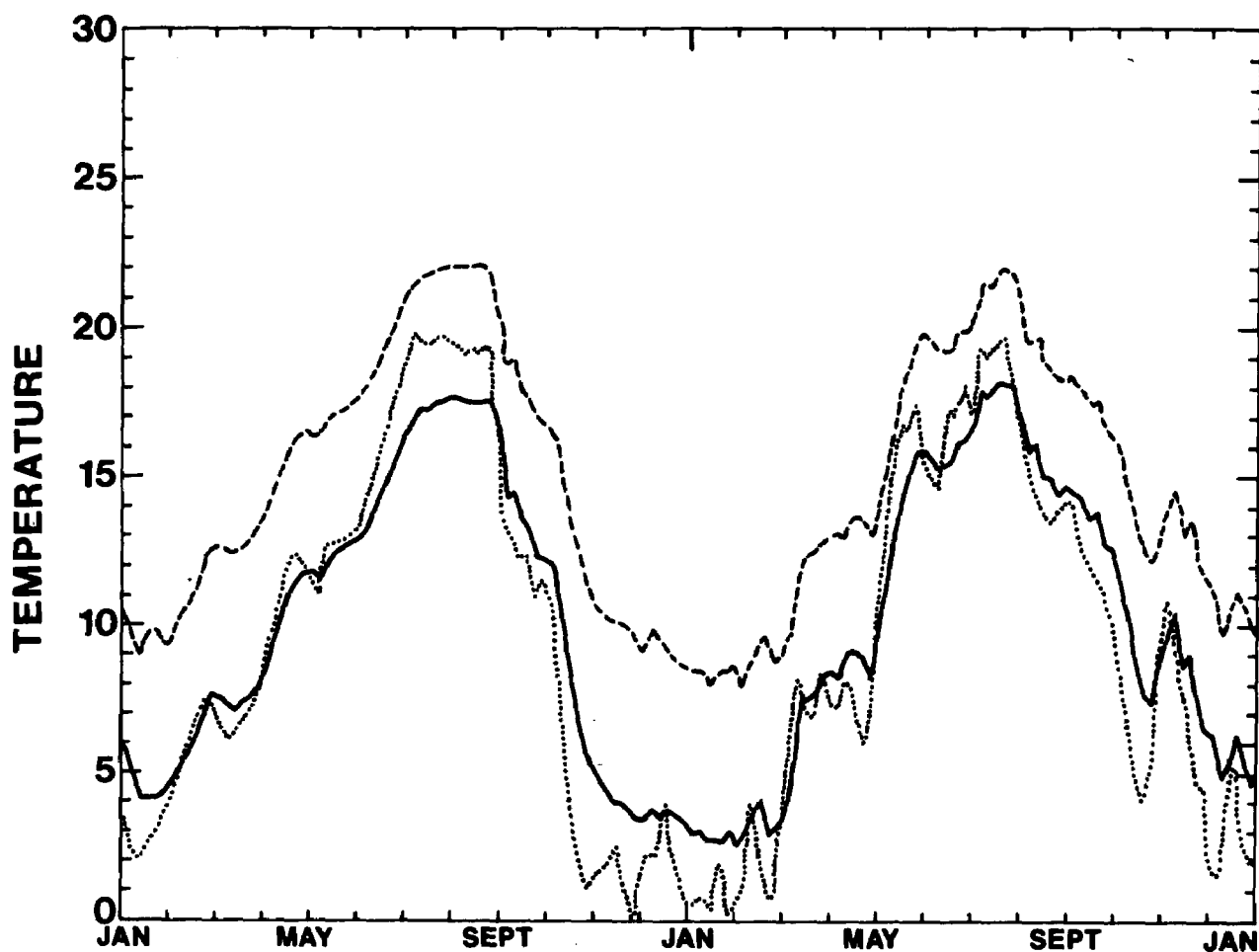


Figure 25. Temperatures 150 m west of the cooling-lake dike in cross-section A-A' of Figure 15 at a depth of 0.6 m. (---) = simulated temperatures for 1984-86; (—) = actual temperatures for 1976-78; (···) = simulated temperatures for 1976-78.

The temperature changes simulated for cross-section A-A' are believed to be representative of the changes in temperature that will occur in the vegetation rooting zone in the wetland along the dike. The ground-water flow patterns, which are determined by the subsurface stratigraphy, determine that the obvious temperature changes will occur within 350 m of the dike. The increase in temperatures will be somewhat greater in the southern part of the wetland since the average annual lake temperature increases from approximately 21° C at the intake to 24° C at the south end of the lake. This difference is shown in Figure 26 (a-c), which presents simulated temperatures in cross-section B-B' of Figure 15. This cross section is 200 m south of the cooling lake intake and 1,500 m south of cross-section A-A'. Temperatures were simulated for 1985-87 at a depth of 0.6 m and at 2, 50, and 200 m west of the dike. Temperatures 2 m west of the dike (Figure 26a) averaged about 3° C higher than temperatures at a similar point on cross-section A-A'.

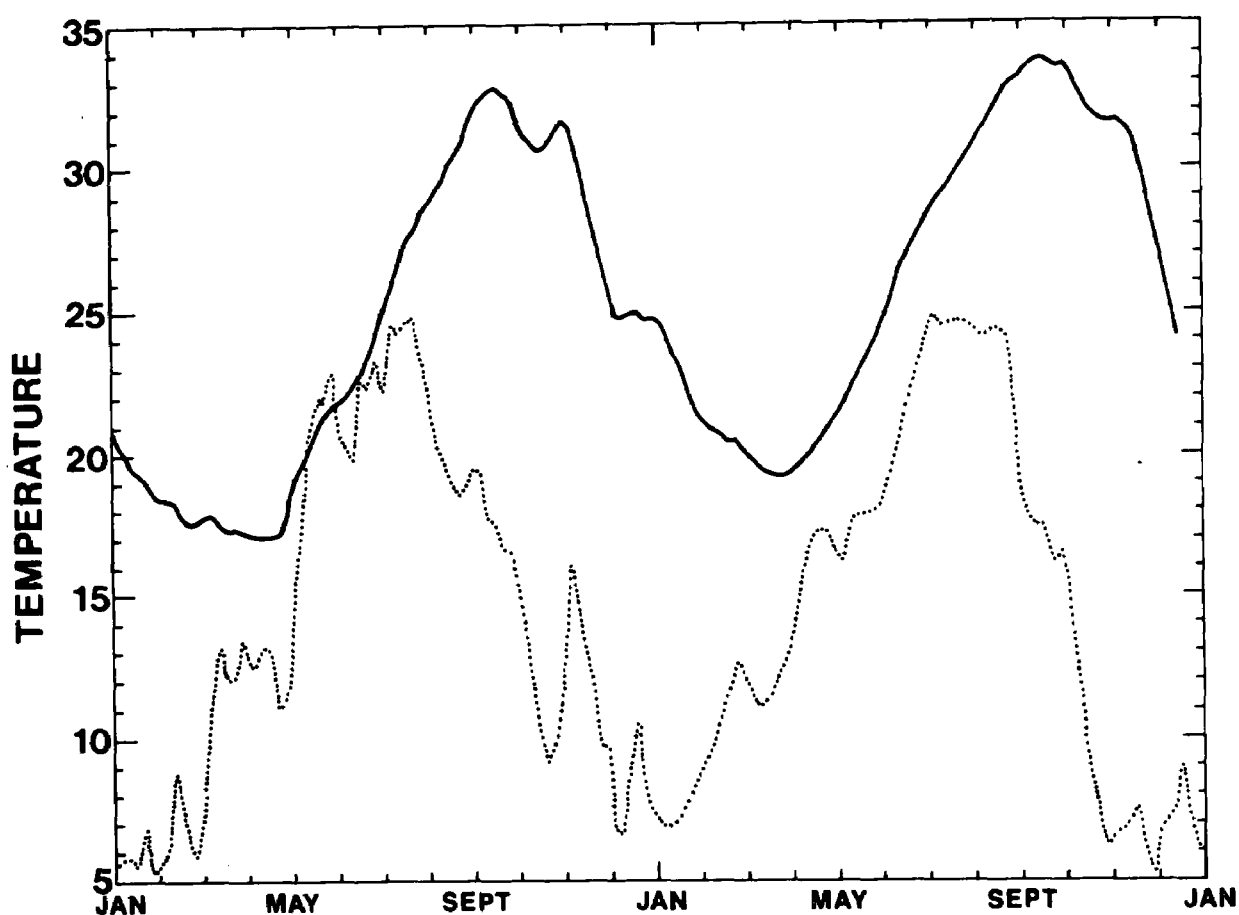


Figure 26a. Temperatures in cross-section B-B' of Figure 15 at a depth of 0.6 m and at 2 m west of the cooling-lake dike. (—) = simulated temperatures for 1985-87; (···) = simulated temperatures for 1976-78 assuming no cooling lake was present.

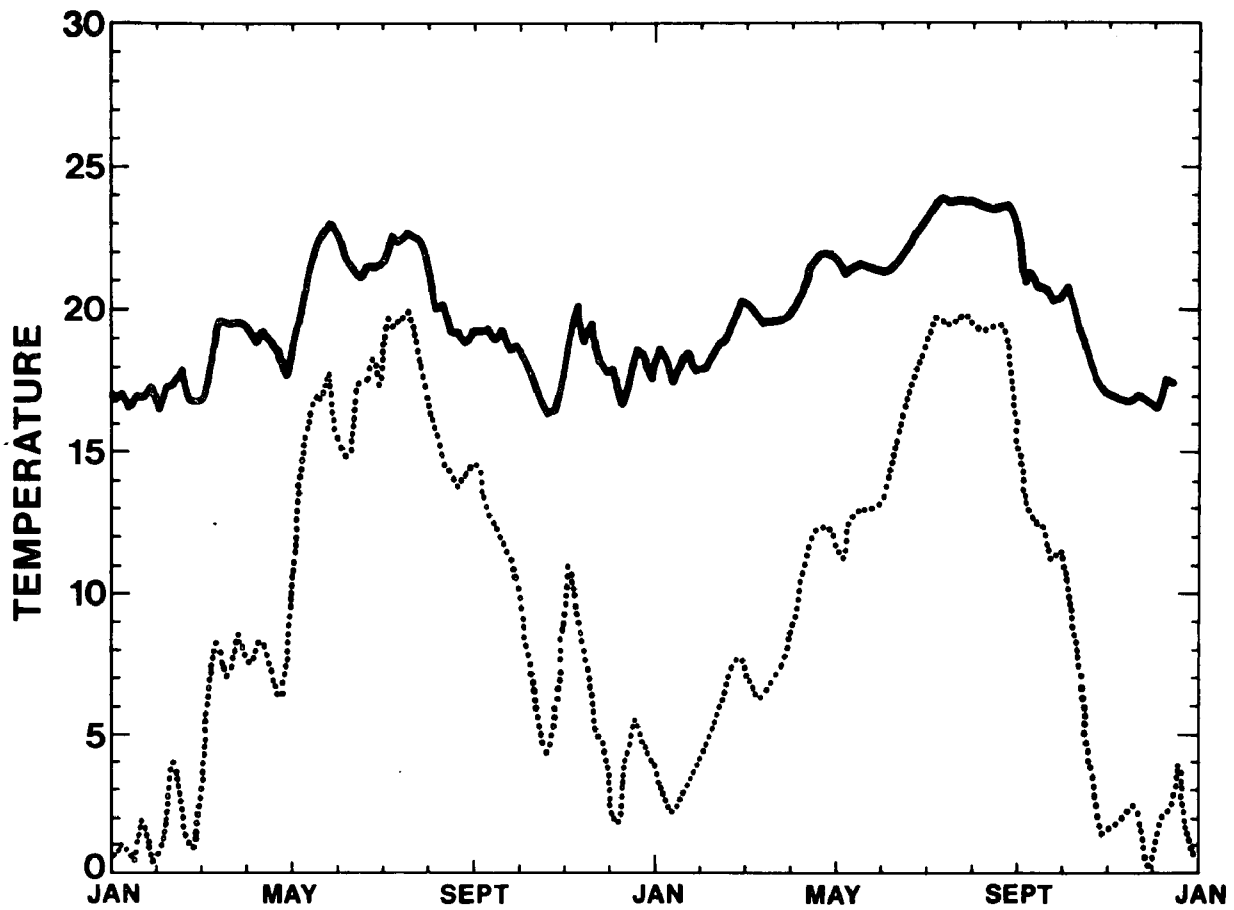


Figure 26b. Temperatures in cross-section B-B' of Figure 15 at a depth of 0.6 m and at 50 m west of the cooling-lake dike. (—) = simulated temperatures for 1985-87; (...) = simulated temperatures for 1976-78 assuming no cooling lake was present.

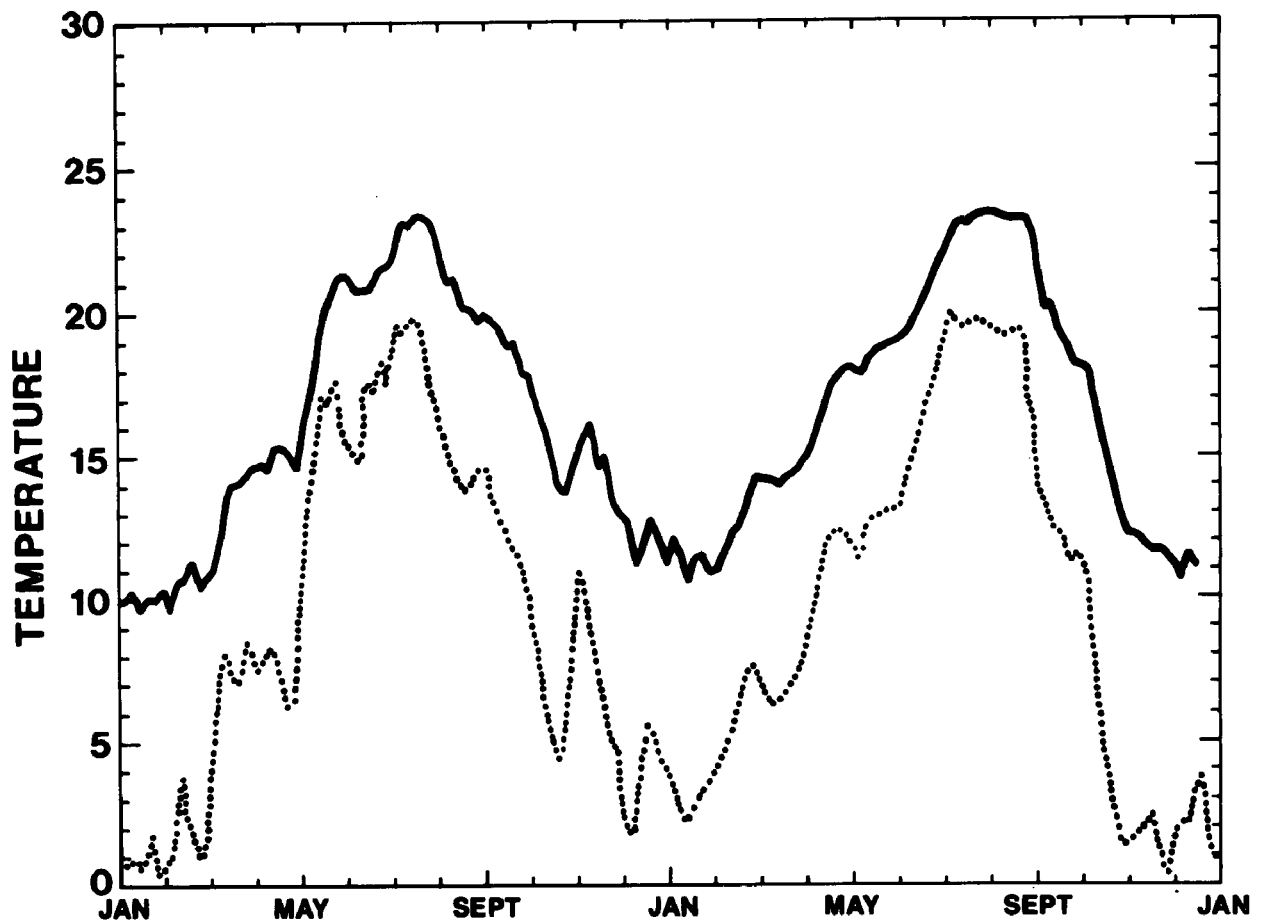


Figure 26c. Temperatures in cross-section B-B' of Figure 15 at a depth of 0.6 m and at 200 m west of the cooling-lake dike. (—) = simulated temperatures for 1985-87; (···) = simulated temperatures for 1976-78 assuming no cooling lake was present.

REFERENCES

- Anderson, M.P. 1979. Using models to simulate the movement of contaminants through groundwater systems. J. Environ. Control, CRC Reviews, in press.
- Anderson, M.P., and C.B. Andrews. 1977. Hydrogeology, p. 83-109. In Documentation of environmental change related to the Columbia Electric Generating Station. Institute of Environmental Studies, Rep. 82, Univ. Wisconsin-Madison, Madison, Wis.
- Andrews, C.B. 1976. An analysis of the impact of a coal-fired power plant on the groundwater supply of a wetland in central Wisconsin. M.S. Thesis. Univ. Wisconsin-Madison, Madison, Wis. 83 p.
- Andrews, C. 1978. The impact of the use of heat pumps on ground-water temperatures. Ground Water 16:437-443.
- Andrews, C.B., and M.P. Anderson. 1978. Impact of a power plant on the groundwater system of a wetland. Ground Water 16:105-111.
- Andrews, C.B., and M.P. Anderson. 1979. Thermal alteration of groundwater caused by seepage from a cooling lake. Water Resour. Res., in press.
- Bay, R. 1967. Groundwater and vegetation in two peat bogs in northern Minnesota. Ecology 48:308-310.
- Bear, J. 1972. Dynamics of fluids in porous media. American Elsevier, New York. 764 p.
- Bedford, B. 1977. Changes in wetland vegetation associated with leakage from the cooling lake of a coal-fired power plant. M.S. Thesis. Univ. Wisconsin-Madison, Madison, Wis. 39 p.
- Bedford, B. 1978. Alterations in the growth and phenology of wetland plants as indicators of environmental change. Proc. Jt. Conf. Sensing Environ. Pollut. New Orleans, La. p. 170-174.
- Boulter, D. 1972. Water table drawdown around an open ditch in organic soils. J. Hydrol. 15:329-340.
- Boyle, J.M., and Z.A. Saleem. 1978. Determination of recharge rate using temperature depth profiles in wells (abstract). EOS 59(4):280.

- Bredehoeft, J.D., H. Counts, S. Robson, and J. Robertson. 1976. Solute transport in groundwater systems, p. 229-256. *In* Facets of hydrology. John Wiley and Sons, New York.
- Bredehoeft, J.D., and I.S. Papadopoulos. 1965. Rates of vertical groundwater movement estimated from the earth's thermal profile. *Water Resour. Res.* 1:325-328.
- Bredehoeft, J., and G. Pinder. 1970. Digital model of areal flow in multiaquifer groundwater systems: A quasi three-dimensional model. *Water Resour. Res.* 6:883-888.
- Bredehoeft, J.D., and G.F. Pinder. 1973. Mass transport in flowing groundwater. *Water Resour. Res.* 9:194-210.
- Cartwright, K. 1970. Ground-water discharge in the Illinois Basin as suggested by temperature anomalies. *Water Resour. Res.* 6:912-918.
- Cartwright, K. 1973. The effect of shallow groundwater flow systems on rock and soil temperatures. Ph.D. Thesis. Univ. Illinois-Urbana, Urbana, Ill. 128 p.
- Cherry, J.A., R.W. Gillham, and J.F. Pickens. 1975. Contaminant hydrogeology. Part 1: Physical processes. *Geosci. Can.* 2(2):76-84.
- Cook, R.D. 1974. Concepts and applications of finite element analysis. John Wiley and Sons, Inc., New York. 402 p.
- Cooley, R. 1977. A method of estimating parameters and assessing reliability for models of steady state groundwater flow, 1: Theory and numerical properties. *Water Resour. Res.* 13:318-324.
- Cooper, H.H., J.D. Bredehoeft, I.S. Papadopoulos. 1967. Response of a finite-diameter well to an instantaneous charge of water. *Water Resour. Res.* 3:263-269.
- Desai, C.S., and J.F. Abel. 1972. Introduction to the finite element method. Van Nostrand Reinhold Co., New York. 477 p.
- Dix, R.L., and F.E. Smeins. 1967. The prairie, meadow, and marsh vegetation of Nelson County, North Dakota. *Can. J. Bot.* 45:21-58.
- Freeze, R.A., and P.A. Witherspoon. 1966. Theoretical analysis of regional groundwater flow, I: Analytical and numerical solutions to the mathematical model. *Water Resour. Res.* 2:641-656.
- Gass, T.E., and J.H. Lehr. 1977. Ground water energy and the ground water heat pump. *Water Well J.* 31(4):42-47.

- Gibbons, J.W. 1976. Thermal alteration and the enhancement of species populations. In: Thermal Ecology II. Proceedings of a symposium held at Augusta, Georgia, April 2-5. ERDA Symposium Series 40, Report CONF-750425.
- Green, D.W. 1963. Heat transfer with flowing fluid through porous media. Ph.D. Thesis. Univ. Oklahoma, Norman, Okla. 312 p.
- Gringarten, A.C., and J.D. Sauty. 1975. A theoretical study of heat extraction from aquifers with uniform regional flow. J. Geophys. Res. 80:4956-4962.
- Hausz, W., and C.F. Meyer. 1975. Energy conservation: Is the heat storage well the key? Public Util. Fortn. 95:34-38.
- Hoopes, J., and D. Harleman. 1967. Dispersion in radial flow from a discharge well. J. Geophys. Res. 72:3595-3607.
- Intercomp Resource Development and Engineering, Inc. 1976. A model for calculating effects of liquid waste disposal in deep saline aquifers. Vol. 1. U.S. Geol. Surv., Water Resour. Invest., 76-61. p.
- Jaeger, J.C. 1958. The measurement of thermal conductivities and diffusivity with cylindrical probes. Trans. Am. Geophys. Union 39:708-710.
- Jobson, H.E. 1972. Effect of using averaged data on the computed evaporation. Water Resour. Res. 8:513-518.
- Keys, W.S., and R.F. Brown. 1978. The use of temperature logs to trace the movement of injected water. Ground Water 16:32-48.
- Kirge, L.J. 1939. Borehold temperatures in the Transvaal and Orange Free State. Proc. Roy. Soc. London, Ser. A, 173:450-474.
- Kley, W., and H. Nieskens. 1975. Möglichkeiten der Warmespeicherung in einem Porengrundwasserleiter und technische Probleme bei einer Rückgewinnung der Energie. Z. Dtsch. Geol. Ges. 126:397-409.
- Konikow, L. 1976. Modeling chloride movement in the alluvial aquifer at the Rocky Mountain Arsenal, Colorado. U.S. Geol. Surv., Water-Supply Pap. 2044., Washington, D.C. 43 p.
- Konikow, L.F., and D.B. Grove. 1977. Derivation of solute transport in ground water. U.S. Geol. Surv., Water-Resour. Invest. 77-19. Washington, D.C. 30 p.
- Lee, D.R. 1977. A device for measuring seepage flux in lakes and estuaries. Limnol. Oceanogr. 22:140-147.
- Mercer, J.W., G.F. Pinder, I.G. Donaldson. 1975. A Galerkin finite element analysis of the hydrothermal system at Wairakei, New Zealand. J. Geophys. Res. 80:2608-2621.

- Meyer, C.F., and D.K. Todd. 1973. Conserving energy with heat storage wells. *Environ. Sci. Technol.* 7:512-516.
- Millar, J.B. 1973. Vegetation changes in shallow marsh wetlands under improving moisture regime. *Can. J. Bot.* 51:509-522.
- Mink, J.F. 1964. Groundwater temperatures in a tropical island environment. *J. Geophys. Res.* 69:5225-5230.
- Mitchell, J., W. Beckman, R. Bailey, and W. Porter. 1975. Microclimate modeling of the desert, p. 275-286. In D.A. de Vries and N.H. Afgan [ed.] *Heat and mass transfer in the biosphere*. Scripta Book Co., Washington, D.C.
- Molz, F.J., J.C. Warman, and T.E. Jones. 1976. Transport of water and heat in an aquifer used for hot-water storage: experimental study (abstract). *EOS* 57:918.
- Molz, F.S., J.C. Warman, T.E. Jones, and G.E. Cook. 1976. Experimental study of the subsurface transport of water and heat as related to the storage of solar energy. *Proc. Int. Solar Energy Soc. (Canadian and American sections)* 8:238-244.
- Myers, G.E. 1971. *Analytical methods in conduction heat transfer*. McGraw-Hill, New York. 508 p.
- Myers, G.E. 1978. The critical time step for finite element solutions to two-dimensional heat-conduction transients. *J. Heat Transfer* 100:120-127.
- Neuman, S.P. 1973. Calibration of distributed parameter groundwater flow models viewed as a multiple objective decision process under uncertainty. *Water Resour. Res.* 9:1006-1021.
- Nightingale, H. 1975. Ground-water recharge rates from thermometry. *Ground Water* 13:340-344.
- Ogata, A., and R. Banks. 1961. A solution of the differential equation of longitudinal dispersion in porous media, U.S. Geol. Surv. Prof. Pap. 411-A. Washington, D.C. 7 p.
- Parsons, M.G. 1970. Ground-water recharge rates from thermometry. *Ground Water* 13:340-344.
- Pickens, J., and W. Lennox. 1977. Numerical simulation of waste movement in steady groundwater flow systems. *Water Resour. Res.* 12:171-180.
- Pinder, G. 1973. A Galerkin-finite element simulation of groundwater contamination on Long Island, New York. *Water Resour. Res.* 9:1657-1669.
- Pinder, G., and J. Bredehoeft. 1968. Application of a digital computer for aquifer evaluation. *Water Resour. Res.* 4:1069-1093.

- Pinder, G.F., and W.G. Gray. 1977. Finite element simulation in surface and subsurface hydrology. Academic Press, New York. 295 p.
- Reddel, D.L., and D.K. Sunada. 1970. Numerical simulation of dispersion in groundwater aquifer. Colorado State Univ., Hydrol. Pap. 41. 79 p.
- Robertson, J.B. 1974. Digital modeling of radioactive and chemical waste transport in the Snake River plain aquifer of the national reactor testing station, Idaho, U.S. Geol. Surv., open file report. Washington, D.C. 41 p.
- Robson, S.G. 1978. Application of digital profile modeling techniques to ground-water solute transport at Barstow, California. U.S. Geol. Surv., Water-Supply Pap. 2050. Washington, D.C. 28 p.
- Sammuel, E.A. 1968. Convective flow and its effect on temperature logging in small diameter wells. Geophysics 33:1004-1012.
- Scheidegger, A.E. 1961. General theory of dispersion in porous media. J. Geophys. Res. 66:3273-3278.
- Schneider, R. 1962. An application of thermometry to the study of ground water. U.S. Geol. Surv., Water Supply Pap. 1566-H. Washington, D.C. 16 p.
- Schneider, R. 1964. Relation of temperature distribution of ground-water movement in carbonate rocks in central Israel. Bull. Geol. Soc. Am. 75:209-214.
- Sorey, M.L. 1971. Measurement of vertical groundwater velocity from temperature profiles in wells. Water Resour. Res. 7:963-970.
- Stallman, R.W. 1960. Notes on the use of temperature data for computing groundwater velocity. Soc. Hydrotech. France (Nancy, France), Rapp. 3. p. 1-7. (Reprinted, 1963, in U.S. Geol. Surv., Water-Supply Pap. 1544H. Washington, D.C. p. 36-46.)
- Stallman, R.W. 1965. Steady one-dimensional fluid flow in a semi-infinite porous medium with sinusoidal surface temperature. J. Geophys. Res. 70:2821-2827.
- Steinhart, J.S., and S.R. Hart. 1968. Calibration curves for thermistors. Deep-Sea Res. 15:497-503.
- Supkow, D.J. 1971. Subsurface heat flow as a means for determining aquifer characteristics in the Tucson Basin, Pima County, Arizona. Ph.D. Thesis. Univ. Arizona, Tucson, Ariz. 182 p.
- Tanner, C., and W. Pelton. 1960. Potential evapotranspiration estimates by the approximate energy balance of Perman. J. Geophys. Res. 65: 3391.

- Tsang, C.F., M.J. Lippmann, and P.A. Witherspoon. 1976. Numerical modeling of cyclic storage of hot water in aquifers. Trans. Am. Geophys. Union, EOS 57:918.
- Vadas, R.L., M. Keser, P.C. Rusanowski, and B.R. Larson. 1976. The effects of thermal loading on the growth and ecology of a northern population of Spartina alterniflora. Thermal Ecology II, National Technical Information Service (CONF-750425). Springfield, Va. p. 54-63.
- Van Wijk, W.R., and D.A. de Vries. 1963. Periodic temperature variation. In W.R. Van Wijk [ed.] Physics of plant environment. North Holland Publishing Co., Amsterdam, Holland.
- Von Herzen, R., and A.E. Maxwell. 1959. The measurement of thermal conductivity of deep sea sediments by a needle probe method. J. Geophys. Res. 64:1557-2563.
- Walker, B.H., and R.T. Coupland. 1968. An analysis of vegetation-environment relationships in Saskatchewan sloughs. Can. J. Bot. 46:509-522.
- Werner, O., and W. Kley. 1977. Problems of heat storage in aquifers. J. Hydrol. 34:35-43.
- Willard, D.E., W. Jones, B. Bedford, M. Jaeger, and J. Benforado. 1976. Wetland ecology, p. 89-135. In Documentation of change related to the Columbia Electric Generating Station, Institute of Environmental Studies, Rep. 69, Univ. Wisconsin-Madison, Madison, Wis.
- Willard, D.E., W. Jones, B. Bedford, M. Jaeger, and J. Benforado. 1977. Wetland ecology, p. 110-125. In Documentation of environmental related to the Columbia Electric Generating Station, Institute of Environmental Studies, Rep. 82, Univ. Wisconsin-Madison, Madison, Wis.
- Winslow, J.D. 1962. Effect of stream infiltration on ground-water temperatures near Schenectady, New York. U.S. Geol. Surv., Prof. Pap. 450-C, Art. III. Washington, D.C. p. C-125-C-128.
- Wisconsin Public Service Commission. 1974. Final environmental impact statement for Generating Unit No. II of the Columbia Electric Generating Station. Madison, Wis. 147 p.
- Zienkiewicz, O.C. 1971. The finite element method in engineering science. McGraw-Hill, London. 521 p.
- Zienkiewicz, O.C. 1977. The finite element method in engineering science. McGraw-Hill, London.

APPENDIX A

DATA SPECIFICATIONS FOR THE WATER-FLOW MODEL

This appendix details procedures used at the site of the Columbia Generating Station to gather field data on the hydrogeologic system. The data were collected from 1971 to 1975. They were used to document changes in the system caused by construction and operation of the generating station and to establish the boundary conditions and parameters for the model of the ground-water flow system.

DATA FOR SPECIFYING BOUNDARIES

Side Boundaries

The position of the site in the regional ground-water flow system was needed to determine the size of the area to be modeled. Water-level data and well logs were collected from more than 100 domestic wells in the vicinity of the Columbia Generating station. Most of the data were obtained from the U.S. Geological Survey in Madison, Wis. The data were used to estimate aquifer transmissivity, flow rates, and the extent of the regional ground-water flow system. Transmissivity was estimated from pump tests and specific capacity data. Flow rates were computed by using the estimated transmissivity value and the water-table gradients existing in the field. The extent of the flow system was estimated by contouring water-level data from the wells open to the sandstone aquifer in the vicinity of the site.

The information on the regional ground-water system was used to justify the assumption that the left and bottom boundaries of the cross section modeled were no-flow boundaries and to specify the flow rates for the right boundary of the cross sections modeled.

Upper Boundary

Over 80 well point piezometers 3.2 cm in diameter were installed on the site to monitor the position of the water table. The piezometers had 46-cm, 80-gauge screens. They were driven in place in the lowlands and augered into place in the uplands. They were positioned so that they were open to the aquifer just below the water table. Monitoring was done with a steel measuring tape at monthly intervals beginning in summer 1971. The water levels in two wells were recorded continuously. Beginning in fall 1974 water levels were recorded at 14 points in the wetlands on a monthly basis. All observation points were surveyed to establish relative elevations. The locations of the wells are shown in Figure A-1.

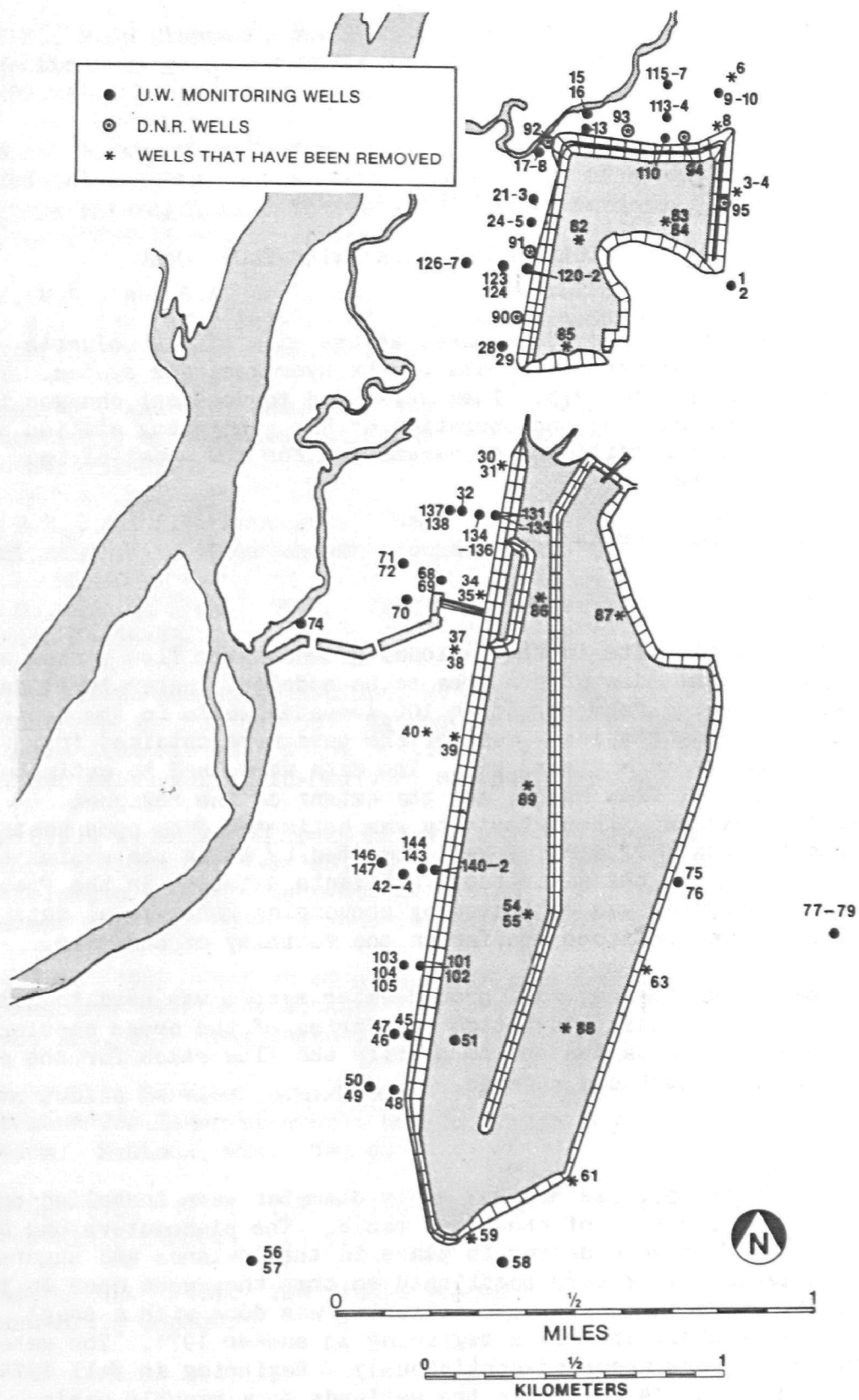


Figure A-1. Location of monitoring wells at the Columbia site.

Water-level data from all monitoring wells were punched onto IBM Cards. A computer program was written in PL/1 (Programming Language, University of Maryland) that graphs the water level in each well by water year, computes the rate of change in water levels, and computes the water-table gradient between the observation points and the rate of change in the gradients. These water-level data were used to specify ground-water potential along the upper boundary of the cross sections modeled and to justify the use of a steady-state model.

DATA FOR SPECIFYING STATE VARIABLES

Permeabilities

The range of permeabilities for the various materials on the site was determined by combining data from a pump test, slug tests, and laboratory permeability tests with lithologic and grain-size information. Permeability distribution in the system was then modeled by using lithologic and grain-size information from over 100 borings on the site. (The locations of the borings are shown in appendix B.) A pump test was run in the alluvial materials on the site in winter 1972 by the Lane Engineering Firm of Chicago, Ill. The data were analyzed by using the Dupuit-Theim equation for steady radial flow without vertical movement. Slug tests were run on 23 of the observation wells on the site. Water was withdrawn from the wells, and the recovery time was recorded. The data from these tests were analyzed with the techniques developed by Cooper, Bredehoeft, and Papadopoulos (1965).

Laboratory permeabilities were run on 23 samples with soil test permeameters under both falling and constant head conditions and under various density conditions. Grain-size analyses (percentages of medium sand, fine sand, silt, and clay) were run on 43 diverse samples from the site. The information was then correlated with the permeability tests, and a working model was formulated between lithology and permeability. This correlation of permeabilities with lithologies was used with the logs of the borings to develop seven cross-sectional permeability models.

Temperature

Temperatures were monitored bimonthly beginning in 1973 by lowering a Yellow Springs Instrument thermistor into observation wells. Before the temperature was recorded, the observation well was pumped with a hand-operated vacuum pump until the temperature of the water became nearly constant.

CALIBRATION DATA

In addition to the data collected to define the boundary and state variables in the system, extensive field data were collected to provide a check on model simulations.

Piezometer Nests

Nineteen observation wells were installed in the lowlands at the site. They were open between 4.5 and 7.6 m below the water table. Seven wells were installed in the uplands so that they were open between 9.1 and 18.3 m below the water table. These wells were placed adjacent to an observation well open just below the water table. Water levels in these wells were monitored at monthly intervals. The vertical gradients and the rate of change of vertical gradients have been computed for each of these wells for each monitoring date. The data from these wells were used to judge the fit of the models' simulations of the ground-water system to the actual situation.

Direct Measurements of Flow

Surface water in the wetland west of the cooling lake drains through well-defined channels during low river stages. The amount of discharge through these channels was monitored several times during fall 1975 on overcast days with a rod-suspended pygmy current meter. Measurements were taken at 0.6 of the total depth at 1-ft intervals across the streams. By similar methods the flow in the drainage ditch on the east side of the cooling lake was measured several times at both the northeast corner and the southwest corner of the cooling lake.

Discharge into the drainage ditch on the east side of the lake from the ground-water system was monitored with seepage collectors. Seepage collectors are 55-gal barrels cut in half whose open end is positioned into the substrate at the bottom of the ditch (Lee 1977). On the closed end, which is also submerged, the spout is covered by a plastic bag. The flow of water into the plastic bag is recorded, which provides a direct measurement of the ground-water inflow into the ditch in the area covered by the barrel. By means of the seepage collectors, rates of ground-water flow into the drainage ditch on the east side of the lake were determined at various locations on several different dates.

APPENDIX B

TECHNIQUES FOR DETERMINING BOUNDARY CONDITIONS AND PARAMETERS IN THE HEAT-FLOW MODEL

The model developed to simulate the transport of heat away from the cooling lake at the Columbia Generating Station requires for its solution the specification of initial and boundary conditions for the partial differential equations describing heat flow and the equations describing water flow. Five sets of parameters are also required: Hydraulic conductivity, storage coefficient, thermal conductivity, heat capacity, and dispersivity. The field and laboratory techniques used to define the boundary conditions and the parameters needed for the water-flow equation were described in appendix A. The field techniques used to measure temperature and the laboratory techniques used to measure thermal conductivity and heat capacity are described in this appendix. The technique used for specifying the dispersivity parameters is described in section 6.

TEMPERATURE MEASUREMENTS

Temperatures were recorded weekly at 40-110 points in the subsurface in the vicinity of the Columbia Generating Station site from August 1976 to January 1978 (Figure B-1). The depths at which temperatures were taken, the dates when readings were taken, and the manner in which temperatures were measured are listed in Table B-1.

Most temperatures in the field were measured with an electronic device with a thermistor as the temperature sensor. A thermistor sensor system was used because of its accuracy and its versatility. A relative accuracy of 0.1°C is easy to maintain in the field, and probes could be buried, lowered down wells, or located far from an accessible point. Liquid expansion thermographs with an accuracy of $+ 0.5^{\circ}\text{C}$ were used for continuous temperature recording because these mechanical devices are much easier to maintain and less expensive than a continuous recording device with a thermistor sensor.

An electronic temperature measuring device is extremely simple in concept (Figure B-2). It consists of a thermistor whose electrical resistance is almost entirely a function of its temperature as the sensing device and an electronic measuring device to measure either directly or indirectly the resistance of the sensor, generally an ohmmeter or a wheatstone bridge. Two types of thermistors and three measuring devices were used at the Columbia Generating Station site.

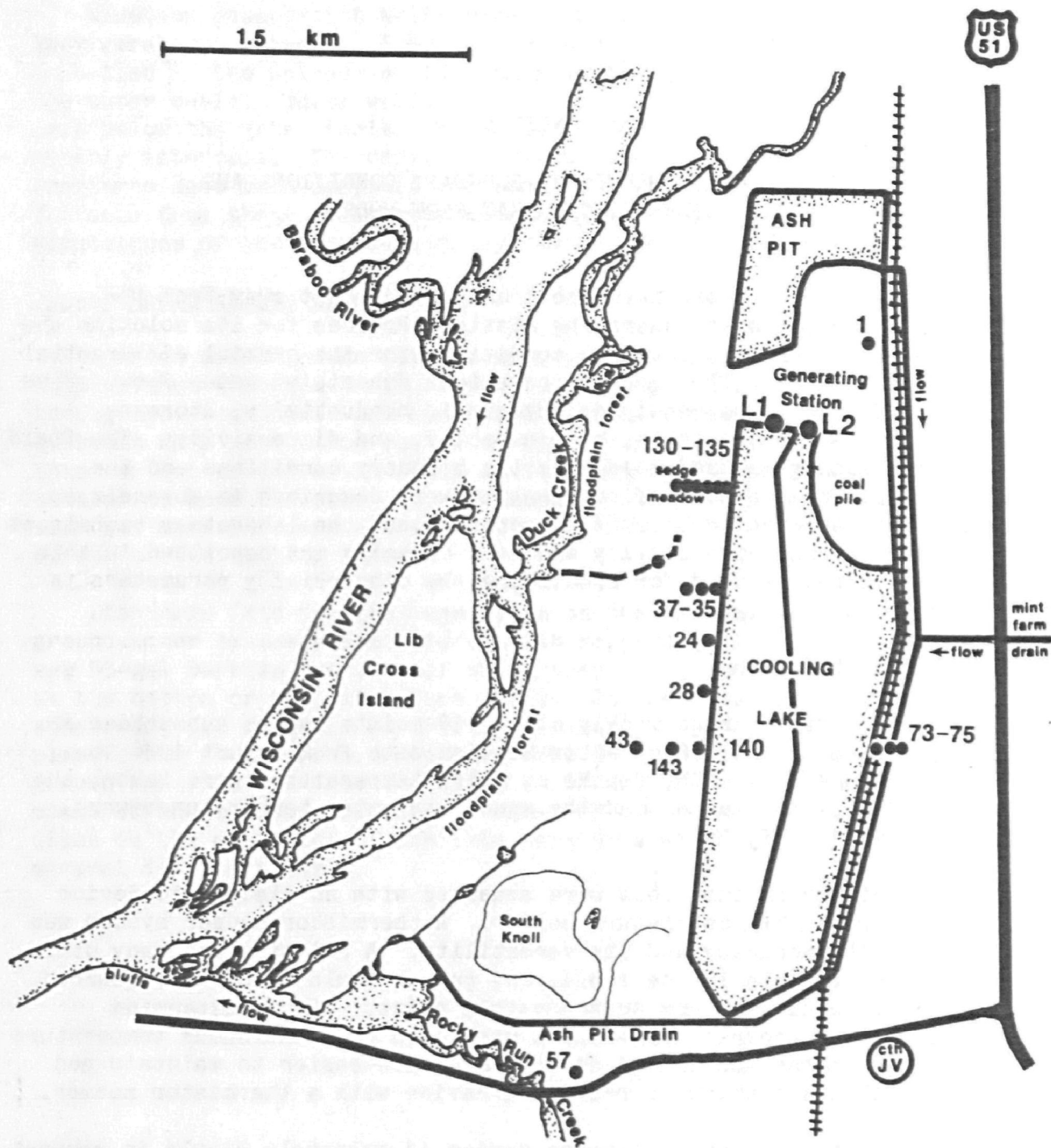


Figure B-1. Location of temperature sampling points at the Columbia Generating Station site.

TABLE B-1. TEMPERATURE SAMPLING POINTS: LOCATIONS, DEPTHS, PROBES, AND FREQUENCIES OF READINGS

Sampling point number	Distance from dike (m)	Depth below surface at which temperature was measured (m)	Probe used to take temperature	Approximate frequency of readings
130	2	0.15, 0.91, 1.52, 3.05, 6.10, 8.70	<u>in situ</u> probe	8/8/76-8/77 weekly 9/77-1/78 monthly
131	15	0.15, 0.46, 0.91, 1.51, 3.05, 4.57, 6.10, 9.76	<u>in situ</u> probe	8/8/76-8/77 weekly 9/77-1/78 monthly
132	32.5	0.15, 0.46, 0.91, 1.52, 3.05, 4.57, 6.10, 9.76	<u>in situ</u> probe	8/8/76-8/77 weekly 9/77-1/78 monthly
133	51		<u>in situ</u> probe	8/8/76-8/77 weekly 9/77-1/78 monthly
134	86		<u>in situ</u> probe	8/8/76-8/77 weekly 9/77-1/78 monthly
135	131.5		<u>in situ</u> probe	8/8/76-8/77 weekly 9/77-1/78 monthly
35	3	2,3,4,5,6,7,8,9	probe lowered down 3.175 cm; PVC pipe	8/8/76-1/17/78 weekly
36	31	2,4,6,7,8	probe lowered down 3.175 cm; PVC pipe	8/10/77-1/18/78 weekly
37	61	2,3,4,5	probe lowered down 3.175 cm; PVC pipe	8/10/77-1/18/78 weekly
68	194	4,6,8,10,12	probe lowered down 3.175 cm; galvanized pipe	8/10/77-1/18/78 weekly
24	2	3,4,5,6,7,8,9,10	probe lowered down 3.175 cm; PVC pipe	5/31/77-1/18/78 weekly
28	2	2,4,6,8,10,12,13	probe lowered down 3.175 cm; PVC pipe	8/10/77-1/18/78 weekly
140	3	2,4,6,8	probe lowered down 3.175 cm; galvanized pipe	4/22/77-1/18/78 weekly

TABLE B-1 (continued).

Sampling point number	Distance from dike (m)	Depth below surface at which temperature was measured (m)	Probe used to take temperature	Approximate frequency of readings
143	37	2,4,6,8	probe lowered down 3.175 cm; galvanized pipe	4/22/77-1/18/78 weekly
43	126	2,4,6,8,10	probe lowered down 3.175 cm; galvanized pipe	4/22/77-1/18/78 weekly
73	west side of ditch	1,2,3,4,5,6,7,8,9	probe lowered down 2.54 cm; PVC pipe	5/31/77-1/18/78 weekly
74	east side of ditch	1,2,3,4	probe lowered down 3.175 cm; PVC pipe	5/31/77-1/18/78 weekly
75	14 m east of ditch	4,6,8,10,12,16,18,20,21	probe lowered down 3.175 cm; galvanized pipe	5/31/77-1/18/78 weekly
1		10,12,14,16,18,20	probe lowered down 3.175 cm; galvanized pipe	10/1/76-12/12/78 monthly
57		8,10,12,14	probe lowered down 3.175 cm; galvanized pipe	10/1/76-12/12/78 monthly
L1/L2	Lake inlet and outlet		thermistor	daily average value recorded every day plant is operating
Areal coverage of marsh (not shown in Figure B-1)		0.1, 0.9 m at 45 locations in marsh	<u>in situ</u>	10/28/76, 11/6/76, 11/13/76, 12/4/76
Transect 1 to transect 42 (not shown on Figure B-1)	0.2 m	1.0, 3.0 m	shallow temperature probe	9/30/77, 10/23/77, 12/03/77, 1/10/78, 3/30/78

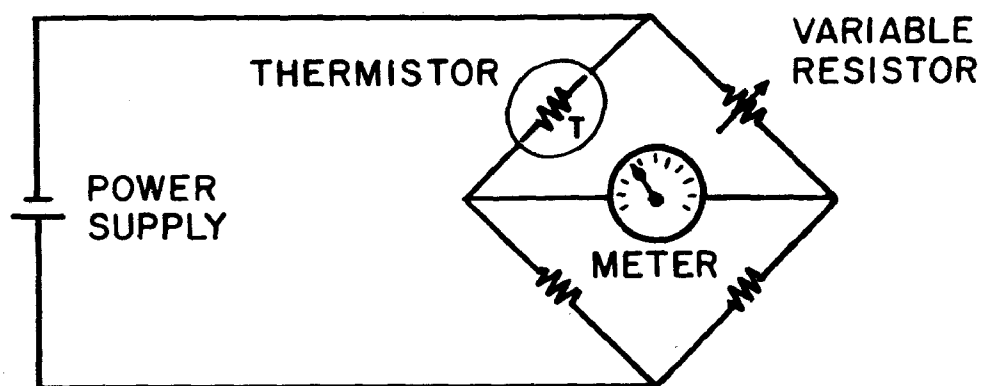


Figure B-2. A simple circuit for measuring temperature.

Thermistors

Most of the temperature data at the Columbia Generating Station site were taken with Yellow Springs Instrument Company Series 400 thermistors. These thermistors are calibrated by Yellow Springs, and all thermistors of this type have the same calibration curve with a maximum error of 0.1°C . The probes are guaranteed to remain calibrated for 1 yr. The temperature-resistance characteristics of these probes, as well as the resistance change for a 0.1°C temperature change, are shown in Figure B-3. The thermistors were used in three modes: as sensors that were lowered down a well, as sensors mounted on 2-m brass rods, and as sensors placed semipermanently in the subsurface.

The easiest and least expensive means for measuring temperature in the subsurface is to lower a probe down a fluid-filled well and take readings at various depths on the way down. The only problem with this technique is that the temperature profile in the well will not correspond to the temperature profile in the subsurface materials if the temperature gradients are above a critical value. For a 3.175-cm well the critical gradient is approximately $1^{\circ}\text{C}/\text{m}$ at 10°C and 0.2°C at 25°C (Sammel 1968). The critical gradient was exceeded in many cases at the Columbia site. The error induced in the temperature readings is probably less than $+0.5^{\circ}\text{C}$ if the critical gradient is exceeded by less than 1 order of magnitude. Near the surface, where the gradient can be large, the induced error was greater. Nevertheless, because of the advantages of simply lowering a probe down a well, this technique was used to record temperatures at many locations in the subsurface.

The thermistors that were lowered down wells were purchased as a unit designed for this purpose. These thermistors were sealed by the manufacturer in an epoxy resin and attached to a shielded cable. The maximum diameter of the assembly was 0.4 cm. The time constant of these thermistors is 7 s. A thermistor assembly as described above was mounted inside a 0.95-cm brass rod, 2.1 m long, for use as a shallow temperature probe for accurately measuring temperatures near the surface. The probe could easily be pushed into the soft sediments on the Columbia site to a depth of 2 m. The thermistors purchased as a unit were calibrated with respect to each other so that temperatures between probes could be compared with an accuracy of $\pm 0.05^{\circ}\text{C}$.

In one plane perpendicular to the dike (Figure B-1), 42 thermistors were mounted in six wells with six to eight thermistors in each well. These thermistors were purchased as unmounted thermistors. Each thermistor was soldered to three wires on a cable, two wires were soldered to one lead, and the assembly was potted with silicon sealer inside a piece of tygon tubing 0.64 cm by 5 cm (Figure B-4). The wires soldered to each thermistor were of sufficient length to reach the surface. All the thermistors to be placed in a well were bound together and wired to a connector that was placed at the surface when the thermistors were inserted in the well. A cable was wired from the thermistors at each of the six wells to a control box on the dike. The control box on the dike was equipped with a 48-position switch to allow access to each thermistor. Three wires were connected to each thermistor so that the lead-wire resistance could be measured and subtracted from the resistance measured for the thermistor plus lead wire.

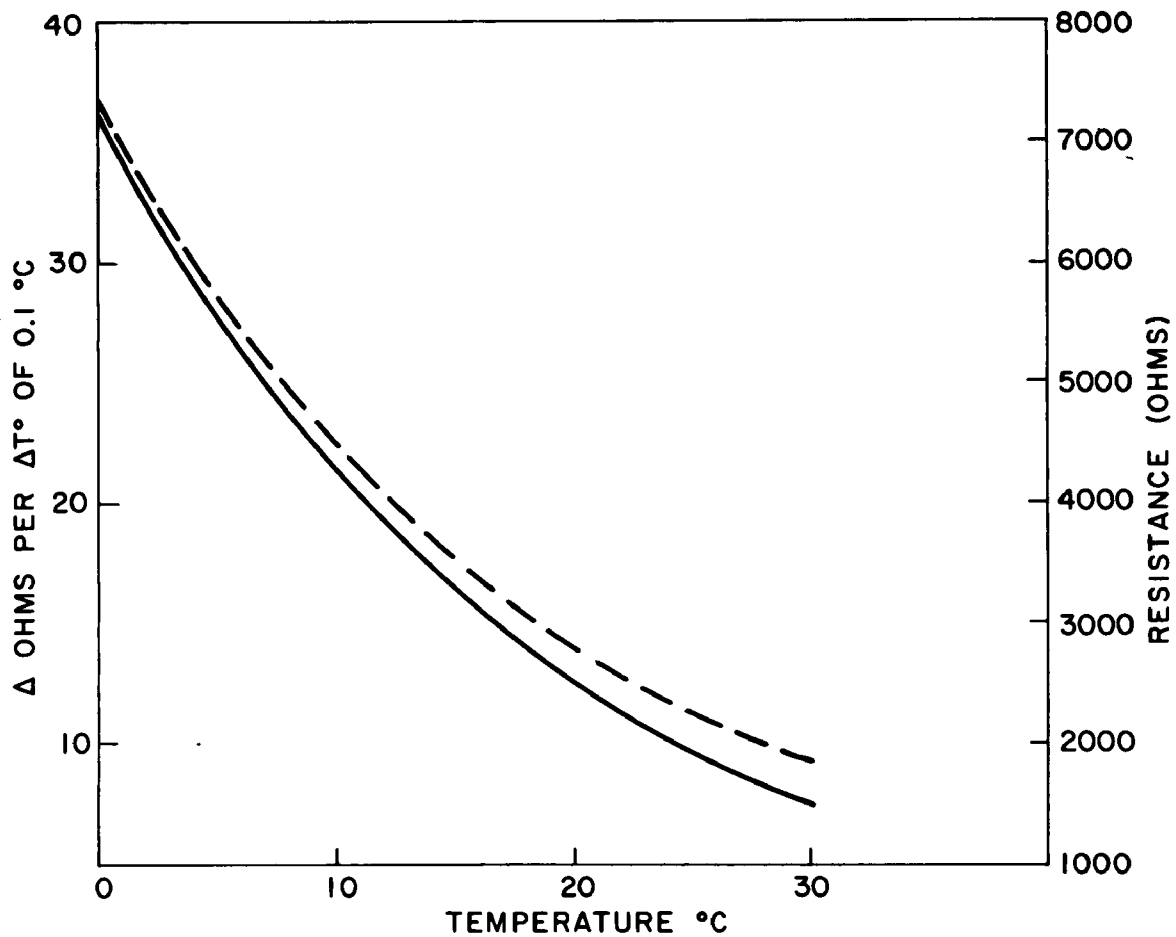


Figure B-3. Temperature-resistance characteristics of Yellow Springs Series 400 thermistors (— = right axis) and the change in resistance with a 0.1° C change in temperature (--- = left axis).

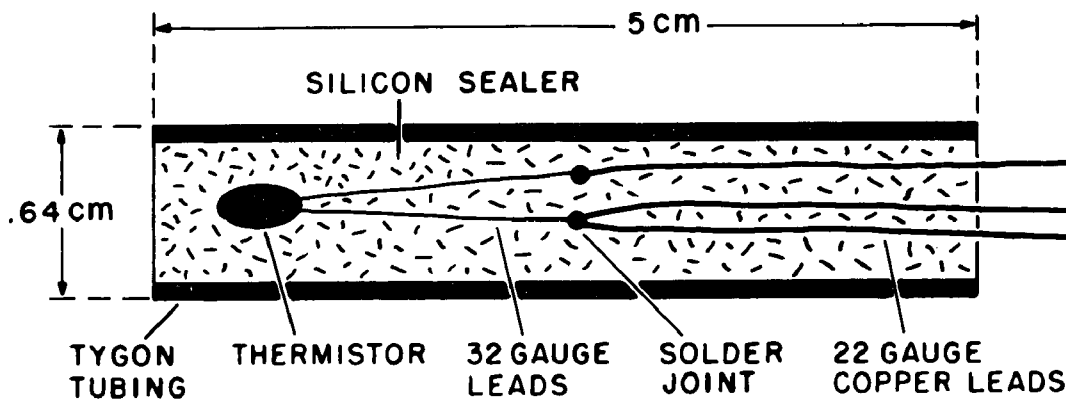


Figure B-4. Potted thermistor assembly showing the details of the thermistor mounts.

The wells into which the thermistors were placed were 10-m deep, water-filled wells constructed with 3.175-cm schedule-40 PVC pipe jettied into place to minimize disturbance of subsurface materials. After the cables were placed in the wells, Fiberglas insulation was stuffed into the remaining space to minimize convection. Thermistors at depths of 0.1, 0.4, and 0.8 m were installed near the well rather than in the well. The field arrangement is shown schematically in Figure B-5. The thermistors on each cable were not calibrated relative to each other, but the cables were pulled twice during the 18 months of temperature-data collection to check for deviation from the calibrated range.

In addition to the in situ thermistors described above, 200 additional thermistors (Fenwall Disc Type JB31J1) were placed at 60 locations in 12 lines perpendicular to the dike in the marsh at depths of 0.1 and 0.9 m. Each line of thermistors was wired to a control box on the dike. Four sets of readings were taken in October and November 1976, but in December the multicolored 22-gauge copper wire, which was used to connect the thermistors to the control boxes on the dikes, became incorporated in the winter dwellings of the marsh muskrats.

Meters Used for Temperature Monitoring

Because of delays in obtaining equipment, three meters were used during the 17 months of temperature monitoring. All meters were frequently calibrated against a known resistance.

From August through December 1976 all thermistor resistances were measured on a Shallcraft four-dial wheatstone bridge with a 5 A full scale needle galvanometer. Resistances could be read accurately to $\pm 3\Omega$ at 4,000 Ω with this meter, and it probably had an operating accuracy of $\pm 10\Omega$.

A Digitec digital recording ohmmeter mounted in a vehicle was used for measuring resistances from January 1977 through January 1978. Most of the resistance measurements were made with this instrument. This instrument had an operating accuracy at 4,000 Ω of approximately $\pm 4\Omega$ and was operated at all times in the field with a 12 VDC to 120 VAC square wave converter and at a temperature of at least 20°C.

A four-dial wheatstone bridge with a digital null meter was constructed as a backup for the digital ohmmeter and as a portable field meter (Figure B-6). This meter had a working accuracy at 4,000 Ω of approximately $\pm 5\Omega$ and was used primarily with the shallow temperature probe for measuring temperatures near the surface.

Temperature Measurements

Two resistances for each location were recorded in the field, a line resistance and a total resistance. The resistances were then coded, punched, cross checked for errors, and then converted to temperature by the following equation (Steinhart and Hart 1968):

$$T^{-1} = A + B \log R + C(\log R)^3 ,$$

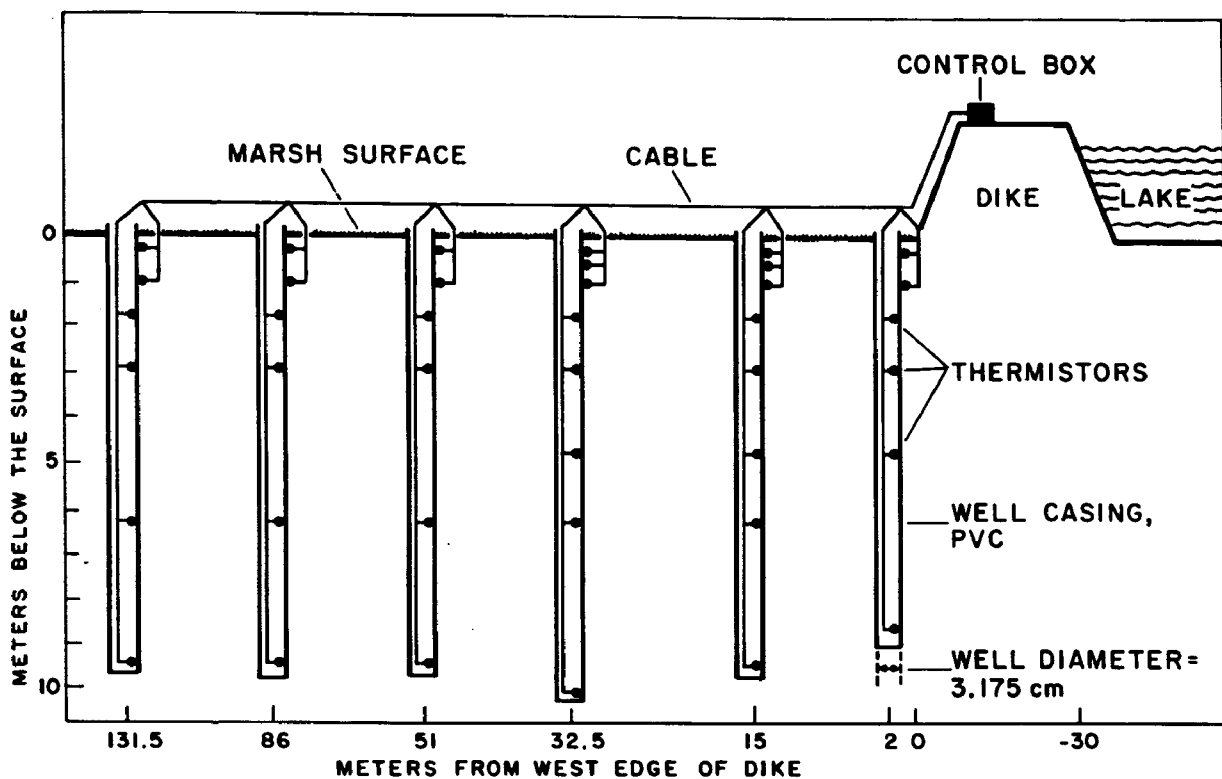


Figure B-5. Schematic of thermistor placement in subsurface wells at the Columbia Generating Station site. The wells shown correspond to locations 130-135 of Figure B-1. Horizontal dimensions are distorted, but vertical dimensions are approximately correct.

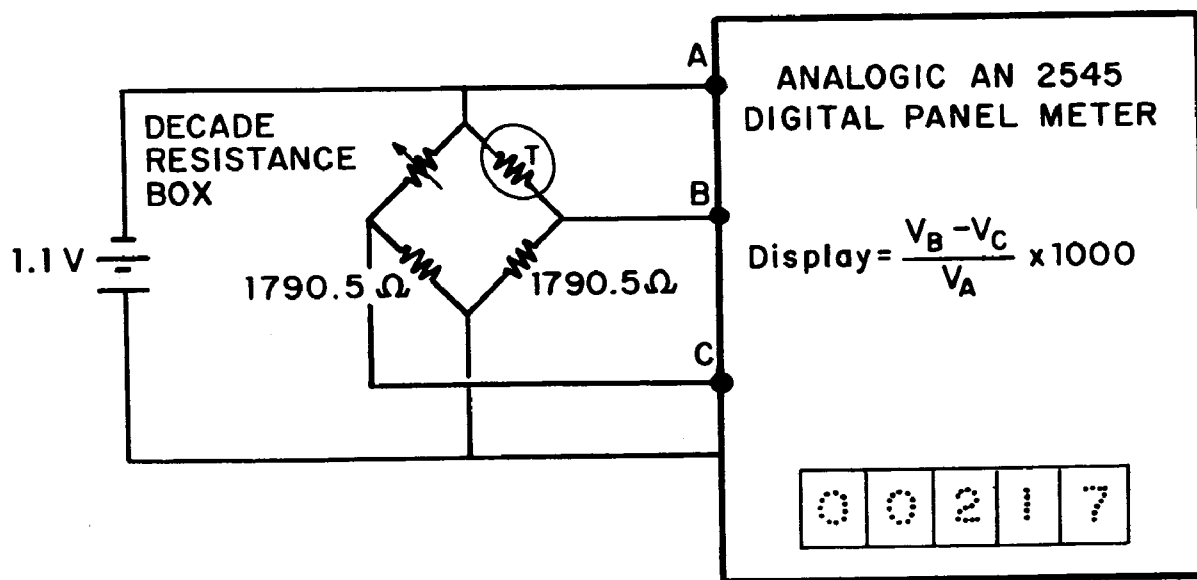


Figure B-6. Schematic of digital bridge circuit used as a portable field meter for measuring ground-water temperatures.

where the constants A, B, and C were determined from the thermistor calibration data, and T^{-1} is the inverse Kelvin temperature.

The relative accuracy of all temperature measurements taken in the study is within $\pm 0.5^\circ\text{C}$ of the actual temperature of the thermistor probe. The main sources of error were thermistor calibration, meter drift, and incorrect meter calibration. The correspondence of probe temperatures to actual subsurface temperatures is unknown. The deviation between these temperatures is a function of the mode of measurement used and was assumed to be small in all cases.

THERMAL CONDUCTIVITY DETERMINATION

The thermal conductivities of unconsolidated materials at the Columbia Generating Station site were measured by the needle probe method (Von Herzen and Maxwell 1959). In the needle probe method, which was developed for determining the thermal conductivity of deep sea sediments, a thin needle is inserted into a sample and is heated along its length. The sample can be as small as 3 cm in radius and 7 cm long. From a record of temperature increase in the needle over time, the thermal conductivity can be easily calculated. The probe and the experimental arrangement for measuring thermal conductivity for this study are shown in Figure B-7. The thermistor in the probe was calibrated to 0.05°C . The needle probe was not checked for accuracy against a known standard.

The theory for the needle probe has been worked out in detail by Jaeger (1958). His analysis shows that temperature increase of the probe is approximated by

$$T = \frac{q}{4K\pi} \ln \left(\frac{4\alpha t}{1.7811 a^2} \right), \quad t > a^2/\alpha,$$

where α = thermal diffusivity of the sediment sample, L^2/t ; a = probe radius, L ; t = time, t ; and q = heat input per unit length per unit time, H/tL .

A plot of T versus $\ln t$ will give a straight line, the slope of which determines K for known values of q . The data collected from measurements of the thermal conductivity of three samples from the Columbia Generating Station site are shown in Figure B-8. All samples were checked for reproducibility, the standard error was less than 3%, and in all measurements thermal conductivity was assumed to be independent of direction.

DETERMINATION OF HEAT CAPACITY

Since heat capacity of a composite material can be determined from a weighted average of the heat capacities of the individual parts in the composite, it was assumed that the heat capacity of the unconsolidated materials at the Columbia Generating Station site could be determined from the relation

$$\rho C_s = \rho C_w X_w + \rho C_{org} X_{org} + \rho C_{qtz} X_{qtz} + \rho C_{clay} X_{clay},$$

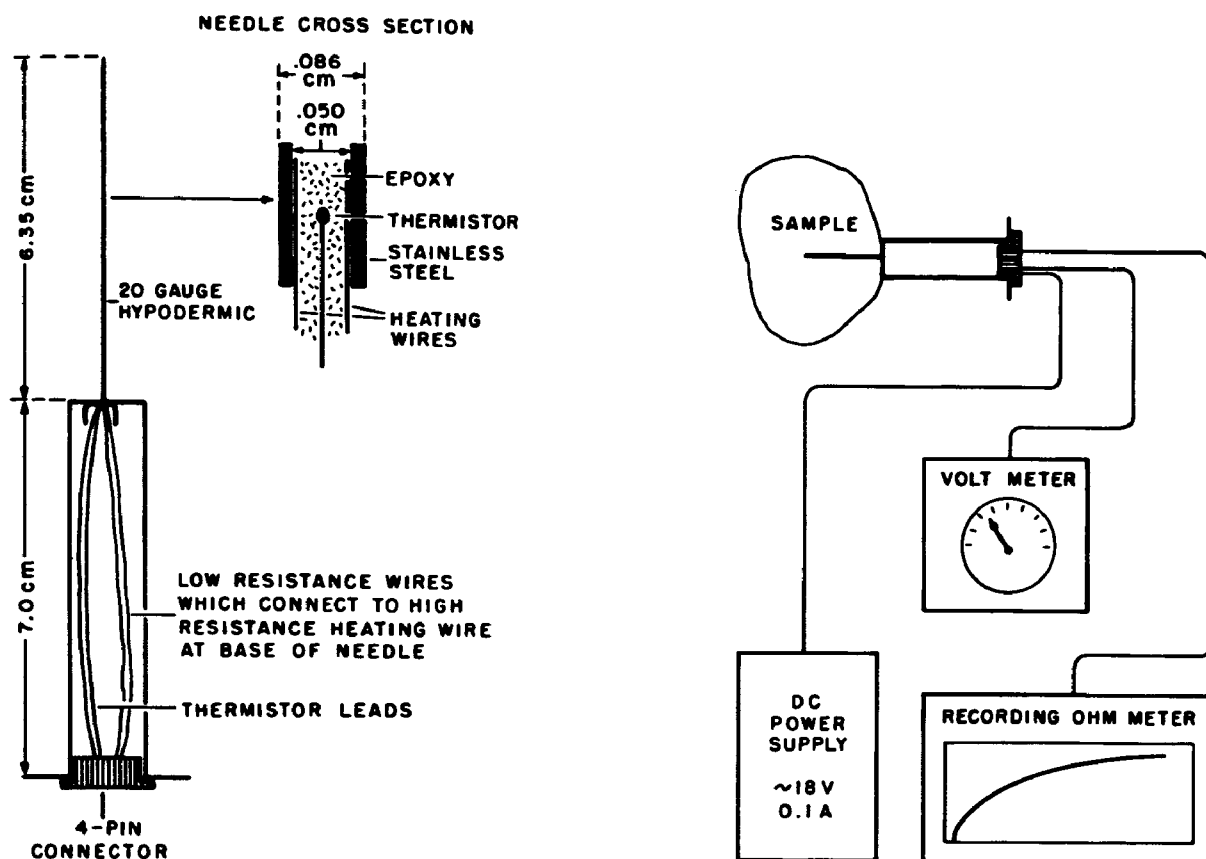


Figure B-7. Details of (a) the needle probe and (b) the experimental arrangement to measure thermal conductivities of unconsolidated materials. The power supply was used to supply a constant voltage to the needle probe. The voltage was then monitored on the volt meter, and the ohmmeter was used to record the resistance changes in the thermistor embedded in the thermistor.

where X_w , X_{org} , X_{qtz} , and X_{clay} denote fractional parts of the material made up of water, organic material, quartz and feldspar, and clay minerals, respectively. The heat capacities of these four components are listed in Table B-2. In a given sample all volatiles were assumed to be organic, all materials greater than 0.001 mm in diameter were assumed to be quartz and feldspars, and all materials less than 0.001 mm in diameter were assumed to be clay minerals. The water content of the samples was determined in the Quarternary Laboratory at the University of Wisconsin-Madison, and the organic, sand and silt, and clay fractions were determined by the Soil and Plant Laboratory of the University of Wisconsin-Madison.

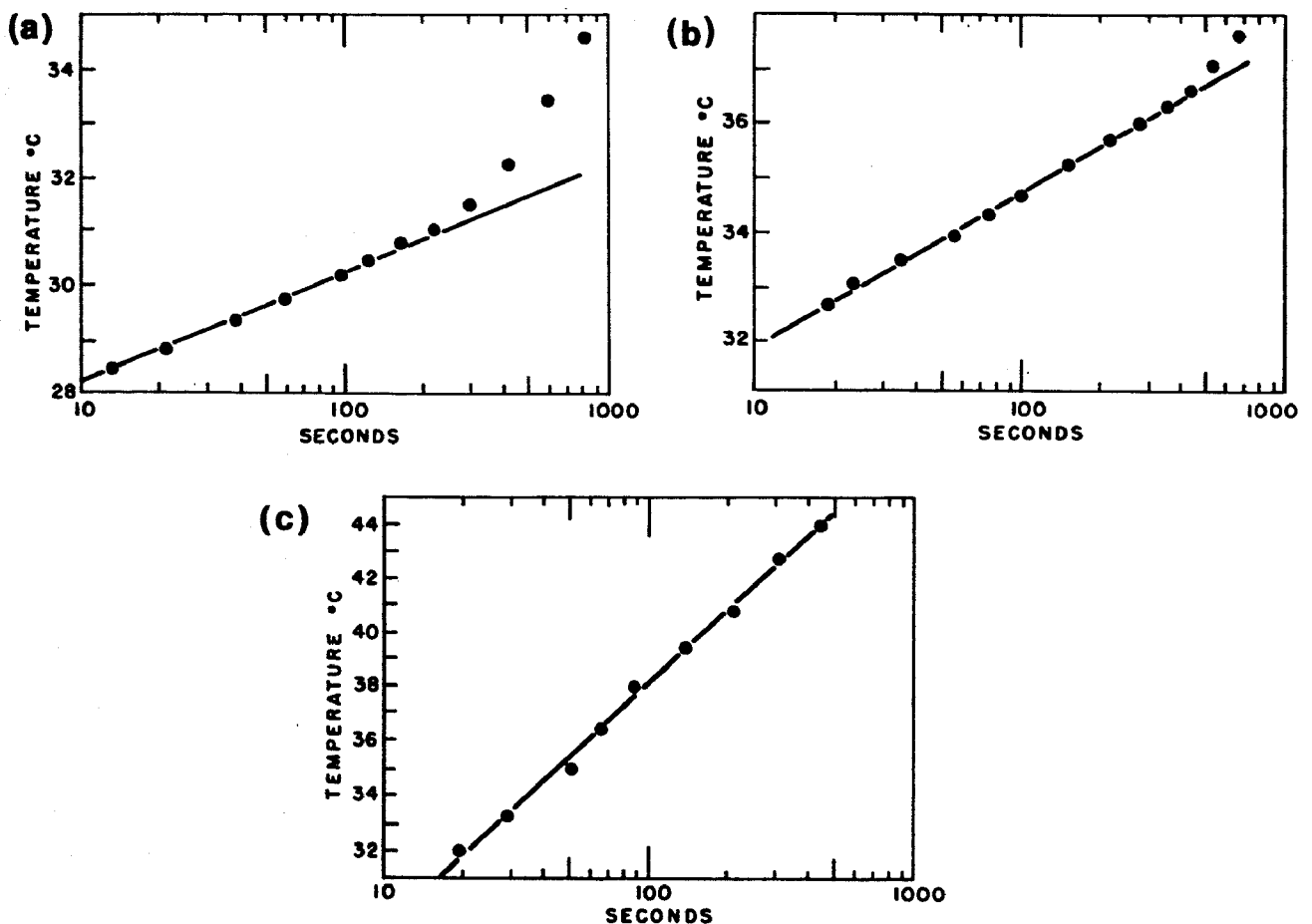


Figure B-8. Thermal conductivities of three ground-water samples from the Columbia Generating Station site which were analyzed with the needle probe. Thermal conductivities were calculated to be 4.9×10^{-3} cal/°C cm sec for medium to fine sand (a), 5.0×10^{-3} cal/°C cm sec for fine sand (b), and 1.5×10^{-3} cal/°C cm sec for hemic peat (c).

TABLE B-2. HEAT CAPACITIES OF THE COMMON COMPONENTS OF UNCONSOLIDATED GLACIAL MATERIALS^a

Component	Heat capacity (cal/m ³ °C)
Quartz and feldspar	0.51×10^6
Clay minerals	0.51×10^6
Organic matter	0.60×10^6
Water @ 25°C	1.00×10^6

^aAdapted from Van Wijk and de Vries (1963).

APPENDIX C

A FINITE ELEMENT PROGRAM TO SIMULATE SINGLE-PHASE HEAT FLOW OR CONSERVATIVE MASS TRANSPORT IN AN AQUIFER

BRIEF DESCRIPTION OF THE MODEL

The following computer code is designed to solve the two-dimensional equations of ground-water flow and heat or mass transport for an aquifer by using the finite element method. The program was written to facilitate the analysis of ground-water contamination in shallow glacial aquifers. The program solves for aquifer potentials and temperatures or concentrations. However, simultaneous simulation of the transfer of heat and mass in an aquifer is not possible. The aquifer to be simulated may be artesian, a water table, or a combination of both. It may be heterogeneous and anisotropic and may have irregular boundaries. The program was designed to simulate cross-sectional problems, but it has also been used successfully to simulate areal problems.

The basic procedure is to solve a ground-water flow problem for potentials in an aquifer and then to use the potential information to compute a velocity distribution in the aquifer. The heat or mass transport equation is then solved for temperatures or concentrations (Figure C-1).

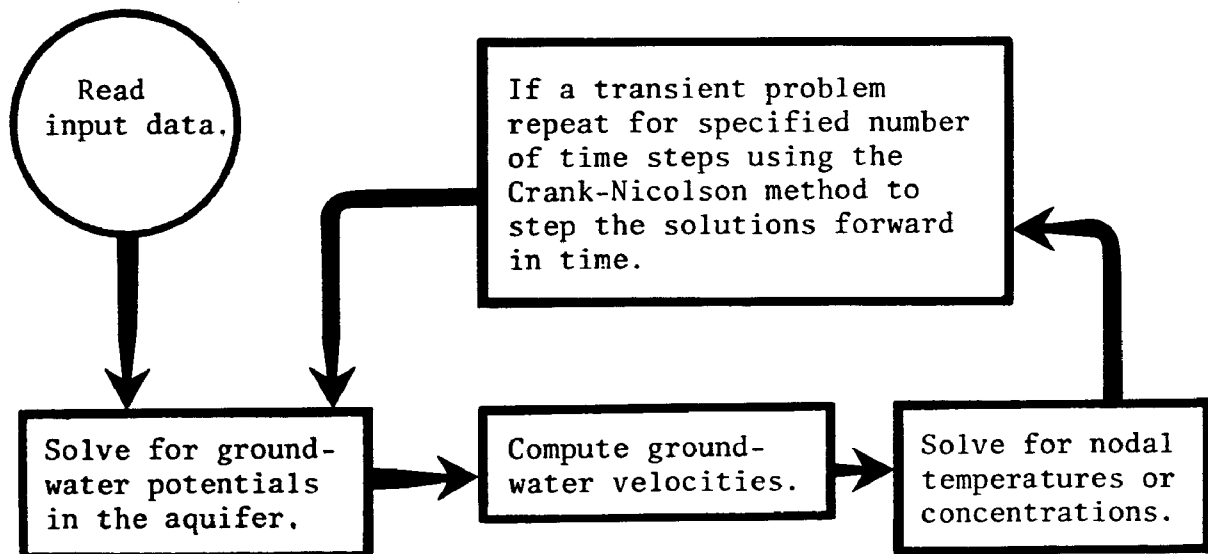


Figure C-1. The basic procedure for linking the ground-water flow and the transport equations of the model. In general, smaller time steps will be used for the heat/mass transport equation than for the water-flow equation.

This flexible program includes these features:

- 1) Neuman, Dirichlet, and mixed boundary conditions can be handled.
- 2) The basic element shape is a quadrilateral. The sides of the elements can be linear, quadratic, or cubic, and thus element sides can have two, three, or four nodes. Any given element can have four linear sides or any mix of linear, quadratic, and cubic sides. This feature allows considerable flexibility in designing a finite element grid.
- 3) The program handles hydrodynamic dispersion.
- 4) Point, line, or areal sources of water, heat, or mass can be represented.
- 5) The problem need not be a linked problem; if desired, the model can be used to solve only for aquifer potentials.
- 6) Hydraulic conductivity can be represented as a function of temperature.

The program is relatively simple to use, but those unfamiliar with the development of the equation describing the convective-dispersive transport of heat or mass in an aquifer, or those unfamiliar with the limitation of the numerical approximation technique, may experience difficulties in using the program. Oscillations and instabilities are frequently encountered in solving the convective-dispersive equation because (1) the equation behaves like a hyperbolic partial differential equation when convective transport dominates over diffusive transport; (2) in the numerical technique used in the program velocities are not continuous everywhere; and (3) the numerical scheme cannot transmit sharp contaminant fronts. Oscillations and instabilities can generally be dampened by reducing element size or by reducing the time step.

THE EQUATIONS SOLVED BY THE PROGRAM

The program was written to solve the differential equation describing mass or energy transport in a ground-water aquifer. Since the rate of transport is a function of ground-water velocity, the first step in solving the transport equation is to solve the ground-water flow equation so that ground-water velocities can be determined.

Water-Flow Equation

The following partial differential equation, which can be used to describe ground-water flow in a confined or water-table aquifer, is solved by the program

$$\frac{\partial}{\partial x_i} (bK_{ij} \frac{\partial \phi}{\partial x_j}) + W - S \frac{\partial \phi}{\partial t} = 0, \quad i, j = 1, 2, \quad (C-1)$$

where K_{ij} are the components of the hydraulic conductivity tensor, which may be a function of temperature, Lt^{-1} ; b = aquifer thickness, L ; ϕ = ground-water potential, L ; W = flux of recharge per unit area, L/T ; and S = storage coefficient for a confined aquifer, or the specific yield in a water-table

aquifer, dimensionless. Boundary conditions may be some combination of the following:

$$\phi = \text{constant}, \quad (\text{C-2})$$

$$\frac{\partial \phi}{\partial x_i} = \text{constant}. \quad (\text{C-3})$$

Equation C-1 can be used only if the aquifer is assumed to be incompressible and if the linearized Dupuit-Forcheimer assumptions apply for unconfined flow for an areal problem. Pinder and Bredehoeft (1968) discuss the development of Eq. (C-1) for modeling a confined aquifer, and Bredehoeft and Pinder (1970) discuss the use of Eq. (C-1) for modeling a water-table aquifer.

Mass/Heat Transport Equation

The program solves the following partial differential equation, which can be used to model the flow of heat or mass in porous media and is commonly referred to as the convective-dispersive equation:

$$\frac{\partial}{\partial x_i} (D_{ij} \frac{\partial C}{\partial x_j}) + \frac{\partial}{\partial x_i} (g D'_{ij} \frac{\partial C}{\partial x_j}) - g q_i \frac{\partial C}{\partial x_i} - R - \rho \frac{\partial C}{\partial t} = 0, \quad (\text{C-4})$$

where

$$D'_{11} = \alpha_L \frac{q_1 q_1}{q} + \alpha_T \frac{q_2 q_2}{q};$$

$$D'_{21} = D_{12} = (\alpha_L - \alpha_T) \frac{q_1 q_2}{q};$$

$$D'_{22} = \alpha_L \frac{q_2 q_2}{q} + \alpha_T \frac{q_1 q_1}{q};$$

α_L = longitudinal dispersivity, L; α_T = transverse dispersivity, L; q_i = velocity or specific discharge, which is calculated by

$$q_i = -K_{ij} \frac{\partial \phi}{\partial x_j}; \quad (\text{C-5})$$

q = mean velocity, $(q_1 + q_2)^{1/2}$, L/t.

The remainder of the parameters are defined differently for a mass transport problem and for a heat transport problem (Table C-1). Boundary conditions may be some combination of the following:

$$C = \text{constant}, \quad (\text{C-6})$$

$$\frac{\partial C}{\partial x_i} = \text{constant}, \quad (\text{C-7})$$

$$\frac{\partial C}{\partial x_i} \propto q_i C_i, \quad (\text{C-8})$$

TABLE C-1. PARAMETERS FOR BOTH MASS AND HEAT TRANSPORT PROBLEMS

	Mass transport problem	Heat transport problem
D_{ij}	Components of molecular diffusion tensor, L^2/t ;	Components of the thermal conductivity tensor for the saturated medium, $H/t LT$;
C	Mass concentration, M ;	Temperature, T ;
g	Unity, dimensionless;	Heat capacity of water, H/L^3T ;
	Effective porosity, dimensionless;	Heat capacity of the saturated medium, H/L^3T ;
R	Mass recharge rate, M/t .	Heat generation or recharge rate, H/L^3t .

$$\frac{\partial C}{\partial x_i} \propto q_i C^\infty, \quad (C-9)$$

$$\frac{\partial C}{\partial x_i} \propto C - C^\infty \quad (C-10)$$

where C^∞ = concentration beyond an exterior boundary.

A physical significance can be ascribed to each of the terms in Eq. (C-4), since the equation can be thought of as a mass balance equation which states that flow into and out of a differential volume sums to zero. The processes described by each of the terms are: transfer by molecular diffusion,

$\frac{\partial}{\partial x_i} (D_{ij} \frac{\partial C}{\partial x_j})$; transfer by velocity fluctuations, called dispersive

transfer, $\frac{\partial}{\partial x_i} (g D'_{ij} \frac{\partial C}{\partial x_j})$; convective transfer, $g q_i \frac{\partial C}{\partial x_i}$; source

or sink, R: storage changes, $\rho \frac{\partial C}{\partial t}$.

The use of Eq. (C-4) to describe mass or heat transport in an aquifer implies the following assumptions: (1) the system is chemically inert, (2) the aquifer is incompressible, (3) density is constant within the system, (4) all transport occurs by molecular diffusion, mechanical dispersion, and convective transport, (5) flow can be represented in two dimensions, and (6) the flow of water is laminar. Bear (1972) and Konikow and Grove (1977) present derivations of Eq. (C-4) to describe solute transport in ground water. The development of Eq. (C-4) to describe energy transport in ground water will be discussed.

THE APPROXIMATION TECHNIQUE

The finite element method is used in the program to approximate Eq. (C-1) and Eq. (C-4) to solve for the unknown potentials and concentrations in an aquifer. The finite element method, like the finite difference method, is a discretization technique. The continuous aquifer is represented by a number of regions, called elements, each bounded by a set of nodes. Integral equations describing water flow and heat or mass flow are developed for each region, giving two sets of simultaneous algebraic equations which are solved to determine the unknown potentials and concentrations. The finite element method generates the integral equation from the governing differential equation and evaluates the integral over an element by a numerical integration scheme. Thus, the finite element method operates on a region, whereas the finite difference technique only operates on a point.

The finite element method has several advantages over the finite difference method for solving Eq. (C-1) and Eq. (C-4), and, in fact, the finite difference method may be unacceptable for solving Eq. (C-4) (Pinder 1973). The advantages are: (1) The finite element method is characterized by less overshoot and less numerical smearing of a concentration front (Pinder and Gray 1977); (2) velocities can have a functional representation, which reduces oscillations in the solution to Eq. (C-4); (3) boundary conditions are much easier to treat in the finite element method, and (4) irregular boundaries are easier to handle with the finite element method.

Two techniques can be used in formulating the approximating integral equations that are the foundation of the finite element method. The procedure used in this study to develop the required finite element formulation is the Rayleigh-Ritz procedure, or the minimum potential energy procedure, which is based on the calculus of variation. The other procedure, the Galerkin method, is more general in application and has been in favor in the literature. It was used by Pinder and Gray (1977) to develop the approximating integral

equations for equations similar to Eq. (C-1) and Eq. (C-4). Both methods yield identical finite element formulations for Eq. (C-1) and Eq. (C-4).

The Finite Element Formulation

The basis of the variational principle is to develop an integral equation describing the total energy within a region and then to minimize the integral. This principle implies that potentials and concentrations in an aquifer will always be at levels that minimize total energy for a given set of boundary conditions.

Integral equations can be developed from first principles by quantifying potential energy in the system, but the Euler-Lagrange equation (Myers 1971) facilitates the process by transforming the governing partial differential equations to integral equations that describe total energy within a region.

The variational statements for Eq. (C-1) and Eq. (C-4) for an element within the aquifer are

$$\Pi_w = 1/2 \iint K_{ij} \left(\frac{\partial \phi}{\partial x_i} \frac{\partial \phi}{\partial x_j} \right) dx_1 dx_2 - 1/2 \iint [2W\phi + S \frac{\partial \phi^2}{\partial t}] dx_1 dx_2 ; \quad (C-11)$$

and

$$\begin{aligned} \Pi_T = 1/2 \iint [D_{ij} \left(\frac{\partial C}{\partial x_i} \frac{\partial C}{\partial x_j} \right) + g(D'_{ij}) \frac{\partial C}{\partial x_i} \frac{\partial C}{\partial x_j} - g q_i \frac{\partial C}{\partial x_i} C - 2RC \\ - \rho \frac{\partial C^2}{\partial t}] b dx_1 dx_2 + 1/2 \int H(C^2 - 2CC\infty) b ds + 1/2 \int g q_i C^2 b ds \\ + 2 \int g q_i C\infty C b ds ; \end{aligned} \quad (C-12)$$

where Π_w = total potential for water flow, Π_T = total potential for heat or mass transport, H = convection coefficient (units depend on type of problem), and b = aquifer thickness.

The next step is to minimize Eq. (C-11) and Eq. (C-12), which is accomplished by setting the first derivatives of Π_w and Π_T equal to zero. Before this is done, it is convenient to introduce the following approximating functions to describe the system at any interior point as a function of nodal values:

$$\phi = [N] \{\phi_N\} , \quad (C-13)$$

$$\partial \phi / \partial x = [n, x] \{\phi_N\} , \quad (C-14)$$

$$C = [N'] \{C_N\}, \text{ and} \quad (C-15)$$

$$\partial C / \partial x = [N', x] \{C_N\} , \quad (C-16)$$

where ϕ , C = potential and concentration respectively at any interior point; $\{\phi_N\}$ = ground-water potentials at nodal points in an element, a column matrix; $\{C_N\}$ = concentrations at nodal points in an element, a column matrix; and $[N]$, $[N']$ = shape functions which relate nodal values of potential or concentration to values at any point in the element, a row matrix. This program allows each element to have a minimum of 4 and a maximum of 12 nodes. For example, if an element has six nodes the shape function has the following form:

$$\phi = [N] \{\phi_N\} = N_1\phi_1 + N_2\phi_2 + N_3\phi_3 + N_4\phi_4 + N_5\phi_5 + N_6\phi_6 , \quad (C-17)$$

where $\phi_1 = \dots \phi_6$ are nodal values of potential.

Derivation of the coefficients of the shape functions is not straightforward, but an understanding of how they are derived is not necessary for a general understanding of the finite element method. It is sufficient to know that if an element side has two nodes the shape function is linear, if the element side has three nodes the shape function is quadratic, and if the element side has four nodes the shape function is cubic. Therefore, the more nodes in an element, the higher the order of the polynomial used to approximate an interior point. This program uses isoparametric elements of the serendipity family. (See Pinder and Gray 1977 for more details.)

To solve the flow problem Eq. (C-11) is then minimized as follows:

$$\begin{aligned} \frac{\partial \Pi_W}{\partial \{\phi_N\}} = & \quad bK_{ij} [N, x_i]^T [N, x_j] \partial x_1 \partial x_2 \{\phi_N\} - W[N] \partial x_1 \partial x_2 \\ & - S \frac{\partial \{\phi_N\}}{\partial \{\partial t\}} , \quad [N]^T [N] \partial x_1 \partial x_2 = 0 . \end{aligned} \quad (C-18)$$

The integrations are performed using Gaussian quadrature (Zienkiewicz 1971). After the equation is integrated, it is convenient to combine terms and put the equation in the following form:

$$[S] \{\phi_N\} = [C] \frac{\partial \{\phi_N\}}{\partial t} - [R] , \quad (C-19)$$

where $[s] = bK_{ij} [N, x_i]^T [N, x_j] \partial x_1 \partial x_2$, which is often called the element structure matrix; $[c] = S [N]^T [N] \partial x_1 \partial x_2$, which is called the element capacitance matrix; and $[r] = W [N] \partial x_1 \partial x_2$, which is called the element recharge matrix.

An equation in the form of Eq. (C-19) is developed for each element in an aquifer. These equations are then added to give the following equation:

$$[S] \{\phi_N\} = [C] \frac{\partial \{\phi_N\}}{\partial t} - [R] , \quad (C-20)$$

where $[S]$ = global structure matrix, $[C]$ = global capacitance matrix, and $[R]$ = global recharge matrix.

The column matrix will have one column for each node, and the square matrices will have a column and a row for each node. The square matrices will be symmetric and banded, and only half the matrix will be stored in the program.

The time derivative is evaluated by the Crank-Nicolson approximation:

$$([C] + \frac{\Delta t}{2} [S]) \{\phi_N\}^{i+1} = ([C] - [S] \frac{\Delta t}{2}) \{\phi_N\}^i + [R] \Delta t . \quad (C-21)$$

The final matrix equation is solved by Gaussian elimination (Cook 1974).

To solve the mass or heat transport problem, Eq. (C-12) is minimized as follows:

$$\begin{aligned} \frac{\Pi_T}{\partial \{C_N\}} = & [D_{ij} [N, x_i]^T [N, x_j] + g D'_{ij} [N, x_i]^T [N, x_j]] b dx_1 dx_2 \{C_N\} \\ & - g q_1 [N, x_i]^T [N] b \partial x_1 \partial x_2 \{C_N\} - \rho \frac{\partial \{C_N\}}{\partial t} [N]^T [N] b \partial x_1 \partial x_2 \\ & + H[N]^T [N] b dS \{C_N\} - H[N] C_\infty dS + q_1 g [N]^T [N] b dS \\ & \{C_N\} + q_1 g C_\infty [N] b dS - R[N] b \partial x_1 \partial x_2 = 0 . \end{aligned} \quad (C-22)$$

This equation can be reduced to a form analogous to Eq. (C-19). As before, one equation is developed for each element, and these equations are summed to give an equation analogous in form to Eq. (C-20). The time derivative is again evaluated by the Crank-Nicolson approximation. The final matrix equation, which is assymmetric due to the presence of the terms $[N, x_i]^T [N]$ in Eq. (C-22), is solved by the Gauss-Doolittle method (Desai and Abel 1972).

CONSIDERATIONS IN DESIGNING A FINITE ELEMENT GRID

The basic step in using a finite element scheme is to subdivide the region of interest into an assemblage of smaller regions called elements. The process of discretizing is an exercise of engineering judgment in which one must choose the number, shape, size, and configuration of elements in such a way that the original continuum is simulated as closely as possible. A grid configuration that provides a greater number of nodes will generate a more accurate solution, but at the same time will lead to more computational effort. In general, the mesh should be refined in the region of steep gradients. The element shapes are quadrilaterals having straight boundaries, although curved boundaries are also possible.

All boundary conditions described for Eq. (C-1) and (C-4), except for constant flux boundaries, are handled explicitly by the program and are explained in the data-input section of the appendix. A constant flux boundary of zero flux is assumed by the finite element method if no other boundary condition is specified. A finite flux boundary is treated by assigning a line source or sink of the appropriate magnitude. Four sample problems will be presented to illustrate the discretization procedure.

In designing the finite element grid, 10 considerations should be observed.

- 1) All elements should be made nearly rectangular, since distorted element shapes decrease the solution accuracy.
- 2) Elements with more than four nodes should be used sparingly. Although an element with more than four nodes uses a higher order approximation function for interior points, replacing an element with six nodes by two elements with four nodes each usually provides as good an approximation with less computational effort. (This occurs because a lower order Gaussian quadrature scheme can be used for elements with only four nodes.) Elements with more than four nodes are best utilized for refining the finite element grid in critical areas (Figure C-2).

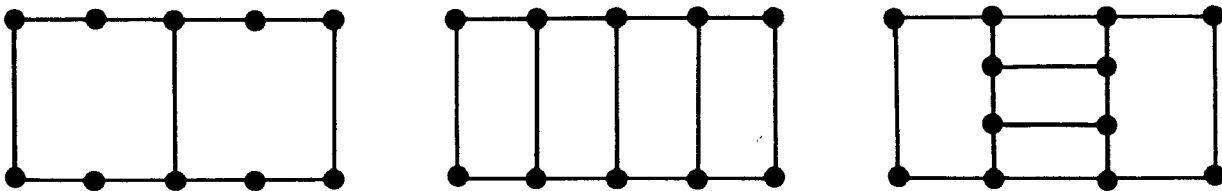


Figure C-2. Examples of refinement of a finite element grid. Left: bad use of multi-node sides; center: the preferred way of discretizing a region; right: good use of multi-node sides.

- 3) Nodes should be placed close together in areas where system parameters exhibit spatial changes, in areas where velocity is relatively rapid or the velocity distribution is complex, and in areas where a sharp temperature or concentration front is expected.
- 4) Exterior element boundaries across which a flux of mass or energy occurs must have only two nodes.
- 5) The velocity field near an exterior element boundary across which a flux of mass or energy occurs must not be complex. Preferably, all flow is normal to the boundary. This can be insured by setting up dummy elements along a boundary with a high hydraulic conductivity in a direction normal to the boundary. Likewise, the boundary should be oriented normal to one of the principle directions of the hydraulic conductivity tensor.
- 6) Boundaries within the area to be modeled should be located accurately. Distant boundaries can be located approximately with fewer nodes by expanding

the grid. Elements with more than four nodes are very useful for expanding the grid away from critical areas.

7) Constant concentration boundaries are generally unrealistic for the transport equation. Transport into the system can best be represented by multiplying the water flux across the boundary by the concentration exterior to the system.

8) The grid should be oriented to coincide with the principle directions of the hydraulic conductivity tensor.

9) The core requirements and computation time are proportional to the number of nodes representing the aquifer and to the number of times system parameters or time steps are changed.

10) If no boundary condition is specified along an exterior boundary, a no-flow boundary is assumed.

DATA DECK INSTRUCTIONS

The Data Groups

All data are read into the model with a free format, except for alphanumeric data. In free format, the data requested by one read statement may be put on one input card or as many input cards as the reader desires. Each bit of data, however, must be followed by either a comma or a blank. The data for each read statement must begin on a new card. Two read statements cannot read from the same card. The data and program output for four sample problems will be presented to illustrate the data deck preparation procedures. Several aspects of the data preparation that may be confusing are explained in more detail in the data notes following this section. The read statements that must be included on every program execution are underlined.

Group 1--

This group of data, which is read by both the main program and the data input subroutine, contains data required to dimension the model and data required to determine the type of problem.

<u>Read Statement</u>	<u>Variable</u>	<u>Definition</u>
1 and 2	TITLE	Any title that the user wishes to print on two lines at the start of output. The input must contain two cards.
3	LM	Number of elements
	LN	Number of nodes
	MBAND	Bandwidth (notes 1 and 2)

	KTYPE	An integer that can have values in the range of one to five. 1--problem to be solved is a steady-state ground-water problem. 2--problem to be solved is a transient ground-water problem. 3--problem to be solved is a steady-state ground-water problem linked to a transient heat or mass transfer problem. 4--problem to be solved is a transient ground-water problem linked to a transient heat or mass transfer problem. 5--problem to be solved is a transient mass or heat transfer problem.
	KPRINT	An integer that can have values of 0 or 1. Set to 0 to suppress printing of input data; otherwise set to 1.
	LON	Set to 99 for calculating coefficient matrix stability for a transient problem (see note 3); otherwise set to zero.
	MQ	Set to 2 if one card is to be read in for each element giving the element node numbers. Set to 0 if the spatial structure for the problem is rectangular and all elements have only four nodes (data group 11).
	NLA	An integer specifying the method to be used for calculating velocities in a linked problem. Set to 1 if velocities are to be calculated at each of the Gauss points; this is generally the better method. Set to 2 if velocities are to be calculated only at the center of each element. Set to 0 if the problem is not linked problem.
	CFACT	Set as 1E13; this value is used to maintain the specified boundary conditions. Set higher if specified boundaries are not reproduced by model.
5 and 6	V(I)	Format statement for printing out nodal values. Two cards are required (note 4).
7 and 8	VV(I)	Format statement for printing out element values. Two cards are required.

Group II--

The data contained in this group of cards are required to specify the spatial structure of the nodal array. The type of data to be input is determined by the value previously specified for variable MQ. If the structure is rectangular with four nodes per element, the program automatically generates a grid and numbers the nodes and elements, and the data input is simple. If the structure is not rectangular, the location of each node must be input as must cards specifying the nodes defining each element (notes 5, 6, 7, and 8).

<u>Read Statement</u>	<u>Variable</u>	<u>Definition</u>
1	Q	Input the alphanumeric characters--up 11.

IF MQ equals 2 only:

one card for each node	J XLOC YLOC	node number X location of the node Y location of the node
one card for each element	J NOD(K,1) NOD(K,2) NOD(K,3) NOD(K,4) NOD(K,5) . . NOD(K,1)	element number The element node numbers. The node numbers for each element <u>must</u> be listed counter-clockwise, starting at the corner nearest the origin. List the nodes in sequence; if a node is not a corner node, place an asterisk after it. Repeat the first node as the last value on each card.

IF MQ equals 0 only:

2	KSPACX KSPACY	Number of nodes in the X direction. Number of nodes in the Y direction.
3	B(I)	KSPACX values, listing the X coordinates in order; <u>smallest</u> value should be listed first.
4	C(I)	KSPACY values, listing the Y coordinates in order; <u>largest</u> value should be listed first.
5	MLS	Optional (note 8).
6	D(I)	Optional (note 8).

Group III--

This group of data contains information on the initial conditions and on the specified boundary conditions. The data to be read in depends on the value specified for KTYPE.

<u>Read Statement</u>	<u>Variable</u>	<u>Definition</u>
1	Q	Input the alphanumeric characters-- Ill.
IF KTYPE equals 1:		
2	HEA(I)	Array used to specify constant potential boundaries. A zero is entered if a potential is not specified at the node; otherwise the specified potential value is entered. See note 9 for the format for entering these values.
IF KTYPE equals 2:		
2	ALPH ALPHM	The length of each time step. Multiplication factor for each time step. Length of the next time step is equal to the length of the old time step multiplied by ALPHM. The program works most efficiently if ALPHM equals 1.
	KBOUND	Set to 1 if subroutine BOUND is to be called at each time step during execution of water-flow equation. Set to 2 if subroutine BVAL is to be called at each time step during execution of water-flow equation (note 13). Set to 99 when determining structure matrix stability for water-flow equation (note 3). Otherwise set to 0.
3	R1(I)	Array used to specify the initial potential at each node (use format explained in note 9).
4	HEA(I)	See above.
IF KTYPE equals 3:		
2	ALPHA ALPHAM KBOUND	The length of time step for heat/mass equation. Multiplication factor for the time step. An integer then can have values 0, 1, 2, or 99. See KBOUND above, except KBOUND applies to the heat or mass flow equation.
	PCW	Heat capacity of water, or 1 in a mass transport problem with units of meters, grams, and ppm.
3	R(I)	An array used to specify the initial temperature or concentration at each node (note 9).

4	HEA(I)	See above. Specified potential values.
5	HEAD(I)	Array used to identify specified concentration boundaries. A zero is entered if temperature or concentration is not specified at the node; otherwise the specified value is entered (note 9).

IF KTYPE equals 4 or 5:

2	ALPH ALPHM BOUN	See description above.
3	R1(I)	See description above.
4	ALPHA ALPHAM BOUND PCW	See description above.
5	R(I)	See description above.
6	HEA(I)	See description above.
7	HEAD(I)	See description above.

Group IV--

This group of data contains information on the model parameters.

<u>Read Statement</u>	<u>Variable</u>	<u>Definition</u>
1	Q	Input the alphanumeric characters-- Group IV.
2	NMATA	An integer, less than 51, specifying the number of different material types in the problem. A homogeneous area has only one material type.
3	FACTH	This card contains multiplication factors for the parameters to be input later. Factor for X direction hydraulic conductivity.
	FACTV	Factor for Y direction hydraulic conductivity.
	FACTWS	Factor for storage coefficient.
	FACTH1	Factor for X direction thermal conductivity.
	FACTV1	Factor for Y direction thermal conductivity.
	FACTHS	Factor for specific heat capacity of saturated medium.

	FACTDL	Factor for longitudinal dispersivity.
	FACTDT	Factor for transverse dispersivity.
<u>4</u>	MAT(J)	Type of material array. Integer values in the range of 1-50 are entered for each element, indicating the type of material in that element (format explained in note 9).
<u>NMATA cards</u> , one card for each material type.	J	Integer number in the range of 1-15 identifying the material type.
	WX	X-direction hydraulic conductivity
	WY	Y-direction hydraulic conductivity
	STO	Storage coefficient
	PX	X direction thermal conductivity, or molecular diffusion coefficient.
	PY	Y direction thermal conductivity or Y direction molecular diffusion coefficient.
	PCX	Heat capacity of the saturated medium, or in a mass transfer problem the porosity.
	DIFF(J,1)	Dispersivity coefficient, lateral.
	DIFF(J,2)	Dispersivity coefficient, transverse.

NOTE: Only values for J, WX, WY, and STO need be entered if KTYPE equals 1 or 2. If KTYPE equals 5, values for WX, WY, and STO must not be entered.

Group V--

This group of data contains information on sources and sinks. Line, areal, or point or sinks can be handled directly. Sources are positive, sinks are negative. If there are no or sinks, three cards must be entered, each with two zeros.

<u>Read Statement</u>	<u>Variable</u>	<u>Definition</u>
<u>1</u>	Q	Input the alphanumeric characters--Group V.
<u>2</u>	KGEN	Set to 1 if there is a uniform source or sink of water over at least one element in the problem; otherwise set to zero.
	KGENH	Set to 1 if there is a uniform source of energy or mass over one element in the problem; otherwise set to 0.
<u>3</u>	INFLOW(J)	Include this only if KGEN is not equal to 0. One value for each element specifying the rate of water generation per unit area per unit time in the element (note 9).
<u>4</u>	HEAT(J)	Include this only if KGENH is greater than 0. One value for each element specifying

		the rate of mass or heat generation per unit area per unit time in the element (note 9).
5	LWATER	Integer values specifying the number of point or sinks of water.
	LHEAT	The number of point sources or sinks of energy or mass.
6	NWATER(J)	Node number of a point source or sink of water.
	AWATER(J)	Rate of water pumpage per unit time. Enter sufficient cards to contain a node number and a rate for each water point source.
7	NHEAT(J)	Node number of point source of energy or mass.
	AHEAT(J)	Rate of energy or mass generation per unit time at the specified source. Enter sufficient cards to contain a node number and a rate for each point source.
8	LINEW	An integer specifying the number of line sources or sinks of water.
	LINEH	An integer specifying the number of line sources or sinks of heat.
9	NLINEW(I,1) NLINEW(I,2)	Element number of line source of water and boundary code (note 10). Enter sufficient cards to contain an element number and a code for each line source of water.
10	ALINEW(I)	Enter one value for each line source giving the rate of water recharge or discharge per unit length per unit time.
11	NLINEH(I,1) NLINEH(I,2)	Element number of line source of heat or mass and boundary code (note 8). Enter two values for each line source of heat or mass.
12	ALINEH(I)	Enter one value for each line source giving rate of heat input or output per unit length per unit time.

Group VI--

Data specifying if the problem is a cross-section problem or an areal problem.

<u>Read Statement</u>	<u>Variable</u>	<u>Definition</u>
1	Q	Input the alphanumeric characters--Group VI.
2	KAREAL	Set to 0 for cross-section problems; set to 1 for areal problems.
3	ER	Error criteria on ground-water potential for a steady-state problem. Solution is reached by an iterative procedure in which transmissivities are adjusted until the potential changes by less than the error criteria.
	ITER	Number of iterations permitted for a steady-state solution to be reached.
4	BOT(I)	Include only if KAREAL equals 1. Enter the bottom elevation of the aquifer at each node (note 9).
5	R1(I)	Initial potential values in the aquifer (use format explained in note 9). Do not input values if the initial values were input in data Group III.

Group VII--

This group of data contains information on the location of flow and convective flux boundaries. These types of boundaries are only used in the mass or heat transport equations. Skip cards 2-7 of this group if the problem is not a linked one. Flow and convective boundaries are discussed in data note 11.

<u>Read Statement</u>	<u>Variable</u>	<u>Definition</u>
1	Q	Input the alphanumeric characters--Group VII.
2	NCONV	An integer specifying the number of convective boundaries.
3	NCON(I,1)	Element number of the element containing this type of boundary.
	NCON(I,2)	This boundary code identifying the side across which the flux occurs.
	CONV(I)	The value of the convection (transfer) coefficient for a convective boundary.
		Include sufficient cards to contain three values for each boundary of this type.

4	TINF(I)	The temperature at a distance from the boundary (temperature at infinity). List one value for each boundary identified by card 3 of this group, and list them in the same order as on card 3.
5	LEL	An integer specifying the number of element sides across which a flux of water occurs.
6	NEL(I,1) NEL(I,2)	Element number and the boundary code. Include two values for each element boundary of this type.
7	AEL(I,2)	One value for each element boundary of this type specifying the temperature or concentration of the incoming fluid.

Group VIII--

This group of data contains information needed for calculating a mass balance. The data identifies the exterior boundaries on which potential, temperature, or concentration are specified (refer to data note 12).

<u>Read Statement</u>	<u>Variable</u>	<u>Definition</u>
1	Q	Input the alphanumeric characters-- Group VIII.
2	LFLUXW	An integer specifying the number of exterior element sides on which potential is specified.
	LFLUXH	An integer specifying the number of exterior element sides on which temperature or concentration is specified.
3		Include only if LFLUXW is greater than 0. Use sufficient cards to list two values for each element side.
	NFLUXW(I,1)	Element number of element with a specified potential on an exterior side.
	NFLUXW(I,2)	Side index number, identifying which of the four element sides the flux is across. An integer in the range of 1 to 4. See explanation notes.
4	NFLUXH(I,1) NFLUXH(I,2)	Include only if LFLUXH is greater than zero. Format is the same as above, except that here boundaries must be identified on which temperature or concentration is specified.

Group IX--

This group of data contains information that controls the flow of the program and allows access to routines for changing boundary conditions at each time step, and it includes a routine for a moving boundary in a cross-section problem (see data note 14).

<u>Read Statement</u>	<u>Variable</u>	<u>Definition</u>
1	Q	Input the alphanumeric characters--Group IX.
2	LA	Set to 0 unless ENTRY LAKE is to be called; if so set to 1.
	LD	Set to 0 unless ENTRY CHANG or ENTRY CHAN is to be called; if so set to 1.
	LE	Set to 0 unless water flows are to recompute at uneven intervals; if so, LE should equal the number of intervals at which water flows are to be recomputed (must be less than 100).
	LF	Set to 0 unless the problem is to be posed in radial coordinates; if so, set to 1.
	LG	Set to 0 unless the problem is to have a moving boundary; if so, set LG equal to the number of nodes which are to move.
	LH	Set to 0.
3	NTIME(I)	Include only if LE is greater than 0. LE values listing the time steps at which flows are to be recomputed; values must be listed in increasing order.
4		Include only if LF is equal to 1. Input 1,1,1,0,0,0 if problem is to be quasi-radial with aquifer thickness being equal to the x coordinate. Input -1,1,1,0,0,0 if problem is to be quasi-radial with aquifer thickness being equal to the y coordinate.
5		Input values needed by ENTRY LAKE.
6		Input values needed by subroutine ADJUST (note 14).

If KTYPE equals 1:

7	Mw	Set to 1 if potentials are to be written on file 14; otherwise set to 2.
---	----	--

If KTYPE equals 2:

7	MA	Total number of time units for the simulation.
	MB	Number of time steps between printing of head values.
	MW	Number of time steps between writing heads on file 14.
	MC	Number of time steps between printing of mass balance.
	MD	Number of time steps between printing of flows. (MA, MB, MW, MC, and MD must not equal zero.)

If KTYPE equals 3, 4, or 5:

7	MO	Total number of time units for the simulation.
	MP	Number of time steps between printing nodal values.
	MV	Number of time steps between printing nodal values on file 14.
	MQ	Number of time steps between printing of mass balance; if set to a negative number, mass balances will not be computed which results in a considerable savings in CPU time.
	MR	Number of time steps between recomputing water flows.
	MS	Set to 1 if initial hydraulic conductivity values are to be adjusted for changing temperature in the aquifer; otherwise set to 0 (note 15).
	MT	Set to 1 if using dispersivities greater than zero; otherwise set to 0.
	MU	Set to 1 if water flows are not to be printed when flows are recomputed; otherwise set to 0. (MO, MP, MV, MQ, and MR must not equal zero.)
	ME	Set to 1 if the program is to stop after water flows are computed; otherwise set to 0.

Data Explanation Notes

1) Program size--

The storage required for the program is approximately

$$2000 + \text{LN}(11 + \text{MBAND} \times 4) + \text{LM} \times 25,$$

where LN is the number of nodes, LM is the number of elements, and MBAND is the bandwidth.

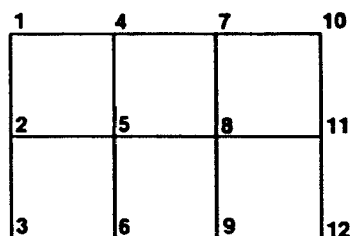
The second statement in the main program is used to change the amount of storage allocated for the program. The parameter variable N specifies the maximum number of nodes, the parameter variable L specifies the maximum number of elements, and the parameter variable M specifies the maximum bandwidth. On a UNIVAC 1110, if the program is compiled in FORTRAN V, the combination of 297 nodes, 260 elements, and a bandwidth of 13 is the maximum permissible. This arrangement uses 64K of memory. If the program is compiled in ASCII FORTRAN on a UNIVAC 1110, the program size could be quadrupled.

If the program is being used only to solve potential problems, the value of the parameter variable M in statement of 1 of the main program need only be equal to one-half the bandwidth plus one. For a linked problem M must be equal to or less than the bandwidth.

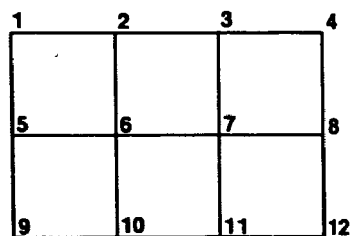
Also, if LWATER, LHEAT, NWATER, NHEAT, LINEW, LINEH (data Group V), NCONV, LEL (data Group VII), LFLUXW, or LFLUXH (data Group VIII) exceed 50, statement 1 of the main program must be changed. The parameter variable Z must be changed from Z = 50 to Z = the maximum value of the above-listed variables.

2) Bandwidth--

The bandwidth depends upon the largest difference between any two nodes in a single element and is equal to the maximum difference between any two nodes in an element in a structure plus one (Figure C-3).



(a) bandwidth equals five



(b) bandwidth equals six

Figure C-3. Examples of numbering of nodes in a structure.

The nodes in a structure should be numbered so as to make the bandwidth as small as possible.

3) Calculation of Stability for a Transient Problem--

The ELGEN subroutine computes the maximum (critical) time step that can be used in a transient simulation to insure that the solution computed by the Crank-Nicolson method will be nonoscillatory. The routine is based on a modified Eigen value extraction technique developed by Myers (1978). The scheme slightly underestimates the maximum (critical) time step. The equation used to estimate the critical time step is

$$\Delta t_c = \frac{1}{2} \min_{i=1}^{LN} \left(\frac{C_{i,i}}{LN \sum_{j=1, j \neq i}^{LN} |S_{i,j}|} \right)$$

where Δt_c = safe estimate of the critical time step, $S_{i,j}$ = the j th entry in the i th row of the structure matrix, and $C_{i,i}$ = the diagonal term in the i th row of the capacitance matrix.

The critical time step is a function of system parameters, the x and y spacing, and boundary conditions. The routine prints out the maximum time step for each node in the structure and prints out the critical time step.

4) Standard FORTRAN formats--

Standard FORTRAN formats are used for printing node and elements values. Values are printed consecutively starting with the value for node or element 1. The format input statements allow the user to specify how the values are to be printed out. This option can be very helpful if an irregular grid is used.

Typical formats for printing out node and element values for a grid 5 nodes by 5 nodes would be: (1X,5(5G12.6//)) for the node values; and (1X,4(4G12.6//)) for the element values. (The word FORMAT is not used; the '(' goes in column one of the data card.) The node values would then be printed out on five lines, five values on each line.

5) Orientation of the Finite Element Grid--

The finite element grid must be orientated correctly, since flows and boundary conditions will be treated incorrectly if the grid is orientated incorrectly. The program requires a standard cartesian orientation (Figure C-4).

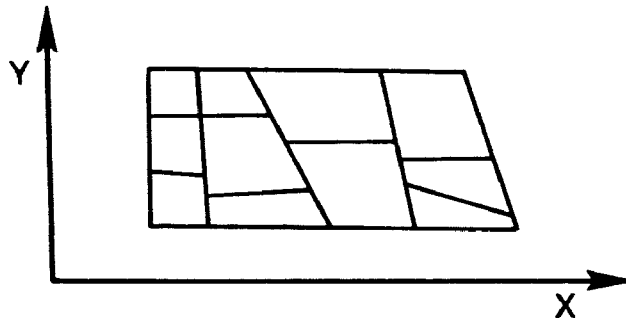


Figure C-4. Cartesian orientation of finite element grid.

Values in the x direction must increase from left to the right and values in the y direction must increase from the bottom to the top.

6) Element Node Numbering--

Typical elements are shown in Figure C-5 to illustrate the manner in which element node numbers must be input to the program.

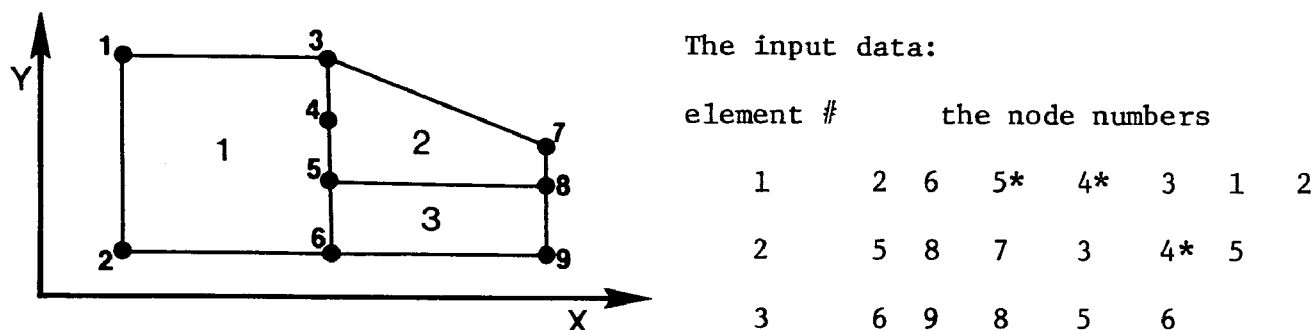


Figure C-5. Typical elements of a finite element grid and the correct method of numbering the elements.

7) The Rectangular Grid Generator--

The rectangular grid generator generates a grid in which the nodes and elements are numbered in the form shown in Figure C-6.

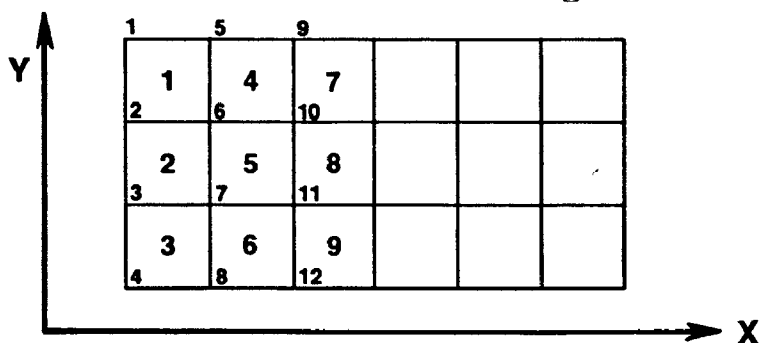


Figure C-6. Numbering of nodes and elements in a rectangular grid.

The program assigns to node 1 the first x and y coordinates read in. For proper orientation the list of x-coordinate values read in must be arranged so the smallest value is read in first, and the list of y coordinates must be arranged so that the largest value is read in first.

8) Selection of Variants of Rectangular Grid--

The program can create the two variants of a rectangular grid shown in Figure C-7.

To select the options shown in Figure C-7:

1) set $KSPACX = -KSPACX$.

2) set $MLS = 0$ for option (a); set $MLS = 1$ for option (b).

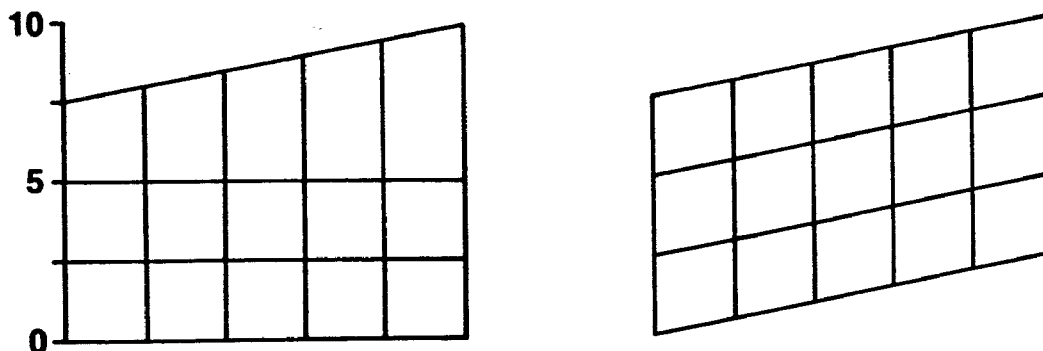


Figure C-7. Two variants of a rectangular grid that can be generated.
Left: grid with sloping upper surface; right: grid with all rows sloping.

3) Input KSPACX values for the D array. Input one value for each set of nodes in the x direction. These values specify how much the y coordinates of the nodes are to be adjusted from the values specified by C(I). For the examples illustrated above the values in the D array would be: 0, 0.5, 1.0, 1.5, 2.0, 2.5. These values need not increase or decrease monotonically.

9) Format for Reading in Array Data--

Several options are provided to the user to simplify the often arduous task of initializing array value. The user must initially specify one value to be assigned to every position in the array. The user then has the options of (1) leaving the array as is, (2) reinitializing the entire array by inputting one value for each position in the array, or (3) selectively changing the initialization. The last option is accomplished by specifying the array position that is to be reinitialized and the new value. An array position will correspond to a node or element number. This format may be used when initializing R, R1, HEA, HEAD, MAT, and BOT.

The format to be used is:

<u>Read Statement</u>	<u>Variable</u>	<u>Definition</u>
1	QI	Value to be assigned initially to each position in the array.
	IZ	Three options: a. set to -1 if one value is to be input for each node or element. b. set to 0 if all values in the array equal QI. c. set to a positive integer specifying the number of array values to be different from QI.
	FACT	Factor by which each of the array values is to be multiplied.

If IZ = -1:

2
(sufficient cards to
contain one value for
each node or element)

Enter the values to be assigned to each node or element. Values are to be entered consecutively beginning with node or element 1. After one value is entered for each node or element, enter 999 which is a sentinel character.

If IZ = 0:

No cards are needed.

If IZ > 0:

2
(sufficient cards to
contain IZ x 2 values)

Enter a node or element number and the value to be assigned to this node or element. Enter two values for each array position that is to be reinitialized.

10) Boundary Codes--

When specifying line fluxes and boundary fluxes, the side of an element across which the flux is occurring must be designated. The sides of an element are coded as shown in Figure C-8.

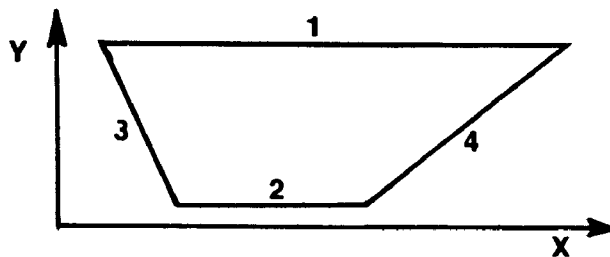


Figure C-8. Numbering of sides of an element.

11) Flow Boundaries--

Data Group VII allows the user to specify several types of boundary fluxes. The type of boundary fluxes permitted across an element side are:

convective, where transfer is equal to $AH(T_i - T^\infty)$;

flow out, where transfer is equal to $V_i T_i A$;

flow in, where transfer is equal to $V_i T^\infty A$;

where A = the length of the element side multiplied by the aquifer thickness;
 H = a transfer coefficient; for heat transfer the units are, $H/L^2 t T$; T_i = temperature or concentration on the boundary; T^∞ = temperature or concentration beyond the boundary; and V_i = water velocity normal to the boundary.

If the boundary is to have more than one type of flux, for example, a flow and a convective flux, it should be treated for purposes of data input as though there were two separate boundaries.

12) Mass Balance--

The mass balance routine computes an approximate mass balance. Several types of boundary fluxes are computed only approximately by the mass balance routine, and often the mass balance errors calculated by this routine will be much higher than they really are. The program generally has mass balance errors of less than 1% for both the water-flow and the transport equations. The user must identify the specified head and temperature or concentration boundary conditions. The program identifies the other boundary conditions and sources and sinks.

13) Boundary Conditions That Vary With Time--

Because the program could handle a variety of boundary conditions that might change at each time step, a program to cover all possibilities could not be written. The user must write additional routines to change boundary values at each time step.

Several entry points in subroutine BOUND are provided for this. Starting addresses for all arrays in which a user is likely to change values at each time step are passed to this subroutine as well as the time step counter KS. The entry points available in this subroutine are:

(a) ENTRY LAKE

The routine is called if LA = 1 (data Group IX). This routine is called immediately after the data input routine and is called only once for a given program execution. The routine can be used to read in information to be used in altering boundary conditions during execution of the program.

(b) ENTRY BOUND

Called during solution of the water-flow equation by subroutine LOAD if KBOUN (data Group III) equals 1, or called during solution of the transport equation by subroutine LOAD if KBOUND equals 1.

(c) ENTRY BVAL

Called during solution of the water-flow equation by subroutine LOAD if KBOUN equals 2, or called during solution of the transport equation by subroutine LOAD if KBOUND equals 2.

(d) ENTRY CHANG

Called during solution of the transport equation by subroutine LOAD if LD = 1 (data Group IX).

(e) ENTRY CHAN

Called during solution of the water-flow equation by subroutine LOAD if LD = 1. The program logic is shown on the program flow chart, which shows the position of the calls to the entry points in BOUNDA by subroutine LOAD.

14) Documentation for Moving Boundary Routine--

For cross-section problems the surface boundary can be programmed to move in response to changing recharge rates. Only boundaries with boundary code 1 may move (note 10). The moving boundary routine is called by setting the 5th value (LG) on card 1, Group IX, equal to the number of nodes that will move. The following cards are then added in the appropriate position in data group IX.

<u>Read Statement</u>	<u>Variable</u>	<u>Definition</u>
1	NSTEP	Number of time periods to be stimulated.
	NPRINT	Number of time periods between printing of potentials.
	NPR	Number of time periods between printing flows and mass balance.
	ERROR	Change allowed in node location before structure matrix is recomputed.
	FACTOR	Factor to be multiplied by recharge rates.
2	Four values for each moving boundary:	
	NMOV(J,1)	Element number on left of node*,
	NMOV(J,2)	Element number on right of node*,
	BMOV(J,3)	Storage coefficient,
	BMOV(J,6)	Initial recharge rate.

*Note: If several nodes are to be constrained to rise and fall at the same rate, the left and right element number for each node of this type must be preceded by a minus sign (-).

After the last card of Group IX one card is added for each pumping period.

<u>Read Statement</u>	<u>Variable</u>	<u>Definition</u>
	BKS	Identifier for this time period.
	TIME	Length of this time period.
	FACT	Factor that relates initial recharge rates to recharge rates at this time step. The current recharge rates are calculated by multiplying FACT by initial recharge rate.

15) Hydraulic Conductivity as a function of Temperature--

The program in subroutine PE adjusts hydraulic conductivities for changing temperature distributions. The following relations are used:

$$\mu = (1.917 - 0.05635T + 0.0071T^2) \times 10^{-3}, \text{ and}$$

$$K_1 = K_{150} \times 1.21/\mu ,$$

where μ = the kinematic viscosity in centimeter-gram-second units, and T = the temperature in degrees centigrade.

The relationship is only valid for temperatures between 0° and 50°C. The relation also assumes that the initial hydraulic conductivities are specified at a temperature of 15°C. The relationship could easily be reprogrammed to cover a different temperature range or to relate hydraulic conductivities to concentration.

DERIVATION OF A HEAT TRANSPORT EQUATION

The processes that control the transport of heat in an aquifer are in many ways analogous to the processes that control the transport of mass in an aquifer. The partial differential equation describing the transport of mass is well known, and its derivation is clearly explained in Konikow and Grove (1977) and is rigorously derived in Bear (1972). Rather than derive the heat transport equation from first principles, which would in many respects repeat Konikow and Grove (1977), we show how the mass transport equation can be modified to apply to the transport of heat.

These assumptions are made in this derivation:

- 1) The aquifer is incompressible and chemically inert with respect to the fluid;
- 2) Fluid density is constant;
- 3) Hydraulic head is the only driving force; coupled processes, Onsanger relationships, and density driven convections are not considered;
- 4) Fluid flow is laminar; and
- 5) Divergence of velocity equals zero.

In addition to these five assumptions the generalized mass transport equation

$$\frac{\partial}{\partial x_i} \left(D_{ij} \frac{\partial C}{\partial x_j} \right) + \frac{\partial}{\partial x_i} \left(D'_{ij} \frac{\partial C}{\partial x_j} \right) - q_i \frac{\partial C}{\partial x_i} - R - n \frac{\partial C}{\partial t} = 0 , \quad (C-23)$$

as derived by Bear (1972) and Konikow and Grove (1977), assumes the following about the processes that transport mass in an aquifer: (1) Velocity driven convection, molecular diffusion, and mechanical dispersion are the only transfer processes; and (2) no transfer of mass occurs within the solid phase.

In an aquifer the basic modes of heat transfer are (Lagarde 1965, quoted in Bear 1972, p. 640) heat transfer through the solid phase by conduction,

heat transfer through the fluid phase by conduction, heat transfer through the fluid phase by convection, and heat transfer by dispersion.

Each of the terms in Eq. (C-23) is discussed sequentially to demonstrate how a similar form for each term can be used to describe the transport of heat in an aquifer.

Molecular Diffusion

Heat, unlike mass, is readily transmitted through the solid phase of most porous media if a temperature gradient exists. In the derivation of the first term of Eq. (C-23), it was assumed that transport does not occur in the solid phase. The coefficient of molecular diffusion in the mass transport equation is defined on the basis of tortuosity (Bear 1972), a concept that is applicable if transfer only takes place through the fluid phase.

The transfer of heat by molecular diffusion (conduction) through the solid phase and the fluid phase can be treated by assuming a simple parallel conduction model in which conduction through the fluid phase occurs separately but simultaneously with no interchange of heat between the two media. The real situation is more complex since heat is interchanged continuously between the two phases. Experimental data (Houpert 1965, quoted in Bear 1972, p. 646) suggest that the simple model is sufficient, and the assumption of simultaneousness is valid if the time period is greater than a few minutes.

Therefore, heat conduction can be described by

$$\frac{n\partial}{\partial x_i} (k_{f_{ij}} \frac{\partial C}{\partial x_j}) + (1-n) \frac{\partial}{\partial x_i} (k_{s_{ij}} \frac{\partial C}{\partial x_j}) , \quad (C-24)$$

where $k_{f_{ij}}$ = coefficient of thermal molecular diffusion for the fluid phase, $k_{s_{ij}}$ = coefficient of thermal molecular diffusion for the solid phase, and n = the porosity.

Dispersive Transfer of Heat

The form of the second term in Eq. (C-23) was derived from experimental data for mass transport in porous media. Green (1963) concludes on the basis of experimental data that in the range of Darcian flow the influence of the passage of heat through the solid phase will be insignificant and that the dispersive transfer of mass and heat will be identical. (Dispersive transfer is a term used to describe convective transfer that occurs due to velocity fluctuations in the fluid.)

Internal Generation of Heat

Heat will be generated by a moving fluid because of energy dissipation by viscous stresses. The rate of dissipation, E , can be estimated from

$$E = \rho q g \frac{\partial \phi}{\partial x} ,$$

where g = the gravitational constant and ρ = fluid density.

A fluid flowing at a rate of 1 m/day, with a gradient of 1 m/m, will dissipate energy at the rate of 10^{-13} cal/m³ per day. Therefore, heat dissipation is considered to be negligible.

The Absorption of Heat by the Solid Phase

The absorption of heat by the solid phase can be treated analogously to the adsorption of mass by the solid phase when the process is characterized by a linear adsorption isotherm. The last term of E. (C-23) can be modified (Bear 1972, Pickens and Lennox 1977) to

$$n \frac{\partial C}{\partial t} + (1-n) A \frac{\partial C}{\partial t} \quad (C-25)$$

to treat the adsorption of mass by the solid phase, where A = the adsorption distribution coefficient that describes the ratio of solute on the solid phase to solute in the fluid phase.

If A is defined to be the ratio of heat in the solid phase to heat in the fluid phase, Eq. (C-25) can be used to describe the absorption of heat by the solid phase in a porous medium.

The heat transport equation can then be obtained by substituting the terms developed above into Eq. (C-23):

$$\begin{aligned} \frac{\partial}{\partial x_i} \left[(n k_{f_{ij}} \frac{\partial C}{\partial x_j}) + (1-n) k_{s_{ij}} \frac{\partial C}{\partial x_j} \right] + (D'_{ij} \frac{\partial}{\partial x_i}) - q_i \frac{\partial C}{\partial x_i} \\ - R - n \frac{\partial C}{\partial t} - (1-n) A \frac{\partial C}{\partial t} = 0 . \end{aligned} \quad (C-26)$$

By convention the concentration of heat is generally expressed as a temperature, where concentration equals temperature multiplied by the heat capacity. The heat capacities of a fluid and solid phase are generally not the same. Each term in Eq. (C-26) refers to heat transfer in either the solid or the fluid phase; no term refers to a combined heat transfer. Making the appropriate substitutions, Eq. (C-26) can be written as:

$$\begin{aligned} \frac{\partial}{\partial x_i} \left[(n \rho C_w k_{f_{ij}} \frac{\partial T}{\partial x_j}) + (1-n) \rho C_{sol} k_{s_{ij}} \frac{\partial T}{\partial x_j} \right] + \frac{\partial}{\partial x_i} \rho C_w (D_{ij} \frac{\partial T}{\partial x_j}) \\ - \rho C_w q_i \frac{\partial T}{\partial x_i} - R - \rho C_w \frac{\partial T}{\partial t} - \rho C_w (1-n) A \frac{\partial T}{\partial t} = 0 , \end{aligned} \quad (C-27)$$

where ρC_w = heat capacity of the fluid, H/L³°C; and ρC_{sol} = heat capacity of the solid phase, H/L³°C. The equation can be simplified by introducing the following conventions.

$$1) K_{ij} = (1-n) \rho C_{sol} k_{s_{ij}} + n \rho C_w k_{f_{ij}},$$

where K_{ij} are the components of the thermal conductivity tensor for the saturated media. It is much simpler to determine experimentally the combined coefficient than the individual ones, which are a function not only of phase composition but also of phase geometry.

2) The absorption distribution coefficient $A = \rho C_{sol}/\rho C_w$. This relationship holds by definition.

3) The heat capacity of a whole is equal to the sum of the heat capacities of its parts: $\rho C_s = n\rho C_w + (1-n)\rho C_{sol}$.

Equation (C-27) then reduces to the following form when the substitutions are made which is in the same form as Eq. (C-23):

$$\frac{\partial}{\partial x_i} (K_{ij}^T \frac{\partial T}{\partial x_j}) + \frac{\partial}{\partial x_i} \rho C_w (D_{ij} \frac{\partial T}{\partial x_j}) - \rho C_w q_i \frac{\partial T}{\partial x_i} - R - \rho C_s \frac{\partial T}{\partial t} = 0, \quad (C-28)$$

SAMPLE PROBLEMS

Linear Heat Transport

This example problem demonstrates the use of all linear elements and the use of mixed higher order elements to solve a one-dimensional convective heat transport problem. The problem analyzed and the finite element grids used to discretize the problem are shown in Figure C-9. The parameters used in the problem are listed in Table C-2. The input data and the program-generated output for both sample simulations are listed in Figures C-10, C-11, C-12, and C-13. The simulated temperatures are nearly identical for both the grid with mixed elements and the one with all linear elements (Table C-3). Simulated temperatures differ by less than 0.5°C.

In analogy to Ogata and Banks (1961), an analytical solution to the linear convective heat transport problem is:

$$T = T_o/Z \left[\operatorname{erfc}\left(\frac{x-q't}{Z(K't/\rho C_s)^{1/2}}\right) + \exp\left(-\frac{xq\rho C_w}{K'}\right) \operatorname{erfc}\left(\frac{x+q't}{Z(K't/\rho C_s)^{1/2}}\right) \right], \quad (C-29)$$

where $q' = q\rho C_w/\rho C_s$, and $K' = K^t + q\alpha_T \rho C_w$, in which the following boundary conditions are used:

$$\begin{aligned} T(x,0) &= 0, \quad x > 0; \\ T(0,t) &= T_o, \quad t \geq 0; \text{ and} \\ T(\infty,t) &= 0, \quad t \geq 0. \end{aligned}$$

The analytical solutions at $t = 25, 50, 75$ days are shown with the simulated temperatures in Figure C-14. The analytical solution at $t = 50$ days is compared to the simulated temperatures at $t = 50$ days in Table C-3. In addition, the simulated temperatures for the all linear element grid with nodes 21 and 22 specified at 15°C at $t = 50$ days are also presented in Table

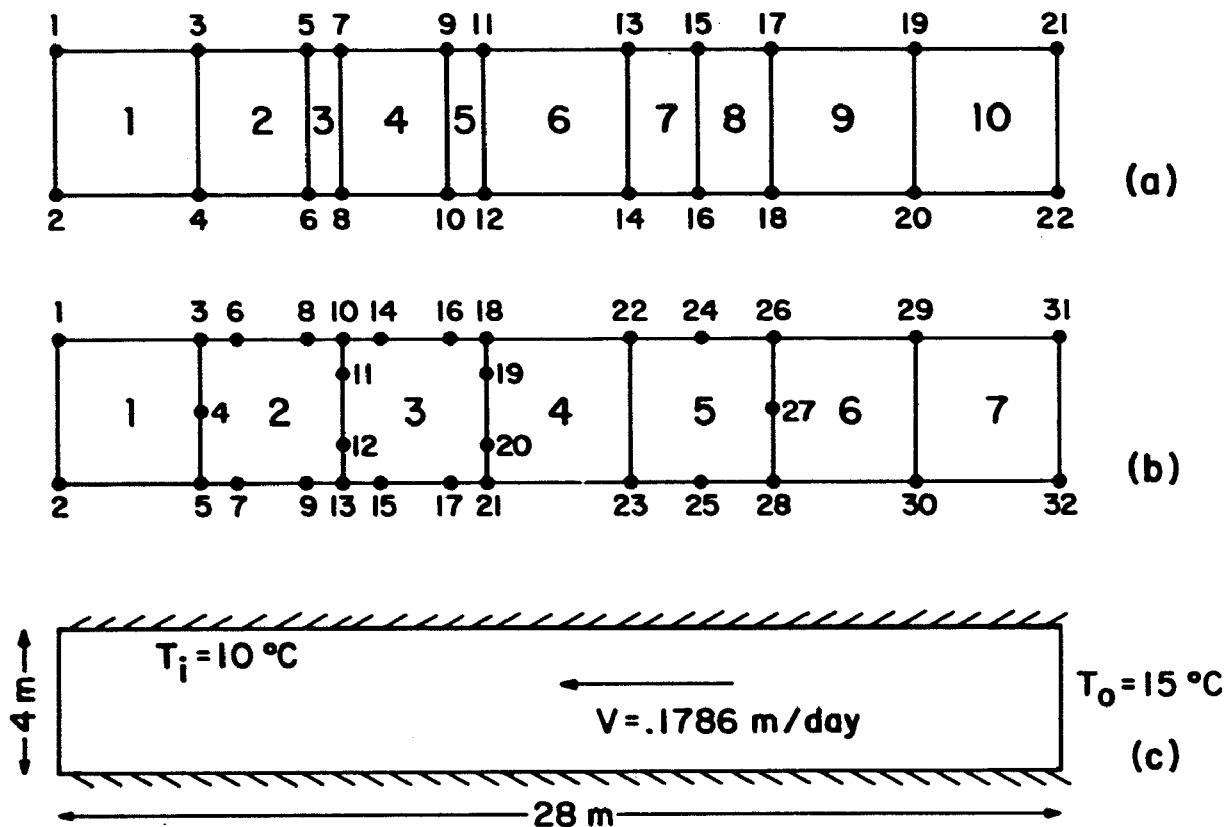


Figure C-9. Finite element grids used to discretize a linear heat transport problem. The problem is depicted in (c). The grid with all linear elements is shown in (a), and the grid with mixed higher order elements is shown in (b). Both node numbers and element numbers are shown in (a) and (b).

Convective test problem rectangular matrix
Units used are meters, days, celsius, calories

```

10 22 4
3 0 0 0 1 1E13
(1x,2G12.6)

(1x,7G12.6)

GROUP II
11 2
0 4 7 8 11 12 16 18 20 24 28
4 0
GROUP III
.5 1 0 1E6
10 0 1
0 4 1
1 100 2 100 21 105 22 105
0 0 1
GROUP IV
1
1 1 1 1 1 1 1 1
1 0 1
1 1 1 0 55000 55000 700000 .1 .1
GROUP V
0 0
0 0
0 0
GROUP VI
0
GROUP VII
1
1 3 0
10
1
10 4 0
15
GROUP VIII
2 0
1 3 10 4
GROUP IX
0 0 0 0 0 0 0 0
75 50 150 50 150 0 1 0

```

Figure C-10. The input data used to model one-dimensional heat transport with all linear elements.

TABLE C-2. PARAMETERS, INITIAL CONDITIONS, AND BOUNDARY CONDITIONS
USED FOR THE HEAT-FLOW EQUATION IN THE LINEAR HEAT TRANSPORT PROBLEM^a

Parameters		Initial conditions	Boundary conditions
V	0.1786 m/day	$T_i = 10^\circ\text{C}$ at all nodes	Dirichlet (convective flow) boundaries at $x = 0$ and $x = 28$
kt	$0.55_i \times 10^5 \text{ cal/m day } ^\circ\text{C}$		
ρC_w	$0.1 \times 10^7 \text{ cal/m}^2 \text{ } ^\circ\text{C}$		Temperature of incoming fluid: 15°C
ρC_s	$0.7 \times 10^6 \text{ cal/m}^2 \text{ } ^\circ\text{C}$		
time step	0.5 day		No flow at all other boundaries

^aThe water-flow equation was solved for head gradient of 0.1786 m/m with hydraulic conductivity and porosity set to unity to obtain the specified velocity.

CONVECTIVE TEST PROBLEM RECTANGULAR MATRIX
UNITS USED ARE METERS, DAYS, CELSIUS, CALORIES

04//07/78
17:01:09

#OF NODES 22 # OF ELEMENTS 10 BANDWIDTH 4

VELOCITIES ARE BEING CALCULATED AT CURRENT TIME STEP 1

THE X-SPACING IS

0.0	4.0000	7.0000	8.0000	11.0000	12.0000	16.0000	18.0000
20.0000	24.0000	28.0000					

THE Y-SPACING IS

4.0000 0.0

EQUATION 2 TIME STEP .500000 HEAT OR MASS CAPACITY COEFFICIENT .100000+07

PARAMETER FACTORS--IN ORDER 1.00000 1.00000 1.00000 1.00000 1.00000 1.00000 1.00000 1.00000 1.00000

MATERIAL	HOR PERM	VER PERM	STORAGE	HOR THERM COND	VERT THERM COND	SPECIFIC DISPERSION COEFS HEAT
1	1.000	1.000	.0000	.5500+05	.5500+05	.7000+06 .1000+00 .1000+00

THE VALUES IN THE TYPE OF MATERIAL MATRIX ARE

1.00000	1.00000	1.00000	1.00000	1.00000	1.00000	1.00000
1.00000	1.00000	1.00000				

INFORMATION FOR MASS OR HEAT TRANSFER ACROSS A SPECIFIED HEAD BOUNDARY
ELEMENT NUMBER--BOUNDARY CODE--TEMPERATURE OR CONCENTRATION OF INCOMING FLUID

10 4 15.000

CONVECTIVE OUT AND CONDUCTIVE BOUNDARY INFORMATION

1 3 .000000

ELEM #--BOUNDARY CODE--TRANSFER COEFFICIENT

Figure C-11. Program output for one-dimensional heat transport problem with linear elements.(continued)

WATER FLOW BOUNDARIES--ELEM # AND BOUNDARY CODE

1 3 10 4

POTENTIAL DISTRIBUTION AT TIME STEP .000000

100.0000	100.0000
100.714	100.714
101.250	101.250
101.429	101.429
101.964	101.964
102.143	102.143
102.857	102.857
103.214	103.214
103.571	103.571
104.286	104.286
105.000	105.000

CUMULATIVE MASS BLANCE

RATES FOR THIS STEP

B. FLUX RECHARGE	.714288	.714288
B. FLUX DISCHARGE	.714281	.714281
CHANGE IN STORAGE	.000000	.000000
QUANTITY PUMPED	.000000	.000000
DIFFERENCE	.715256-05	.715256-05

TIME STEP .000000

FLOWS IN THE X DIRECTION

.714281	.714284	.714285	.714286	.714287	.714286	.714287
.714288	.714288	.714288				

FLOWS IN THE Y DIRECTION

.000000	.715256-06	.119209-06	.357628-06	.000000	.476837-06	.000000
.000000	-.476837-06	.000000				

THE DISPERSION ROUTINE IS BEING USED

-108-

Figure C-11. (continued)

TEMPERATURE DISTRIBUTION AT TIME STEP		25.0000
10.0001	10.0002	
9.99935	9.99949	
10.0014	10.0016	
10.0074	10.0074	
9.99971	9.99992	
9.96143	9.96156	
9.90413	9.90422	
10.3286	10.3286	
11.4248	11.4248	
14.1568	14.1569	
15.3485	15.3486	

	CUMULATIVE MASS BLANCE	RATES FOR THIS TIME STEP
CONDUCTIVE TRANSFER	.000000	.000000
CONVECTIVE TRANSFER--OUT	.178571+09	.357147+07
CONVECTIVE TRANSFER--IN	.267858+09	.535716+07
B. FLUX RECHARGE	.000000	.000000
B. FLUX DISCHARGE	.000000	.000000
CHANGE IN STORAGE	.892868+08	.178568+07
QUANTITY PUMPED	.000000	.000000
DIFFERENCE	429.500	8.37500

TEMPERATURE DISTRIBUTION AT TIME STEP		50.0000
10.0037	10.0039	
9.97586	9.97601	
9.94439	9.94460	
10.0029	10.0029	
10.4781	10.4783	
10.9284	10.9285	
12.8394	12.8395	
14.0114	14.0115	
14.5750	14.5750	
15.1468	15.1468	
14.9093	14.9093	

Figure C-11. (continued)

	CUMULATIVE MASS BLANCE	RATES FOR THIS TIME STEP
CONDUCTIVE TRANSFER	.000000	.000000
CONVECTIVE TRANSFER-OUT	.357165+09	.357283+07
CONVECTIVE TRANSFER-IN	.535716+09	.535716+07
B. FLUX RECHARGE	.000000	.000000
B. FLUX DISCHARGE	.000000	.000000
CHANGE IN STORAGE	.178550+09	.178431+07
QUANTITY PUMPED	.000000	.000000
DIFFERENCE	896.781	14.2500

TEMPERATURE DISTRIBUTION AT TIME STEP		75.0000
10.0302	10.0304	
10.5080	10.5082	
11.6597	11.6599	
12.1306	12.1306	
13.4834	13.4837	
13.8607	13.8608	
14.9332	14.9333	
14.9278	14.9278	
15.0309	15.0309	
15.0045	15.0045	
14.9912	14.9913	

	CUMULATIVE MASS BLANCE	RATES FOR THIS TIME STEP
CONDUCTIVE TRANSFER	.000000	.000000
CONVECTIVE TRANSFER-OUT	.535367+09	.358047+07
CONVECTIVE TRANSFER-IN	.803574+09	.535716+07
B. FLUX RECHARGE	.000000	.000000
B. FLUX DISCHARGE	.000000	.000000
CHANGE IN STORAGE	.268205+09	.177668+07
QUANTITY PUMPED	.000000	.000000
DIFFERENCE	1372.56	7.93750

Figure C-11. Program output for one-dimensional heat transport problem with linear elements.

CONVECTIVE TEST PROGRAM
 UNITS USED ARE METERS, DAYS, CELCIUS, CALORIES

7 32 12
 3 0 0 2 1 1E13
 (1x,2G12.6/3G12.6/2G12.6/2G12.6/4G12.6/2G12.6/2G12.6/4G12.6/2G12.6/2G12.6/
 3G12.6/2G12.6/2G12.6)
 (1x,7G12.6)

GROUP II

1 0 4
 2 0 0
 3 4 4
 4 4 2
 5 4 0
 6 5 4
 7 5 0
 8 7 4
 9 7 0
 10 8 4
 11 8 3
 12 8 1
 13 8 0
 14 9 4
 15 9 0
 16 11 4
 17 11 0
 18 12 4
 19 12 3
 20 12 1
 21 12 0
 22 16 4
 23 16 0
 24 18 4
 25 18 0
 26 20 4
 27 20 2
 28 20 0
 29 24 4
 30 24 0
 31 28 4
 32 28 0
 1 2 5 4* 3 1 2
 2 5 7* 9* 13 12* 11* 10 8* 6* 3 4* 5
 3 13 15* 17* 21 20* 19* 18 16* 14* 10 11* 12* 13
 4 21 23 22 18 19* 20* 21
 5 23 25* 28 27* 26 24* 22 23
 6 28 30 29 26 27* 28
 7 30 32 31 29 30

(continued)

Figure C-12. The data deck used to model one-dimensional heat transport with mixed elements.

GROUP III

```
.5 1 0 1E6
10 0 1
0 4 1
1 100 2 100 31 105 32 105
0 0 1
```

GROUP IV

```
1
1 1 1 1 1 1 1 1
1 0 1
1 1 1 0 55000 55000 700000 .1 .1
```

GROUP V

```
0 0
0 0
0 0
```

GROUP VI

```
0
```

GROUP VII

```
1
1 3 0
10
1
7 4 0
15
```

GROUP VIII

```
2 0
1 3 7 4
```

GROUP IX

```
0 0 0 0 0 0 0 0
75 50 150 50 150 0 1 0
```

Figure C-12. The data deck used to model one-dimensional heat transport with mixed elements.

CONVECTIVE TEST PROGRAM
UNITS USED ARE METERS, DAYS, CELCIUS, CALORIES

04/07/76
17:00:46

OR NODES 32 # OF ELEMENTS 7 BANDWIDTH 12

VELOCITIES ARE BEING CALCULATED AT CURRENT TIME STEP 1

EQUATION 2 TIME STEP .500000 HEAT OR MASS CAPACITY COEFFICIENT .100000+07

PARAMETER FACTORS--IN ORDER 1.00000 1.00000 1.00000 1.00000 1.00000 1.00000 1.00000 1.00000

MATERIAL	HOR PERM	VER PERM	STORAGE	HOR THERM COND	VERT THERM COND	SPECIFIC HEAT	DISPERSION COEFS
1	1.000	1.000	.0000	.5500+05	.5500+05	.7000+06	.1000+00 .1000+00

THE VALUES IN THE TYPE OF MATERIAL MATRIX ARE

1.00000 1.00000 1.00000 1.00000 1.00000 1.00000 1.00000

INFORMATION FOR MASS OR HEAT TRANSFER ACROSS A SPECIFIED HEAD BOUNDARY
ELEMENT UNSER--BOUNDARY CODE--TEMPERATURE OR CONCENTRATION OF INCOMING FLUID

7 4 15.000

CONVECTIVE OUT AND CONDUCTIVE BOUNDARY INFORMATION ELEM #--BOUNDARY CODE--TRANSFER COEFFICIENT

1 3 .000000

WATER FLOW BOUNDARIES--ELEM # AND BOUNDARY CODE

1 3 7 4

POTENTIAL DISTRIBUTION AT TIME STEP .000000

100.0000	100.0000		
100.714	100.714	100.714	
100.893	100.893		
101.253	101.253		
101.429	101.429	101.429	101.429
101.657	101.657		
101.964	101.964		
102.143	102.143	102.143	102.143
102.857	102.857		

(continued)

Figure C-13. Program output for the one-dimensional heat transport problem with mixed elements.

103.214 103.214
 103.571 103.571 103.571
 104.236 104.236
 103.000 105.000

	CUMULATIVE MASS BLANCE	RATES FOR THIS TIME STEP
B. FLUX RECHARGE	.714289	.714289
B. FLUX DISCHARGE	.714202	.714262
CHANGE IN STORAGE	.000000	.000000
QUANTITY PUMPED	.000000	.000000
DIFFERENCE	.267029-04	.267029-04

TIME STEP .000000
 FLOWS IN THE X DIRECTION
 .714262 1.42996 .1.74388 .915181 .714290 .714292 .714289

FLOWS IN THE Y DIRECTION
 -.476837-56 .558137-05 .540157-05 -.548363-05 .00-000 -.953674-06 .000000

THE DISPERSION ROUTINE IS BEING USED

TEMPERATURE DISTRIBUTION AT TIME STEP 25.0000

10.0005	10.0006		
10.0001	9.99989	10.0002	
9.99925	9.99977		
10.0025	10.0026		
10.0077	10.0058	10.0076	
10.0073	10.0079		
9.99686	9.9551		
9.90961	9.97127	9.97589	9.96879
9.79857	9.89727		
10.3231	10.3737		
11.4719	11.4715	11.4717	
14.1362	14.1365		
13.3683	15.3502		

	CUMULATIVE MASS BLANCE	RATES FOR THIS TIME STEP
CONDUCTIVE TRANSFER	.000000	.000000
CONVECTIVE TRANSFER-OUT	.178569+09	.357150+07
CONVECTIVE TRANSFER-IN	.267858+09	.535716+07
B. FLUX RECHARGE	.000000	.000000
B. FLUX DISCHARGE	.000000	.000000
CHANGE IN STORAGE	.589193+08	.180833+07
QUANTITY PUMPED	.000000	.000000
DIFFERENCE	370063.	-22663.4

Figure C-13. (continued)

TEMPERATURE DISTRIBUTION AT TIME STEP 50.0000

10.0049	10.0050	
9.96511	9.93723	9.98017
9.96235	9.96254	
9.96261	9.95263	
10.0013	9.95-12	9.99911 10.0018
17.1391	17.1396	
17.54??	17.54?4	
17.??3	17.3997	10.8995 10.8954
12.??73	12.9877	
13.9537	13.9556	
14.5316	14.5311	14.5313
15.1661	15.1663	
14.8985	14.5984	

	CUMULATIVE MASS BLANCE	RATES FOR THIS TIME STEP
CONDUCTIVE TRANSFER	.000000	.000000
CONVECTIVE TRANSFER-OUT	.357160+09	.357313+07
CONVECTIVE TRANSFER-IN	.535716+09	.535716+07
B. FLUX RECHARGE	.000000	.000000
B. FLUX DISCHARGE	.000000	.000000
CHANGE IN STORAGE	.17257+09	.179040+07
QUANTITY PUMPED	.000000	.000000
DIFFERENCE	.330007+07	-6372.50

TEMPERATURE DISTRIBUTION AT TIME STEP 75.0000

10.8259	10.0261	
10.5035	17.5926	10.5035
10.6??9	17.9895	
11.6724	11.6724	
12.1127	12.1154	12.1154 12.1135
12.5?53	12.5?66	
13.4747	13.4742	
13.7692	13.5693	13.8603 13.86?5
14.9299	14.93?4	
14.9297	14.9296	
15.0453	15.044?	15.0451
15.??1?	15.??22	
14.9917	14.9917	

Figure C-13. (continued)

	CUMULATIVE MASS BLANCE	RATES FOR THIS TIME STEP
CONDUCTIVE TRANSFER	.000000	.000000
CONVECTIVE TRANSFER-OUT	.635375+09	.357859+07
CONVECTIVE TRANSFER-IN	.000000	.000000
B. FLUX RECHARGE	.000000	.000000
B. FLUX DISCHARGE	.000000	.000000
CHANGE IN STORAGE	.567842+09	.183896+07
QUANNTITY PUMPED	.000000	.000000
DIFFERENCE	356718.	-60682.3
EXGT		

Figure C-13. Program output for the one-dimensional heat transport problem with mixed elements.

TABLE C-3. ANALYTICAL SOLUTION AT $t = 50$ DAYS FOR THE PROBLEM POSED IN FIGURE C-9 AND FINITE ELEMENT NUMERICAL SOLUTIONS AT $t = 50$ DAYS FOR TWO GRID CONFIGURATIONS AND TWO TYPES OF BOUNDARY CONDITIONS

	Analytical	Linear elements (a)	Mixed elements	Linear elements with nodes 21 & 22 specified at 15°C
$x = 0$	15.0 ^a	14.901	14.899	15.0
$x = 4$	14.982	15.147	15.166	15.081
$x = 8$	14.649	14.575	14.531	14.484
$x = 10$	14.017	14.011	13.945	13.981
$x = 12$	12.962	12.840	12.867	13.036
$x = 16$	10.787	10.929	10.900	10.724
$x = 20$	10.062	10.003	9.999	10.095
$x = 24$	10.002	9.976	9.976	9.763

^aAll values listed are temperatures in degrees centigrade. $x = 0$ is at the right in Figure C-10.

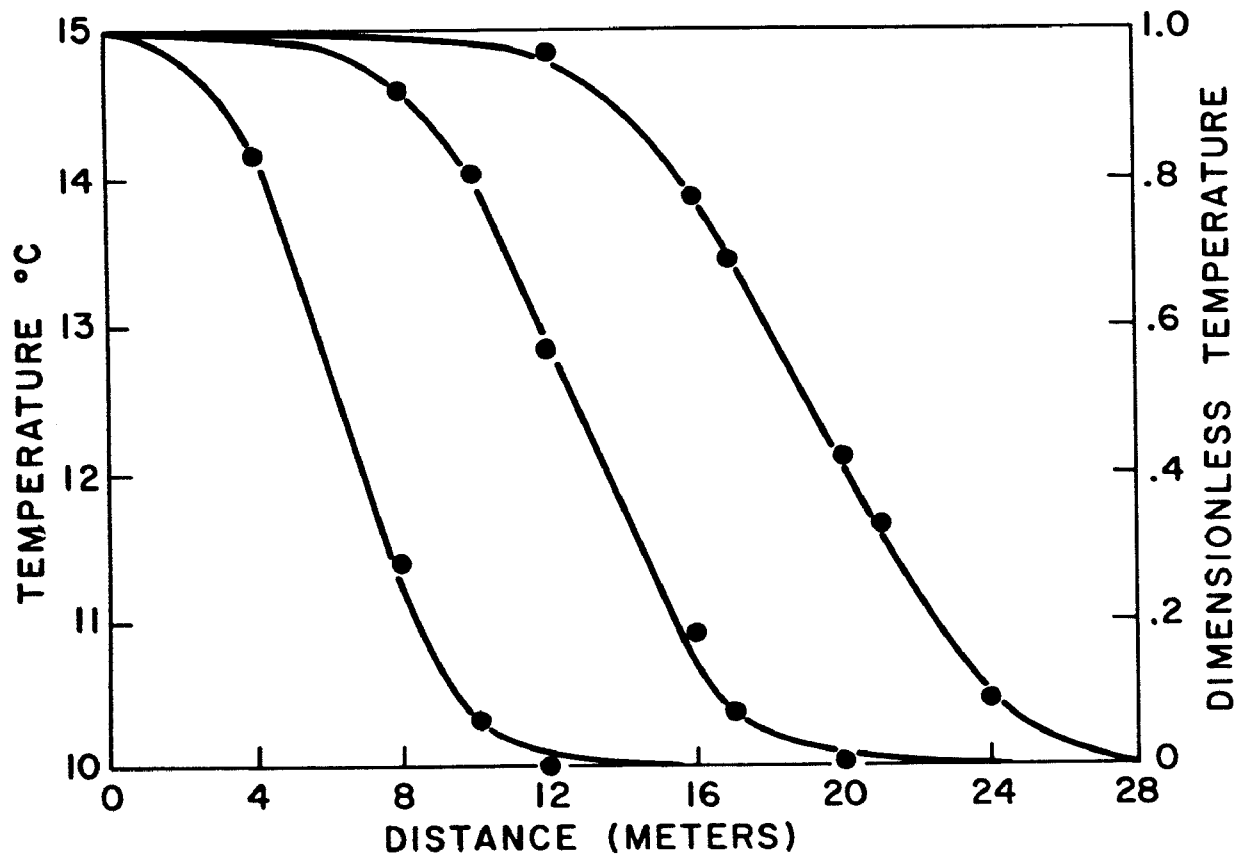


Figure C-14. Analytical solutions (solid lines) and numerical solutions (dots) for the linear heat transport problem for $t = 25, 50$ and 75 days.

C-3. Specification of the boundary temperature, rather than use of a convective boundary, constrains the solution from oscillating as much near the origin and is the exact boundary condition used by Ogata and Banks (1961).

The Mohawk River

This problem demonstrates the use of the program to solve an areal problem to investigate the effect of stream infiltration on ground-water temperatures in an alluvial aquifer along the Mohawk River near Schenectady, N.Y. (Figure C-15).

The flood plain of the Mohawk River in the vicinity of Lock and Dam 8, about 2 miles west of the city of Schenectady, is underlain by more than 100 ft of unconsolidated deposits. From the surface downward the deposits consist of 30 ft of flood-plain alluvium, 20-100 ft of sandy gravel and sand, and, immediately above the bedrock, a layer of glacial till 25-50 ft thick (Figure C-16). The sandy gravel and sand deposit is tapped by the well fields of the city of Schenectady and town of Rotterdam. Winslow (1962) monitored temperatures in this aquifer and concluded that most of the water pumped from the well fields originated as infiltration from the Mohawk River. This model was programmed to determine if the temperature patterns observed by Winslow could be simulated.

The grid used to model the aquifer is shown in Figure C-17. The boundary conditions and parameters used in the simulation are listed in Table C-4. All water flow was assumed to occur within the principal aquifer, and the principal aquifer was assumed to be thermally insulated from the overlying flood-plain deposits and the underlying glacial tills. (This assumption greatly simplified the data input, but it could be relaxed if a better approximation is desired.)

The temperature of the river water was changed at each time step. River temperatures for a 1-yr period were read in at the beginning of program execution by a call to ENTRY LAKE and were then altered at each time step by a call to ENTRY BOUND. ENTRY CHANG was called at each time step to compute heat flow out of the system with the pumped water. Heat flow at the wells for each time step was set equal to the temperature at the wells multiplied by the heat capacity and the rate of pumpage.

The data and the program output for a 10-day simulation, with pumpage rates only 10% of actual rates, are listed in Figure C-18 and Figure C-19. If actual pumpage rates are used, a time step of 0.1 day must be used to insure solution stability, unless a corrector is applied near the wells to force stability.

TABLE C-4. PARAMETERS, INITIAL CONDITIONS, AND BOUNDARY CONDITIONS USED FOR THE SIMULATION OF TEMPERATURES IN THE MOHAWK RIVER ALLUVIAL AQUIFER

Water flow

Boundary conditions

Mohawk River	Specified head of 100 ft ^a
--------------	---------------------------------------

All other boundaries	No flow
----------------------	---------

Parameters (principle aquifer)

$K_{11} = K_{22}$	100,000 gal/day ft ²
-------------------	---------------------------------

Wells--discharge rates

Node 70	2,000,000 gal/day
---------	-------------------

Nodes 130, 131, 145, 146	4,500,000 gal/day at each node
--------------------------	--------------------------------

Heat flow

Initial conditions	$T_1 = 10^{\circ}\text{C}$
--------------------	----------------------------

Boundary conditions

River	Convective flux in
-------	--------------------

All other boundaries	No flow
----------------------	---------

Parameters

$K_{11}^t = K_{22}^t$	$1.3 \times 10^4 \text{ cal/day ft}^{\circ}\text{C}$
-----------------------	--

ρC_s	$2.1 \times 10^4 \text{ cal/ft}^3 \text{ }^{\circ}\text{C}$
------------	---

α_L	10 ft
------------	-------

α_T	1 ft
------------	------

Time step	1 day
-----------	-------

^aUnits of feet, gallons, calories, and days were used in this simulation.

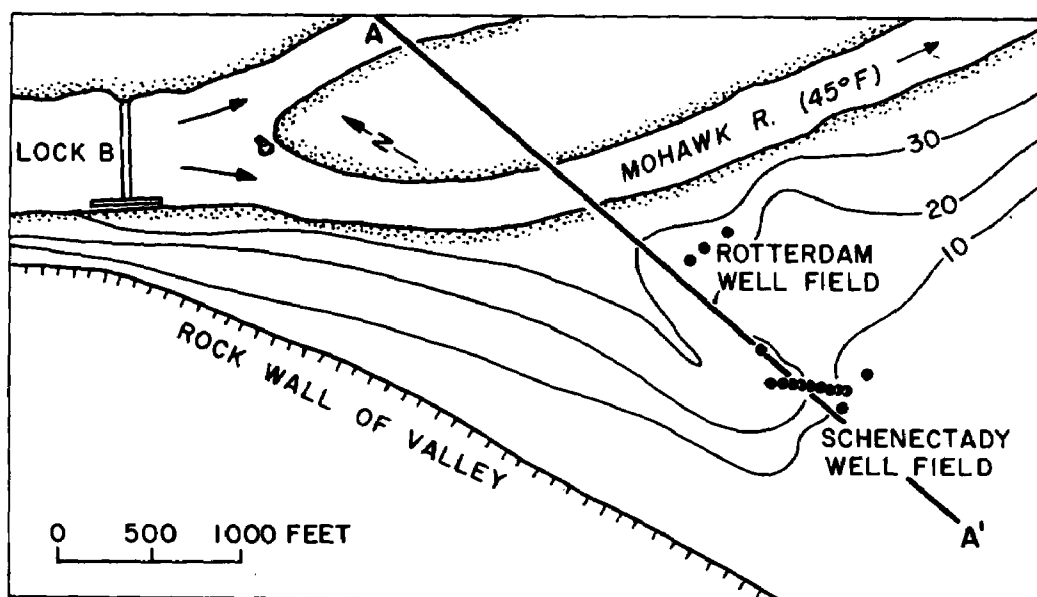


Figure C-15. Areal view of the Mohawk River Valley showing location of the Schenectady and Rotterdam well fields (Winslow 1962).

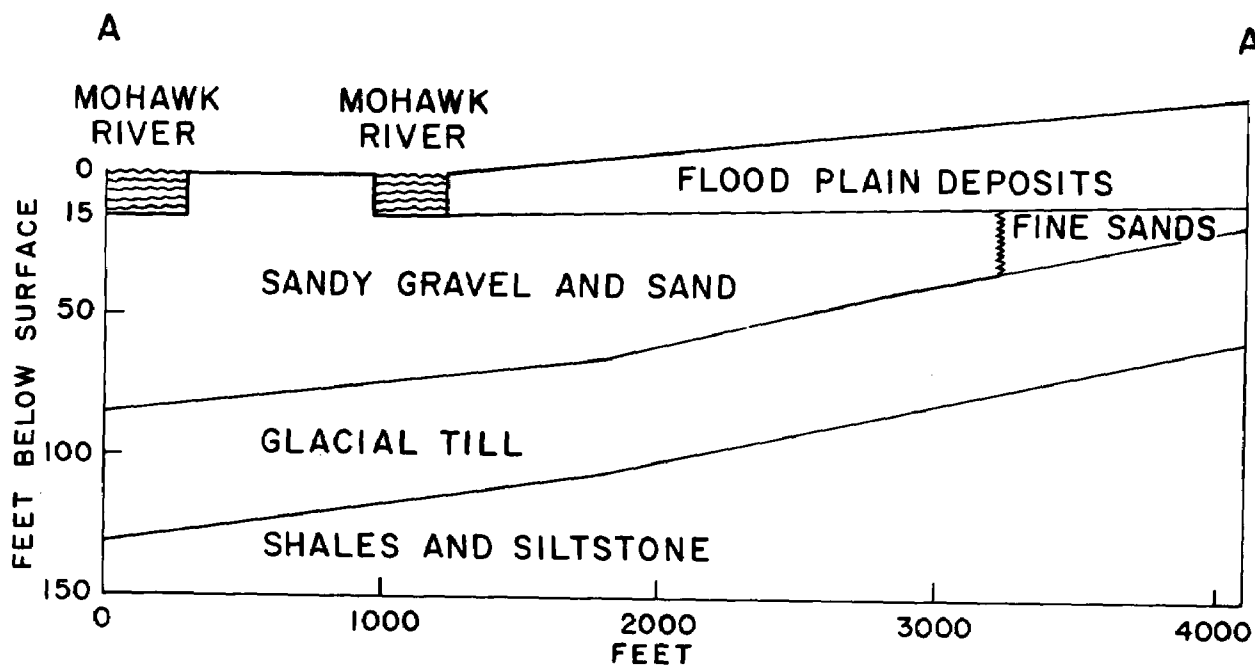


Figure C-16. Cross-sectional view of the Mohawk River alluvial aquifer along section A-A' of Figure C-15.

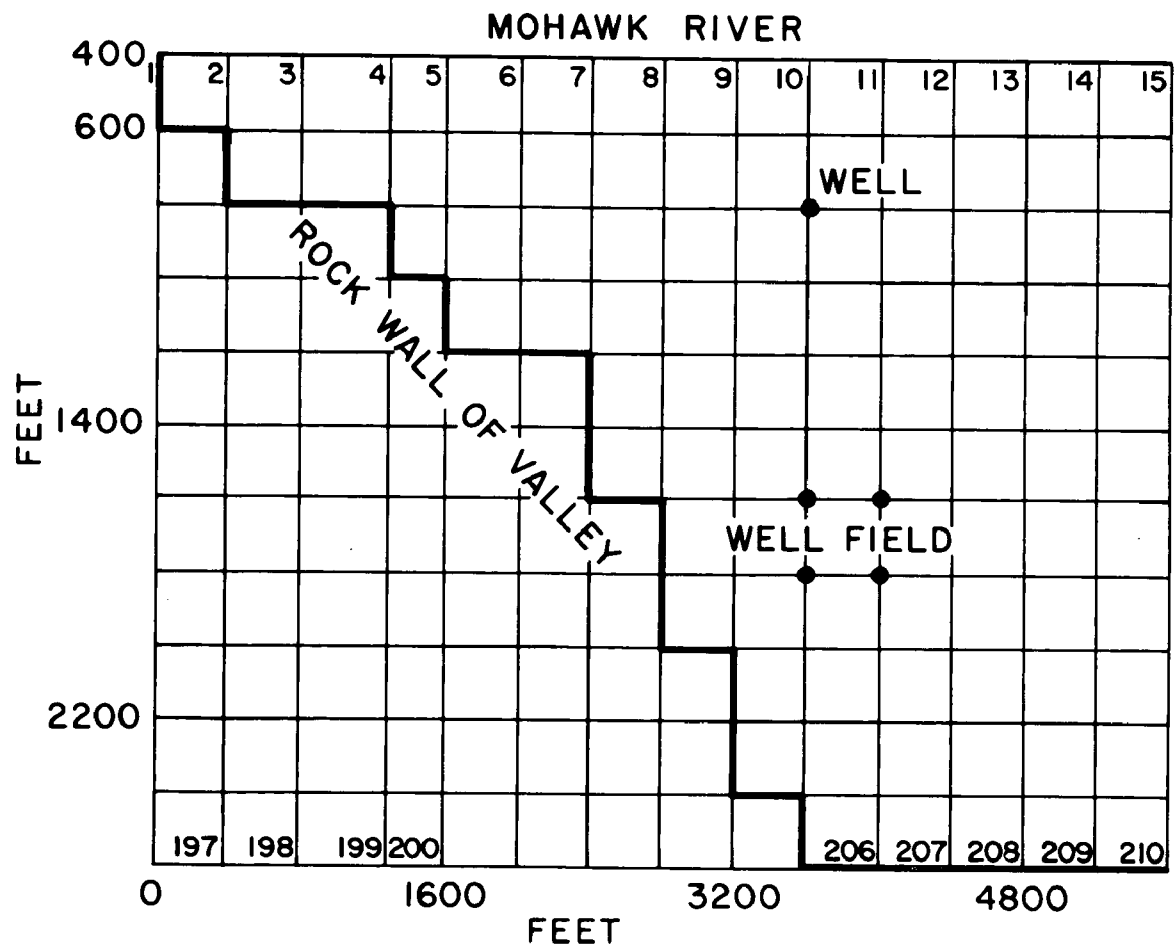


Figure C-17. Grid used to discretize the Mohawk River problem. (The node numbers in the first and last rows are listed.)

```

MOHAWK RIVER PROBLEM
UNITS ARE GALLONS DAYS FEET
182 210 17
3 0 0 0 1 1E16
(1x,15F6.2)

(1x,14F6.2)

GROUP II
14 15
400 450 500 600 800 1000 1200 1400 1600 1800 2000 2200 2400 2600
5600 5200 4800 4480 4000 3600 3200 2800 2400 2000 1600 1200 800 400 0
GROUP III
1 1 1 3785.68
10 0 1
0 -1 1
100 100 100 100 100 100 100 100 100 100 100 100 100 100 100
0 0 0 0 0 0 0 0 0 0 0 0 0 0 0 0 0 0 0 0 0 0 0 0 0 0 0 0 0 0 0 0
0 0 0 0 0 0 0 0 0 0 0 0 0 0 0 0 0 0 0 0 0 0 0 0 0 0 0 0 0 0 0 0
0 0 0 0 0 0 0 0 0 0 0 0 0 0 0 0 0 0 0 0 0 0 0 0 0 0 0 0 0 0 0 0
0 0 0 0 0 0 0 0 0 0 0 0 0 0 0 0 0 0 0 0 0 0 0 0 0 0 0 0 0 0 0 0
0 0 0 0 0 0 0 0 0 0 0 0 0 0 0 0 0 0 0 0 0 0 0 0 0 0 0 0 0 0 0 0
0 0 0 0 0 0 0 0 0 0 0 0 0 0 0 0 0 0 0 0 0 0 0 0 0 0 0 0 0 0 0 0
999
0 0 1
GROUP IV
4
1 1 1 1 1 1 1 1 1 1
0 -1 1
1 1 1 1 1 1 1 1 1 1 1 1 1 1 1 1
2 2 2 2 2 2 2 2 2 2 2 2 2 2 2 2
2 2 2 2 2 2 2 2 2 2 2 2 2 2 2 2
4 2 2 2 2 2 2 2 2 2 2 2 2 2 2 2
4 4 4 2 2 2 2 2 2 2 2 2 2 2 2 2
4 4 4 4 2 2 2 2 2 2 2 2 2 2 2 2
4 4 4 4 4 2 2 2 2 2 2 2 2 2 2 2
4 4 4 4 4 4 2 2 2 2 2 2 2 2 2 2
4 4 4 4 4 4 4 2 2 2 2 2 2 2 2 2
4 4 4 4 4 4 4 4 2 2 2 2 2 2 2 2
4 4 4 4 4 4 4 4 4 3 3 3 3 3 3 3
4 4 4 4 4 4 4 4 4 3 3 3 3 3 3 3
4 4 4 4 4 4 4 4 4 3 3 3 3 3 3 999
1 100000 1000000 0 13000 13000 21000 10 1
2 100000 1000000 0 13000 13000 21000 10 1
3 500 500 0 13000 13000 21000 10 1
4 0.001 0.001 0.001 0.001 0.001 0.001 0.001 0.001
GROUP VI
0 0
5 5
130 -4.5E5 131 -4.5E5 145 -4.5E5 146 -4.5E5 70 -2E5
130 1 131 1 145 1 146 1 70 1

```

(continued)

Figure C-18. The data deck used to model heat flow in the Mohawk River alluvial aquifer.

```

0 0
GROUP VI 1
1
1 3
0 -1 1
1 1 1 1 1 10 20 30 40 50 50 50 50 50 50
1 1 1 1 1 10 20 30 40 50 50 50 50 50 50
1 1 1 1 1 10 20 30 40 50 50 50 50 50 50
1 1 1 1 1 10 20 30 40 50 50 50 50 50 50
1 1 1 1 1 10 20 30 40 50 50 50 50 50 50
99 99 99 20 20 25 35 45 50 55 55 55 55 55 55
99 99 99 99 40 45 50 55 60 60 60 60 60 60 60
99 99 99 99 99 99 65 65 65 60 60 60 60 60 60
99 99 99 99 99 99 70 70 70 70 70 70 70 70 70
75 75 75 75 75 75 75 75 75 75 75 75 75 75
80 80 80 80 80 80 80 80 80 80 80 80 80 80
80 80 80 80 80 80 80 80 80 80 80 80 80 80
80 80 80 80 80 80 80 80 80 80 80 80 80 80
80 80 80 80 80 80 80 80 80 80 80 80 80 80
100 0 1
GROUP VII
14
1 3 3000 2 3 3000 3 3 3000 4 3 3000 5 3 3000 6 3 3000 7 3 3000
8 3 3000 9 3 3000 10 3 3000 11 3 3000 12 3 3000 13 3 3000 14 3 3000
0 0 0 0 0 0 0 0 0 0 0 0 0 0 0
14
1 3 2 3 3 3 4 3 5 3 6 3 7 3 8 3 9 3 10 3 11 3 12 3 13 3 14 3
0 0 0 0 0 0 0 0 0 0 0 0 0 0 0
GROUP VIII
14 0
1 3 2 3 3 3 4 3 5 3 6 3 7 3 8 3 9 3 10 3 11 3 12 3 13 3 14 3
GROUP IX
1 1 0 0 0 0
0 220 220 1 220 220 1 220 220 1 1 1
277 860
      1.0000      29.5000      41.0000
      2.0000      28.5000      35.9000
      3.0000      27.5000      30.8000
      4.0000      27.4600      30.5000
      5.0000      27.4100      30.2000
      6.0000      27.3700      29.9000
      7.0000      27.3300      29.6000
      8.0000      27.2900      29.3000
      9.0000      27.2400      29.0000
      10.0000     27.2000      28.7000
10 10 10 10 10 1 1 1

```

Figure C-18. The data deck used to model heat flow in the Mohawk River alluvial aquifier.

MOHAWK RIVER PROBLEM
UNITS ARE GALLONS DAYS FEET

04/07/78
17:01:49

OF NODES 210 # OF ELEMENTS 182 BANDWIDTH 17

VELOCITIES ARE BEING CALCULATED AT CURRENT TIME STEP 1

THE X-SPACING IS

400.0000	450.0000	500.0000	600.0000	800.0000	1000.0000	1200.0000	1400.0000
1600.0000	1800.0000	2000.0000	2200.0000	2400.0000	2600.0000		

THE Y-SPACING IS:

5600.0000	5200.0000	4800.0000	4480.0000	4000.0000	3600.0000	3200.0000	2800.0000
2400.0000	2000.0000	1600.0000	1200.0000	800.0000	400.0000	0.0	

EQUATION 2 TIME STEP 1.00000

HEAT OR MASS CAPACITY COEFFICIENT 3785.68

PARAMETER FACTORS- IN ORDER 1.00000 1.00000 1.00000 1.00000 1.00000 1.00000 1.00000 1.00000 1.00000

MATERIAL	HOR PERM	VER PERM	STORAGE	HOR THERM COND	VERT THERM COND	SPECIFIC HEAT	DISPERSION	COEFS
1	.1000+06	.1000+06	.0000	.1300+05	.1300+05	.2100+05	10.00	1.000
2	.1000+06	.1000+06	.0000	.1300+05	.1300+05	.2100+05	10.00	1.000
3	500.0	500.0	.0000	.1300+05	.1300+05	.2100+05	10.00	1.000
4	.1000-02	.1000-02	.1000-02	.1000-02	.1000-02	.1000-02	.1000-02	.1000-02

THE VALUES IN THE TYPE OF MATERIAL ARE

1.00	1.00	1.00	1.00	1.00	1.00	1.00	1.00	1.00	1.00	1.00	1.00	1.00	1.00	1.00
2.00	2.00	2.00	2.00	2.00	2.00	2.00	2.00	2.00	2.00	2.00	2.00	2.00	2.00	2.00
2.00	2.00	2.00	2.00	2.00	2.00	2.00	2.00	2.00	2.00	2.00	2.00	2.00	2.00	2.00
4.00	2.00	2.00	2.00	2.00	2.00	2.00	2.00	2.00	2.00	2.00	2.00	2.00	2.00	2.00
4.00	4.00	4.00	2.00	2.00	2.00	2.00	2.00	2.00	2.00	2.00	2.00	2.00	2.00	2.00
4.00	4.00	4.00	4.00	2.00	2.00	2.00	2.00	2.00	2.00	2.00	2.00	2.00	2.00	2.00
4.00	4.00	4.00	4.00	4.00	2.00	2.00	2.00	2.00	2.00	2.00	2.00	2.00	2.00	2.00
4.00	4.00	4.00	4.00	4.00	4.00	2.00	2.00	2.00	2.00	2.00	2.00	2.00	2.00	2.00
4.00	4.00	4.00	4.00	4.00	4.00	4.00	2.00	2.00	2.00	2.00	2.00	2.00	2.00	2.00
4.00	4.00	4.00	4.00	4.00	4.00	4.00	4.00	3.00	3.00	3.00	3.00	3.00	3.00	3.00
4.00	4.00	4.00	4.00	4.00	4.00	4.00	4.00	3.00	3.00	3.00	3.00	3.00	3.00	3.00
4.00	4.00	4.00	4.00	4.00	4.00	4.00	4.00	3.00	3.00	3.00	3.00	3.00	3.00	3.00

Figure C-19. Program output for Mohawk River problem.

(continued)

POINT SOURCES OF WATER--NODE # AND AMOUNT

130	-450000.	131	-450000.	145	-450000.	146	-450000.	70	-200000.
-----	----------	-----	----------	-----	----------	-----	----------	----	----------

POINT SOURCES OF HEAT

130	1.00000	131	1.00000	145	1.00000	146	1.00000	70	1.00000
-----	---------	-----	---------	-----	---------	-----	---------	----	---------

ELEVATION OF THE AQUIFER BOTTOM

1.00	1.00	1.00	1.00	1.00	10.00	20.00	30.00	40.00	50.00	50.00	50.00	50.00	50.00	50.00
1.00	1.00	1.00	1.00	1.00	10.00	20.00	30.00	40.00	50.00	50.00	50.00	50.00	50.00	50.00
1.00	1.00	1.00	1.00	1.00	10.00	20.00	30.00	40.00	50.00	50.00	50.00	50.00	50.00	50.00
1.00	1.00	1.00	1.00	1.00	10.00	20.00	30.00	40.00	50.00	50.00	50.00	50.00	50.00	50.00
1.00	1.00	1.00	1.00	1.00	10.00	20.00	30.00	40.00	50.00	50.00	50.00	50.00	50.00	50.00
99.00	99.00	99.00	20.00	20.00	25.00	35.00	45.00	50.00	55.00	55.00	55.00	55.00	55.00	55.00
99.00	99.00	99.00	99.00	40.00	45.00	50.00	55.00	60.00	60.00	60.00	60.00	60.00	60.00	60.00
99.00	99.00	99.00	99.00	99.00	99.00	65.00	65.00	65.00	65.00	60.00	60.00	60.00	60.00	60.00
99.00	99.00	99.00	99.00	99.00	99.00	70.00	70.00	70.00	70.00	70.00	70.00	70.00	70.00	70.00
75.00	75.00	75.00	75.00	75.00	75.00	75.00	75.00	75.00	75.00	75.00	75.00	75.00	75.00	75.00
80.00	80.00	80.00	80.00	80.00	80.00	80.00	80.00	80.00	80.00	80.00	80.00	80.00	80.00	80.00
80.00	80.00	80.00	80.00	80.00	80.00	80.00	80.00	80.00	80.00	80.00	80.00	80.00	80.00	80.00
80.00	80.00	80.00	80.00	80.00	80.00	80.00	80.00	80.00	80.00	80.00	80.00	80.00	80.00	80.00
80.00	80.00	80.00	80.00	80.00	80.00	80.00	80.00	80.00	80.00	80.00	80.00	80.00	80.00	80.00

INFORMATION FOR MASS OR HEAT TRANSFER ACROSS A SPECIFIED HEAD BOUNDARY

ELEMENT NUMBER--BOUNDARY CODE--TEMPERATURE OR CONCENTRATION OF INCOMING FLUID

1	3	.00000	2	3	.00000	3	3	.00000	4	3	.00000	5	3	.00000
6	3	.00000	7	3	.00000	8	3	.00000	9	3	.00000	10	3	.00000
11	3	.00000	12	3	.00000	13	3	.00000	14	3	.00000			

CONVENTIVE OUT AND CONDUCTIVE BOUNDARY INFORMATION

ELEM #--BOUNDARY CODE--TRANSFER COEFFICIENT

1	3	3000.00	2	3	3000.00	3	3	3000.00	4	3	3000.00	5	3	3000.00
6	3	3000.00	7	3	3000.00	8	3	3000.00	9	3	3000.00	10	3	3000.00
11	3	3000.00	12	3	3000.00	13	3	3000.00	14	3	3000.00			

WATER FLOW BOUNDARIES--ELEM # AND BOUNDARY CODE

1	3	2	3	3	3	4	3	5	3	6	3	7	3	8	3	9	3	10	3
10	3	11	3	12	3	13	3	14	3										

Figure C-19. (continued)

ITERATIONS NEEDED FOR CONVERGENCE 1

POTENTIAL DISTRIBUTION AT TIME STEP .000000

100.00	100.00	100.00	100.00	100.00	100.00	100.00	100.00	100.00	100.00	100.00	100.00	100.00	100.00	100.00	100.00
100.00	100.00	100.00	100.00	100.00	100.00	100.00	100.00	99.99	99.99	99.99	99.99	99.99	99.99	100.00	100.00
100.00	100.00	100.00	100.00	100.00	100.00	100.00	100.00	99.99	99.99	99.98	99.98	99.99	99.99	99.99	99.99
100.00	100.00	100.00	100.00	100.00	100.00	100.00	99.99	99.98	99.97	99.96	99.97	99.97	99.98	99.98	99.98
100.00	100.00	100.00	100.00	100.00	100.00	99.99	99.98	99.97	99.95	99.92	99.93	99.94	99.96	99.97	99.97
100.00	100.00	100.00	100.00	99.99	99.99	99.97	99.95	99.92	99.89	99.89	99.89	99.91	99.93	99.95	99.95
99.97	99.97	99.98	99.99	99.99	99.99	99.96	99.93	99.89	99.84	99.84	99.84	99.88	99.91	99.93	99.94
99.94	99.94	99.94	99.96	99.98	99.97	99.94	99.91	99.85	99.78	99.78	99.84	99.89	99.89	99.92	99.93
99.91	99.91	99.91	99.91	99.91	99.91	99.93	99.88	99.82	99.68	99.68	99.82	99.88	99.91	99.92	99.92
99.90	99.90	99.90	99.90	99.90	99.89	99.89	99.89	99.84	99.79	99.63	99.63	99.80	99.87	99.90	99.91
99.90	99.90	99.90	99.90	99.90	99.89	99.88	99.87	99.83	99.77	99.65	99.65	99.78	99.86	99.90	99.91
99.90	99.90	99.90	99.90	99.89	99.86	99.85	99.81	99.72	99.69	99.70	99.77	99.84	99.88	99.90	99.90
99.90	99.90	99.90	99.89	99.89	99.87	99.84	99.79	99.70	99.70	99.72	99.77	99.83	99.87	99.89	99.89
99.90	99.90	99.90	99.89	99.89	99.87	99.84	99.79	99.70	99.70	99.72	99.77	99.83	99.87	99.88	99.88

CUMULATIVE MASS BLANCE

RATES FOR THIS TIME STEP

B. FLUX RECHARGE
B. FLUX DISCHARGE
CHANGE IN STORAGE
QUANTITY PUMPED
DIFFERENCE

.200989+07
.000000
.000000
-.200000+07
9886.42

.200989+07
.000000
.000000
-.200000+07
9886.42

THE DISPERSION ROUTINE IS BEING USED

NODE # AND TEMP AT INF.	1	15.04	2	15.04	3	15.04	4	15.04	5	15.04	6	15.04	7	15.04	8	15.04
9	15.04	10	15.04	11	15.04	12	15.04	13	15.04	14	15.04					
NODE # AND TEMP AT INF.	1	15.52	2	15.52	3	15.52	4	15.52	5	15.52	6	15.52	7	15.52	8	15.52
9	15.52	10	15.52	11	15.52	12	15.52	13	15.52	14	15.52					
NODE # AND TEMP AT INF.	1	16.00	2	16.00	3	16.00	4	16.00	5	16.00	6	16.00	7	16.00	8	16.00
9	16.00	10	16.00	11	16.00	12	16.00	13	16.00	14	16.00					
NODE # AND TEMP AT INF.	1	16.48	2	16.48	3	16.48	4	16.48	5	16.48	6	16.48	7	16.48	8	16.48
9	16.48	10	16.48	11	16.48	12	16.48	13	16.48	14	16.48					
NODE # AND TEMP AT INF.	1	16.96	2	16.96	3	16.96	4	16.96	5	16.96	6	16.96	7	16.96	8	16.96
9	16.96	10	16.96	11	16.96	12	16.96	13	16.96	14	16.96					
NODE # AND TEMP AT INF.	1	17.44	2	17.44	3	17.44	4	17.44	5	17.44	6	17.44	7	17.44	8	17.44
9	17.44	10	17.44	11	17.44	12	17.44	13	17.44	14	17.44					
NODE # AND TEMP AT INF.	1	17.92	2	17.92	3	17.92	4	17.92	5	17.92	6	17.92	7	17.92	8	17.92
9	17.92	10	17.92	11	17.92	12	17.92	13	17.92	14	17.92					

Figure C-19. (continued)

NODE # AND TEMP AT INF.	1	18.40	2	18.40	3	18.40	4	18.40	5	18.40	6	18.40	7	18.40	8	18.40
9	18.40	10	18.40	11	18.40	12	18.40	13	18.40	14	18.40					
NODE # AND TEMP AT INF.	1	18.88	2	18.88	3	18.88	4	18.88	5	18.88	6	18.88	7	18.88	8	18.88
9	18.88	10	18.88	11	18.88	12	18.88	13	18.88	14	18.88					
NODE # AND TEMP AT INF.	1	19.36	2	19.36	3	19.36	4	19.36	5	19.36	6	19.36	7	19.36	8	19.36
9	19.36	10	19.36	11	19.36	12	19.36	13	19.36	14	19.36					

TEMPERATURE DISTRIBUTION AT TIME STEP														10.000
10.69	10.70	10.76	10.91	11.38	12.20	13.50	14.99	16.49	17.48	17.25	16.63	15.86	15.15	14.87
9.82	9.82	9.81	9.77	9.67	9.52	9.39	9.46	9.93	10.67	10.49	10.03	9.69	9.52	9.48
10.04	10.04	10.04	10.04	10.06	10.07	10.07	10.02	9.91	9.84	9.86	9.90	9.96	10.01	10.02
9.98	9.99	9.99	9.99	9.99	9.99	9.99	10.00	10.02	10.03	10.02	10.02	10.01	10.00	10.00
10.01	10.00	10.00	10.00	10.00	10.00	10.00	10.00	10.00	9.99	10.00	10.00	10.00	10.00	10.00
10.00	10.00	10.00	10.00	10.00	10.00	10.00	10.00	10.00	10.00	10.00	10.00	10.00	10.00	10.00
10.01	10.01	10.01	10.00	10.00	10.00	10.00	10.00	10.00	10.00	10.00	10.00	10.00	10.00	10.00
10.01	10.01	10.02	10.02	10.01	10.01	10.00	10.00	10.00	10.02	10.02	10.00	10.00	10.00	10.00
10.00	10.00	10.00	10.00	10.00	10.00	10.00	10.00	10.02	9.98	9.98	10.01	10.00	10.00	10.00
10.00	10.00	10.00	10.00	10.00	9.99	10.00	9.99	10.04	9.92	9.92	10.03	9.99	10.00	10.00
10.00	10.00	10.00	10.00	10.00	10.00	10.00	10.00	10.00	10.03	10.03	10.00	10.00	10.00	10.00
10.00	10.00	10.00	10.00	10.00	10.00	10.00	10.00	10.00	9.99	9.99	10.00	10.00	10.00	10.00
10.00	10.00	10.00	10.00	10.00	10.00	10.00	10.00	10.00	10.00	10.00	10.00	10.00	10.00	10.00
10.00	10.00	10.00	10.00	10.00	10.00	10.00	10.00	10.00	10.00	10.00	10.00	10.00	10.00	10.00

B. FLUX DISCHARGE	.000000	.000000
CHANGE IN STORAGE	.620931+12	.794988+11
QUANTITY PUMPED	-.755490+12	-.754061+11
DIFFERENCE	-.471091+07	-502208.
	CUMULATIVE MASS BLANCE	RATES FOR THIS TIME STEP
CONDUCTIVE TRANSFER	.676988+11	.759752+10
CONVECTIVE TRANSFER--OUT	.000000	.000000
CONVECTIVE TRANSFER--IN	.130872+13	.147307+12
B. FLUX RECHARGE	.000000	.000000

Figure C-19. Program output for Mohawk River problem.

The Columbia Generating Station Site

This example is representative of the application described in section 5 of this report in which temperatures and water flows in the alluvial aquifer along the Wisconsin River were simulated after construction of a cooling lake on the river flood plain. Temperatures and water flows were simulated in an aquifer cross section shown in the schematic diagram in Figure C-20, and a finite element grid was used to discretize the cross section (Figure C-21). The parameters, boundary conditions, and initial conditions used in the simulation are listed in Table C-5.

The input data and the program output for a 9-day simulation are listed in Figure C-22 and Figure C-23. ENTRY BOUND was called at each time step to change the temperature of the water in the cooling lake and the air temperature.

TABLE C-5. PARAMETERS, INITIAL CONDITIONS, AND BOUNDARY CONDITIONS
USED IN THE COLUMBIA GENERATING STATION PROBLEM

Water flow

Boundary conditions

River	Specified head at 778 ft ^a
Marsh	Specified head at 780 ft
Lake	Specified head at 789.2 ft
All other boundaries	No flow

Parameters

K_{11} , K_{22}	Ten sets of values specified (refer to program output)
---------------------	---

Heat flow

Initial conditions	$T_1 = 10^\circ\text{C}$
--------------------	--------------------------

Boundary conditions

Lake	Convective flux in
Marsh, River	Convective flux out and conductive flux
All other boundaries	No flow

Parameters

K_{11}^t , K_{22}^t , ρC_s	Ten sets of values specified (refer to program output)
α_L	0.33 ft
α_T	0.08 ft
Time step	3 days

^aThe units of feet, gallons, calories, and days were used in this simulation.

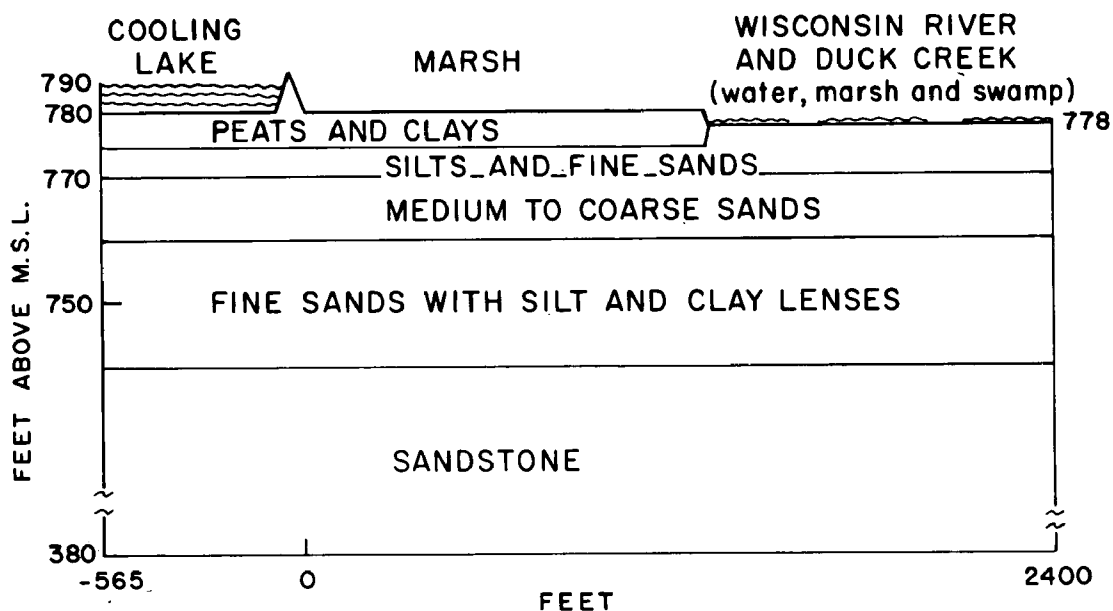


Figure C-20. Schematic cross section of the Columbia Generating Station site along an east-west line.

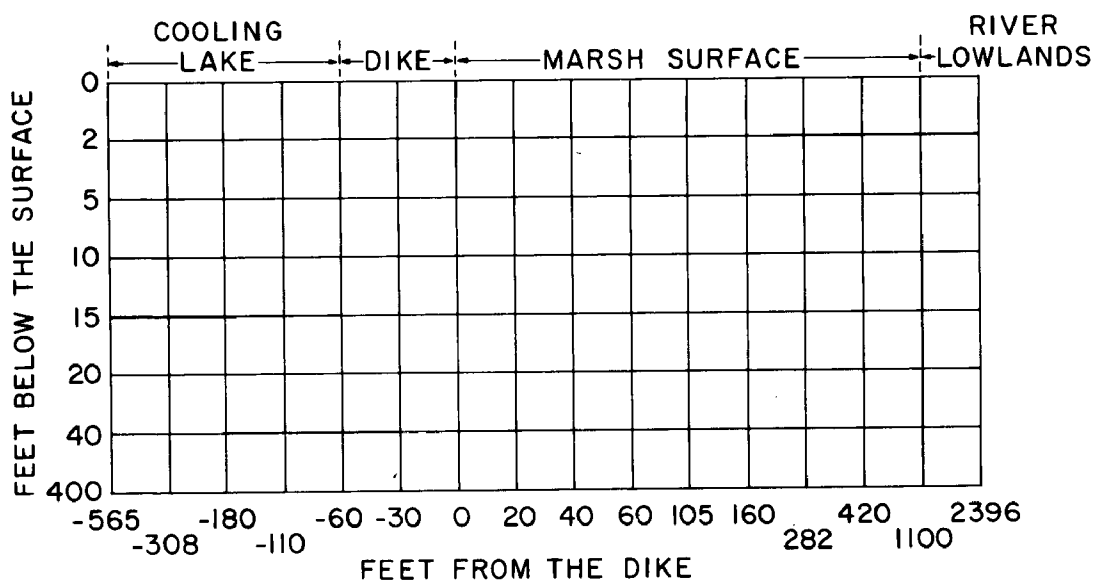


Figure C-21. The grid used to discretize the cross section simulated at the Columbia Generating Station site.

```

CGS 130'S
UNITS USED ARE GALLONS FOR FLOW, FT FOR DISTANCE, CAL, CENTIGRADE
105 128 10
3 0 0 0 1 1E14
(1X,8G12.6)

(1X,7G12.6)

GROUP 22
16 8
-565 -308 -180 -110 -60 -30 0 20 40 60 105 160 260 420 1100 2396
0 -2 -5 -10 -15 -20 -40 -400
GROUP III
3 1 1 3785.68
10 0 1
0 -1 1
89.3 0 0 0 0 0 0 0 89.3 0 0 0 0 0 0 0 89.3 0 0 0 0 0 0 0
89.3 0 0 0 0 0 0 0 89.3 0 0 0 0 0 0 0 84.5 0 0 0 0 0 0 0
80 0 0 0 0 0 0 0 80 0 0 0 0 0 0 0 80 0 0 0 0 0 0 0 80 0 0 0 0 0 0 0
80 0 0 0 0 0 0 0 80 0 0 0 0 0 0 0 80 0 0 0 0 0 0 0 79 0 0 0 0 0 0 0
78.5 0 0 0 0 0 0 0 78.5 0 0 0 0 0 0 0 999
0 0 1
GROUP IV CGS 130'S CARDS USED FOR SAVANNAH PAPER
10
1.6 1.6 1 .7 .7 1 .2 .2
1 -1 1
1 2 3 4 4 6 5
1 2 3 4 4 6 5
1 2 3 4 4 6 5
1 2 3 4 4 6 5
7 2 3 4 4 6 5
7 2 10 8 8 6 5
1 9 10 8 8 6 5
1 9 10 8 8 6 5
1 9 10 8 8 6 5
1 9 10 8 8 6 5
1 9 10 8 8 6 5
1 9 10 8 8 6 5
1 9 10 8 8 6 5
1 1 10 8 8 6 5
1 1 10 8 8 6 5 999
1
100 20 0 20000 20000 26000 .33 .08
2
1 1 0 8000 8000 26000 .33 .08
3

```

(continued)

Figure C-22. The data deck used to model heat flow at the Columbia Generating Station site.

Figure C-22. The data deck used to model heat flow at the Columbia Generating Station site.

CGS 130'S UNITS USED ARE GALLONS FOR FLOW, FT FOR DISTANCE, CAL, CENTIGRADE
 # OF NODES 128 # OF ELEMENTS 105 PANDWIDTH 10

VELOCITIES ARE BEING CALCULATED AT CURRENT TIME STEP 1

THE X-SPACING IS

-565.0000	-508.0000	-160.0000	-110.0000	-60.0000	-30.0000	0.0	20.0000
40.0000	60.0000	105.0000	-160.0000	260.0000	420.0000	1100.0000	2396.0000

THE Y-SPACING IS

0.0	-4.0000	-5.0000	-10.0000	-15.0000	-20.0000	-40.0000	-400.0000
-----	---------	---------	----------	----------	----------	----------	-----------

EDUCATION 2 TIME STEP 3.00000 HEAT OR MASS CAPACITY COEFFICIENT 3785.68

PARAMETER FACTORS--IN ORDER		1.60000	1.60000	1.00000	.700000	.700000	1.00000	.200000	.200000
MATERIAL	HOR PERM	VER PERM	STORAGE	HOR THERM COND	VERT THERM COND	SPECIFIC DISPERSION COEFS HEAT			
1	160.0	32.00	.0000	.1400+05	.1400+.05	.2600+05	.6600-01	.1600-01	
2	1.800	1.600	.0000	5600.	5600.	.2600+05	.6600-01	.1600-01	
3	160.0	32.00	.0000	.1190+05	.1190+05	.2100+05	.6600-01	.1600-01	
4	800.0	80.00	.0000	.1190+05	.1190+05	.2100+05	.6600-01	.1600-01	
5	16.00	16.00	.0000	5600.	5600.	.2600+05	.6600-01	.1600-01	
6	200.0	19.20	.0000	.1190+05	.1190+05	.2100+05	.6600-01	.1600-01	
7	1.800	1.600	.0000	5600.	5600.	.2600+05	.6600-01	.1600-01	
8	1600.	160.0	.0000	.1190+05	.1190+05	.2100+05	.6600-01	.1600-01	
9	3.200	3.200	.0000	5600.	5600.	.2600+05	.6600-01	.1600-01	
10	280.0	40.00	.0000	.1190+05	.1190+05	.2100+05	.6600-01	.1600-01	

Figure C-23. Program output for Columbia Generating Station problem. (continued)

THE VALUES IN THE TYPE OF MATERIAL MATRIX ARE

1.00000	2.00000	3.00000	4.00000	4.00000	6.00000	5.00000
1.00000	2.00000	3.00000	4.00000	4.00000	6.00000	5.00000
1.00000	2.00000	3.00000	4.00000	4.00000	6.00000	5.00000
1.00000	2.00000	3.00000	4.00000	4.00000	6.00000	5.00000
7.00000	2.00000	3.00000	4.00000	4.00000	6.00000	5.00000
7.00000	2.00000	10.0000	8.00000	8.00000	6.00000	5.00000
1.00000	9.00000	10.0000	8.00000	8.00000	6.00000	5.00000
1.00000	2.00000	10.0000	8.00000	8.00000	6.00000	5.00000
1.00000	9.00000	10.0000	8.00000	8.00000	6.00000	5.00000
1.00000	9.00000	10.0000	8.00000	8.00000	6.00000	5.00000
1.00000	9.00000	10.0000	8.00000	8.00000	6.00000	5.00000
1.00000	9.00000	10.0000	8.00000	8.00000	6.00000	5.00000
1.00000	9.00000	10.0000	8.00000	8.00000	6.00000	5.00000
1.00000	9.00000	10.0000	8.00000	8.00000	6.00000	5.00000
1.00000	1.00000	10.0000	8.00000	8.00000	6.00000	5.00000
1.00000	1.00000	10.0000	8.00000	8.00000	6.00000	5.00000

INFORMATION FOR MASS OR HEAT TRANSFER ACROSS A SPECIFIED HEAD BOUNDARY

ELEMENT NUMBER--BOUNDARY CODE--TEMPERATURE OR CONCENTRATION OF INCOMING FLUID

1	1	.00000	8	1	.00000	15	1	.00000	22	1	.00000	29	1	.00000
---	---	--------	---	---	--------	----	---	--------	----	---	--------	----	---	--------

36 1

CONVECTIVE OUT AND CONDUCTIVE BOUNDARY INFORMATION

1	1	12000.0	8	1	12000.00	15	1	12000.0
50	1	.000000	57	1	.000000	64	1	.000000
85	1	.000000	92	1	.000000	99	1	.000000
64	1	8000.00	71	1	8000.00	75	1	8000.00
99	1	8000.00						

ELEM #--BOUNDARY CODE--TRANSFER COEFFICIENT

22	1	12000.0	43	1	.000000
71	1	.000000	78	1	.000000
50	1	8000.00	57	1	8000.00
85	1	8000.00	92	1	8000.00

WATER FLOW BOUNDARIES--ELEM # AND BOUNDARY CODE

1	1	8	1	15	1	22	1	29	1	36	1	43	1	50	1	57	1	64	1
71	1	78	1	85	1	92	1	99	1										

POTENTIAL DISTRIBUTION AT TIME STEP

			.00000																	
89.3000	89.3805	88.70000	88.6525	88.6355	88.6218	88.4519	86.8035													
89.3000	89.2615	88.3858	87.9897	87.9564	87.9318	87.6714	85.9030													
89.3000	89.2224	86.9984	85.8184	86.7581	86.7171	86.3573	84.9464													
89.3000	89.2390	85.9284	85.6591	85.5716	85.5204	85.2024	84.4145													
89.3000	89.0895	84.7128	84.3900	84.3048	84.2692	84.2345	84.0487													
84.5000	89.8503	83.3893	84.3395	83.3358	83.3626	83.6783	83.8094													
80.0000	80.2692	82.5679	82.7641	82.8003	82.8165	83.1117	83.5782													

Figure C-23. (continued)

-51.5399	-39.3041	-31.2270	-22.3388	-10.7826	-4.78335	-.416066
-31.6491	-34.3912	-33.3403	-24.6573	-12.7486	-4.72700	-.530258
-30.5509	-29.3358	-28.9887	-22.8616	-12.2211	-4.62473	-.619473
-53.6430	-54.0320	-52.3883	-41.7264	-23.2787	-9.53972	-1.59924
-48.1144	-45.1488	-44.7073	-35.9204	-20.6327	-9.53262	-2.14461
-34.1526	-38.6777	-33.9313	-20.7011	-19.2395	-11.5253	-3.85953
-35.987	-15.4392	-35.8504	-31.1358	-22.1957	-14.5765	-5.71147
-134.856	-156.379	-129.908	-105.243	-64.2157	-34.1659	-12.2147
12.9762	18.4182	12.3757	9.10431	3.91385	.408686	-.678204

THE DISPERSION ROUTINE IS BEING USED

MODE # AND TEMP AT INF.		1	25.76	8	25.76	15	25.76	22	25.76	43	25.76	50	25.76	57	9.00	64	9.00
71	9.00	78	9.00	85	9.00	92	9.00	99	9.00	50	9.00	57	9.00	64	9.00		
71	9.00	78	9.00	35	9.00	92	9.00	99	9.00								

TEMPERATURE DISTRIBUTION AT TIME STEP .00000

23.0526	10.6176	9.98973	10.0160	9.99720	10.0002	9.99999	10.0000
24.0723	10.8383	9.88251	10.0196	9.99675	10.0002	9.99999	10.0000
23.2023	11.3082	9.35211	10.0222	9.99657	10.0002	9.99999	10.0000
28.3750	12.0244	9.32307	10.0226	9.99680	10.0002	9.99999	10.0000
28.4317	11.7903	9.80178	10.0184	9.99758	10.0001	10.00000	10.0000
9.36313	9.22293	10.8940	10.0030	9.98476	10.0030	10.0000	10.00000
10.6118	10.1791	9.97268	10.0030	9.99928	10.0001	10.00000	10.0000
9.68002	9.95359	10.0947	9.99947	10.0001	10.0000	10.00000	10.00000
9.38139	10.0437	9.99198	10.0016	9.99978	10.0000	10.0000	10.0000
9.48225	10.0148	9.99649	10.0011	9.99965	10.0001	10.00000	10.0000
9.42817	10.0091	9.99830	10.0004	9.99997	9.99996	10.0000	10.00000
9.44609	10.3090	10.6900	10.0791	10.0001	9.99995	10.0000	10.00000
9.35584	9.97909	10.8035	9.99838	10.0001	9.99998	10.0000	10.00000
9.43319	9.99364	10.0908	9.99995	10.00000	9.99996	10.0000	10.00000
9.38966	9.98055	10.0016	9.99975	10.0001	9.99997	10.0000	10.00000
9.40101	9.98236	10.0016	9.99369	10.0001	9.99998	10.0000	10.00000

	CUMULATIVE MASS BLANCE	RATES FOR THIS TIME STEP
CONDUCTIVE TRANSFER	.114876+09	.114876+09
CONVECTIVE TRANSFER--OUT	.446673+08	.448673+08
CONVECTIVE TRANSFER--IN	.118618+09	.112618+09
B. FLUX RECHARGE	.000000	.000000
B. FLUX DISCHARGE	.000000	.000000
CHANGE IN STORAGE	.188595+09	.188595+09
QUANTITY PUMPED	.000000	.000000
DIFFERECE	32501.0	32501.0

QXQT

Figure C-23. Program output for Columbia Generating Station problem.

80.0000	80.1100	82.1493	82.4126	82.4586	82.4821	82.7735	83.4091
80.0000	80.1228	81.6793	82.1055	82.1513	82.1748	82.4630	83.2320
80.0000	80.1019	81.6384	81.8778	81.8771	81.3987	82.1775	83.0495
80.0000	80.0735	81.1874	81.3707	81.3596	81.3761	81.6172	82.8280
80.0000	80.0499	80.7483	80.8439	80.5631	80.8744	81.0584	82.1134
80.0000	80.0004	80.1561	80.1600	80.1619	80.1647	80.2634	81.2531
79.0000	79.0329	79.0889	79.1506	79.1630	79.1703	79.2952	80.1966
78.5000	78.4972	79.4910	78.4856	78.4846	78.4842	78.4326	78.5328
78.5000	78.5814	79.0047	78.5070	78.5075	78.5077	78.5085	78.4860
			CUMULATIVE MASS BLANCE	RATES FOR THIS TIME STEP			
B. FLUX RECHARGE		417.916			417.916		
B. FLUX DISCHARGE		417.716			417.916		
CHANGE IN STORAGE		.000000			.000000		
QUANTITY PUMPED		.000000			.000000		
DIFFERECE		.200280			.200280		
TIME STEP	.000000						
FLOWS IN THE X DIPRECTION							
-.996091-02	-.502178-02	-1.66834	-8.87056	-9.05049	-9.72060	-16.0007	
-.414756-01	-.179398-01	-5.99535	-31.4491	-32.0244	-33.5617	-43.3976	
-.281315-01	-.315544-01	-10.8207	-56.9305	-57.8404	-57.0730	-58.9506	
-.378952	-.552483-01	-16.8848	-86.1615	-85.5518	-75.3980	-65.2530	
-.453898	-.444803	-26.8867	-114.767	-106.215	-82.8756	-64.8656	
-.366091	-.499161	-27.6845	-105.815	-122.489	-63.0097	-65.0647	
-1.08199	-.117809	-22.8950	-117.353	-114.864	-57.1372	-62.0496	
.372479-01	-.524130-01	-17.1250	-104.200	-104.412	-52.4734	-59.6368	
-.141957	-.533644-01	-1511524	-92.2431	-93.4833	-47.7045	-57.2477	
-.359611-01	-.434412-01	-12.6539	-77.3605	-78.5292	-40.8782	-53.3715	
-.532992-01	-.343201-01	-10.0149	-60.7450	-61.6645	-32.7559	-47.7426	
-.673201-01	-.251925-01	-7.56603	-47.0623	-47.9377	-25.5635	-40.4953	
-1.67195	-.515699-01	-7.71698	-42.0485	-42.3296	-20.8387	-30.9582	
-.208530	-.339984	-1.10422	-6.71201	-6.81793	-3.74431	-8.90867	
.443338-03	.275349-02	.159093-01	.115948	.121541	.647594-01	-.394883-01	
FLOWS IN THE Y DIRECTION							
101.654	102.223	100.305	87.9404	66.8651	45.0807	18.5753	
100.988	98.5690	96.0592	81.4697	57.0099	32.3655	7.68152	
80.2117	87.2790	85.4840	70.3572	43.8252	19.3443	2.90531	
109.236	86.4973	80.4588	58.7120	29.4592	7.18937	.918946	
8.97147	32.7361	30.5889	18.1331	1.79816	-3.43804	.399501-01	
3.87355	-12.4882	-14.9164	-13.2480	-17.5263	-7.47321	-.338393	

Figure C-23. (continued)

The Heat Pump Problem

This problem was coded to study the impact of the injection of cooled waters from a heat pump into a shallow ground-water aquifer. The problem is discussed in more detail by Andrews (1978).

The finite element grid used to discretize the problem is shown in Figure C-24. Since the problem is symmetric, only half the system was modeled. A novel feature of the finite element grid is that the thickness of each element is proportional to distance along the horizontal axis from the wells--a quasi-radial formulation. The program input data and a sample program output are listed in Figure C-25 and Figure C-26.

A few unusual features are incorporated into this problem. The heat pump problem was programmed to recompute flows at odd intervals, corresponding to the end of each of the seasons. The intervals at which flows were recomputed are listed on cards 3 and 4 of data group IX. ENTRY CHAN was called each time flows were recomputed to read in the pumping schedule for the current interval. Air temperatures for the entire simulation period were read in by a call to ENTRY LAKE at the beginning of program execution.

The major subroutines and the tasks performed by each are listed in a program flow chart (Figure C-27).

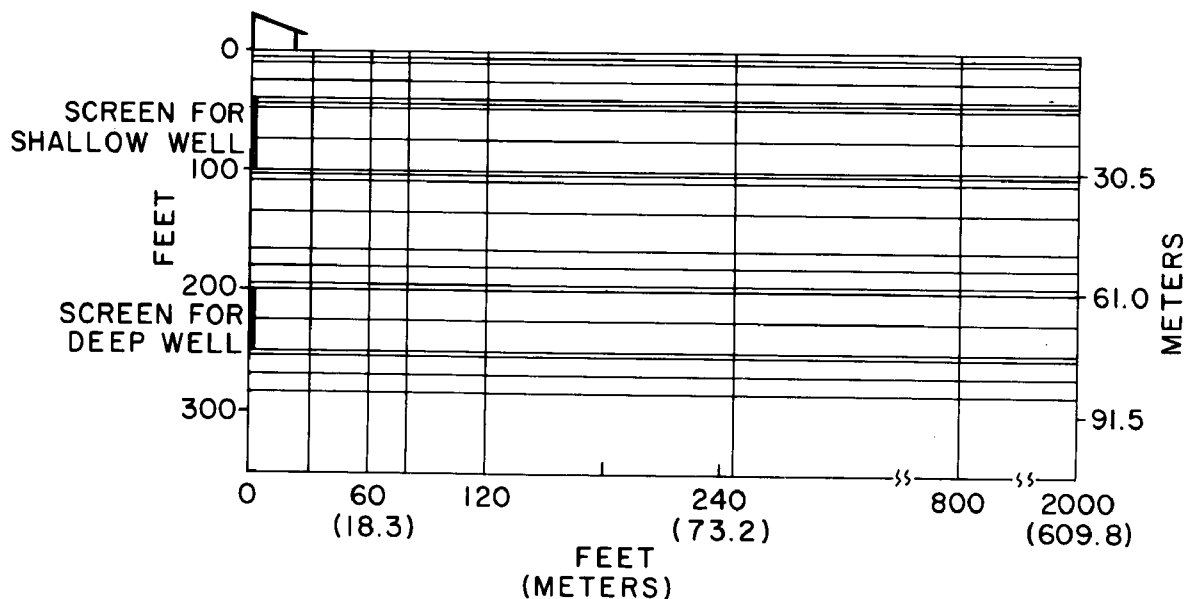


Figure C-24. Grid used to discretize the aquifer simulated in the heat pump problem.

Figure C-25. The data deck used to model the heat pump simulation with no regional groundwater flow.

```

1000 100 0 17000 21000 .33 .08
9 2 2 0 8000 8000 26000 .33 .08
10
175 25 0 17000 17000 21000 .33 .08
GROUP V
0 0
0 0
0 0
GROUP VI
0
GROUP VII
21
1 1 12000 8 1 12000 15 1 12000 22 1 12000
43 1 0 50 1 0 57 1 0 64 1 0 71 1 0 78 1 0 85 1 0 92 1 0 99 1 0
50 1 8000 57 1 8000 64 1 8000 71 1 8000 78 1 8000 85 1 8000 92 1 8000 99 1 8000
0 0 0 0 0 0 0 0 0 0 0 0 0 0 0 0 0 0 0 0 0 0
6
1 1 8 1 15 1 22 1 29 1 36 1
0 0 0 0 0 0 0
GROUP VIII
15 0
1 1 8 1 15 1 22 1 29 1 36 1 43 1 50 1 57 1 64 1 71 1 78 1 85 1 92 1 99 1
GROUP IX
1 0 0 0 0 8
53 69 93 101 52 68 92 100
1 140 140 1 140 140 1 140 140 1 3
5
10 860
      1.0000      29.5000      41.0000
      2.0000      28.5000      35.9000
      3.0000      27.5000      30.8000
1 1 1 1 1 1 1 0

```

Figure C-25. The data deck used to model the heat pump simulation with no regional groundwater flow.

HOME HEATING AND COOLING--SYMMETRICAL SET-UP
UNITS FEET GALLONS DAYS CALORIES

04/07/78
17:02:33

OF NODES 198 # OF ELEMENTS 168 BANDWIDTH 11

VELOCITIES ARE BEING CALCULATED AT CURRENT TIME STEP 1

THE X-SPACING IS

0.0	2.0000	10.0000	25.0000	40.0000	48.0000	50.0000	75.0000
100.0000	102.0000	110.0000	135.0000	165.0000	180.0000	195.0000	200.0000
225.0000	250.0000	255.0000	270.0000	285.0000	350.0000		

THE Y-SPACING IS

2000.000	800.0000	250.0000	160.0000	120.0000	80.0000	60.0000	30.0000
0.0							

EQUATION 2 TIME STEP 15.0000

HEAT OR MASS CAPACITY COEFFICIENT 3785.68

PARAMETER FACTORS--IN ORDER 1.00000 1.00000 1.00000 .700000 .700000 1.00000 1.00000 1.00000

MATERIAL	HOR PERM	VER PERM	STORAGE	HOR THERM COND	VERT THERM COND	SPECIFIC HEAT	DISPERSION	COEFS
1	.1000+00	.1000+00	.0000	5600.	5600.	.1700+05	10.00	1.000
2	10.00	100.0	.0000	.1190+05	.1190+05	.2100+05	10.00	1.000
3	25.00	250.00	.0000	.1190+05	.1190+05	.2100+05	10.00	1.000
4	10.00	100.0	.0000	.1190+05	.1190+05	.2100+05	10.00	1.000

THE VALUES IN THE TYPE OF MATERIAL MATRIX ARE

1.00000	1.00000	1.00000	1.00000	1.00000	1.00000	1.00000	1.00000
2.00000	2.00000	2.00000	2.00000	2.00000	2.00000	2.00000	2.00000
2.00000	2.00000	2.00000	2.00000	2.00000	2.00000	2.00000	2.00000
3.00000	3.00000	3.00000	3.00000	3.00000	3.00000	3.00000	3.00000
4.00000	4.00000	4.00000	4.00000	4.00000	4.00000	4.00000	4.00000
4.00000	4.00000	4.00000	4.00000	4.00000	4.00000	4.00000	4.00000
4.00000	4.00000	4.00000	4.00000	4.00000	4.00000	4.00000	4.00000
4.00000	4.00000	4.00000	4.00000	4.00000	4.00000	4.00000	4.00000
4.00000	4.00000	4.00000	4.00000	4.00000	4.00000	4.00000	4.00000

Figure C-26. Program output for the heat pump problem.

(continued)

-142-

JOHN	SOURCE OF WATER	WELL #	WELL DEPTH	WELL TYPE	WELL STATUS	WELL LOCATION	WELL DATE	WELL COMMENTS
63	1.00000	72	1.00000	81	1.00000	144	1.00000	153 1.00000
162	1.00000							

63	1.00000	72	1.00000	81	1.00000	144	1.00000	153	1.00000
162	1.00000								

ELEM #--BOUNDARY CODE--TRANSFER COEFFICIENT

LAI FLOW BOUNDARIES		NODE #		FWD BOUNDARY CODE													
1	3	2	3	3	3	4	3	5	3	6	3	7	3	8	3	9	3

.250000

Figure C-26. (continued)

10.0000	10.0000	10.0000	10.0000	10.0000	10.0000	10.0000	10.0000	10.0000
10.0000	10.0000	10.0000	10.0000	10.0000	10.0000	10.0000	10.0000	10.0000
10.0000	10.0000	10.0000	10.0000	10.0000	10.0000	10.0000	10.0000	10.0000
10.0000	10.0000	10.0000	10.0000	10.0000	10.0000	10.0000	10.0000	10.0000
10.0000	10.0000	10.0000	10.0000	10.0000	10.0000	10.0000	10.0000	10.0000
POTENTIAL DISTRIBUTION AT TIME STEP .000000								
10.00000	10.00000	10.00000	10.00000	10.00000	10.00000	10.00000	10.00000	10.00000
10.0013	10.0011	9.98874	9.97939	9.97459	9.96998	9.96806	9.96583	9.96433
10.0014	10.0012	9.98832	9.97842	9.97322	9.96813	9.96599	9.96346	9.96173
10.0015	10.0013	9.98773	9.97589	9.96883	9.96082	9.95687	9.95193	9.94858
10.0015	10.0014	9.98772	9.97457	9.96588	9.95443	9.94715	9.93387	9.91940
10.0015	10.0015	9.98799	9.97279	9.96126	9.94321	9.92931	9.89177	9.78885
10.0015	10.0015	9.98807	9.97238	9.96016	9.94052	9.92456	9.88408	9.72716
10.0016	10.0018	9.98989	9.97052	9.95306	9.92129	9.89284	9.81196	9.52379
10.0017	10.0022	9.99331	9.97712	9.96360	9.94163	9.92412	9.88125	9.72221
10.0017	10.0022	9.99365	9.97797	9.96504	9.94436	9.92863	9.88812	9.78247
10.0017	10.0023	9.99511	9.98172	9.97125	9.95580	9.94514	9.92506	9.90286
10.0018	10.0026	10.0005	9.99548	9.99222	9.98861	9.98716	9.98618	9.98653
10.0019	10.0029	10.0075	10.0129	10.0164	10.0203	10.0221	10.0242	10.0256
10.0019	10.0031	10.0109	10.0215	10.0291	10.0391	10.0449	10.0528	10.0565
10.0020	10.0033	10.0139	10.0295	10.0419	10.0611	10.0753	10.1086	10.1655
10.0020	10.0034	10.0148	10.0319	10.0458	10.0683	10.0860	10.1293	10.2876
10.0020	10.0037	10.0183	10.0393	10.0557	10.0903	10.1192	10.2003	10.4890
10.0019	10.0041	10.0201	10.0383	10.0527	10.0755	10.0933	10.1367	10.2951
10.0019	10.0042	10.0203	10.0373	10.0502	10.0698	10.0842	10.1176	10.1746
10.0019	10.0044	10.0206	10.0336	10.0421	10.0527	10.0588	10.0669	10.0708
10.0019	10.0046	10.0206	10.0298	10.0346	10.0396	10.0417	10.0442	10.0460
10.0018	10.0051	10.0198	10.0222	10.0227	10.0229	10.0228	10.0227	10.0225
CUMULATIVE MASS BLANCE								
B. FLUX RECHARGE	.000000				RATES FOR THIS TIME STEP			
B. FLUX DISCHARGE	.000000				.000000			
CHANGE IN STORAGE	.000000				.000000			
QUANTITY PUMPED	.000000				.000000			
DIFFERENCE	.000000				.000000			

Figure C-26. Program output for the heat pump problem.

I. BRIEF DESCRIPTION OF THE PROGRAM ROUTINES

A. Main Routine

This routine controls the flow of the program and the program dimensions. The parameter variables L, N, M control the maximum number of elements, nodes, and bandwidth respectively.

1. Internal Subroutine ITERAT

This subroutine controls the solution of a steady-state areal problem by an iterative method.

2. Internal Subroutine FLOADD

This subroutine adds in a constant specified flow rate to the values calculated by the water-flow equation.

B. Subroutine DATAIN

This subroutine reads in the program data.

1. ENTRY DI

This entry point passes arguments from the main routine to subroutine DATAIN.

2. Internal Subroutine ELREAD

This subroutine reads in the element node numbers.

3. Internal Subroutine P

This subroutine creates a rectangular grid and numbers the nodes and elements in the grid.

C. Subroutine STRUCT

This subroutine assembles the global structure matrix and the global capacitance matrix.

D. Subroutine GAUSS

This subroutine forms the element structure and capacitance matrices by Gaussian Quadrature.

1. ENTRY DERIVE

The main entry point for subroutine GAUSS.

2. Internal Subroutine CONVEC

This routine handles the convective boundaries.

E. Subroutine SHAPE1

This subroutine computes the shape functions for a linear element.

F. Subroutine SHAPE

This subroutine computes the shape functions for elements with one or more nonlinear sides.

G. Subroutine LOAD

This subroutine computes the global recharge matrix by adding in the various sources and sinks.

1. ENTRY HEATE
The main entry point for subroutine LOAD.
2. Internal Subroutine CB
This subroutine computes mass or heat flow across a specified potential boundary.

H. Subroutine SOLVE

This subroutine is a symmetric banded matrix equation solver.

1. ENTRY BACK
Entry point for the back substitution of the recharge matrix.
2. ENTRY MULTI
Entry point for the multiplication in a transient problem.

I. Subroutine ASOLVE

This subroutine is an assymetric banded matrix equation solver.

1. ENTRY ABACK
Entry point for the back substitution.
2. ENTRY AMULTI
Entry point for matrix multiplication in a transient problem.

J. Subroutine BALAN

This subroutine computes a mass balance.

1. ENTRY MASBAL
The main entry point for subroutine BALAN.
2. ENTRY BPRINT
The entry point for the printing of the mass balance.
3. ENTRY WATER
Entry point for computing water flows in each element.
4. ENTRY VELO
Computes water velocities at the Gauss points.
5. ENTRY VCENT
Computes water velocities at the center of each element.
6. Internal Subroutine FLOWW
Subroutine for computing element flows.

K. Subroutine FLOWS

This subroutine prints out element flows and nodal values.

1. ENTRY FFLOW
Entry point for the printing of nodal potentials on file 14.

2. ENTRY FFFLOW
Entry point for the printing of nodal temperatures or concentrations on file 14.
3. ENTRY WFLOW
Entry point for printing water flows for each element.
4. ENTRY HPRINT
Entry point for printing nodal temperature or concentration values.
5. ENTRY WPRINT
Entry point for printing nodal potential values.

L. Subroutine PARAM

This subroutine computes element parameters that are a function of velocity or temperature and localized coordinates.

1. ENTRY MECD
Entry point for computing dispersivity.
2. ENTRY CORD
Entry point for the computation of localized coordinates.
3. ENTRY PE
Entry point for computing hydraulic conductivity as a function of temperature.
4. ENTRY PEE
Entry point for the computation of aquifer thickness in an areal problem.

M. Subroutine BOUNDA

This routine is used to change parameter values or boundary conditions at each time step. Five entry points, ENTRY LAKE, ENTRY BVAL, ENTRY BOUND, ENTRY CHANG, ENTRY CHAN, are provided for user programming.

N. Subroutine EIGEN

This subroutine is used to compute the maximum stable time step for a transient problem.

O. Subroutine ADJUST

This subroutine moves the upper boundary in a cross-section problem.

1. ENTRY ADJUST
The main entry point for subroutine ADJUST.

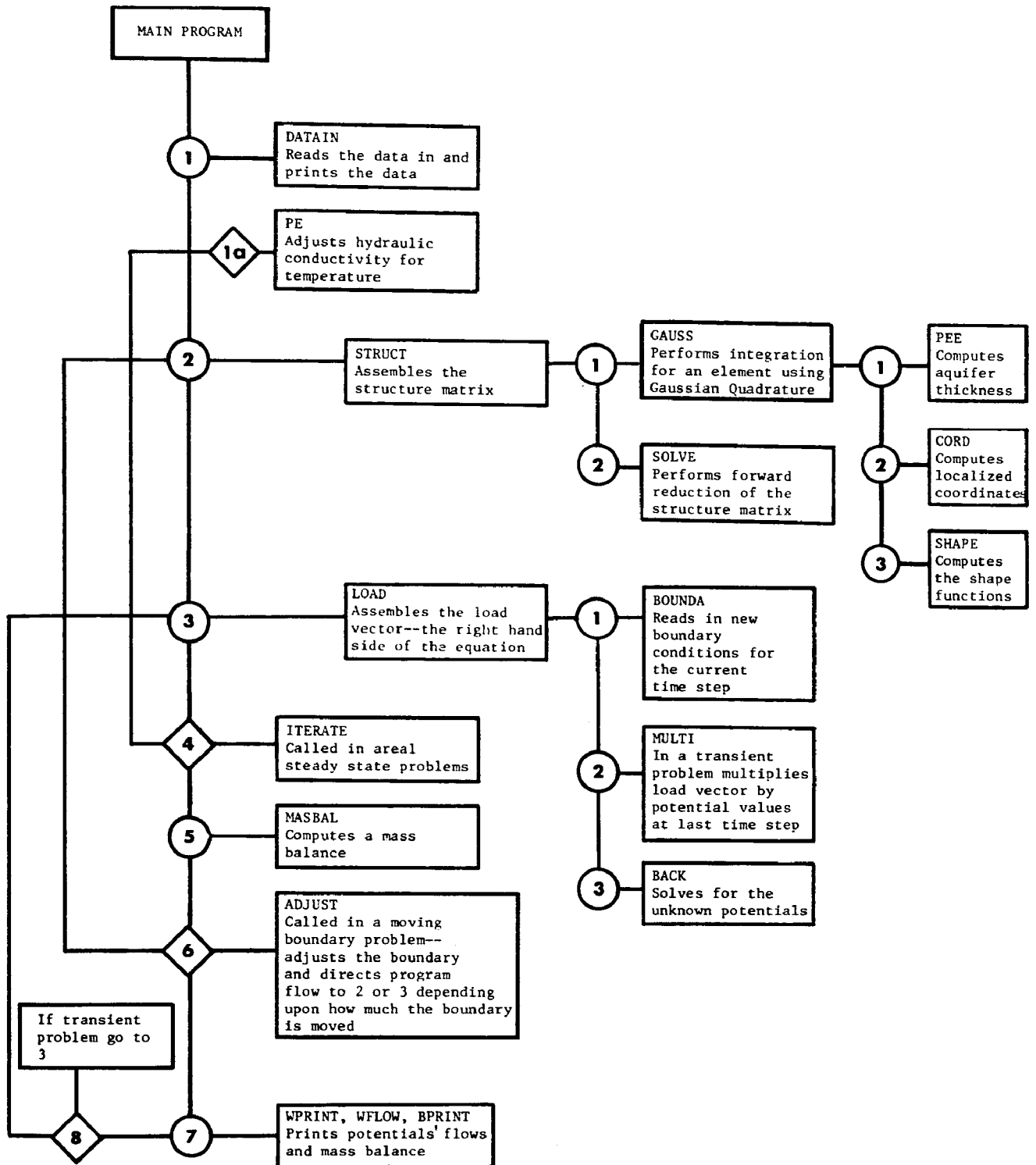


Figure C-27. Program flow chart.

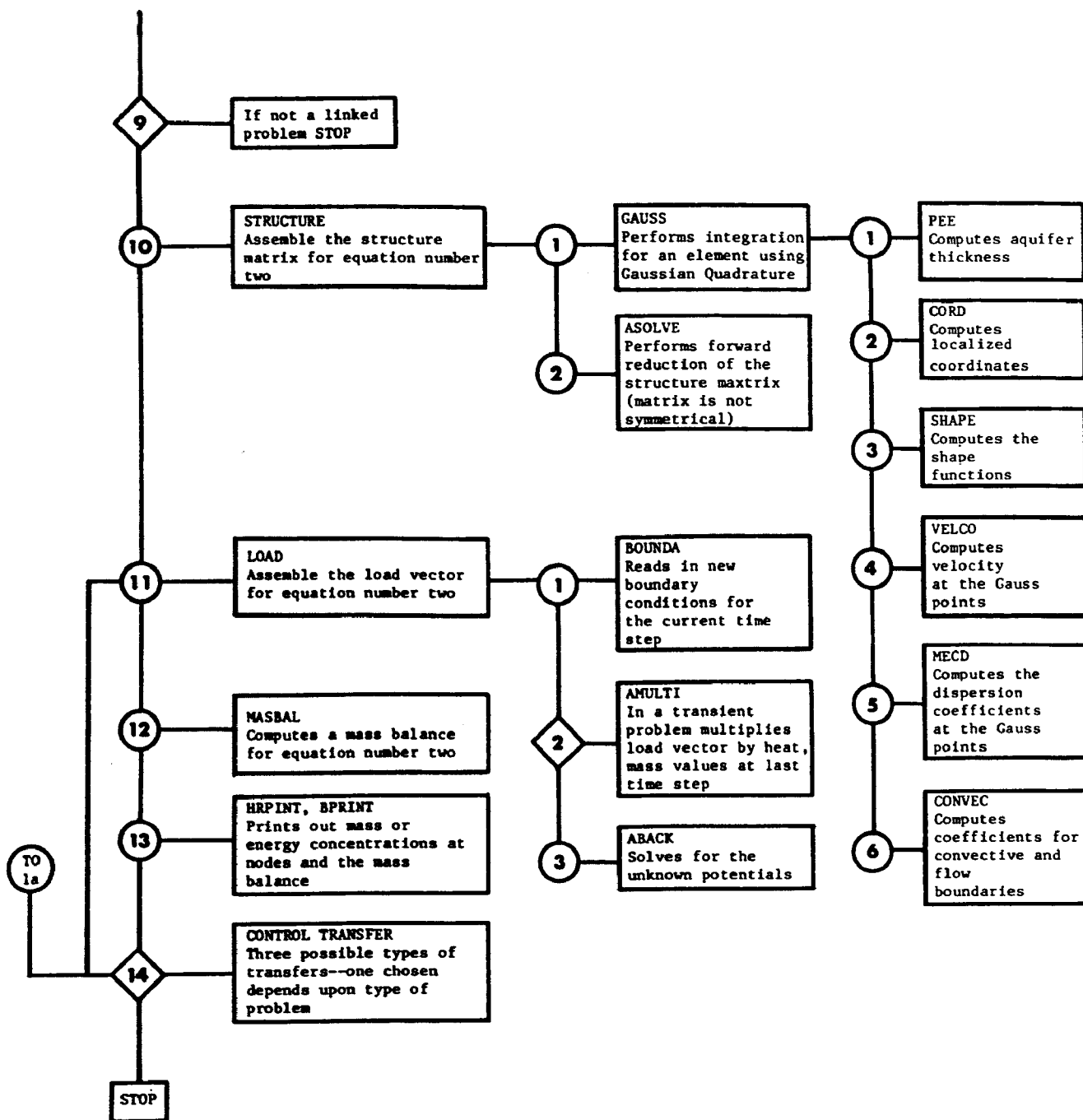


Figure C-27 (continued)

THE FINITE ELEMENT PROGRAM LISTING

C		MAI	100
C	*****	MAI	200
C		MAI	300
C	THE MAIN ROUTINE FOR THE FINITE ELEMENT PROGRAM	MAI	400
C	BY CHARLES ANDREWS	MAI	500
C		MAI	600
C		MAI	700
C	*****	MAI	800
C		MAI	900
C		MAI	1000
C	THE PARAMETER STATEMENTS	MAI	1100
C	L--NUMBER OF ELEMENTS, N--NUMBER OF NODES.	MAI	1200
C	M-- BANDWIDTH, Z--SIZE OF ARRAYS CONTAINING SOURCE	MAI	1300
C	SINK, AND BOUNDARY INFORMATION	MAI	1400
C		MAI	1500
C	PARAMETER M=17,N=160,L=130,Z=50	MAI	1600
C		MAI	1700
C		MAI	1800
C	*****	MAI	1900
C	PARAMETER P=M*2-1,BBB=N	MAI	2000
C	INTEGER AY(4),AZ(4)	MAI	2100
C	DATA AY/4,1,4,3/	MAI	2200
C	DATA AZ/3,2,1,2/	MAI	2300
C	DOUBLE PRECISION S,T	MAI	2400
C	REAL MAT INFLOW	MAI	2500
C	COMMON/ACC/KK(12),K1,K2,K3,K4	MAI	2600
C	COMMON/AM/NLA,PCT/CON/MC1,MC2,NCONV	MAI	2700
C	*/CONT/LA,LB,LC,LD,LE,LF,LG LH	MAI	2800
C	COMMON/HI/TITLE(25),V(26),VV(26)	MAI	2900
C	COMMON/HM/PXX,PYY,PXY,KAD/HH/LFLOW,LON/ME/MEQ	MAI	3000
C	COMMON/ATHICK/ASIZE,NTHICK,THICK ERROR	MAI	3100
C	MODEL PARAMETERS--1	MAI	3200
C	DIMENSION WX(L),WY(L),STO(L),INFLOW(L)	MAI	3300
C	--MODEL PARAMETERS--2	MAI	3400
C	DIMENSION PX(L),PY(L),PCX(L),HEAT(L),DIFF(L,2)	MAI	3500
C	--BOUNDARY CONDITIONS	MAI	3600
C	DIMENSION HEAD(N),HEA(N)	MAI	3700
C	--INITIAL CONDITIONS AND ANSWERS	MAI	3800
C	DIMENSION R(N),R1(N)	MAI	3900
C	--THE GRID CHARACTERISTICS	MAI	4000
C	DIMENSION XLOC(N),YLOC(N),NOD(12,L),NODE(L),MAT(L)	MAI	4100
C	--LINKING INFORMATION	MAI	4200
C	DIMENSION YSPACE(20) FLOWX(N),FLOWY(N)	MAI	4300
C	--MATRICIES USED FOR TEMPORARY STORAGE	MAI	4400
C	DIMENSION TPX(L),TPY(L),RI(N),G(N),NTIME(100),NSPACE(50)	MAI	4500
C	--INFORMATION FOR POINT SOURCES	MAI	4600
C	DIMENSION NFLUXW(Z,2),AFLUXW(Z),NFLUXH(Z,2),AFLUXH(Z)	MAI	4700
C	--INFORMATION FOR LINE SOURCES OF MASS OR WATER	MAI	4800
C	*.ALINEW(Z),ALINEH(Z),NLINEW(Z,2),NLINEH(Z,2)	MAI	4900
C	--INFORMATION FOR MASS BALANCE ON FLOW BOUNDARIES	MAI	5000
C	DIMENSION N WATER(Z),A WATER(Z),NHEAT(Z),AHEAT(Z)	MAI	5100
C	--ELEVATION AT THE BOTTOM OF THE AQUIFER	MAI	5200
C	DIMENSION BOT(BBB)	MAI	5300
C	--INFORMATION ON CONVECTIVE BOUNDARIES	MAI	5400
C	*.NCON(Z,3).TINF(Z),CONV(Z),ALOC(Z),NEL(Z,2).AEL(Z,2).CBAL(Z,2)	MAI	5500
C	--STRUCTURE MATRICIES	MAI	5600
C	DIMENSION GG(N), S(N,P),T(N,P)	MAI	5700

	CALL URDATE(IDATE,IYEAR)	MAI 5800
	CALL URTIMD(ETIME,ISEC)	MAI 5900
1	FORMAT(1X,'MAXIMUM NUMBER OF NODES PERMITTED EXCEEDED')	MAI 6000
3	FORMAT(1X,'MAXIMUM NUMBER OF ELEMENTS EXCEEDED')	MAI 6100
4	FORMAT(1X,1H1)	MAI 6200
	READ 7,(TITLE(J),J=1,24)	MAI 6300
	PRINT 300 (TITLE(J),J=1,24),IDATE,IYEAR,ETIME,ISEC	MAI 6400
7	FORMAT(12A6)	MAI 6500
	READ,LM,LN,MBAND	MAI 6600
	PRINT 8,LN,LM,MBAND	MAI 6700
8	FORMAT(1X,'#OF NODES',I4 ' # OF ELEMENTS',I4 ' BANDWIDTH',I4)	MAI 6800
	IF(LM.GT.L) PRINT 3	MAI 6900
	IF(LN.GT.N) PRINT 1	MAI 7000
	MPP=MBAND*2-1	MAI 7100
	NAA=0	MAI 7200
C	*****	MAI 7300
C	INPUT THE DATA	MAI 7400
C		MAI 7500
	CALL DATAIN(LM,LN,MBAND,MAT,R1,R,HEA,HEAD,WX,WY,STO,INFLOW,PX,PY,	MAI 7600
	*PCX,HEAT,XLOC,YLOC,NOD,TPX,TPY,KRANA,CFACT,CFACT1,	MAI 7700
	*ALPHA,KSTEP,KBOUND,KFT,PCW,KRAN,ALPH,KSTE,KBOUN,KF,PCH,DIFF,	MAI 7800
	*Z,NCON,TINF,CONV,ALOC,LWATER,NWATER,AWATER,LHEAT,NHEAT,AHEAT,	MAI 7900
	*LFLUXW,NFLUXW,AFLUXW,LFLUXH,NFLUXH,AFLUXH,BBB,BOT,KTYPE	MAI 8000
	*,NODE,NEL,AEL)	MAI 8100
	CALL DI(KAREAL,ALPHM,ALPHAM,ER,ITER,LEL	MAI 8200
	*LINEW,LINEH,NLINEW,NLINEH,ALINEW,ALINEH)	MAI 8300
C		MAI 8400
C	*****	MAI 8500
C	INITIALIZE THE STARTING ADDRESSES AND STARTING VALUES	MAI 8600
C		MAI 8700
	CALL FLOWS(LM,LN,R,R1,FLOWX,FLOWY)	MAI 8800
C		MAI 8900
	CALL BOUND(LM,LN,Z,R,R1,HEAD,HEA,FLOWX,FLOWY,HEAT,INFLOW	MAI 9000
	*NWATER,AWATER,NHEAT,AHEAT,NCON,TINF	MAI 9100
	*CONV,ALOC,NEL,AEL,CBAL,LEL,LHEAT,LWATER,PCW,AY,AZ	MAI 9200
	*,LINEW,LINEH,NLINEW,NLINEH,ALINEW,ALINEH)	MAI 9300
	CALL PARAM(LM,LN,BBB,XLOC,YLOC,NOD,PCX,DIFF,R,R1,WX,WY,TPX	MAI 9400
	*,TPY,BOT,KAREAL)	MAI 9500
	CALL VELOC(LN,LM,R1,WX,WY)	MAI 9600
C		MAI 9700
	MU=0	MAI 9800
C	*****	MAI 9900
C	PROGRAM CONTROL IS ESTABLISHED	MAI 10000
	READ,LA,LD,LE,LF,LG,LH	MAI 10100
	IF(LE.GT.0) READ,(NTIME(I),I=1,LE)	MAI 10200
	IF(LF.EQ.1) READ,ASIZE,NTHICK,MTHICK,ERROR,XADD,YADD	MAI 10300
	IF(LH.GT.0) READ,(HSPACE(I),I=1,LH)	MAI 10400
	IF(LA.EQ.1) CALL LAKE	MAI 10500
	IF(LG.GT.0) CALL ADJUST(LG,LM,LN,Z,HEA,XLOC,YLOC,NOD	MAI 10600
	*,FLOWX,FLOWY,R1)	MAI 10700
	GO TO(10,20,30,30,30),KTYPE	MAI 10800
10	CONTINUE	MAI 10900
	MA=-1	MAI 11000
	MB=1	MAI 11100
	MC=1	MAI 11200
	MD=1	MAI 11300
	ME=1	MAI 11400
	READ,MW	MAI 11500
	GO TO 120	MAI 11600
20	READ,MA,MB,MW,MC,MD	MAI 11700
	IF(MD.LE.0) MU=1	MAI 11800
	ME=1	MAI 11900
	GO TO 120	MAI 12000

30	READ,MO,MP,MV,MQ,MR,MS,MT MU,ME	MAI12100
	MA=-1	MAI12200
	MB=1	MAI12300
	MC=1	MAI12400
	MD=1	MAI12500
	ME=0	MAI12600
	MW=9999999999	MAI12700
	ALPH=0.0	MAI12800
120	CONTINUE	MAI12900
C	NA IS A COUNTER	MAI13000
	NA=0	MAI13100
C	THESE LINES ESTABLISH NO CONVECTIVE BOUNDARIES IN EQN 1	MAI13200
	NCC=NCONV	MAI13300
	NCONV=0	MAI13400
C	NO DISPERSION IN EQN 1	MAI13500
	KAD=0	MAI13600
C	CONTROL FOR SYM OR ASSYM SOLUTION TECHNIQUE	MAI13700
	NLB=NLA	MAI13800
	NLA=LC	MAI13900
	IF(KTYPE.EQ.5) GO TO 160	MAI14000
124	CONTINUE	MAI14100
125	CONTINUE	MAI14200
C		MAI14300
C	*****	MAI14400
C		MAI14500
C	EQUATION NUMBER ONE	MAI14600
C		MAI14700
C	*****	MAI14800
C	ADJUST PERMEABILITIES FOR CHANGING TEMPERATURES	MAI14900
	IF(MS.EQ.1) CALL PE(MS)	MAI15000
C	MULTIPLICATION FACTOR FOR TIME STEP	MAI15100
	IF(KS.GT.0.OR.NA.GT.0) ALPH=ALPH*ALPHM	MAI15200
C		MAI15300
C	*****	MAI15400
C	INITALIZE STARTING ADDRESSES IN HEATER GAS AND BALANCE FOR EQUATION	MAI15500
	MEQ=1	MAI15600
	CALL LOAD(LM,LN,MBAND,NOD,NODE,R1,RI,G	MAI15700
	*.GG,INFLOW,HEA,ALPH,KBOUN,KF,PCH,KRANA,CFACT1 KS,	MAI15800
	*Z,NCON,TINF,CONV,ALOC,LWATER,NWATER,AWATER,CBAL,AY,AZ	MAI15900
	*.AEL,NEL,MEQ,LEL,CBAL,LINEW,NLINEW,ALINEW)	MAI16000
	CALL BALAN(LM,LN,R1,WX,WY,STO HEA,INFLOW,Z,LWATER,AWATER	MAI16100
	*.LFLUXW,NFLUXW,WA,WB,WC,WD,WE,MPRINT,NTYPE,RI,NODE,NOD	MAI16200
	*FLOWX.FLOWY.PCW,MEQ,CBAL,CBALA,AY,AZ,NCON,KRANA)	MAI16300
C		MAI16400
C		MAI16500
	CALL GAUSS(LLL,LM,LN,XLOC,YLOC,NOD,WY,WX,INFLOW,STO,ALPH,KBOUN,	MAI16600
	* KRANA,Z,NCON,CONV,ALOC,NODE,CBAL,AY,AZ)	MAI16700
	CALL STRUCT(LN,LM,MBAND,MPP,R1,S T,G,GG,RI,HEA,XLOC,	MAI16800
	*YLOC,NOD,NODE,CFACT1,KRANA,ALPH,KBOUN)	MAI16900
C		MAI17000
	NAA=NAA+1	MAI17100
130	NA=NA+1	MAI17200
	BKS=BKS+ALPH	MAI17300
	IF(ALPH.LT.0.0001) BKS=AKS	MAI17400
	CALL HEATE(KS)	MAI17500
	IF(KAREAL.EQ.1) CALL ITERAT(ER,ITER,KSA,\$124)	MAI17600
	KSA=0	MAI17700
	IF(MC.GT.0) CALL MASBAL(ALPH)	MAI17800
	M1=NA/MD	MAI17900
	MM1=M1*MD	MAI18000
	IF(MM1.EQ.NA.AND.MU.EQ.0) CALL WATER	MAI18100
C		MAI18200
C		MAI18300
	IF(LG.GT.0) CALL ADJUS(\$125,\$130)	MAI18400

C		MAI18500
C		MAI18600
	M1=NA/MB	MAI18700
	M1=M1*MB	MAI18800
	IF(M1.EQ.NA) CALL WPRINT(BKS)	MAI18900
	M1=NA/MC	MAI19000
	M1=M1*MC	MAI19100
	IF(M1.EQ.NA) CALL BPRINT	MAI19200
C		MAI19300
C	ADDS IN A CONSTANT BACKGROUND FLOW RATE	MAI19400
C		MAI19500
	IF(XADD.EQ.0.AND.YADD.EQ.0) GO TO 145	MAI19600
C		MAI19700
	CALL FLOADD	MAI19800
C		MAI19900
145	CONTINUE	MAI20000
C		MAI20100
C		MAI20200
	IF(MM1.EQ.NA.AND.MU.EQ.0) CALL WFLOW(BKS)	MAI20300
	M1=NA/MW	MAI20400
	M1=M1*MW	MAI20500
	IF(M1.EQ.NA) CALL FFLOW	MAI20600
	IF(MA.LE.BKS) GO TO 155	MAI20700
	IF(ALPHM.GT.1) GO TO 125	MAI20800
	GO TO 130	MAI20900
155	CONTINUE	MAI21000
	IF(ME.EQ.1) STOP	MAI21100
160	CONTINUE	MAI21200
C	*****	MAI21300
C		MAI21400
C	EQUATION NUMBER TWO	MAI21500
C		MAI21600
C	*****	MAI21700
	NTHICK=MTHICK	MAI21800
	NCONV=NCC	MAI21900
	KAD=MT	MAI22000
	NLA=NLB	MAI22100
C	*****	MAI22200
C	MULTIPLICATION FACTOR FOR THE TIME STEP	MAI22300
	IF(KS.GT.0) ALPHA=ALPHA*ALPHAM	MAI22400
C		MAI22500
C		MAI22600
C	INITIALIZE STARTING ADDRESSES IN HEATER AND BALANCE FOR EQUATION 2	MAI22700
	MEQ=2	MAI22800
C		MAI22900
	CALL LOAD(LM, LN, MBAND, NOD, NODE, R, RI, G,	MAI23000
	*GG, HEAT, HEAD, ALPHA, KBOUND, KFT, PCW, KRAN, CFACT, KS,	MAI23100
	*Z, NCON, TINF, CONV, ALOC, LHEAT, NHEAT, AHEAT, CBAL, AY, AZ	MAI23200
	* , AEL, NEL, MEQ, LEL, CBALA, LINEH, NLINEH, ALINEH)	MAI23300
	CALL BALAN(LM, LN, R, PX, PY, PCX, HEAD, HEAT, Z, LHEAT, AHEAT, LFLUXH,	MAI23400
	* NFLUXH, HA, HB, HC, HD, HE, MPRINT, NTYPE, RI, NODE, NOD, FLOWX, FLOWY, PCW,	MAI23500
	* MEQ, CBAL, CBALA, AY, AZ, NCON, KRAN)	MAI23600
C		MAI23700
C		MAI23800
C		MAI23900
	CALL GAUSS(LLL, LM, LN, XLOC, YLOC, NOD, PY, PX, HEAT, PCX, ALPHA, KBOUND, KRMAI24000	
	*AN, Z, NCON, CONV, ALOC, NODE, CBAL, AY, AZ)	MAI24100
C		MAI24200
	CALL STRUCT(LN, LM, MBAND, MPP, R, S, T, G, GG, RI, HEAD, XLOC, YLOC,	MAI24300
	* NOD, NODE, CFACT, KRAN, ALPHA, KBOUND)	MAI24400
C		MAI24500
C		MAI24600

200	CONTINUE	MAI24700
	KS=KS+1	MAI24800
	AKS=AKS+ALPHA	MAI24900
C		MAI25000
C		MAI25100
C		MAI25200
C		MAI25300
	CALL HEATE(KS)	MAI25400
	IF(LH.EQ.0) GO TO 209	MAI25500
	DO 208 I=1,LH	MAI25600
	J=NSPACE(I)	MAI25700
208	YSPACE(I)=R(J)	MAI25800
	WRITE(15,V) (YSPACE(I),I=1,LH)	MAI25900
209	CONTINUE	MAI26000
	IF(MQ.GT.0) CALL MASBAL(ALPHA)	MAI26100
	IF(ASIZE.NE.-1.0) GO TO 212	MAI26200
	DO 211 I=2,LN 2	MAI26300
	R(I)=(R(I)+R(I-1))/2	MAI26400
211	R(I-1)=R(I)	MAI26500
212	CONTINUE	MAI26600
	M1=KS/MP	MAI26700
	M1=M1*MP	MAI26800
	IF(M1.EQ.KS) CALL HPRINT(AKS)	MAI26900
	M1=KS/MV	MAI27000
	M1=M1*MV	MAI27100
	IF(M1.EQ.KS) CALL FFFLOW	MAI27200
	M1=KS/MQ	MAI27300
	M1=M1*MQ	MAI27400
	IF(M1.EQ.KS) CALL BPRINT	MAI27500
	IF(MO.LE.AKS) STOP	MAI27600
	C NTIME CONTAINS INFORMATION ON WHEN FLOWS ARE TO BE RECOMPUTED	MAI27700
	C NAA IS A COUNTER INDICATING THE NUMBER OF TIMES FLOWS HAVE BEEN COMP	MAI27800
	IF(LE.EQ.1.AND.NTIME(NAA).EQ.KS) GO TO 120	MAI27900
	M1=KS/MR	MAI28000
	M1=MR*M1	MAI28100
	IF(M1.NE.KS) GO TO 200	MAI28200
	GO TO 120	MAI28300
C		MAI28400
300	FORMAT(1H1/1X,130(''')/1X,3(''',T130,''/1X),	MAI28500
	* 2(''',35X,12A6,T130,''/1X),'',T130,''/1X,	MAI28600
	* 2(''',T100,A6,A2,T130.''/1X),130('''))	MAI28700
C		MAI28800
C	*****	MAI28900
C	*****	MAI29000
C		MAI29100
	SUBROUTINE ITERAT(ER,ITER,KS.*)	MAI29200
	IF(KRANA.NE.0) RETURN	MAI29300
	A=0	MAI29400
	DO 1J=1,LN	MAI29500
	B=RI(J)-R1(J)	MAI29600
	B=ABS(B)	MAI29700
1	A=AMAX1(B,A)	MAI29800
	KS=KS+1	MAI29900
	IF(A.LT.ER.OR.KS.GT.ITER) PRINT 5,KS	MAI30000
	IF(A.LT.ER.OR.KS.GT.ITER) RETURN	MAI30100
	RETURN 4	MAI30200
5	FORMAT(1X//1X,'ITERATIONS NEEDED FOR CONVERGENCE ',I5)	MAI30300
C		MAI30400

C*****	MAI30500
C	MAI30600
SUBROUTINE FLOADD	MAI30700
C	MAI30800
DO 140 KSS=1,LM	MAI30900
CALL CORD(KSS)	MAI31000
Y=YLOC(K4)-YLOC(K1)+YLOC(K3)-YLOC(K2)	MAI31100
Y=ABS(Y)/2	MAI31200
X=XLOC(K4)+XLOC(K1)-XLOC(K3)-XLOC(K2)	MAI31300
X=ABS(X)/2	MAI31400
XX=1.0	MAI31500
YY=1.0	MAI31600
IF(NTHICK.EQ.0) GO TO 135	MAI31700
YY=(YLOC(K1)+YLOC(K4))/2*ASIZE	MAI31800
XX=(XLOC(K3)+XLOC(K4))/2*ASIZE	MAI31900
XX=ABS(XX)	MAI32000
YY=ABS(YY)	MAI32100
135 CONTINUE	MAI32200
FLOWY(KSS)=FLOWY(KSS)+YADD*X/YY	MAI32300
FLOWX(KSS)=FLOWX(KSS)+XADD*Y/XX	MAI32400
140 CONTINUE	MAI32500
END	MAI32600

C*****	DAT 100
C	DAT 200
C THIS ROUTINE IS USED TO READ IN THE DATA	DAT 300
C	DAT 400
SUBROUTINE DATAIN(LM, LN, MBAND, MAT, R1, R, HEA, HEAD, WX, WY, STO	DAT 500
*, INFLOW, PX, PY, PCX, HEAT, XLOC, YLOC, NOD, TPX, TPY, KRANA, CFACT, CFACT1,	DAT 600
*ALPHA, KSTEP, BOUND, KFT, PCW, KRAN, ALPH, KSTE, BOUN, KF, PCH, DIFF,	DAT 700
*Z, NCON, TINF, CONV, ALOC, LWATER, NWATER, AWATER, LHEAT, NHEAT, AHEAT,	DAT 800
, LFLUXW, NFLUXW, AFLUXW, LFLUXH, NFLUXH, AFLUXH, BBB, BOT, KTYPE	DAT 900
*, NODE, NEL, AEL)	DAT 1000
INTEGER BOUND, BOUN, BBB, Z	DAT 1100
REAL INFLOW, MAT	DAT 1200
COMMON/HI/TITLE(25), V(26), VV(26)/HH/LFLOW, LON	DAT 1300
COMMON/A1/M, MM, NUMNP, NSIZE/AM/NLA, PCT	DAT 1400
COMMON/CON/MC1, MC2, NCONV	DAT 1500
DIMENSION NCON(Z, 3), TINF(Z), CONV(Z), ALOC(Z), NWATER(Z),	DAT 1600
* AWATER(Z), NHEAT(Z), AHEAT(Z), NFLUXW(Z, 2), AFLUXW(Z), NFLUXH(Z, 2),	DAT 1700
*AFLUXH(Z), BOT(BBB), AEL(Z, 2), NEL(Z, 2)	DAT 1800
DIMENSION MAT(LM), R1(LN), R(LN), HEA(LN), HEAD(LN), WX(LM), WY(LM)	DAT 1900
DIMENSION STO(LM), INFLOW(LM), PX(LM), PY(LM), PCX(LM), HEAT(LM)	DAT 2000
DIMENSION XLOC(LN), YLOC(LN), NOD(12, LM), TPX(LM), TPY(LM)	DAT 2100
DIMENSION FF(8), Q(12), A(8, 50), DIFF(LM, 2), NODE(LM)	DAT 2200
RETURN	DAT 2300
C	DAT 2400
C	DAT 2500
ENTRY DI(KAREAL, ALPHM, ALPHAM, ER, ITER, LEL,	DAT 2600
*LINEW, LINEH, NLINEW, NLINEH, ALINEW, ALINEH)	DAT 2700
DIMENSION NLINEW(Z, 2), NLINEH(Z, 2), ALINEW(Z), ALINEH(Z)	DAT 2800
C*****	DAT 2900
C	DAT 3000
DO 2 J=1, LM	DAT 3100
HEAD(J)=0.0	DAT 3200
2 HEA(J)=0.0	DAT 3300
C	DAT 3400
C	DAT 3500
C*****	DAT 3600
C	DAT 3700
7 FORMAT(12A6)	DAT 3800
READ, KTYPE, KPRINT, LON, MQ, NLA, CFACT	DAT 3900
CFACT1=CFACT	DAT 4000
NUMNP=LN	DAT 4100
NSIZE=NUMNP	DAT 4200
M=LM	DAT 4300
MM=M	DAT 4400
READ 40, (V(I), I=1, 26)	DAT 4500
READ 40, (VV(I), I=1, 26)	DAT 4600
IF(NLA.GT.0) PRINT 155, NLA	DAT 4700
C	DAT 4800
READ 7, (Q(J), J=1, 12)	DAT 4900
C*****	DAT 5000
C	DAT 5100
C DATA GROUP II	DAT 5200
C READ IN DATA ON THE SPATIAL STRUCTURE	DAT 5300
C	DAT 5400
IF(MQ.LT.0.0001) GO TO 12	DAT 5500
DO 8 I=1, NUMNP	DAT 5600
READ, J, XLOC(J), YLOC(J)	DAT 5700
8 CONTINUE	DAT 5800
DO 9 II=1, LM	DAT 5900
CALL ELREAD	DAT 6000
9 CONTINUE	DAT 6100
GO TO 15	DAT 6200

12	CONTINUE	DAT 6300
	READ,KSPACX,KSPACY	DAT 6400
	CALL P(KSPACX,KSPACY)	DAT 6500
	MQ=ABS(MQ)	DAT 6600
	DO 14 J=1,LM	DAT 6700
14	NODE(J)=4	DAT 6800
15	CONTINUE	DAT 6900
C		DAT 7000
	READ 7,(Q(J),J=1,12)	DAT 7100
C	*****	DAT 7200
C		DAT 7300
C	DATA GROUP III	DAT 7400
C	INPUT INITIAL CONDITIONS AND BOUNDARY CONDITIONS	DAT 7500
C		DAT 7600
	KRAN=0	DAT 7700
	KRANA=0	DAT 7800
	GO TO (21,20,23,22,22),KTYPE	DAT 7900
20	READ,ALPH,ALPHM,BOUN	DAT 8000
	PCH=1.0	DAT 8100
	KF=0	DAT 8200
	PRINT 150,ALPH	DAT 8300
	KRANA=1	DAT 8400
	CALL READER(LN,R1,I)	DAT 8500
	IF(I.NE.999) STOP R1	DAT 8600
21	CALL READER(LN,HEA,I)	DAT 8700
	IF(I.NE.999) STOP HEA	DAT 8800
	GO TO 24	DAT 8900
22	READ,ALPH,ALPHM,BOUN	DAT 9000
	KF=0	DAT 9100
	PCH=1.0	DAT 9200
	PRINT 150,ALPH	DAT 9300
	KRANA=1	DAT 9400
	CALL READER(LN,R1,I)	DAT 9500
	IF(I.NE.999) STOP R1	DAT 9600
23	READ,ALPHA,ALPHAM,BOUND,PCW	DAT 9700
	KFT=0	DAT 9800
	IF(NLA.EQ.0) KFT=1	DAT 9900
	PCT=PCW	DAT10000
	PRINT 151,ALPHA,PCW	DAT10100
	KRAN=1	DAT10200
	CALL READER(LN,R,I)	DAT10300
	IF(I.NE.999) STOP R	DAT10400
	CALL READER(LN,HEA,I)	DAT10500
	IF(I.NE.999) STOP HEA	DAT10600
	CALL READER(LN,HEAD,I)	DAT10700
	IF(I.NE.999) STOP HEAD	DAT10800
24	CONTINUE	DAT10900
	IF(KFT.EQ.1) PRINT 156	DAT11000
C		DAT11100
	READ 7,(Q(J),J=1,12)	DAT11200
C	*****	DAT11300
C		DAT11400
C	DATA GROUP IV	DAT11500
C	INPUT PARAMETERS	DAT11600
C		DAT11700
	READ, NMATA	DAT11800
	IF(KTYPE.GT.2) READ,(FF(I),I=1,8)	DAT11900
C		DAT12000
	IF(KTYPE.LT.3) READ,FF(1),FF(2),FF(3)	DAT12100
	PRINT 105,(FF(I),I=1,8)	DAT12200
	PRINT 102	DAT12300
	CALL READER(LM,MAT,I)	DAT12400
	IF(I.NE.999) STOP MAT	DAT12500

DO 32 JJ=1,NMATA	DAT12600
IF(KTYPE.LT.3) READ,J,(A(I,J),I=1,3)	DAT12700
IF(KTYPE.EQ.5) READ,J,(A(I,J),I=4,8)	DAT12800
IF(KTYPE.GT.2) READ,J,(A(I,J),I=1,8)	DAT12900
DO 31 I=1,8	DAT13000
31 A(I,J)=A(I,J)*FF(I)	DAT13100
PRINT 104,J,(A(I,J),I=1,8)	DAT13200
32 CONTINUE	DAT13300
DO 34 K=1,LM	DAT13400
DO 33 J=1,50	DAT13500
KZX=MAT(K)	DAT13600
IF(KZX.NE.J) GO TO 33	DAT13700
WX(K)=A(1,J)	DAT13800
WY(K)=A(2,J)	DAT13900
STO(K)=A(3,J)	DAT14000
PX(K)=A(4,J)	DAT14100
PY(K)=A(5,J)	DAT14200
PCX(K)=A(6,J)	DAT14300
DIFF(K,1)=A(7,J)	DAT14400
DIFF(K,2)=A(8,J)	DAT14500
GO TO 34	DAT14600
33 CONTINUE	DAT14700
34 CONTINUE	DAT14800
DO 35 J=1,LM	DAT14900
TPX(J)=WX(J)	DAT15000
35 TPY(J)=WY(J)	DAT15100
C	DAT15200
PRINT 120	DAT15300
PRINT VV,(MAT(J),J=1,LM)	DAT15400
C	DAT15500
READ 7,(Q(J),J=1,12)	DAT15600
C*****	DAT15700
C	DAT15800
C INPUT DISTRIBUTED SOURCES	DAT15900
C	DAT16000
READ,KGEN,KGENH	DAT16100
IF(KGEN.EQ.1) CALL READER(LM,INFLOW,I)	DAT16200
IF(I.NE.999) STOP INFL	DAT16300
IF(KGENH.EQ.1) CALL READER(LM,HEAT,I)	DAT16400
IF(I.NE.999) STOP HEAT	DAT16500
C*****	DAT16600
C	DAT16700
C INPUT POINT SOURCES OF WATER AND HEAT	DAT16800
READ,LWATER,LHEAT	DAT16900
IF(LWATER.EQ.0) GO TO 61	DAT17000
READ,(NWATER(I),AWATER(I),I=1,LWATER)	DAT17100
PRINT 131,(NWATER(I),AWATER(I),I=1,LWATER)	DAT17200
61 CONTINUE	DAT17300
IF(LHEAT.EQ.0) GO TO 63	DAT17400
READ,(NHEAT(I),AHEAT(I),I=1,LHEAT)	DAT17500
PRINT 132,(NHEAT(I),AHEAT(I),I=1,LHEAT)	DAT17600
63 CONTINUE	DAT17700
C	DAT17800
C	DAT17900
C INPUT LINE SOURCES OF WATER AND HEAT	DAT18000
READ,LINEW,LINEH	DAT18100
IF(LINEW.EQ.0) GO TO 66	DAT18200
READ,(NLINEW(I,1),NLINEW(I,2),I=1,LINEW)	DAT18300
READ,(ALINEW(I),I=1,LINEW)	DAT18400
PRINT 278,(NLINEW(I,1),NLINEW(I,2),ALINEW(I),I=1,LINEW)	DAT18500
66 IF(LINEH.EQ.0) GO TO 68	DAT18600
READ,(NLINEH(I,1),NLINEH(I,2),I=1,LINEH)	DAT18700
READ,(ALINEH(I),I=1,LINEH)	DAT18800
PRINT 279,(NLINEH(I,1),NLINEH(I,2),ALINEH(I),I=1,LINEH)	DAT18900

68	CONTINUE	DAT19000
C		DAT19100
C		DAT19200
	READ 7,(Q(J),J=1,12)	DAT19300
C	*****	DAT19400
C		DAT19500
C	DATA GROUP VI	DAT19600
C		DAT19700
C	INPUT INFORMATION NEEDED FOR A 2-D AREAL VIEW OF THE SYSTEM	DAT19800
	READ,KAREAL	DAT19900
	IF(KAREAL.EQ.0) GO TO 41	DAT20000
	READ,ER,ITER	DAT20100
	CALL READER(LN,BOT,I)	DAT20200
	IF(I.NE.999) STOP BOT	DAT20300
	CALL READER(LN,R1,I)	DAT20400
	IF(I.NE.999) STOP R1 2	DAT20500
40	FORMAT(2(13A6,A2/))	DAT20600
	PRINT 276	DAT20700
	PRINT V,(BOT(I),I=1,LN)	DAT20800
C		DAT20900
41	CONTINUE	DAT21000
	READ 7,(Q(J),J=1,12)	DAT21100
C	*****	DAT21200
C	INPUT CONVECTIVE BOUNDARY INFORMATION	DAT21300
C		DAT21400
C	DATA GROUP VII	DAT21500
	IF(KTYPE.LT.3) GO TO 59	DAT21600
	READ,NCONV	DAT21700
	IF(NCONV.EQ.0) GO TO 55	DAT21800
	READ,(NCON(I,1),NCON(I,2),CONV(I),I=1,NCONV)	DAT21900
C		DAT22000
	READ,(TINF(I),I=1,NCONV)	DAT22100
55	CONTINUE	DAT22200
C		DAT22300
C		DAT22400
C	INFORMATION NEEDED FOR HEAT OR MASS TRANSFER ACROSS A BOUNDARY	DAT22500
C	WITH A SPECIFIED HEAD	DAT22600
C		DAT22700
	READ,LEL	DAT22800
	IF(LEL.EQ.0) GO TO 56	DAT22900
	READ,(NEL(J,1),NEL(J,2),J=1,LEL)	DAT23000
	READ,(AEL(J,2),J=1,LEL)	DAT23100
	PRINT 157,(NEL(J,1),NEL(J,2),AEL(J,2),J=1,LEL)	DAT23200
56	CONTINUE	DAT23300
	PRINT 110,(NCON(I,1),NCON(I,2),CONV(I),I=1,NCONV)	DAT23400
59	CONTINUE	DAT23500
	READ 7,(Q(I),I=1,12)	DAT23600
C		DAT23700
C	*****	DAT23800
C		DAT23900
C	DATA GROUP VIII	DAT24000
C	INPUT LOCATION OF FLOW BOUNDARIES	DAT24100
C	INPUT NODE # AND THEN THE BOUNDARY CODE	DAT24200
	READ,LFLUXW,LFLUXH	DAT24300
	IF(LFLUXW.EQ.0) GO TO 71	DAT24400
	READ,(NFLUXW(I,1),NFLUXW(I,2),I=1,LFLUXW)	DAT24500
	PRINT 133,(NFLUXW(I,1),NFLUXW(I,2),I=1,LFLUXW)	DAT24600
71	CONTINUE	DAT24700
	IF(LFLUXH.EQ.0) GO TO 73	DAT24800
	READ,(NFLUXH(I,1),NFLUXH(I,2),I=1,LFLUXH)	DAT24900
	PRINT 134,(NFLUXH(I,1),NFLUXH(I,2),I=1,LFLUXH)	DAT25000
73	CONTINUE	DAT25100
C		DAT25200
	READ 7,(Q(I),J=1,12)	DAT25300

```

C
C FORMAT INFORMATION--INFORMATION PRINTED ON EVERY RUN
102  FORMAT(1X//1X,T10,'MATERIAL',T20,'HOR PERM',T32,' VER PERM',T50,
    *'STORAGE',T65,'HOR THERM COND',T85,'VERT THERM COND',T103,
    *'SPECIFIC DISPERSION COEFS'/1X,T103,'HEAT')
104  FORMAT(1X,T12,G9.4,T22,G9.4,T34,G9.4,T50,G9.4,T68,G9.4,T88,
    *G9.4,T105,G9.4,T115,2G9.4/)
105  FORMAT(1X//1X,'PARAMETER FACTORS--IN ORDER      ',8(G10.6,1X))
110  FORMAT(1X,'CONVECTIVE OUT AND CONDUCTIVE BOUNDARY INFORMATION',1X
    *, 'ELEM #--BOUNDARY CODE--TRANSFER COEFFICIENT'
    */1X,20(1X,5(I4,1X,I1,1X,G11.6,2X)/))
120  FORMAT(1X//1X,'THE VALUES IN THE TYPE OF MATERIAL MATRIX ARE')
131  FORMAT(1X//1X,'POINT SOURCES OF WATER--NODE # AND AMOUNT'/1X,
    *5(I4,1X,G12.6,5X))
132  FORMAT(1X//1X,'POINT SOURCES OF HEAT'/1X,5(I4,1X,G12.6,5X))
133  FORMAT(1X//1X,'WATER FLOW BOUNDARIES--ELEM # AND BOUNDARY CODE'/
    *10(I4,2X,I1,5X))
134  FORMAT(1X//1X,'HEAT FLOW BOUNDARIES--NODE # AND BOUNDARY CODE'/
    *10(I4,2X,I1,5X))
150  FORMAT(1X//1X,'EQUATION 1 TIME STEP',G12.6)
151  FORMAT(1X//1X,'EQUATION 2 TIME STEP',G12.6,10X,'HEAT OR MASS CAPACIT
    *ITY COEFFICIENT',G12.6)
155  FORMAT(1X//1X,'VELOCITIES ARE BEING CALCULATED AT CURRENT TIME STEP
    *EP      ',I1)
156  FORMAT(1X//1X,'VELOCITIES ARE BEING CALCULATED AT THE PREVIOUS TIME
    *ME STEP')
157  FORMAT(1X//1X,'INFORMATION FOR MASS OR HEAT TRANSFER ACROSS'
    *,1X,'A SPECIFIED HEAD BOUNDARY'/1X,'ELEMENT NUMBER--BOUNDARY CODE'
    *,1X,'--TEMPERATURE OR CONCENTRATION OF INCOMING FLUID'
    */1X,5(2X,I4,1X,I2,1X,2X,G10.5)/)
C*****
C      THE ROUTINE THAT PRINTS OUT THE INITIAL CONDITIONS
C      SPECIFIED BY THE INPUT DATA
C
    IF(KPRINT.EQ.0) GO TO 300
    PRINT 199,(TITLE(J),J=1,24)
199  FORMAT(1H1,1X//,20('* ',12A6,20('* ')/1X,10X,'THE UNITS USED ARE',
    *12A6))
    PRINT 210,NUMNP,M
210  FORMAT(1X,'NUMBER OF NODES ',I3,'    NUMBER OF ELEMENTS ',I3//)
    PRINT 211,ALPHA,PCW
211  FORMAT(1X,10X,'TIME STEP',F5.2,' UNITS',10X,'PC=',G10.5)
    PRINT 220
220  FORMAT(1X,'ELEMENT DATA'/1X,'NODE NUMBER',T20,'X-LOCATION',T40,
    *'Y-LOCATION',T60,'SPEC. HEAD',T75,'SPEC. T',T90,'INITIAL T',
    * T110,'INITIAL HEAD')
    DO 240 J=1,NUMNP
    PRINT 225,J,XLOC(J),YLOC(J),HEA(J),HEAD(J),R(J),R1(J)
225  FORMAT(1X,T5,I3,T20,G10.5,T40,G10.5,T60,G10.5,T75,G10.5,T90,G10.5,
    * T110,G10.5)
240  CONTINUE
    PRINT 250
250  FORMAT(1X,2X//1X,'ELEMENT PROPERTIES'/1X, 'ELEMENT',T12,'HCX',
    *T22,'HCY',T32,'STO',T42,'TCX',T52,'TCY',T63,'PC',T72,
    * ' THE ELEMENT NODES      ',T102,'HEATIN',T112,'WATER IN')
    DO 270 J=1,M
    PRINT 275,J,WX(J),WY(J),STO(J),PX(J),PY(J),PCX(J),(NOD(LZ,J),LZ=1,
    * 4),HEAT(J),INFLOW(J)
275  FORMAT(1X,T4,I3,T10,G8.3,T20,G8.3,T30,G8.3,T40,G8.3,,T50,G8.3,
    * T60,G8.3,T70,4I3,T100,G8.3,T110,G8.3)
276  FORMAT(1X//1X,'ELEVATION OF THE AQUIFER BOTTOM',1X/)
278  FORMAT(1X,'LINE SOURCES OF WATER--ELEMENT NUMBER,BOUNDARY CODE,RAD
    *TE'/1X,6(I4,1X,I2,1X,G10.5,2X))

```


279	FORMAT(1X,'LINE SOURCES OF HEAT--ELEMENT NUMBER,BOUNDARY CODE, RADAT31700	
	*TE'/1X,6(I4,1X,I2,1X,G10.5,2X))	DAT31800
270	CONTINUE	DAT31900
300	CONTINUE	DAT32000
C	ROUTINE TO ORIENTATE THE MATRIX--INSURES THAT ALL PROBLEMS ARE ORIENTADAT32100	
C	IN THE SAME MANNER	DAT32200
		DAT32300
	IF(MQ.EQ.0) GO TO 294	DAT32400
	IF(MQ.EQ.2) GO TO 294	DAT32500
	AC=0	DAT32600
	AB=0	DAT32700
	DO 282 J=1,LN	DAT32800
	AB=AMAX1(XLOC(J),AB)	DAT32900
282	AC=AMAX1(YLOC(J),AC)	DAT33000
	IF(MQ.EQ.4) GO TO 288	DAT33100
	DO 284 J=1,LN	DAT33200
284	YLOC(J)=AC-YLOC(J)	DAT33300
	IF(MQ.EQ.1) GO TO 294	DAT33400
288	CONTINUE	DAT33500
	DO 290 J=1,LN	DAT33600
290	XLOC(J)=AB-XLOC(J)	DAT33700
294	CONTINUE	DAT33800
C		DAT33900
C*****		DAT34000
	RETURN	DAT34100
	• SUBROUTINE ELREAD	DAT34200
	DIMENSION DIGIT(10), CHAR(80)	DAT34300
	DATA DIGIT/'0','1','2','3','4','5','6','7','8','9'/'	DAT34400
54	FORMAT(1X,'PROBLEMS--BAD CHARACTER',1X,A1,3X,'ELEMENT',I6)	DAT34500
55	FORMAT(1X,'PROBLEM--NOT ENOUGH NODAL DATA FOR ELEMENT ',I6)	DAT34600
	READ 1,(CHAR(J),J=1,80)	DAT34700
1	FORMAT(80A1)	DAT34800
	KC=0	DAT34900
	KE=4	DAT35000
	KS=2	DAT35100
	J=0	DAT35200
	KL=0	DAT35300
8	NUM=0	DAT35400
9	J=J+1	DAT35500
	IF(CHAR(J).EQ.' ') GO TO 9	DAT35600
10	I=0	DAT35700
11	I=I+1	DAT35800
	IF(I.LE.10) GO TO 12	DAT35900
	PRINT 54,CHAR(J),L	DAT36000
	STOP	DAT36100
12	IF(CHAR(J).NE.DIGIT(I)) GO TO 11	DAT36200
	NUM=10*NUM+I-1	DAT36300
	J=J+1	DAT36400
	IF(CHAR(J).EQ.' ') GO TO 13	DAT36500
	IF(CHAR(J).EQ.'*') GO TO 14	DAT36600
	GO TO 10	DAT36700
13	KL=KL+1	DAT36800
	IF(KL.EQ.1) L=NUM	DAT36900
	IF(KL.EQ.1) GO TO 8	DAT37000
	KL=KL+1	DAT37100
	KC=KC+1	DAT37200
	IF(KC.EQ.5) GO TO 15	DAT37300
	MOD(KC,L)=NUM	DAT37400
	IF(KS.EQ.0) KE=KE+2	DAT37500
	IF(KS.EQ.1) KE=KE+1	DAT37600
	KS=0	DAT37700
	GO TO 8	DAT37800
14	KE=KE+1	DAT37900
	KS=KS+1	DAT38000

```

      NOD(KE,L)=NUM
      IF(J.LT.65) GO TO 8
      PRINT 55,L
      STOP
15    MTM=4
      DO 16 I=5,12
      IF(NOD(I,L).EQ.0) GO TO 16
      MTM=MTM+1
16    CONTINUE
      NODE(L)=MTM
      RETURN
C
C*****
C
      SUBROUTINE P(KX,KY)
      DIMENSION D(50), B(50),C(50)
      J=0
      MN=0
      IF(KX.LT.0) MN=1
      KX=ABS(KX)
      KXA=KX-1
      KYA=KY-1
      DO 2 L=1,KXA
      DO 1 K=1,KYA
      J=J+1
      NOD(4,J)=L-1+J
      NOD(3,J)=L+J+KYA
      NOD(1,J)=L+J
      NOD(2,J)=L+J+KY
1    CONTINUE
2    CONTINUE
      READ,(B(J),J=1,KX)
      PRINT 10
      PRINT,(B(J),J=1,KX)
      READ,(C(J),J=1,KY)
      PRINT 11
      PRINT,(C(J),J=1,KY)
      J=0
      DO 4 L=1,KX
      DO 3 K=1,KY
      J=J+1
      YLOC(J)=C(K)
      XLOC(J)=B(L)
3    CONTINUE
4    CONTINUE
      IF(MN.EQ.0) RETURN
      READ,MLD
      MLB=1
      IF(MLD.EQ.0) MLB=KY
      READ,(D(J),J=1,KX)
      KXX=LN-KY+1
      DO 20 K=MLB,KY
      L=0
      DO 20 JJ=1,KXX,KY
      J=JJ+K-1
      L=L+1
20   YLOC(J)=YLOC(J)+D(L)
      RETURN
10   FORMAT(1X/1X,'THE X-SPACING IS')
11   FORMAT(1X/1X,'THE Y-SPACING IS')
      RETURN
      SUBROUTINE READER(LZ,Q,I)

```

```

DAT38100
DAT38200
DAT38300
DAT38400
DAT38500
DAT38600
DAT38700
DAT38800
DAT38900
DAT39000
DAT39100
DAT39200
DAT39300
DAT39400
DAT39500
DAT39600
DAT39700
DAT39800
DAT39900
DAT40000
DAT40100
DAT40200
DAT40300
DAT40400
DAT40500
DAT40600
DAT40700
DAT40800
DAT40900
DAT41000
DAT41100
DAT41200
DAT41300
DAT41400
DAT41500
DAT41600
DAT41700
DAT41800
DAT41900
DAT42000
DAT42100
DAT42200
DAT42300
DAT42400
DAT42500
DAT42600
DAT42700
DAT42800
DAT42900
DAT43000
DAT43100
DAT43200
DAT43300
DAT43400
DAT43500
DAT43600
DAT43700
DAT43800
DAT43900
DAT44000
DAT44100
DAT44200

```

```

1  DIMENSION Q(LZ)
    READ,QI,IZ,FACT
    DO 1 IP=1,LZ
      Q(IP)=QI
      IF(IZ.GE.0) GO TO 2
      READ,(Q(IP),IP=1,LZ),I
      GO TO 3
2  I=999
      IF(IZ.EQ.0) GO TO 3
      READ,(J,Q(J),IP=1,IZ)
3  CONTINUE
      DO 5 IP=1,LZ
5  Q(IP)=Q(IP)*FACT
    RETURN
    END

```

```

DAT44300
DAT44400
DAT44500
DAT44600
DAT44700
DAT44800
DAT44900
DAT45000
DAT45100
DAT45200
DAT45300
DAT45400
DAT45500
DAT45600
DAT45700

```

C*****	STR	100
C	STR	200
C	STR	300
C	THIS ROUTINE ASSEMBLES THE STRUCTURE MATRICIES AND PREFORMS	STR 400
C	A FORWARD REDUCTION OF THE STIFNESS MATRIX BY GAUSS ELIMINATION	STR 500
C	STR	600
	SUBROUTINE STRUCT(LN,LM,MBAND,MP,R,S,T,G,GG,RI,HEAD,XLOC,	STR 700
	*YLOC,NOD,NODE,CFACT,TT,ALPHA,KBOUND)	STR 800
	INTEGER TT	STR 900
	REAL JAC	STR 1000
	DOUBLE PRECISION AA,SE,TE,S,T	STR 1100
	COMMON/AAA/XL(4),YL(4),DETJAC,JAC(4,4)/A1/M,MM,NUMNP,NSIZE	STR 1200
	COMMON/AB/AA(6),W(4)/ABB/SE(12,12),TE(12,12)	STR 1300
	COMMON/AC/RE(12),GE(12)/ACC/KK(12),K1,K2,K3,K4	STR 1400
	COMMON/HH/LFLOW,LON/HM/PXX,PYY,PXY,KAD/AM/KSYM,PCT	STR 1500
	DIMENSION XLOC(LN),YLOC(LN),NOD(12,LM),R(LN),S(LN,MP)	STR 1600
	DIMENSION T(LN,MP),G(LN),GG(LN),RI(LN),NODE(LM),HEAD(LN)	STR 1700
	LFLOW=1	STR 1800
	AA(1)=- (1/3)**.5	STR 1900
	AA(2)=-AA(1)	STR 2000
C	STR	2100
	DO 50 J=1,LN	STR 2200
	GG(J)=0.0	STR 2300
	DO 50 I=1,MP	STR 2400
	S(J,I)=0.0	STR 2500
50	T(J,I)=0.0	STR 2600
C	PRINT MESSAGE IF DISPERSION ROUTINE IS USED	STR 2700
	IF(KAD.EQ.1) PRINT 10	STR 2800
C	STR	2900
C*****	STR	3000
C	STR	3100
C	THE STIFFNESS MATRIX FORMULATION ROUTINE	STR 3200
C	STR	3300
	DO 150 LLL=1,MM	STR 3400
	PXX=0	STR 3500
	PYY=0	STR 3600
	PXY=0	STR 3700
	M4=NODE(LLI)	STR 3800
	CALL DERIVE(LLI,M4)	STR 3900
C*****	STR	4000
C	THE STRUCTURE STIFFNESS MATRIX ASSEMBLER	STR 4100
	K=0	STR 4200
	DO 110 I=1,M4	STR 4300
100	K=K+1	STR 4400
	IF(NOD(K,LLL).EQ.0) GO TO 100	STR 4500
110	KK(I)=NOD(K,LLL)	STR 4600
	DO 140 I=1,M4	STR 4700
	IF(KK(I).LE.0) GO TO 140	STR 4800
	II=KK(I)	STR 4900
C	STR	5000
	GG(II)=GG(II)+GE(I)	STR 5100
120	CONTINUE	STR 5200
	DO 140 J=1,M4	STR 5300
	IF(KSYM.GT.0) GO TO 130	STR 5400
	IF(KK(J).LT.II) GO TO 140	STR 5500
	JJ=KK(J)-II+1	STR 5600
	GO TO 135	STR 5700
130	CONTINUE	STR 5800
	JJ=KK(J)-II+MBAND	STR 5900
135	CONTINUE	STR 6000
	IF(JJ.GT.MP) PRINT 20,LLL,JJ	STR 6100
	S(II,JJ)=S(II,JJ)+SE(I,J)	STR 6200
	IF(TT.EQ.0) GO TO 140	STR 6300
	T(II,JJ)=T(II,JJ)+TE(I,J)	STR 6400

140	CONTINUE	STR 6500
150	CONTINUE	STR 6600
C		STR 6700
C		STR 6800
C	*****	STR 6900
C		STR 7000
C	--ROUTINE FOR SPECIFIED HEAD BOUNDARY CONDITIONS	STR 7100
	DO 200 N=1,NUMNP	STR 7200
	IF(HEAD(N).EQ.0) GO TO 200	STR 7300
	IF(KSYM.EQ.0) S(N,1)=S(N,1)+CFACT	STR 7400
	IF(KSYM.GT.0) S(N,MBAND)=S(N,MBAND)+CFACT	STR 7500
200	CONTINUE	STR 7600
C		STR 7700
C	*****	STR 7800
C		STR 7900
C	CALL THE ROUTINE THAT CHECKS FOR THE STABILITY OF THE CHOSEN TIME	STR 8000
	KSM=KSYM	STR 8100
	IF(LON.EQ.99.AND.TT.EQ.1) CALL EIGEN(LN,MBAND,MP,KSM,CFACT,S,T,RI,	STR 8200
	*HEAD)	
C	GAUSS ELIMINATION--FORWARD REDUCTION OF STIFNESS, MATRIX	STR 8400
C		STR 8500
	IF(KSYM.EQ.0) CALL SOLVE(LN MBAND,S,T,R,RI)	STR 8600
	IF(KSYM.NE.0) CALL ASOLVE(S,R,RI,LN,MBAND-1,LN,MBAND*2-1,T)	STR 8700
C		STR 8800
C		STR 8900
10	FORMAT(1X/1X,'THE DISPERSION ROUTINE IS BEING USED')	STR 9000
20	FORMAT(1X/1X,'MAX. BANDWIDTH EXCEEDED IN ELEMENT',I4,	STR 9100
	* 'WHERE BANDWIDTH IS ',I4)	STR 9200
	RETURN	STR 9300
C		STR 9400
C		STR 9500
	END	STR 9600

C*****	GAU 100
C*	GAU 200
C THIS ROUTINE FORMS ELEMENT STIFFNESS MATRIX BY GAUSS QUADRATURE	GAU 300
C	GAU 400
SUBROUTINE GAUSS(LLL,LM,LN,XLOC,YLOC,NOD,PY,PX,HEAT,PCX,ALPHA,KBOGAU	GAU 500
*UND,TT,Z,NCON,CONV,ALOC,NODE,CBAL,AY,AZ)	GAU 600
REAL JAC	GAU 700
INTEGER VE, TT,Z,AY(4),AZ(4)	GAU 800
DOUBLE PRECISION AA,NOT,NXI,NET,SE,TE,BB ,DUM1,DUM2,DUM3	GAU 900
COMMON/AA/NXI(12),NET(12),NOT(12)	GAU 1000
COMMON/AAA/XL(4),YL(4),DETJAC,JAC(4,4)	GAU 1100
COMMON/AB/AA(6),W(4)/ABB/SE(12,12),TE(12,12)	GAU 1200
COMMON/AC/RE(12),GE(12)/ACC/KK(12),K1,K2,K3,K4	GAU 1300
COMMON/HH/LFLOW,LON/HM/PXX,PYY,PXY,KAD/ME/MEQ	GAU 1400
COMMON/CON/MC1,MC2,NCONV/AS/BB(2,12)	GAU 1500
DIMENSION NCON(2,3),CONV(2),ALOC(2)	GAU 1600
COMMON/CON1/HE(4),HEE(4,4)/AM/NLA,PCH/AT/XII(4),ETI(4)	GAU 1700
COMMON/ATHICK/ASIZE,NTHICK,THICK,ERROR	GAU 1800
DIMENSION VE(4),AVY(4),AVX(4),VEL(4)	GAU 1900
DIMENSION XLOC(LN),YLOC(LN),PY(LM),PX(LM),HEAT(LM),PCX(LGAU	GAU 2000
*M),CBAL(2,2),AG(6),NODE(LM),NOD(12,LM)	GAU 2100
DATA XII/-1.,1.,1.,-1./	GAU 2200
DATA VE/1,4,2,3/	GAU 2300
DATA ETI/-1.,-1.,1.,1./	GAU 2400
DATA W/.3478549,.6521451,.6521451,.3478549/	GAU 2500
DATA AG/-.5773503,.5773503,-.8611363,-.3399810,.3399810,.8611363/	GAU 2600
RETURN	GAU 2700
C*****	GAU 2800
C	GAU 2900
ENTRY DERIVE(LLL,M4)	GAU 3000
C	GAU 3100
C	GAU 3200
C*****	GAU 3300
C	GAU 3400
CALL CORD(LLL)	GAU 3500
T=1.0	GAU 3600
CALL PEE(T,LLL)	GAU 3700
DO 10 K=1,12	GAU 3800
GE(K)=0.0	GAU 3900
DO 10 L=1,12	GAU 4000
TE(K,L)=0.0	GAU 4100
10 SE(K,L)=0	GAU 4200
C START THE QUADRATURE LOOP	GAU 4300
NP=2	GAU 4400
IF(M4.GT.4) NP=4	GAU 4500
KVE=0	GAU 4600
DO 200 II=1,NP	GAU 4700
DO 200 JJ=1,NP	GAU 4800
KVE=KVE+1	GAU 4900
IF(NP.EQ.4) GO TO 20	GAU 5000
XI=AG(JJ)	GAU 5100
YI=AG(II)	GAU 5200
GO TO 30	GAU 5300
20 XI=AG(JJ+2)	GAU 5400
YI=AG(II+2)	GAU 5500
IF(LFLOW.EQ.0) XI=0.0	GAU 5600
IF(LFLOW.EQ.0) YI=0.0	GAU 5700
30 CONTINUE	GAU 5800
IF(M4.GT.4) CALL SHAPE(LLL,M4,XI,YI,XLOC,YLOC,LM,NOD)	GAU 5900
IF(M4.EQ.4) CALL SHAPE1(II,JJ)	GAU 6000
C	GAU 6100
C*****	GAU 6200

175	CONTINUE	GAU 6300
	THICK=1.0	GAU 6400
	IF(NTHICK.EQ.0) GO TO 176	GAU 6500
	XX=(XLOC(K2)+XLOC(K1))/2	GAU 6600
	XX=ABS(XX)	GAU 6700
	THICK=XX*ASIZE	GAU 6800
	YY=(YLOC(K3)+YLOC(K1))/2	GAU 6900
	YY=ABS(YY)	GAU 7000
	IF(ASIZE.LT.0) THICK=-YY*ASIZE	GAU 7100
176	DUM1=W(II)*W(JJ)*DETJAC*THICK*T	GAU 7200
	IF(M4.EQ.4) DUM1=DETJAC*THICK*T	GAU 7300
C	*****	GAU 7400
C		GAU 7500
	IF(LFLOW.EQ.0) DETJAC=DETJAC*T*THICK	GAU 7600
	IF(LFLOW.EQ.0) RETURN	GAU 7700
C	VELOCITY AND DISPERSION CALCULATIONS	GAU 7800
C		GAU 7900
	VX=0.0	GAU 8000
	VY=0.0	GAU 8100
	IF(NLA.EQ.0) GO TO 178	GAU 8200
	IF(NLA.EQ.1) CALL VELO(LLL,VX,VY)	GAU 8300
	IF(NLA.EQ.2) CALL VCENT(LLL,VX,VY)	GAU 8400
	IF(KAD.EQ.1) CALL MECD(LLL,VX,VY)	GAU 8500
C		GAU 8600
	IF(KVE.GT.4) GO TO 178	GAU 8700
	KEE=VE(KVE)	GAU 8800
	AVY(KEE)=VY	GAU 8900
	AVX(KEE)=VX	GAU 9000
178	CONTINUE	GAU 9100
C		GAU 9200
C	*****	GAU 9300
C		GAU 9400
C		GAU 9500
C	*****	GAU 9600
C		GAU 9700
	DO 200 NROW=1,M4	GAU 9800
	GE(NROW)=GE(NROW)+NOT(NROW)*HEAT(LLL)*DUM1	GAU 9900
	DO 200 NCOL=1,M4	GAU10000
	IF(NLA.EQ.0) GO TO 180	GAU10100
	DUM2=BB(1,NROW)*NOT(NCOL)*PCH*VX+BB(2,NROW)*NOT(NCOL)*PCH*VY	GAU10200
	SE(NROW,NCOL)=SE(NROW,NCOL)+DUM2*DUM1	GAU10300
180	CONTINUE	GAU10400
	DUM2=BB(1,NROW)*BB(1,NCOL)*(PX(LLL)+PXX)	GAU10500
	SE(NROW,NCOL)=SE(NROW,NCOL)+DUM1*DUM2	GAU10600
	DUM2=BB(2,NROW)*BB(2,NCOL)*(PY(LLL)+PYY)	GAU10700
	SE(NROW,NCOL)=SE(NROW,NCOL)+DUM1*DUM2	GAU10800
C	THESE NEXT TWO LINES ADD IN TRANSVERSE TERMS OF CONDUCTIVITY TENSORS	GAU10900
	DUM2=BB(1,NROW)*BB(2,NCOL)*PXY+BB(2,NROW)*BB(1,NCOL)*PXY	GAU11000
	SE(NROW,NCOL)=SE(NROW,NCOL)+DUM1*DUM2	GAU11100
	IF(TT.EQ.0) GO TO 200	GAU11200
	DUM3=NOT(NROW)*NOT(NCOL)*PCX(LLL)	GAU11300
	IF(NLA.EQ.0) DUM3=DUM3/T	GAU11400
	TE(NROW,NCOL)=DUM3*DUM1+TE(NROW,NCOL)	GAU11500
200	CONTINUE	GAU11600
C		GAU11700
C	*****	GAU11800
C	THE CONVECTIVE BOUNDARIES ARE HANDLED	GAU11900
C		GAU12000
	IF(NCONV.EQ.0) GO TO 400	GAU12100
	IF(MEQ.EQ.1) GO TO 400	GAU12200
	DO 301 I=1,NCONV	GAU12300
	II=I	GAU12400
	IF(LLL.EQ.NCON(I,1)) CALL CONVEC	GAU12500
300	CONTINUE	GAU12600

301	CONTINUE	GAU12700
400	CONTINUE	GAU12800
	VYY=(AVY(1)+AVY(2)+AVY(3)+AVY(4))/4	GAU12900
	IF(KBOUND.EQ.99) RETURN	GAU13000
	IF(TT.EQ.0) RETURN	GAU13100
C	*****	GAU13200
C	CRANK-NICOLSON METHOD FOR TREATING TRANSIENT CONDITIONS	GAU13300
C		GAU13400
C		GAU13500
	DO 450 NROW=1,M4	GAU13600
	GE(NROW)=GE(NROW)*ALPHA	GAU13700
	DO 450 NCOL=1,M4	GAU13800
	DUM4=SE(NROW,NCOL)	GAU13900
	SE(NROW,NCOL)=ALPHA/2*SE(NROW,NCOL)+TE(NROW,NCOL)	GAU14000
	TE(NROW,NCOL)=TE(NROW,NCOL)-ALPHA/2*DUM4	GAU14100
450	CONTINUE	GAU14200
800	CONTINUE	GAU14300
C	*****	GAU14400
	RETURN	GAU14500
C	ROUTINE THAT ADDS IN CONVECTIVE BOUNDARY TERMS	GAU14600
C		GAU14700
	SUBROUTINE CONVEC	GAU14800
	LA=NCON(I,2)	GAU14900
	MC1=AY(LA)	GAU15000
	MC2=AZ(LA)	GAU15100
	A=XL(MC1)-XL(MC2)	GAU15200
	MC3=MC1+MC2	GAU15300
	IF(MC3.EQ.5) A=YI(MC1)-YI(MC2)	GAU15400
	A=ABS(A)	GAU15500
	DO 505 J=1,4	GAU15600
505	HE(J)=0.0	GAU15700
	HE(MC1)=.5	GAU15800
	HE(MC2)=.5	GAU15900
	ALOC(II)=A*THICK*T	GAU16000
	CO=CONV(II)	GAU16100
	IF(CO.LT.0.00001) GO TO 600	GAU16200
C		GAU16300
C		GAU16400
	CBAL(II,1)=ALPHA*CO*THICK*T*A	GAU16500
	DO 550 K=1,4	GAU16600
	DO 550 J=1,4	GAU16700
550	SE(K,J)=HE(J)*HE(K)*CO*THICK*T*A+SE(K,J)	GAU16800
C		GAU16900
	RETURN	GAU17000
C	*****	GAU17100
C		GAU17200
600	CONTINUE	GAU17300
	GO TO (603,601,601,603),LA	GAU17400
601	DO 602 J=1,4	GAU17500
	IF(MC3.EQ.5) VEL(J)=AVX(J)	GAU17600
602	IF(MC3.NE.5) VEL(J)=AVY(J)	GAU17700
	GO TO 605	GAU17800
603	DO 604 J=1,4	GAU17900
	IF(MC3.EQ.5) VEL(J)=-AVX(J)	GAU18000
604	IF(MC3.NE.5) VEL(J)=-AVY(J)	GAU18100
605	CONTINUE	GAU18200
C		GAU18300
	CO=-CO	GAU18400
	NCO=CO	GAU18500
	VT=VEL(MC1)/2+VEL(MC2)/2	GAU18600
	IF(NCO.LT.995.OR.NCO.GT.1000) GO TO 700	GAU18700
	IF(NCO.EQ.999) CO=VT*PCH*ERROR	GAU18800
	IF(NCO.EQ.996) CO=(-VT+VYY)*PCH*ERROR	GAU18900

IF(NCO.EQ.997) CO=ERROR	GAU19000
CBAL(II,1)=ALPHA*CO*THICK*T*A	GAU19100
DO 650 K=1,4	GAU19200
DO 650 J=1,4	GAU19300
650 SE(K,J)=HE(J)*HE(K)*CO*THICK*T*A+SE(K,J)	GAU19400
RETURN	GAU19500
C	GAU19600
C*****	GAU19700
C	GAU19800
700 CONTINUE	GAU19900
C CALCULATE HEAT TRANSFER OUT WITH FLOWING WATER	GAU20000
C	GAU20100
CBAL(II,1)=ALPHA*VT*PCH*THICK*T*A	GAU20200
C	GAU20300
DUM1=1-AA(1)	GAU20400
DUM2=1-AA(2)	GAU20500
HE(MC1)=DUM1/4	GAU20600
HE(MC2)=DUM2/4	GAU20700
VELL=VEL(MC1)	GAU20800
DO 720 K=1,4	GAU20900
DO 720 J=1,4	GAU21000
720 SE(K,J)=HE(J)*HE(K)*VELL*PCH*THICK*T*A*2+SE(K,J)	GAU21100
HE(MC1)=DUM2/4	GAU21200
HE(MC2)=DUM1/4	GAU21300
VELL=VEL(MC2)	GAU21400
DO 730 K=1,4	GAU21500
DO 730 J=1,4	GAU21600
730 SE(K,J)=HE(J)*HE(K)*VELL*PCH*THICK*T*A*2+SE(K,J)	GAU21700
RETURN	GAU21800
END	GAU21900

C*****	SH1	100
SUBROUTINE SHAPE1(II,JJ)	SH1	200
C*****	SH1	300
REAL JAC	SH1	400
C	SH1	500
DOUBLE PRECISION AA,NOT,NXI,NET,SE,TE,BB ,DUM1,DUM2	SH1	600
COMMON/AA/NXI(12),NET(12),NOT(12)	SH1	700
COMMON/AAA/XL(4),YL(4),DETJAC,JAC(4,4)	SH1	800
COMMON/AB/AA(6),W(4)/ABB/SE(12,12),TE(12,12)	SH1	900
COMMON/AC/RE(12),GE(12)/ACC/KK(12),K1,K2,K3,K4	SH1	1000
COMMON/HH/LFLOW,LON/HM/PXX,PYY,PXY,KAD	SH1	1100
COMMON/AT/XII(4),ETI(4)/CON/MC1,MC2,NCONV/AS/BB(2,12)	SH1	1200
C COMPUTE THE SHAPE FUNCTIONS AND THEIR DERIVATIVES	SH1	1300
DO 100 I=1,4	SH1	1400
DUM1=(1.+XII(I)*AA(II))*0.25	SH1	1500
DUM2=(1.+ETI(I)*AA(JJ))*0.25	SH1	1600
NXI(I)=XII(I)*DUM2	SH1	1700
NET(I)=ETI(I)*DUM1	SH1	1800
NOT(I)=4.*DUM1*DUM2	SH1	1900
100 CONTINUE	SH1	2000
C	SH1	2100
C*****	SH1	2200
C COMPUTE JACOBIAN, AND ITS DETERMINANT	SH1	2300
DO 150 I=1,2	SH1	2400
DO 150 J=1,2	SH1	2500
150 JAC(I,J)=0.0	SH1	2600
DO 160 I=1,4	SH1	2700
JAC(1,1)=JAC(1,1)+NXI(I)*XL(I)	SH1	2800
JAC(1,2)=JAC(1,2)+NXI(I)*YL(I)	SH1	2900
JAC(2,1)=JAC(2,1)+NET(I)*XL(I)	SH1	3000
JAC(2,2)=JAC(2,2)+NET(I)*YL(I)	SH1	3100
160 CONTINUE	SH1	3200
DETJAC=JAC(1,1)*JAC(2,2)-JAC(2,1)*JAC(1,2)	SH1	3300
DUM1=JAC(1,1)/DETJAC	SH1	3400
JAC(1,1)=JAC(2,2)/DETJAC	SH1	3500
JAC(1,2)=-JAC(1,2)/DETJAC	SH1	3600
JAC(2,1)=-JAC(2,1)/DETJAC	SH1	3700
JAC(2,2)=DUM1	SH1	3800
DO 170 L=1,4	SH1	3900
BB(1,L)=JAC(1,1)*NXI(L)+JAC(1,2)*NET(L)	SH1	4000
BB(2,L)=JAC(2,1)*NXI(L)+JAC(2,2)*NET(L)	SH1	4100
170 CONTINUE	SH1	4200
RETURN	SH1	4300
END	SH1	4400

C	SUBROUTINE SHAPE(L,M,XI,YI,X,Y,NN,NE,IN)	SHA 100
C	*****	SHA 200
C		SHA 300
C	XI/YI THE GAUSS POINTS	SHA 400
C	X/Y THE X AND Y LOCATIONS OF THE ELEMENT NODES	SHA 500
C	NN NUMBER OF NODES	SHA 600
C	NE NUMBER OF ELEMENTS	SHA 700
C	IN ARRAY REFERED TO IN MAIN PROGRAM AS NOD	SHA 800
C	M REFERED TO IN MAIN PROGRAM AS M4, NUMBER OF NODES IN THE ELEMENT	SHA 900
C	DET IS THE DETERMINENT, ONE QUARTER OF THE AREA OF THE ELEMENT	SHA 1000
C		SHA 1100
C		SHA 1200
C	CALLED FROM MNPGM	SHA 1300
C	PURPOSE: TO COMPUTE BASIS FUNCTIONS	SHA 1400
C	ORIGINALLY PROGRAMED BY EMIL O. FRIND	SHA 1500
C	-----	SHA 1600
	DOUBLE PRECISION DFX,DFY,FF,BB	SHA 1700
	DIMENSION X(NN), Y(NN), IN(12,NE)	SHA 1800
	DIMENSION ALF(4), DAX(4), DAY(4), BTX(4), BTY(4), DBX(4),	SHA 1900
	1 DBY(4)	SHA 2000
C	COMMON/AA/DFX(12),DFY(12),FF(12)	SHA 2100
	*/AAA/ZZZ(4),ZZZZ(4),DET,DJAC(4,4)	SHA 2200
	COMMON/AS/BB(2,12)	SHA 2300
C	-----	SHA 2400
C		SHA 2500
C		SHA 2600
C	XI/YI - LOCAL COORDINATES OF THE INTEGRATION POINTS	SHA 2700
	XI1=1.-XI	SHA 2800
	XI2=1.+XI	SHA 2900
	YI1=1.-YI	SHA 3000
	YI2=1.+YI	SHA 3100
C		SHA 3200
C	CORNER NODE SHAPE FUNCTIONS, BASIC PART	SHA 3300
C	ALF - ALPHA PART OF SHAPE FUNCTION	SHA 3400
	ALF(1)=.25*XI1*YI1	SHA 3500
	ALF(2)=.25*XI2*YI1	SHA 3600
	ALF(3)=.25*XI2*YI2	SHA 3700
	ALF(4)=.25*XI1*YI2	SHA 3800
C	DAX/DAY - X- AND Y-DERIVATIVE OF ALPHA PART	SHA 3900
	DAX(1)=-.25*YI1	SHA 4000
	DAX(2)=.25*YI1	SHA 4100
	DAX(3)=.25*YI2	SHA 4200
	DAX(4)=-.25*YI2	SHA 4300
	DAY(1)=-.25*XI1	SHA 4400
	DAY(2)=-.25*XI2	SHA 4500
	DAY(3)=.25*XI2	SHA 4600
	DAY(4)=.25*XI1	SHA 4700
C		SHA 4800
C	CORNER NODE SHAPE FUNCTIONS, SIDE-DEPENDENT PART	SHA 4900
	XQ1=XI-.5	SHA 5000
	XQ2=-XI-.5	SHA 5100
	YQ1=YI-.5	SHA 5200
	YQ2=-YI-.5	SHA 5300
	XC1=1.125*XI*XI-.625	SHA 5400
	XC2=2.25*XI	SHA 5500
	YC1=1.125*YI*YI-.625	SHA 5600
	YC2=2.25*YI	SHA 5700
	J1=1	SHA 5800
	J2=2	SHA 5900
	J3=5	SHA 6000
C	FOR BETA X PART (BTX) OF SHAPE FUNCTION	SHA 6100
	DO 50 J=1,2	SHA 6200
	IF (IN(J3,L).EQ.0) GO TO 10	SHA 6300

	IF (IN(J3+1,L).EQ.0) GO TO 20	SHA 6400
	GO TO 30	SHA 6500
10	CONTINUE	SHA 6600
C	LINEAR . . .	SHA 6700
	BTX(J1)=.5	SHA 6800
	BTX(J2)=.5	SHA 6900
C	DBX - BETA X DERIVATIVE	SHA 7000
	DBX(J1)=0.	SHA 7100
	DBX(J2)=0.	SHA 7200
	GO TO 40	SHA 7300
20	CONTINUE	SHA 7400
C	QUADRATIC . . .	SHA 7500
	BTX(J1)=XQ2	SHA 7600
	BTX(J2)=XQ1	SHA 7700
	DBX(J1)=-1.	SHA 7800
	DBX(J2)=1.	SHA 7900
	GO TO 40	SHA 8000
30	CONTINUE	SHA 8100
C	CUBIC . . .	SHA 8200
	BTX(J1)=XC1	SHA 8300
	BTX(J2)=XC1	SHA 8400
	DBX(J1)=XC2	SHA 8500
	DBX(J2)=XC2	SHA 8600
40	CONTINUE	SHA 8700
	J1=4	SHA 8800
	J2=3	SHA 8900
	J3=9	SHA 9000
50	CONTINUE	SHA 9100
	J1=2	SHA 9200
	J2=3	SHA 9300
	J3=7	SHA 9400
C	FOR BETA Y PART (BTY) OF SHAPE FUNCTION	SHA 9500
	DO 100 J=1,2	SHA 9600
	IF (IN(J3,L).EQ.0) GO TO 60	SHA 9700
	IF (IN(J3+1,L).EQ.0) GO TO 70	SHA 9800
	GO TO 80	SHA 9900
60	CONTINUE	SHA10000
C	LINEAR . . .	SHA10100
	BTY(J1)=.5	SHA10200
	BTY(J2)=.5	SHA10300
C	DBY - BETA Y DERIVATIVE	SHA10400
	DBY(J1)=0.	SHA10500
	DBY(J2)=0.	SHA10600
	GO TO 90	SHA10700
70	CONTINUE	SHA10800
C	QUADRATIC . . .	SHA10900
	BTY(J1)=YQ2	SHA11000
	BTY(J2)=YQ1	SHA11100
	DBY(J1)=-1.	SHA11200
	DBY(J2)=1.	SHA11300
	GO TO 90	SHA11400
80	CONTINUE	SHA11500
C	CUBIC . . .	SHA11600
	BTY(J1)=YC1	SHA11700
	BTY(J2)=YC1	SHA11800
	DBY(J1)=YC2	SHA11900
	DBY(J2)=YC2	SHA12000
90	CONTINUE	SHA12100
	J1=1	SHA12200
	J2=4	SHA12300
	J3=11	SHA12400
100	CONTINUE	SHA12500
C		SHA12600

C	SHAPE FUNCTION DERIVATIVE MATRIX - CORNER NODES	SHA12700
	DO 110 J=1,4	SHA12800
	DFX(J)=DAX(J)*(BTX(J)+BTY(J))+DBX(J)*ALF(J)	SHA12900
	DFY(J)=DAY(J)*(BTX(J)+BTY(J))+DBY(J)*ALF(J)	SHA13000
	FF(J)=ALF(J)*(BTX(J)+BTY(J))	SHA13100
110	CONTINUE	SHA13200
C		SHA13300
C	SHAPE FUNCTION DERIVATIVE MATRIX - EDGE NODES	SHA13400
C	SKIP IF ELEMENT IS LINEAR (M=4)	SHA13500
	IF (M.EQ.4) GO TO 240	SHA13600
	J=4	SHA13700
	XEQ=1.-XI*XI	SHA13800
	YEQ=1.-YI*YI	SHA13900
	XE1=1.-3.*XI	SHA14000
	XE2=1.+3.*XI	SHA14100
	YE1=1.-3.*YI	SHA14200
	YE2=1.+3.*YI	SHA14300
	IF (IN(5,L).EQ.0) GO TO 140	SHA14400
	IF (IN(6,L).EQ.0) GO TO 120	SHA14500
	GO TO 130	SHA14600
120	J=J+1	SHA14700
	DFX(J)=-XI*YI1	SHA14800
	DFY(J)=-.5*XEQ	SHA14900
	FF(J)=.5*XEQ*YI1	SHA15000
	GO TO 140	SHA15100
130	J=J+1	SHA15200
	DFX(J)=-.28125*YI1*(3.*XEQ+2.*XI*XE1)	SHA15300
	DFY(J)=-.28125*XEQ*XE1	SHA15400
	FF(J)=.28125*XEQ*XE1*YI1	SHA15500
	J=J+1	SHA15600
	DFX(J)=.28125*YI1*(3.*XEQ-2.*XI*XE2)	SHA15700
	DFY(J)=-.28125*XEQ*XE2	SHA15800
	FF(J)=.28125*XEQ*XE2*YI1	SHA15900
140	IF (IN(7,L).EQ.0) GO TO 170	SHA16000
	IF (IN(8,L).EQ.0) GO TO 150	SHA16100
	GO TO 160	SHA16200
150	J=J+1	SHA16300
	DFX(J)=.5*YEQ	SHA16400
	DFY(J)=-YI*XI2	SHA16500
	FF(J)=.5*XI2*YEQ	SHA16600
	GO TO 170	SHA16700
160	J=J+1	SHA16800
	DFX(J)=.28125*YEQ*YE1	SHA16900
	DFY(J)=-.28125*XI2*(3.*YEQ+2.*YI*YE1)	SHA17000
	FF(J)=.28125*XI2*YEQ*YE1	SHA17100
	J=J+1	SHA17200
	DFX(J)=.28125*YEQ*YE2	SHA17300
	DFY(J)=.28125*XI2*(3.*YEQ-2.*YI*YE2)	SHA17400
	FF(J)=.28125*XI2*YEQ*YE2	SHA17500
170	IF (IN(9,L).EQ.0) GO TO 200	SHA17600
	IF (IN(10,L).EQ.0) GO TO 180	SHA17700
	GO TO 190	SHA17800
180	J=J+1	SHA17900
	DFX(J)=-XI*YI2	SHA18000
	DFY(J)=.5*XEQ	SHA18100
	FF(J)=.5*XEQ*YI2	SHA18200
	GO TO 200	SHA18300
190	J=J+1	SHA18400
	DFX(J)=.28125*YI2*(3.*XEQ-2.*XI*XE2)	SHA18500
	DFY(J)=.28125*XEQ*XE2	SHA18600
	FF(J)=.28125*XEQ*XE2*YI2	SHA18700
	J=J+1	SHA18800
	DFX(J)=-.28125*YI2*(3.*XEQ+2.*XI*XE1)	SHA18900

	FF(J)=.28125*XEQ*XE1*YI2	SHA19000
	DFY(J)=.28125*XEQ*XE1	SHA19100
200	IF (IN(11,L).EQ.0) GO TO 230	SHA19200
	IF (IN(12,L).EQ.0) GO TO 210	SHA19300
	GO TO 220	SHA19400
210	J=J+1	SHA19500
	DFX(J)=-.5*YEQ	SHA19600
	DFY(J)=-YI*XI1	SHA19700
	FF(J)=.5*XI1*YEQ	SHA19800
	GO TO 230	SHA19900
220	J=J+1	SHA20000
	DFX(J)=-.28125*YEQ*YE2	SHA20100
	DFY(J)=.28125*XI1*(3.*YEQ-2.*YI*YE2)	SHA20200
	FF(J)=.28125*XI1*YEQ*YE2	SHA20300
	J=J+1	SHA20400
	DFX(J)=-.28125*YEQ*YE1	SHA20500
	DFY(J)=-.28125*XI1*(3.*YEQ+2.*YI*YE1)	SHA20600
	FF(J)=.28125*YEQ*YE1*XI1	SHA20700
230	CONTINUE	SHA20800
240	CONTINUE	SHA20900
C		SHA21000
C	JACOBIAN	SHA21100
	SUM1=0.	SHA21200
	SUM2=0.	SHA21300
	SUM3=0.	SHA21400
	SUM4=0.	SHA21500
	K=0	SHA21600
	DO 260 I=1,M	SHA21700
250	K=K+1	SHA21800
	IF (IN(K,L).EQ.0) GO TO 250	SHA21900
	KI=IN(K,L)	SHA22000
	SUM1=SUM1+DFX(I)*X(KI)	SHA22100
	SUM2=SUM2+DFX(I)*Y(KI)	SHA22200
	SUM3=SUM3+DFY(I)*X(KI)	SHA22300
	SUM4=SUM4+DFY(I)*Y(KI)	SHA22400
260	CONTINUE	SHA22500
	DET=SUM1*SUM4-SUM2*SUM3	SHA22600
	DET1=1./DET	SHA22700
	C11=DET1*SUM4	SHA22800
	C12=-DET1*SUM2	SHA22900
	C21=-DET1*SUM3	SHA23000
	C22=DET1*SUM1	SHA23100
C		SHA23200
	DJAC(1,1)=C11	SHA23300
	DJAC(1,2)=C12	SHA23400
	DJAC(2,1)=C21	SHA23500
	DJAC(2,2)=C22	SHA23600
C	SHAPE FUNCTION DERIVATIVES - GLOBAL	SHA23700
	DO 270 J=1,M	SHA23800
	BB(1,J)=C11*DFX(J)+C12*DFY(J)	SHA23900
	BB(2,J)=C21*DFX(J)+C22*DFY(J)	SHA24000
270	CONTINUE	SHA24100
	RETURN	SHA24200
	END	SHA24300

C	*****	LOA	100
C		LOA	200
C	THIS ROUTINE COMPUTES THE COLUMN MATRIX R BY ADDING IN THE VARIOUS	LOA	300
C	SOURCES AND SINKS AND THEN SOLVES FOR THE UNKNOWN COLUMN MATRIX	LOA	400
C		LOA	500
C		LOA	600
	SUBROUTINE LOAD(LM, LN, MBAND, NOD, NODE, R, RI, G	LOA	700
	*, GG, HEAT, HEAD, ALPHA, KBOUND, KFT, PCW, LT, CFACT, KS,	LOA	800
	*Z, NCON, TINF, CONV, ALOC, LSOURC, NSOURC, ASOURC, CBAL, AY, AZ	LOA	900
	*, AEL, NEL, MEQ, LEL, CBALA, LINE, NLINE, ALINE)	LOA	1000
	REAL JAC	LOA	1100
	INTEGER Z, AY(4), AZ(4)	LOA	1200
	DOUBLE PRECISION AA, NET, NXI, NOT	LOA	1300
	COMMON/AAA/XL(4), YL(4), DETJAC, JAC(4,4)/AB/AA(6), W(4)	LOA	1400
	COMMON/A1/M, MM, NUMNP, NSIZE/AA/NXI(12), NET(12), NOT(12)	LOA	1500
	COMMON/ACC/KK(12), K1, K2, K3, K4/AM/KSYM, PCT/HH/LFLOW, LON	LOA	1600
	COMMON/BAL/BLINE/CON/MC1, MC2, NCONV/CONT/LA, LB, LC, LD, LE, LF, LG, LH	LOA	1700
	COMMON/ATHICK/ASIZE, NTHICK, THICK, ERROR, XADD, YADD	LOA	1800
	DIMENSION NCON(Z,3), TINF(Z), CONV(Z), ALOC(Z), NSOURC(Z)	LOA	1900
	DIMENSION AEL(Z,2), CBAL(Z,2), ASOURC(Z), NODE(LM), NOD(12, LM)	LOA	2000
	DIMENSION R(LN), G(LN), GG(LN), RI(LN), HEAD(LN), HEAT(LM)	LOA	2100
	*, NLINE(Z,2), ALINE(Z), NEL(Z,2)	LOA	2200
	RETURN	LOA	2300
C	*****	LOA	2400
C		LOA	2500
	ENTRY HEATE(KS)	LOA	2600
		LOA	2700
		LOA	2800
		LOA	2900
		LOA	3000
		LOA	3100
		LOA	3200
	DO 1 J=1, LN	LOA	3300
	RI(J)=R(J)	LOA	3400
	G(J)=0.0	LOA	3500
1	CONTINUE	LOA	3600
	BLINE=0.0	LOA	3700
	IF(LD.EQ.1.AND.MEQ.EQ.1) CALL CHAN	LOA	3800
	IF(LT.EQ.0) GO TO 300	LOA	3900
C	*****	LOA	4000
C		LOA	4100
C	TRANSIENT LOOP GENERATION AND BOUNDARY CONDITIONS ARE CHANGED AT EACH	LOA	4200
	IF(KBOUND.EQ.1) CALL BOUND(KS)	LOA	4300
C	THREE ENTRY POINTS ARE PROVIDED FOR CHANGING RECHARGE RATES	LOA	4400
C	AND BOUNDARY CONDITIONS AT EACH TIME STEP--ALL ENTRIES IN BOUNDA	LOA	4500
C		LOA	4600
	IF(KBOUND.EQ.2) CALL BVAL(KS, ALPHA)	LOA	4700
C		LOA	4800
	IF(LD.EQ.1.AND.MEQ.EQ.2) CALL CHANG	LOA	4900
C		LOA	5000
C	*****	LOA	5100
C		LOA	5200
C	*****	LOA	5300
C		LOA	5400
C	CONVECTIVE BOUNDARY ROUTINE	LOA	5500
	IF(MEQ.EQ.1) GO TO 50	LOA	5600
C		LOA	5700
	IF(NCONV.EQ.0) GO TO 40	LOA	5800
C		LOA	5900
	DO 30 I=1, NCONV	LOA	6000
	LLL=NCON(I,1)	LOA	6100
	LA=NCON(I,2)	LOA	6200

MC1=AY(LA)	LOA 6300
MC2=AZ(LA)	LOA 6400
MA=NOD(MC1,LLL)	LOA 6500
NA=NOD(MC2,LLL)	LOA 6600
K=NA	LOA 6700
ONV=ABS(CONV(I))	LOA 6800
CBAL(I,2)=ONV*ALOC(I)*TINF(I)*ALPHA	LOA 6900
C H*LENGTH PF BOUNDARY*TEMP AT INFINITY*TIME STEP	LOA 7000
G(K)=ONV*ALOC(I)*.5*TINF(I)*ALPHA+G(K)	LOA 7100
K=MA	LOA 7200
G(K)=ONV*ALOC(I)*.5*TINF(I)*ALPHA+G(K)	LOA 7300
30 CONTINUE	LOA 7400
C	LOA 7500
40 CONTINUE	LOA 7600
C	LOA 7700
C ROUTINE THAT CALCUALTES CONVECTIVE INPUTS IS CALLED	LOA 7800
IF(LEL.GT.0) CALL CB(ALPHA)	LOA 7900
C	LOA 8000
C	LOA 8100
50 CONTINUE	LOA 8200
C*****	LOA 8300
C--MATRIX MULTIPLICATION LOOP	LOA 8400
C	LOA 8500
IF(KSYM.EQ.0) CALL MULTI	LOA 8600
IF(KSYM.NE.0) CALL AMULTI	LOA 8700
C	LOA 8800
C*****	LOA 8900
C	LOA 9000
C	LOA 9100
C GENERATION TERMS ARE ADDED INTO THE RIGHT SIDE OF THE EQUATION	LOA 9200
C	LOA 9300
C	LOA 9400
C GENERATION TERMS FROM POINT SOURCES	LOA 9500
C	LOA 9600
300 IF(LSOURC.EQ.0) GO TO 360	LOA 9700
DO 350 LLL=1,LSOURC	LOA 9800
K=NSOURC(LLL)	LOA 9900
IF(ALPHA.LE.0) AS=ASOURC(LLL)	LOA10000
IF(ALPHA.GT.0) AS=ASOURC(LLL)*ALPHA	LOA10100
IF(LT.EQ.0) GG(K)=GG(K)+AS	LOA10200
IF(LT.EQ.1) G(K)=G(K)+AS	LOA10300
350 CONTINUE	LOA10400
360 CONTINUE	LOA10500
C	LOA10600
C GENERATION TERMS FROM LINE SOURCES ARE COMPUTED AND ADDED IN	LOA10700
C	LOA10800
IF(LINE.EQ.0) GO TO 378	LOA10900
DO 375 L=1,LINE	LOA11000
LLL=NLINE(L,1)	LOA11100
CALL CORD(LLL)	LOA11200
LA=NLINE(L,2)	LOA11300
LY=AY(LA)	LOA11400
LZ=AZ(LA)	LOA11500
MC3=LY+LZ	LOA11600
IF(MC3.EQ.5) A=ABS(YL(LY)-YL(LZ))	LOA11700
IF(MC3.NE.5) A=ABS(XL(LY)-XL(LZ))	LOA11800
AS=ALINE(L)*A	LOA11900
IF(ALPHA.GT.0) AS=AS*ALPHA	LOA12000
BLINE=BLINE+AS	LOA12100
LY=NOD(LY,LLL)	LOA12200
LZ=NOD(LZ,LLL)	LOA12300
IF(LT.EQ.0) GO TO 372	LOA12400

	G(LY)=G(LY)+AS/2	LOA12500
	G(LZ)=G(LZ)+AS/2	LOA12600
	GO TO 375	LOA12700
372	GG(LY)=GG(LY)+AS/2	LOA12800
	GG(LZ)=GG(LZ)+AS/2	LOA12900
375	CONTINUE	LOA13000
C		LOA13100
378	CONTINUE	LOA13200
C		LOA13300
	DO 380 N=1,NSIZE	LOA13400
380	R(N)=R(N)+G(N)	LOA13500
C		LOA13600
C	*****	LOA13700
C		LOA13800
C	GENERATION TERMS FROM SOURCES ARE ADDED IN	LOA13900
C	AND SPECIFIED HEADS ARE TREATED	LOA14000
C		LOA14100
	DO 410 N=1,NSIZE	LOA14200
	IF(LT.EQ.0) R(N)=CFACT*HEAD(N)+GG(N)	LOA14300
410	IF(LT.EQ.1) R(N)=R(N)+CFACT*HEAD(N)+GG(N)	LOA14400
C		LOA14500
C	*****	LOA14600
C		LOA14700
C	FORWARD REDUCTION OF THE LOAD MATRIX IS PREFORMED AND BACK	LOA14800
C	SUBSTITUTION IS PREFORMED TO SOLVE FOR THE UNKNOWN MATRIX	LOA14900
C		LOA15000
	IF(KSYM.EQ.0) CALL BACK	LOA15100
	IF(KSYM.NE.0) CALL ABACK	LOA15200
550	CONTINUE	LOA15300
C		LOA15400
C	*****	LOA15500
	RETURN	LOA15600
C		LOA15700
C	*****	LOA15800
C		LOA15900
C		LOA16000
	SUBROUTINE CB(ALPHA)	LOA16100
C		LOA16200
C	*****	LOA16300
	DIMENSION JA(4),JB(4),JC(4),JD(4)	LOA16400
	DATA JA/1,1,1,2/JB/2,1,2,2/JC/2,2,1,2/JD/2,1,1,1/	LOA16500
	IF(LEL.EQ.0) RETURN	LOA16600
	AA(1)=-((1/3)**.5	LOA16700
	AA(2)=-AA(1)	LOA16800
	FACT1=0.7886751	LOA16900
	FACT2=0.2113249	LOA17000
	CBALA=0.0	LOA17100
	LFLOW=0	LOA17200
	DO 10 J=1,LEL	LOA17300
	LLL=NEL(J,1)	LOA17400
	M4=4	LOA17500
	CALL DERIVE(LLL,M4)	LOA17600
	T=1.0	LOA17700
	CALL PEE(T,LLL)	LOA17800
	LA=NEL(J,2)	LOA17900
	LY=AY(LA)	LOA18000
	LZ=AZ(LA)	LOA18100
	IF(LA.GT.2) A=Y(LY)-Y(LZ)	LOA18200
	IF(LA.LT.3) A=X(LY)-X(LZ)	LOA18300
	A=ABS(A)*T*THICK	LOA18400
	LY=NOD(LY,LLL)	LOA18500
	LZ=NOD(LZ,LLL)	LOA18600
C		LOA18700
C	COMPUTE VELOCITIES AT THE GAUSS POINTS	LOA18800

C			LOA18900
C	VX IS ASSOCIATED WITH ARRAY AY	VXX IS ASSOCIATED WITH ARRAY AZ	LOA19000
	JJ=JA(LA)		LOA19100
	II=JB(LA)		LOA19200
	CALL SHAPE1(JJ,II)		LOA19300
	CALL VELO(LLL,VX,VY)		LOA19400
	JJ=JC(LA)		LOA19500
	II=JD(LA)		LOA19600
	CALL SHAPE1(JJ,II)		LOA19700
	CALL VELO(LLL,VXX,VYY)		LOA19800
C			LOA19900
	IF(LA.GT.2) GO TO 6		LOA20000
	V1=(VY*A/2)		LOA20100
	V2=(VYY*A/2)		LOA20200
	GO TO 7		LOA20300
6	V1=(VX*A/2)		LOA20400
	V2=(VXX*A/2)		LOA20500
7	CONTINUE		LOA20600
	GO TO (9,8,8,9),LA		LOA20700
8	V1=-V1		LOA20800
	V2=-V2		LOA20900
9	CONTINUE		LOA21000
	IF(V1.GE.0) Q=V1*PCW*AEL(J,2)		LOA21100
	IF(V1.LT.0) Q=V1*PCW*R(LY)		LOA21200
	IF(V2.GE.0) QQ=V2*PCW*AEL(J,2)		LOA21300
	IF(V2.LT.0) QQ=V2*PCW*R(LZ)		LOA21400
	G(LY)=G(LY)+Q*ALPHA*FACT1+QQ*ALPHA*FACT2		LOA21500
	G(LZ)=G(LZ)+QQ*ALPHA*FACT1+Q*ALPHA*FACT2		LOA21600
	CBALA=CBALA+Q+QQ		LOA21700
10	CONTINUE		LOA21800
20	FORMAT(1X,'BOUND TEMPS ',7(I4,G8.3,3X))		LOA21900
	RETURN		LOA22000
	END		LOA22100

C*****	SOL 100
C	SOL 200
C FORWARD REDUCTION OF THE S MATRIX BY GAUSS ELIMINATION	SOL 300
C	SOL 400
C SUBROUTINE SOLVE(LN,MBAND,S,T,R,RI)	SOL 500
C	SOL 600
DOUBLE PRECISION S,T,C	SOL 700
COMMON/A1/ M,MM,NUMNP,NSIZE	SOL 800
DIMENSION S(LN,MBAND),T(LN,MBAND),R(LN),RI(LN)	SOL 900
C GAUSS ELIMINATION--FORWARD REDUCTION OF STIFNESS MATRIX	SOL 1000
DO 550 N=1,NSIZE	SOL 1100
DO 530 L=2,MBAND	SOL 1200
IF(S(N,L).EQ.0) GO TO 530	SOL 1300
I=N+L-1	SOL 1400
C=S(N,L)/S(N,1)	SOL 1500
J=0	SOL 1600
DO 510 K=L,MBAND	SOL 1700
J=J+1	SOL 1800
510 S(I,J)=S(I,J)-C*S(N,K)	SOL 1900
S(N,L)=C	SOL 2000
530 CONTINUE	SOL 2100
550 CONTINUE	SOL 2200
RETURN	SOL 2300
C	SOL 2400
C*****	SOL 2500
C BACK SOLUTION OF THE R VECTOR BY GAUSS ELIMINATION	SOL 2600
C	SOL 2700
C ENTRY BACK	SOL 2800
C	SOL 2900
C	SOL 3000
C FORWARD REDUCTION OF THE LOAD MATRIX IS PREFORMED AND BACK	SOL 3100
C SUBSTITUTION IS PREFORMED TO SOLVE FOR THE UNKNOWN MATRIX	SOL 3200
DO 630 N=1,NSIZE	SOL 3300
DO 620 L=2,MBAND	SOL 3400
IF(S(N,L).EQ.0) GO TO 620	SOL 3500
I=N+L-1	SOL 3600
R(I)=R(I)-S(N,L)*R(N)	SOL 3700
620 CONTINUE	SOL 3800
630 R(N)=R(N)/S(N,1)	SOL 3900
DO 660 M=2,NSIZE	SOL 4000
N=NSIZE+1-M	SOL 4100
DO 650 L=2,MBAND	SOL 4200
IF(S(N,L).EQ.0) GO TO 650	SOL 4300
K=N+L-1	SOL 4400
R(N)=R(N)-S(N,L)*R(K)	SOL 4500
650 CONTINUE	SOL 4600
660 CONTINUE	SOL 4700
C	SOL 4800
C RETURN	SOL 4900
C	SOL 5000
C*****	SOL 5100
C MULTIPLICATION OF THE T MATRIX BY THE NODAL VALUES AT THE LAST TIME	SOL 5200
C	SOL 5300
C	SOL 5400
C ENTRY MULTI	SOL 5500
C	SOL 5600
C MATRIX MULTIPLICATION LOOP--CRANK-NICOLSON METHOD	SOL 5700
C	SOL 5800
DO 150 N=1,NSIZE	SOL 5900
R(N)=0.0	SOL 6000
DO 110 M=1,MBAND	SOL 6100
NO=M+N-1	SOL 6200
IF(NO.GT.NSIZE) GO TO 120	SOL 6300

110	R(N)=RI(NO)*T(N,M)+R(N)	SOL 6400
120	CONTINUE	SOL 6500
	MBA=MBAND-1	SOL 6600
	DO 130 M=1,MBA	SOL 6700
	NO=N-M	SOL 6800
	IF(NO.LE.0) GO TO 140	SOL 6900
130	R(N)=RI(NO)*T(NO,M+1)+R(N)	SOL 7000
140	CONTINUE	SOL 7100
150	CONTINUE	SOL 7200
C		SOL 7300
	RETURN	SOL 7400
	END	SOL 7500

C*****	ASO 100
C	ASO 200
SUBROUTINE ASOLVE(B,R,RI,NEQ,IHALFB,NDIM,MDIM,T)	ASO 300
C	ASO 400
C ASSYMMETRIC BAND MATRIX EQUATION SOLVER	ASO 500
C ORIGINALLY PROGRAMED BY J.O. DUGUID	ASO 600
C	ASO 700
DOUBLE PRECISION B,T,PIVOT,C	ASO 800
DIMENSION B(NDIM,MDIM),R(NDIM),T(NDIM,MDIM)	ASO 900
DIMENSION RI(NDIM)	ASO 1000
NRS=NEQ-1	ASO 1100
IHBP=IHALFB+1	ASO 1200
C	ASO 1300
C TRIANGULARIZE MATRIX B USING DOOLITTLE METHOD	ASO 1400
C	ASO 1500
DO 20 K=1,NRS	ASO 1600
PIVOT=B(K,IHBP)	ASO 1700
KK=K+1	ASO 1800
KC=IHBP	ASO 1900
DO 10 I=KK,NEQ	ASO 2000
KC=KC-1	ASO 2100
IF(KC.LE.0) GO TO 20	ASO 2200
C=-B(I,KC)/PIVOT	ASO 2300
B(I,KC)=C	ASO 2400
KI=KC+1	ASO 2500
LIM=KC+IHALFB	ASO 2600
DO 10 J=KI,LIM	ASO 2700
JC=IHBP+J-KC	ASO 2800
10 B(I,J)=B(I,J)+C*B(K,JC)	ASO 2900
20 CONTINUE	ASO 3000
RETURN	ASO 3100
C	ASO 3200
C*****	ASO 3300
C	ASO 3400
ENTRY ABACK	ASO 3500
C	ASO 3600
NN=NEQ+1	ASO 3700
IBAND=2*IHALFB+1	ASO 3800
DO 70 I=2,NEQ	ASO 3900
JC=IHBP-I+1	ASO 4000
JI=1	ASO 4100
IF(JC.LE.0) GO TO 40	ASO 4200
GO TO 50	ASO 4300
40 JC=1	ASO 4400
JI=I-IHBP+1	ASO 4500
50 SUM=0.0	ASO 4600
DO 60 J=JC,IHALFB	ASO 4700
SUM=SUM+B(I,J)*R(JI)	ASO 4800
60 JI=JI+1	ASO 4900
70 R(I)=R(I)+SUM	ASO 5000
C	ASO 5100
C BACK SUBSTITUTION	ASO 5200
C	ASO 5300
R(NEQ)=R(NEQ)/B(NEQ,IHBP)	ASO 5400
DO 90 IBACK=2,NEQ	ASO 5500
I=NN-IBACK	ASO 5600
JP=I	ASO 5700
KR=IHBP+1	ASO 5800
MR=MIN0(IBAND,IHALFB+IBACK)	ASO 5900
SUM=0.0	ASO 6000
DO 80 J=KR,MR	ASO 6100
JP=JP+1	ASO 6200

80	SUM=SUM+B(I,J)*R(JP)	ASO 6300
90	R(I)=(R(I)-SUM)/B(I,IHBP)	ASO 6400
100	RETURN	ASO 6500
C		ASO 6600
C	*****	ASO 6700
C		ASO 6800
	ENTRY AMULTI	ASO 6900
C		ASO 7000
	LN=NDIM	ASO 7100
	MBAND=(MDIM+1)/2	ASO 7200
	DO 150 N=1, LN	ASO 7300
	R(N)=0.0	ASO 7400
	DO 110 M=1, MDIM	ASO 7500
	NO=M+N-MBAND	ASO 7600
	IF(NO.GT.LN) GO TO 120	ASO 7700
	IF(NO.LT.1) GO TO 110	ASO 7800
	R(N)=R1(NO)*T(N,M)+R(N)	ASO 7900
110	CONTINUE	ASO 8000
120	CONTINUE	ASO 8100
150	CONTINUE	ASO 8200
	RETURN	ASO 8300
	END	ASO 8400

C*****	BAL	100
C THIS SUBROUTINE COMPUTES A MASS BALANCE	BAL	200
C	BAL	300
SUBROUTINE BALAN(LM, LN, R, PX, PY, PCX, HEAD, HEAT, Z, LSOURC, ASOURC,	BAL	400
* LFLUX, NFLUX, A, B, C, D, E, MPRINT, NTYPE, RI, NODE, NOD, FLOWX, FLOWY, PCW	BAL	500
* , MEQ, CBAL, CBALA, AY, AZ, NCON, KRAN)	BAL	600
REAL JAC	BAL	700
INTEGER Z, AY, AZ	BAL	800
DOUBLE PRECISION AA, NXI, NET, NOT	BAL	900
COMMON/AAA/XL(4), YL(4), DETJAC, JAC(4.4)/AB/AA(6) .W(4)	BAL	1000
COMMON/CON/M1, M2, NCONV/AA/NXI(12), NET(12), NOT(12)	BAL	1100
COMMON/ACC/KK(12), K1, K2, K3, K4/HH/LFLOW, LON/BAL/BLINE	BAL	1200
DIMENSION RI(LN), R(LN), PX(LM), PY(LM), NODE(LM)	BAL	1300
DIMENSION FLOWX(LM), FLOWY(LM), AY(4), AZ(4)	BAL	1400
DIMENSION NCON(Z, 2), CBAL(Z, 2) , NOD(12, LM)	BAL	1500
DIMENSION PCX(LM), HEAD(LN), HEAT(LM), ASOURC(Z) .NFLUX(Z, 2)	BAL	1600
DIMENSION LOA(4), LOB(4), LOC(4), LOD(4)	BAL	1700
DATA LOA/1, 2, 3, 4/LOB/2, 3, 4, 1/LOC/5, 7, 9, 11/LOD/6 8, 10, 12/	BAL	1800
RETURN	BAL	1900
C*****	BAL	2000
ENTRY MASBAL(ALPHA)	BAL	2100
C	BAL	2200
C---COMPUTE BOUNDARY FLUXES	BAL	2300
C	BAL	2400
ST=0.0	BAL	2500
PUMP=0.0	BAL	2600
F=0.0	BAL	2700
LFLOW=0	BAL	2800
RECH=0.0	BAL	2900
DISCH=0.0	BAL	3000
IF(LFLUX.EQ.0) GO TO 15	BAL	3100
AA(1)=0.0	BAL	3200
AA(2)=0.0	BAL	3300
C	BAL	3400
DO 10 LLA=1, LFLUX	BAL	3500
LLL =NFLUX(LLA, 1)	BAL	3600
K=NFLUX(LLA, 2)	BAL	3700
C	BAL	3800
CALL FLOWW(LLL)	BAL	3900
C	BAL	4000
LT=NFLUX(LLA, 2)	BAL	4100
FLUXX=0.0	BAL	4200
FLUXY=0.0	BAL	4300
IF(LT.GT.2) FLUXX=DHX*ARX*PX(LLL)	BAL	4400
IF(LT.LT.3) FLUXY=DHY*ARY*PY(LLL)	BAL	4500
IF(MEQ.EQ.1) GO TO 8	BAL	4600
LY=AY(LT)	BAL	4700
LZ=AZ(LT)	BAL	4800
LY=NOD(LY, LLL)	BAL	4900
LZ=NOD(LZ, LLL)	BAL	5000
RR=(R(LY)+R(LZ))/2	BAL	5100
IF(LT.GT.2) FLUXX=FLUXX+FLOWX(LLL)*PCW*RR	BAL	5200
IF(LT.LT.3) FLUXY=FLUXY+FLOWY(LLL)*PCW*RR	BAL	5300
8 CONTINUE	BAL	5400
IF(LT.EQ.1.AND.FLUXY.LT.0) DISCH=DISCH-FLUXY	BAL	5500
IF(LT.EQ.1.AND.FLUXY.GT.0) RECH=RECH+FLUXY	BAL	5600
IF(LT.EQ.2.AND.FLUXY.LT.0) RECH=RECH-FLUXY	BAL	5700
IF(LT.EQ.2.AND.FLUXY.GT.0) DISCH=DISCH+FLUXY	BAL	5800
IF(LT.EQ.3.AND.FLUXX.LT.0) RECH=RECH-FLUXX	BAL	5900
IF(LT.EQ.3.AND.FLUXX.GT.0) DISCH=DISCH+FLUXX	BAL	6000
IF(LT.EQ.4.AND.FLUXX.LT.0) DISCH=DISCH-FLUXX	BAL	6100
IF(LT.EQ.4.AND.FLUXX.GT.0) RECH=RECH+FLUXX	BAL	6200
10 CONTINUE	BAL	6300

15	CONTINUE	BAL 6400
C		BAL 6500
C	*****	BAL 6600
C	COMPUTE RATE OF CHANGE IN STORAGE	BAL 6700
C		BAL 6800
	IF(KRAN.EQ.0) GO TO 21	BAL 6900
	ST=0.0	BAL 7000
	DO 20 LLL=1,LM	BAL 7100
	M4=4	BAL 7200
	CALL DERIVE(LLL,M4)	BAL 7300
	IF(MEQ.EQ.1) CALL PEE(T,LLL)	BAL 7400
	IF(MEQ.EQ.1) DETJAC=DETJAC/T	BAL 7500
	RB=0	BAL 7600
	RA=0	BAL 7700
	K=0	BAL 7800
	DO 19 I=1,4	BAL 7900
	L1=LOA(I)	BAL 8000
	L2=LOB(I)	BAL 8100
	L3=LOC(I)	BAL 8200
	L4=LOD(I)	BAL 8300
	L5=NOD(L1,LLL)	BAL 8400
	L6=NOD(L2,LLL)	BAL 8500
	L7=NOD(L3,LLL)	BAL 8600
	L8=NOD(L4,LLL)	BAL 8700
	IF(L7.GT.0) GO TO 23	BAL 8800
	RA=RA+.5*R(L5)+.5*R(L6)	BAL 8900
	RB=RB+.5*RI(L5)+.5*RI(L6)	BAL 9000
	GO TO 19	BAL 9100
23	IF(L8.GT.0) GO TO 24	BAL 9200
	RA=RA+1/3*R(L5)+2/3*R(L7)+1/3*R(L6)	BAL 9300
	RB=RB+1/3*RI(L5)+1/3*RI(L6)+2/3*RI(L7)	BAL 9400
	GO TO 19	BAL 9500
24	RA=RA+1/8*R(L5)+1/8*R(L6)+3/8*R(L7)+3/8*R(L8)	BAL 9600
	RB=RB+1/8*RI(L5)+1/8*RI(L6)+3/8*RI(L7)+3/8*RI(L8)	BAL 9700
19	CONTINUE	BAL 9800
	RA=RA/4	BAL 9900
	RB=RB/4	BAL10000
	ST=ST+(RA-RB)*PCX(LLL)*4*DETJAC	BAL10100
20	CONTINUE	BAL10200
21	CONTINUE	BAL10300
C		BAL10400
C	*****	BAL10500
C	ADD IN PUMPING SOURCES	BAL10600
C		BAL10700
	PUMP=0.0	BAL10800
	PUMP=PUMP+BLINE	BAL10900
	IF(LSOURC.EQ.0) GO TO 31	BAL11000
	DO 30 LLL=1,LSOURC	BAL11100
	PUMP=PUMP+ASOURC(LLL)	BAL11200
30	CONTINUE	BAL11300
31	CONTINUE	BAL11400
C	DISTRIBUTED SOURCES	BAL11500
	DO 40 LLL=1,LM	BAL11600
	IF(HEAT(LLL).EQ.0) GO TO 40	BAL11700
	M4=NODE(LLL)	BAL11800
	CALL DERIVE(LLL,M4)	BAL11900
	PUMP=PUMP+HEAT(LLL)*4*DETJAC	BAL12000
40	CONTINUE	BAL12100
C		BAL12200
C	*****	BAL12300
C		BAL12400

C	ROUTINES TO COMPUTE FLUXES ACROSS CONVECTIVE BOUNDARIES	BAL12500
C		BAL12600
	IF(MEQ.EQ.1) GO TO 48	BAL12700
	IF(NCONV.EQ.0) GO TO 45	BAL12800
	CO=0.0	BAL12900
	COA=0.0	BAL13000
	DO 43 I=1,NCONV	BAL13100
	LLL=NCON(I,1)	BAL13200
	LA=NCON(I,2)	BAL13300
	MC1=AY(LA)	BAL13400
	MC2=AZ(LA)	BAL13500
	MA=NOD(MC1,LLL)	BAL13600
	NA=NOD(MC2,LLL)	BAL13700
	NC=CBAL(I,2)*100	BAL13800
	IF(NC.EQ.0) COA=COA+(R(MA)/4+R(NA)/4+RI(MA)/4+RI(NA)/4)*CBAL(I,1)	BAL13900
	IF(NC.EQ.0) GO TO 43	BAL14000
	CO=CO+CBAL(I,2)-(R(MA)/4+R(NA)/4+RI(MA)/4+RI(NA)/4)*CBAL(I,1)	BAL14100
43	CONTINUE	BAL14200
C		BAL14300
C		BAL14400
45	CONTINUE	BAL14500
48	CONTINUE	BAL14600
C	*****	BAL14700
C		BAL14800
C		BAL14900
	AL=ALPHA	BAL15000
	IF(ALPHA.LT.0.0001) AL=1	BAL15100
	RECH=RECH*AL	BAL15200
	DISCH=DISCH*AL	BAL15300
	PUMP=PUMP*AL	BAL15400
	CBALA=CBALA*AL	BAL15500
C	*****	BAL15600
	A=A+RECH	BAL15700
	B=B+DISCH	BAL15800
	C=C+ST	BAL15900
	D=D+PUMP	BAL16000
	O=O+CO	BAL16100
	OO=OO+COA	BAL16200
	P=P+CBALA	BAL16300
	IF(MEQ.EQ.1) F=RECH-DISCH+PUMP-ST	BAL16400
	IF(MEQ.EQ.2) F=RECH-DISCH+PUMP-ST+CBALA+CO-COA	BAL16500
	E=E+F	BAL16600
	RETURN	BAL16700
	ENTRY BPRINT	BAL16800
	PRINT 50	BAL16900
	IF(MEQ.EQ.2) PRINT 51,O,CO,OO,COA,P,CBALA	BAL17000
	PRINT 52,A,RECH,B,DISCH,C,ST,D,PUMP,E,F	BAL17100
50	FORMAT(1X,T30,'CUMULATIVE MASS BLANCE',	BAL17200
	*T60,'RATES FOR THIS TIME STEP')	BAL17300
51	FORMAT(1X,'CONDUCTIVE TRANSFER',	BAL17400
	* ,T30,G12.6,T60,G12.6,	BAL17500
	* 1X/1X,'CONVECTIVE TRANSFER--OUT ',T30,G12.6,T60,G12.6	BAL17600
	* ,1X/1X,'CONVECTIVE TRANSFER--IN',T30,G12.6,T60,G12.6)	BAL17700
52	FORMAT(BAL17800
	*1X,'B. FLUX RECHARGE',T30,G12.6,T60, G12.6.	BAL17900
	* /1X,'B. FLUX DISCHARGE',T30,G12.6,T60,G12.6,	BAL18000
	* /1X,'CHANGE IN STORAGE',T30,G12.6,T60,G12.6.	BAL18100
	* /1X,'QUANTITY PUMPED',T30,G12.6,T60,G12.6,	BAL18200
	* /1X,'DIFFERECE',T30,G12.6,T60,G12.6)	BAL18300
	RETURN	BAL18400
C		BAL18500

C*****	BAL18600
C	BAL18700
ENTRY WATER	BAL18800
AA(1)=0.0	BAL18900
AA(2)=0.0	BAL19000
LFLOW=0	BAL19100
DO 100 LLL=1,LM	BAL19200
CALL FLOWW(LLL)	BAL19300
C	BAL19400
C FLOW EQUALS THE SLOPE * AREA * PERMEABILITY	BAL19500
C	BAL19600
FLOWX(LLL)=DHX*ARX*PX(LLL)	BAL19700
FLOWY(LLL)=DHY*ARY*PY(LLL)	BAL19800
C	BAL19900
100 CONTINUE	BAL20000
C*****	BAL20100
RETURN	BAL20200
C	BAL20300
C	BAL20400
C*****	BAL20500
C	BAL20600
ENTRY VELOC(LN,LM,RW,WX WY)	BAL20700
DIMENSION WX(LM),WY(LM),RW(LN)	BAL20800
RETURN	BAL20900
C*****	BAL21000
ENTRY VELO(LLLQ,VX,VY)	BAL21100
DHE=0.0	BAL21200
DHN=0.0	BAL21300
K=0	BAL21400
M4=NODE(LLLQ)	BAL21500
DO 500 I=1,M4	BAL21600
400 K=K+1	BAL21700
IF(NOD(K,LLLQ).EQ.0) GO TO 400	BAL21800
KI=NOD(K,LLLQ)	BAL21900
DHE=DHE+NXI(I)*RW(KI)	BAL22000
DHN=DHN+NET(I)*RW(KI)	BAL22100
500 CONTINUE	BAL22200
DHX=JAC(1,1)*DHE+JAC(1,2)*DHN	BAL22300
DHY=JAC(2,1)*DHE+JAC(2,2)*DHN	BAL22400
VX=DHX*WX(LLLQ)	BAL22500
VY=DHY*WY(LLLQ)	BAL22600
RETURN	BAL22700
C	BAL22800
C*****	BAL22900
C	BAL23000
C	BAL23100
ENTRY VCENT(LLLQ,VXQ,VYA)	BAL23200
C THE AREA TO BE USED IN THE FORMULA Q=KIA IS COMPUTED	BAL23300
ARX=(YL(3)+YL(4)-YL(1)-YL(2))/2	BAL23400
ARX=ABS(ARX)	BAL23500
ARY=(XL(2)+XL(3)-XL(1)-XL(4))	BAL23600
ARY=ABS(ARY)/2	BAL23700
VXQ=FLOWX(LLLQ)/ARX	BAL23800
VYA=FLOWY(LLLQ)/ARY	BAL23900
RETURN	BAL24000
C*****	BAL24100
C	BAL24200
C	BAL24300
C SUBROUTINE FLOWW(LLL)	BAL24400
C	BAL24500
DHE=0.0	BAL24600
DHN=0.0	BAL24700
M4=NODE(LLL)	BAL24800

	CALL DERIVE(LLL,M4)	BAL24900
	K=0	BAL25000
	DO 7 I=1,M4	BAL25100
4	K=K+1	BAL25200
	IF(NOD(K,LLL).EQ.0) GO TO 4	BAL25300
	KI=NOD(K,LLL)	BAL25400
	DHE=DHE+NXI(I)*R(KI)	BAL25500
	DHN=DHN+NET(I)*R(KI)	BAL25600
7	CONTINUE	BAL25700
	DHX=JAC(1,1)*DHE+JAC(1,2)*DHN	BAL25800
	DHY=JAC(2,1)*DHE+JAC(2,2)*DHN	BAL25900
C	THE AREA TO BE USED IN THE FORMULA Q=KIA IS COMPUTED	BAL26000
	ARX=(YL(3)+YL(4)-YL(1)-YL(2))/2	BAL26100
	ARX=ABS(ARX)	BAL26200
	ARY=(XL(2)+XL(3)-XL(1)-XL(4))	BAL26300
	ARY=ABS(ARY)/2	BAL26400
	ARXX=ARX	BAL26500
	ARX=DETJAC*4/ARY	BAL26600
	ARY=DETJAC*4/ARXX	BAL26700
C	↑	BAL26800
C		BAL26900
	RETURN	BAL27000
C		BAL27100
C	*****	BAL27200
	END	BAL27300

C THIS ROUTINE IS USED TO PRINT FLOWS AND FLUXES	FLO 100
C	FLO 200
SUBROUTINE FLOWS(LM, LN, R, R1, FLOWX, FLOWY)	FLO 300
DIMENSION R(LN), R1(LN), FLOWX(LM), FLOWY(LM)	FLO 400
COMMON/HI/TITLE(25), V(26), VV(26)	FLO 500
C	FLO 600
C*****	FLO 700
RETURN	FLO 800
ENTRY FFLOW	FLO 900
WRITE(14, V) (R1(I), I=1, LN)	FLO 1000
RETURN	FLO 1100
ENTRY FFFLOW	FLO 1200
WRITE(14, V) (R(I), I=1, LN)	FLO 1300
RETURN	FLO 1400
C	FLO 1500
ENTRY WFLOW(S)	FLO 1600
PRINT 1, S	FLO 1700
1 FORMAT(1X//1X, 'TIME STEP ', G12.6/1X, 'FLOWS IN THE X DIRECTION')	FLO 1800
PRINT VV, (FLOWX(I), I=1, LM)	FLO 1900
PRINT 2	FLO 2000
2 FORMAT(1X/1X, 'FLOWS IN THE Y DIRECTION')	FLO 2100
PRINT VV, (FLOWY(I), I=1, LM)	FLO 2200
RETURN	FLO 2300
C	FLO 2400
C*****	FLO 2500
C	FLO 2600
ENTRY HPRINT(S)	FLO 2700
PRINT 10, S	FLO 2800
10 FORMAT(1X//1X, 'TEMPERATURE DISTRIBUTION AT TIME STEP ', G12.6)	FLO 2900
PRINT V, (R(I), I=1, LN)	FLO 3000
RETURN	FLO 3100
C	FLO 3200
C*****	FLO 3300
C	FLO 3400
ENTRY WPRINT(S)	FLO 3500
PRINT 100, S	FLO 3600
100 FORMAT(1X//1X, 'POTENTIAL DISTRIBUTION AT TIME STEP ', G12.6)	FLO 3700
PRINT V, (R1(I), I=1, LN)	FLO 3800
RETURN	FLO 3900
END	FLO 4000

C*****	PAR 100
SUBROUTINE PARAM(LM, LN, BBB, XLOC, YLOC, NOD, PCX, DIFF, R, R1, WX, WY,	PAR 200
C	PAR 300
C THIS SUBROUTINE IS USED TO COMPUTE THE DISPERSION COEFFICEIENTS,	PAR 400
C THE LOCALIZED COORDINATES, AND CHANGES IN HYDRAULIC	PAR 500
C CONDUCTIVITY WITH TEMPERATURE	PAR 600
C	PAR 700
C*****	PAR 800
* A, B, BOT, KAREAL)	PAR 900
INTEGER BBB	PAR 1000
DIMENSION XLOC(LN), YLOC(LN), NOD(12, LM), PCX(LM), DIFF(LM, 2), R(LN)	PAR 1100
*, R1(LN), WX(LM), WY(LM), A(LM), B(LM), BOT(BBB)	PAR 1200
REAL JAC	PAR 1300
COMMON/AAA/XL(4), YL(4), DETJAC, JAC(4, 4)/ACC/KK(12), K1, K2, K3, K4	PAR 1400
*/HM/PXX, PYY, PXY, KAD/AM/NLA, PCW	PAR 1500
C	PAR 1600
RETURN	PAR 1700
C	PAR 1800
C*****	PAR 1900
C THE ROUTINE THAT CALCULATES THE DISPERSION COEFFICIENTS	PAR 2000
C	PAR 2100
ENTRY MECD(LLL, VX, VY)	PAR 2200
V=VX*VX+VY*VY	PAR 2300
IF(V.LE.0) RETURN	PAR 2400
V=SQRT(V)	PAR 2500
DL=DIFF(LLL, 1)*V	PAR 2600
DT=DIFF(LLL, 2)*V	PAR 2700
PXX=(DL*VX*VX/V/V+DT*VY*VY/V/V)*PCW	PAR 2800
PYY=(DT*VX*VX/V/V+DL*VY*VY/V/V)*PCW	PAR 2900
PXY=((DL-DT)*VX*VY/V/V)*PCW	PAR 3000
PXY=ABS(PXY)	PAR 3100
RETURN	PAR 3200
C	PAR 3300
C*****	PAR 3400
C	PAR 3500
ENTRY CORD(LLLQ)	PAR 3600
COMMON/AF/II, JJ, L1(4)	PAR 3700
C THIS ROUTINE COMPUTES LOCALIZED COORDINATES	PAR 3800
K1=NOD(1, LLLQ)	PAR 3900
K2=NOD(2, LLLQ)	PAR 4000
K3=NOD(3, LLLQ)	PAR 4100
K4=NOD(4, LLLQ)	PAR 4200
AQ=XLOC(K1)	PAR 4300
BB=XLOC(K2)	PAR 4400
C=XLOC(K3)	PAR 4500
D=XLOC(K4)	PAR 4600
E=AMIN1(AQ, BB, C, D)	PAR 4700
XL(1)=AQ-E	PAR 4800
XL(2)=BB-E	PAR 4900
XL(3)=C-E	PAR 5000
XL(4)=D-E	PAR 5100
AQ=YLOC(K1)	PAR 5200
BB=YLOC(K2)	PAR 5300
C=YLOC(K3)	PAR 5400
D=YLOC(K4)	PAR 5500
E=AMIN1(AQ, BB, C, D)	PAR 5600
YL(1)=AQ-E	PAR 5700
YL(2)=BB-E	PAR 5800
YL(3)=C-E	PAR 5900
YL(4)=D-E	PAR 6000
C	PAR 6100
C	PAR 6200
RETURN	PAR 6300

C		PAR 6400
C		PAR 6500
C	*****	PAR 6600
C		PAR 6700
	ENTRY PE(MS)	PAR 6800
C		PAR 6900
	IF(MS.EQ.0) RETURN	PAR 7000
	DO 1 J=1,LM	PAR 7100
	N1=NOD(1,J)	PAR 7200
	N2=NOD(2,J)	PAR 7300
	N3=NOD(3,J)	PAR 7400
	N4=NOD(4,J)	PAR 7500
	T=(R(N1)+R(N2)+R(N3)+R(N4))/4	PAR 7600
C		PAR 7700
C	THE VISCOSITY RELATIONSHIP	PAR 7800
C		PAR 7900
	U=1.917-.05635*T+.00071*T*T	PAR 8000
	WX(J)=1.21/U*A(J)	PAR 8100
	WY(J)=1.21/U*B(J)	PAR 8200
1	CONTINUE	PAR 8300
	RETURN	PAR 8400
	ENTRY PEE(BBQQ,JQQ)	PAR 8500
	IF(KAREAL.EQ.0) RETURN	PAR 8600
	N1=NOD(1,JQQ)	PAR 8700
	N2=NOD(2,JQQ)	PAR 8800
	N3=NOD(3,JQQ)	PAR 8900
	N4=NOD(4,JQQ)	PAR 9000
C	GEOMETRIC MEANS ARE CALCULATED FOR AQUIFER DEPTH	PAR 9100
	BBQQ=(R1(N1)-BOT(N1))*(R1(N2)-BOT(N2))*(R1(N3)-BOT(N3))*(R1(N4)-BOT(N4))	BP
	*OT(N4))	PAR 9200
	BBQQ=ABS(BBQQ)	PAR 9300
	BBQQ=BBQQ**0.25	PAR 9400
	RETURN	PAR 9500
	END	PAR 9600
		PAR 9700

C*****	BOU 100
C THIS ROUTINE IS USED TO CHANGE BOUNDARY CONDITIONS OR PARAMETERS	BOU 200
C AT EACH TIME STEP FIVE ENTRY POINTS ARE PROVIDED	BOU 300
C	BOU 400
SUBROUTINE BOUND(LM, LN, Z, R, R1, HEAD, HEA, FLOWX, FLOWY, HEAT, INFLOW	BOU 500
*, NWATER, AWATER, NHEAT, AHEAT, NCON, TINF, CONV, ALOC, NEL, AEL, CBAL	BOU 600
*, LEL, LHEAT, LWATER, PCW, AY, AZ, LINEW, LINEH, NLINEW, NLINEH,	BOU 700
* ALINEW, ALINEH)	BOU 800
INTEGER Z, AY(4), AZ(4)	BOU 900
REAL INFLOW, N11	BOU 1000
COMMON/ATHICK/ASIZE, NTHICK, THICK, ERROR/BM/RY(4800, 3)	BOU 1100
*/BOUND/DIST, N1, N2, N3, N4, N5, N6, N7, N8, N9, N10	BOU 1200
*/CONT/LA, LB, LC, LD, LE, LF, LG, LH/CON/MC1, MC2, NCONV/ME/MEQ	BOU 1300
C--LINKING INFORMATION	BOU 1400
DIMENSION FLOWX(LM), FLOWY(LM)	BOU 1500
C--INFORMATION FOR POINT SOURCES	BOU 1600
DIMENSION NWATER(Z), AWATER(Z), NHEAT(Z), AHEAT(Z)	BOU 1700
C RECHARGE RATE INFORMATION	BOU 1800
*, HEAT(LM), INFLOW(LM), NLINEW(Z, 2), NLINEH(Z, 2), ALINEW(Z), ALINEH(Z)	BOU 1900
C--INFORMATION ON CONVECTIVE BOUNDARIES	BOU 2000
*, NCON(Z, 3), TINF(Z), CONV(Z), ALOC(Z), NEL(Z, 2), AEL(Z, 2), CBAL(Z, 2)	BOU 2100
C--BOUNDARY CONDITIONS	BOU 2200
DIMENSION HEAD(LN), HEA(LN)	BOU 2300
C--INITIAL CONDITIONS AND ANSWERS	BOU 2400
DIMENSION R(LN), R1(LN)	BOU 2500
C	BOU 2600
RETURN	BOU 2700
C	BOU 2800
C*****	BOU 2900
C	BOU 3000
ENTRY LAKE	BOU 3100
READ, DIST, N1, N2, N3, N4, N5, N6, N7, N8, N9, N10, N11	BOU 3200
READ, M, NUMBER	BOU 3300
DO 110 K=1, M	BOU 3400
110 READ, A, B, C	BOU 3500
MM=NUMBER-M	BOU 3600
DO 111 K=1, MM	BOU 3700
111 READ, RY(K, 3), RY(K, 1), RY(K, 2)	BOU 3800
RETURN	BOU 3900
C	BOU 4000
C*****	BOU 4100
C	BOU 4200
C	BOU 4300
ENTRY BVAL(KSQ, ALPHA)	BOU 4400
K=KSQ*ALPHA	BOU 4500
T1=RY(K, 1)-5.0	BOU 4600
DO 100 J=1, LEL	BOU 4700
100 AEL(J, 2)=T1	BOU 4800
RETURN	BOU 4900
C	BOU 5000
C*****	BOU 5100
C	BOU 5200
ENTRY BOUND(KS)	BOU 5300
C	BOU 5400
K=KS*N10+8	BOU 5500
T1=RY(K, 1)	BOU 5600
T2=RY(K, 2)	BOU 5700
AA=ALOG(T1)	BOU 5800
AB=(ALOG(T2)-AA)/54	BOU 5900
T3=AA+DIST*AB	BOU 6000
T3=EXP(T3)	BOU 6100
DO 59 J=N1, N2, N3	BOU 6200
59 HEAD(J)=T3	BOU 6300
DO 60 J=N4, N5, N6	BOU 6400

60	HEAD(J)=T3-2.5	BOU 6500
	DO 200 J=1,LEL	BOU 6600
	TINF(J)=T3	BOU 6700
200	AEL(J,2)=T3	BOU 6800
	IF(NCONV.LT.1) GO TO 300	BOU 6900
	LEA=LEL+1	BOU 7000
	DO 500 J=LEA,NCONV	BOU 7100
	TINF(J)=RY(K-2,1)-N11	BOU 7200
	IF(RY(K-2,3).LT.50) TINF(J)=RY(K-2,3)-N11	BOU 7300
500	CONTINUE	BOU 7400
	PRINT 555, (NCON(J,1),TINF(J),J=1,NCONV)	BOU 7500
555	FORMAT(1X,'NODE # AND TEMP AT INF.',8(2X,I3,2X,F5.2))	BOU 7600
	GO TO 400	BOU 7700
300	CONTINUE	BOU 7800
	DO 700 J=N7,N8,N9	BOU 7900
700	HEAD(J)=T3-N11	BOU 8000
400	CONTINUE	BOU 8100
	RETURN	BOU 8200
C		BOU 8300
C	*****	BOU 8400
C		BOU 8500
C		BOU 8600
	ENTRY CHANG	BOU 8700
C		BOU 8800
	RR=R(130)+R(131)+R(145)+R(146)	BOU 8900
	RR=RR/4	BOU 9000
	DO 10 J=1,LHEAT	BOU 9100
	N=NHEAT(J)	BOU 9200
10	AHEAT(J)=R(N)*PCW*AWATER(J)	BOU 9300
	RETURN	BOU 9400
C		BOU 9500
	ENTRY CHAN	BOU 9600
	RETURN	BOU 9700
	END	BOU 9800

	SUBROUTINE EIGEN(LN,MBAND,MP,KSYP,CFAC,T,RI,HEAD)	EIG 100
	DOUBLE PRECISION S,T	EIG 200
	DIMENSION HEAD(LN), RI(LN), S(LN,MBAND),T(LN,MBAND)	EIG 300
	COMMON/HI/TITLE(25),V(26),VV(26)	EIG 400
	PRINT 10	EIG 500
	COMMON/HH/LFLOW,LON	EIG 600
C	C=1000	EIG 700
	DO 1 J=1,LN	EIG 800
	A=0	EIG 900
	IF(KSYM.GT.0) GO TO 6	EIG 1000
	IF(HEAD(J).EQ 0) A=S(J,1)	EIG 1100
	DO 2 K=2,MBAND	EIG 1200
	IF(HEAD(J).NE.0) GO TO 1	EIG 1300
	E=S(J,K)	EIG 1400
2	A=ABS(E)+A	EIG 1500
	MBA=MBAND-1	EIG 1600
	DO 4 K=1,MBA	EIG 1700
	NO=J-K	EIG 1800
	IF(NO.LE.0) GO TO 5	EIG 1900
	E=T(NO,K+1)	EIG 2000
4	A=ABS(E)+A	EIG 2100
5	CONTINUE	EIG 2200
	B=T(J,1)*.5/A	EIG 2300
	GO TO 8	EIG 2400
6	DO 7 K=1,MP	EIG 2500
	IF(S(J,K).GT.CFACT) GO TO 1	EIG 2600
	E=S(J,K)	EIG 2700
	E=ABS(E)	EIG 2800
	IF(K.EQ.MBAND) E=S(J,K)	EIG 2900
7	A=E+A	EIG 3000
	B=T(J,MBAND)*0.5/A	EIG 3100
8	CONTINUE	EIG 3200
	RI(J)=B	EIG 3300
	IF(B.LT.C) LQ=J	EIG 3400
	C=AMIN1(B,C)	EIG 3500
1	CONTINUE	EIG 3600
	PRINT V,(RI(J),J=1,LN)	EIG 3700
	PRINT 11,C,LQ	EIG 3800
	STOP	EIG 3900
10	FORMAT(1X/1X,'STABILITY OF SOLUTION USING CRANK NICOLSON METHOD'	EIG 4000
	*,4X/3X,'MAXIMUM TIME STEP FOR EACH NODE')/	EIG 4100
11	FORMAT(1X/1X,'THE CRITICAL TIME STEP IS ',G12.6,'	EIG 4200
	*CONSTRAINED AT NODE',I5)	EIG 4300
	END	EIG 4400
		EIG 4500

C	SUBROUTINE THAT ALLOWS FOR A MOVING BOUNDARY IN A VERTICAL CROSS SEC	ADJ 100
C		ADJ 200
C		ADJ 300
C		ADJ 400
	SUBROUTINE ADJUST(NJUST,LM,LN,Z,HEAD,XLOC,YLOC,NODE,FLOWX,FLOWY,RADJ	ADJ 500
*	*)	ADJ 600
	DIMENSION NMOV(40,2), FLOWX(LM),FLOWY(LM),A(2),B(2),R(LN)	ADJ 700
	DIMENSION BMOV(40,6),HEAD(LN),XLOC(LN),YLOC(LN),NODE(12,LM)	ADJ 800
	READ,NSTEP,NPRINT,NPR,ERROR,FACTOR	ADJ 900
	READ,(NMOV(J,1),NMOV(J,2),BMOV(J,3),BMOV(J,6),J=1,NJUST)	ADJ 1000
	KLT=0	ADJ 1100
	KSS=1	ADJ 1200
	RETURN	ADJ 1300
C		ADJ 1400
C	*****	ADJ 1500
C		ADJ 1600
	ENTRY ADJUS(*,*)	ADJ 1700
	IF(KSS.EQ.2) GO TO 5	ADJ 1800
	DO 4 J=1,NJUST	ADJ 1900
	LL=NMOV(J,1)	ADJ 2000
	LL=ABS(LL)	ADJ 2100
	IF(LL.NE.0) GO TO 2	ADJ 2200
	LL=NMOV(J,2)	ADJ 2300
	LL=ABS(LL)	ADJ 2400
	L=NODE(4,LL)	ADJ 2500
	GO TO 3	ADJ 2600
2	CONTINUE	ADJ 2700
	L=NODE(3,LL)	ADJ 2800
3	CONTINUE	ADJ 2900
	BMOV(J,5)=YLOC(L)	ADJ 3000
4	CONTINUE	ADJ 3100
5	CONTINUE	ADJ 3200
	KLT=KLT+1	ADJ 3300
	READ,BKS,TIME,FACT	ADJ 3400
	DO 6 J=1,NJUST	ADJ 3500
6	BMOV(J,4)=BMOV(J,6)*FACT	ADJ 3600
	DO 8 J=1,NJUST	ADJ 3700
8	BMOV(J,4)=BMOV(J,4)/FACTOR	ADJ 3800
	SLENG=0.00001	ADJ 3900
	FLOW=0	ADJ 4000
	DO 40 J=1,NJUST	ADJ 4100
	DO 10 K=1,2	ADJ 4200
	NS=1	ADJ 4300
	LLL=NMOV(J,K)	ADJ 4400
	IF(LLL.LT.0) NS=2	ADJ 4500
	LLL=ABS(LLL)	ADJ 4600
	IF(LLL.EQ.0) GO TO 10	ADJ 4700
	CALL CORD(LLL)	ADJ 4800
	CALL VCENT(LLL,VX,VY)	ADJ 4900
	LA=NODE(3,LLL)	ADJ 5000
	LB=NODE(4,LLL)	ADJ 5100
	AA=(XLOC(LA)-XLOC(LB))	ADJ 5200
	A(K)=ABS(AA)	ADJ 5300
	B(K)=VY	ADJ 5400
10	CONTINUE	ADJ 5500
	LC=NMOV(J,1)	ADJ 5600
	LC=ABS(LC)	ADJ 5700
	IF(LC.EQ.0) A(1)=A(2)	ADJ 5800
	IF(LC.EQ.0) B(1)=B(2)	ADJ 5900
	IF(LLL.EQ.0) A(2)=A(1)	ADJ 6000
	IF(LLL.EQ.0) B(2)=B(1)	ADJ 6100
	IF(J,LLL.EQ.0) LB=NODE(3,LC)	ADJ 6200

	IF(NS.EQ.2) GO TO 20	ADJ 6300
	C=(B(1)*A(1)+B(2)*A(2))/(A(1)/2+A(2)/2)	ADJ 6400
	YLOC(LB)=YLOC(LB)+((-C+BMOV(J,4))*TIME/BMOV(J,3))	ADJ 6500
	HEAD(LB)=YLOC(LB)	ADJ 6600
	GO TO 40	ADJ 6700
20	CONTINUE	ADJ 6800
	FLOW=B(1)*A(1)/2+B(2)*A(2)/2+FLOW	ADJ 6900
	SLENG=SLENG+A(1)/2+A(2)/2	ADJ 7000
40	CONTINUE	ADJ 7100
C		ADJ 7200
C		ADJ 7300
C LAKE LEVEL LEVELLER		ADJ 7400
C		ADJ 7500
	HE=FLOW/SLENG	ADJ 7600
	DO 50 J=1,NJUST	ADJ 7700
	IF(NMOV(J,2).GT.-0.0001) GO TO 50	ADJ 7800
	LLL=NMOV(J,2)	ADJ 7900
	LLL=ABS(LL)	ADJ 8000
	IF(LL.EQ.0) GO TO 45	ADJ 8100
	MD=NODE(4,LLL)	ADJ 8200
	GO TO 47	ADJ 8300
45	LLL=NMOV(J,1)	ADJ 8400
	LLL=ABS(LL)	ADJ 8500
	MD=NODE(3,LLL)	ADJ 8600
47	CONTINUE	ADJ 8700
	YLOC(MD)=(-HE+BMOV(J,4))*TIME/BMOV(J,3)+YLOC(MD)	ADJ 8800
	HEAD(MD)=YLOC(MD)	ADJ 8900
50	CONTINUE	ADJ 9000
C		ADJ 9100
C PRINTING ROUTINE		ADJ 9200
C		ADJ 9300
	LP=KLT/NPRINT	ADJ 9400
	LQ=KLT/NPR	ADJ 9500
	LP=LP*NPRINT	ADJ 9600
	LQ=LQ*NPR	ADJ 9700
	IF(KLT.EQ.LP) CALL WPRINT(BKS)	ADJ 9800
	IF(KLT.EQ.LQ) CALL WFLOW(BKS)	ADJ 9900
	IF(KLT.EQ.LQ) CALL BPRINT	ADJ 10000
C		ADJ 10100
	IF(KLT.GT.NSTEP) STOP	ADJ 10200
	KSS=2	ADJ 10300
	AC=0	ADJ 10400
	DO 70 J=1,NJUST	ADJ 10500
	LL=NMOV(J,1)	ADJ 10600
	LL=ABS(LL)	ADJ 10700
	IF(LL.NE.0) GO TO 60	ADJ 10800
	LL=NMOV(J,2)	ADJ 10900
	LL=ABS(LL)	ADJ 11000
	L=NODE(4,LL)	ADJ 11100
	GO TO 65	ADJ 11200
60	CONTINUE	ADJ 11300
	L=NODE(3,LL)	ADJ 11400
65	CONTINUE	ADJ 11500
	AD=BMOV(J,5)-YLOC(L)	ADJ 11600
	AD=ABS(AD)	ADJ 11700
	AC=AMAX1(AD,AC)	ADJ 11800
70	CONTINUE	ADJ 11900
	IF(AC.GT.ERROR) KSS=1	ADJ 12000
	IF(KSS.EQ.2) RETURN 2	ADJ 12100
	PRINT 110,BKS,KLT	ADJ 12200
110	FORMAT(1X/1X,'STUCTURE MATRIX RECOMPUTED AT TIME STEP ',G8.3,	ADJ 12300
	*' ITERATION ',I5)	ADJ 12400
	RETURN 1	ADJ 12500
	END	ADJ 12600

APPENDIX D

ESTIMATION OF AQUIFER PARAMETERS BY USING SUBSURFACE TEMPERATURE DATA

Flowing ground water distorts the normal distribution of subsurface temperatures. Researchers interested in determining the geothermal heat flux have long been aware of the distorting influence moving ground water can have on the measured geothermal gradient (Kirge 1939). Only a few ground-water researchers, however, have attempted to use subsurface temperature information to calculate the rate and direction of ground-water flow.

Stallman (1960) aroused interest in the use of subsurface temperature as an indirect manifestation of ground-water velocity with a presentation of a differential equation describing heat transport in the subsurface and with the suggestion that temperature measurements might be a useful means for indirectly determining aquifer characteristics. An analytical solution was developed by Stallman (1965) for determining ground-water velocities in a homogeneous medium when the boundary conditions of heat and water movement are, respectively, (1) a sinusoidal temperature fluctuation of constant amplitude at the land surface, and (2) a constant and uniform percolation rate normal to the land surface. Bredehoeft and Papadopoulos (1965) developed an analytical solution for determining the ground-water velocity from subsurface temperature data in an isotropic, homogeneous, and fully saturated semiconfining layer in which all flow is vertical.

The analytical solution developed by Stallman (1965) has not been used extensively. Its main drawbacks are the assumptions that the water table is at the surface and that all flow is vertical. Taking a different approach, Nightingale (1975) estimated vertical recharge rates from an infiltration pond with a sinusoidal temperature distribution, but he assumed that conductive transfer processes were negligible and that velocity could be calculated by using only the lag between surface temperatures and temperatures at a point in the subsurface.

Several researchers have used Bredehoeft and Papadopoulos's analytical solution. Cartwright (1970) successfully used temperature anomalies to estimate the amount of vertical movement of ground water in the Illinois Basin. He matched the average temperature profile to the $\beta=-1$ curve of Bredehoeft and Papadopoulos (1965) to obtain a discharge rate of 1.52 cm/yr from the deep aquifer, a value that agrees with estimates of ground-water discharge into streams in the basin. Sorey (1971) used the Bredehoeft and Papadopoulos technique to estimate the rate of upward movement through semiconfining beds in the San Luis valley of Colorado and the Roswell basin of New Mexico. His conclusions suggest that pumping tests and water-budget

methods are often preferable because of limitations imposed by instabilities in the borehole fluids and the measurement detail required. Boyle and Saleem (1978) used the technique to estimate vertical flow rates through a clay-rich glacial drift semiconfining layer in the Chicago area. They obtained good agreement with values calculated by using the water-budget method.

The available analytical techniques only provide solutions for a very small group of problems in which flow is in the vertical direction and boundary conditions are specialized. In most aquifers the dominant direction of water movement is horizontal. Noticeable temperature variations have been observed in the horizontal direction in ground-water systems (Winslow 1962, Schneider 1962 and 1964, Mink 1964, Parsons 1970, Supkow 1971, Cartwright 1973). The researchers all implicitly assumed that the variations in temperature were caused by ground-water flow, but none were able to quantify flows by using this information.

In the course of the research reported here an attempt was made to use the measured horizontal and vertical distribution of subsurface temperatures to estimate the rate of flow from a cooling lake situated on an alluvial aquifer. A numerical technique was used by which ground-water velocities and hydraulic conductivities in a two-dimensional system with nonuniform boundary conditions can be determined by a trial-and-error procedure from subsurface temperature information. The procedure is not recommended for use in routine ground-water flow system analysis since traditional methods for defining flow systems are simpler to use and more reliable.

MATHEMATICAL MODEL

Given the following assumptions: (1) thermal equilibrium between the liquid and soil particles is achieved simultaneously, (2) the density of the soil particles is constant, (3) the heat capacity is constant, and (4) the system is chemically inert, then the general differential equation for simultaneous heat and fluid flow in a two-dimensional aquifer is

$$\frac{\partial}{\partial x_1} (D_{1j} \frac{\partial T}{\partial x_j}) - \rho C_w \frac{\partial (q_1 T)}{\partial x_1} - \rho C_s \frac{\partial T}{\partial t} + R = 0, \quad 1, j = 1, 2, \quad (D-1)$$

where T = temperature, T ; D_{1j} = coefficient of dispersion, H/tTL ; ρC_w = heat capacity of water, H/L^3T ; ρC_s = heat capacity of the saturated media, H/L^3T ; q_1 = specific discharge or ground-water velocity, L/t ; R = rate of heat injection or discharge, H/L^3t ; and x_1, x_2 = cartesian coordinates L .

The goal is to solve Eq. (D-1) for the velocity distribution; then hydraulic conductivities can be determined from

$$K_{1j} = -q_1 \left(\frac{\partial \phi}{\partial x_j} \right)^{-1} \quad 1, j = 1, 2; \quad (D-2)$$

where K_{1j} = hydraulic conductivity tensor, L/t ; and ϕ = head, L .

Velocities in the aquifer can be determined from Eq. (D-1) either directly or indirectly according to whether velocities are obtained directly by using

the temperature distribution as a known in the differential equation, or whether velocities are obtained as a solution to a nonlinear optimization problem in which a set of calculated temperatures is matched to an observed set. Direct methods require that the temperature distribution be known completely and that it closely represent the true solution to the differential equations (Neuman 1973). These types of solutions to the inverse problem are currently a subject of active research and were not used in the present study.

The equation describing the two-dimensional flow of water through a nonhomogeneous aquifer in steady state may be written as

$$\frac{\partial}{\partial x_i} (bK_{ij} \frac{\partial \phi}{\partial x_j}) + W = 0, \quad i,j=1,2, \quad (D-3)$$

where W = water recharge rate per unit area, L/t ; and b = thickness, L .

The ground-water velocity or specific discharge can then be determined from

$$q_i = -K_{ij} \frac{\partial \phi}{\partial x_j} \quad i,j=1,2. \quad (D-4)$$

Acquisition of some information on subsurface permeability is desirable for initial estimates of velocities by using the general differential equation describing water flow in an aquifer. Hydraulic conductivities can then be adjusted until the computed velocity distribution, when input into Eq. (D-1), produces a temperature distribution that is reasonably close to the observed temperature data.

The parameter estimation problem could be viewed as a classical nonlinear regression problem in which a solution to the linked differential equations [Eq. (D-1), Eq. (D-3), and Eq. (D-4)] forms the regression equation and in which all unknown quantities are parameters (Cooley 1977). The problem was not viewed in this manner because (1) sufficient temperature data will generally not be available to insure a well-conditioned solution, and (2) Eq. (D-1) behaves as a hyperbolic paraboloid when convective transport dominates, which means that small errors in the input parameters can cause large errors in the output.

Instead, a trial-and-error procedure was used to estimate hydraulic conductivities. This technique is conceptually simple, but has several drawbacks: (1) It can be expensive, (2) it is very time consuming, (3) an answer cannot always be obtained, and (4) if an answer is obtained, it is probably not the best estimate, and its relation to the best estimate is unknown.

Several difficulties are encountered when Eq. (D-1) and Eq. (D-3) are linked and solved in a trial-and-error procedure to estimate hydraulic conductivities. The best documented difficulty is that, when hydraulic conductivities are known, researchers have not been very successful in solving for a known conservative contaminant distribution, even though the conservative mass transfer problem is mathematically simpler than the heat

transport problem. The differential equations are of the same form, but the conservative mass transport problem has two fewer parameters because of the common assumption that molecular diffusion, which is equivalent to thermal conductivity, is negligible.

Attempts to simulate a known conservative contaminant distribution in an aquifer with a deterministic model are not numerous. Pinder (1973) simulated the observed chromium contamination on Long Island; Bredehoeft and Pinder (1973) simulated the known chloride distribution in the Brunswick aquifer; Konikow (1976) simulated the chloride distribution in the vicinity of the Rocky Mountain Arsenal; Robertson (1974) simulated chlorides and other contaminants in the vicinity of the Idaho Test Site; and Robson (1978) simulated total dissolved solids in a shallow alluvial aquifer near Barstow, Calif. In all these simulations velocities within the aquifer were determined by using equations similar to Eq. (D-3) and Eq. (D-4). In these equations hydraulic conductivities were adjusted by a trial-and-error procedure until predicted aquifer heads closely matched observed aquifer heads. An equation similar to Eq. (D-1) was used to simulate transport of contaminants, and the porosity and dispersivity parameters were then adjusted until the observed chemical concentration patterns were matched. Even when hydraulic conductivities are known, the chemical concentration distribution could not be simulated without a trial-and-error adjustment procedure. Also, even after the researchers had obtained what they considered to be a best fit between the simulated and the observed data, the fit in all cases was less than perfect. Anderson (1979) discusses some of the problems involved in applying contaminant transport models.

Since the temperature data will generally be sparse, the trial-and-error procedure of parameter estimation for the linked Eq. (D1) and (D-3) is generally non-tractable unless several of the parameters are constrained. In this analysis, in which hydraulic conductivities in a steady-state water-flow problem were estimated, thermal conductivities, heat capacities, and dispersivities were fixed. The rationale for fixing these parameters was that the thermal conductivity and the heat capacity of most saturated glacial materials fall within a small range, and they can be measured accurately in the laboratory. Dispersivities were assumed to be small because element sizes were chosen so that intra-element inhomogeneities were minimized.

These procedures left only hydraulic conductivities to be adjusted. Generally, even with hydraulic conductivities as the only unknowns, problems were ill conditioned unless the hydraulic conductivities were constrained to be within a small range. Therefore, this technique is only useful for refining estimates of hydraulic conductivity that are determined with other procedures.

The following procedure was used to refine estimates of the hydraulic conductivity distribution at the Columbia Generating Station site by using subsurface temperature data:

- 1) hydraulic conductivity distributions were proposed on the basis of stratigraphic information and field tests, and these distributions were

then tested using Eq. (D-3) to determine if the known potential distribution could be predicted within a set error criterion.

- 2) Once the potential distribution could be predicted, the relative magnitude of the hydraulic conductivities was adjusted in a model linking Eq. (D-1) and Eq. (D-3) to determine which factor gave the best fit to the observed temperature data.
- 3) If the best fit of the temperature data obtained in step 2 was not good, steps 1 and 2 were repeated. If the fit was judged to be acceptable, thermal conductivities and dispersivities were changed to determine the sensitivity of the estimate to changes in these parameters.

SOLUTION PROCEDURE

The finite element method was used to solve Eq. (D-1) and Eq. (D-3) for temperatures in an aquifer subject to the boundary conditions described in section 5 and appendix B. Each cross section modeled was divided into 100-150 quadrilateral elements. The procedure used to link the equations was: (1) Eq. (D-3) was solved for head at each node and Eq. (D-4) was solved for velocity; (2) Eq. (D-1) was solved for temperature at each node; (3) the solution to Eq. (D-1) was stepped forward in time by using the Crank-Nicolson approximation for the time derivative for a specified number of time steps; (4) the hydraulic conductivities, which are a function of temperature, were adjusted for the new temperature distribution; and (5) steps (1) to (4) were repeated.

FIELD DATA

Temperatures were recorded weekly at 40-110 points in the subsurface in the vicinity of the Columbia Generating Station (Figure A-1) from August 1976 to January 1978. The monitoring techniques and the locations of the data points are described in appendix A. The data collected on 7 October 1977 are presented in a fence diagram in Figure (D-1). The data collected in cross-section A-A' and B-B' of Figure 6 are presented in section 5. Temperatures recorded in an array of wells on the east side of the cooling lake are shown in Figure (D-2).

RESULTS

The temperature data from cross-sections A-A' and B-B' were used to refine estimates of hydraulic conductivity and to refine previous estimates of flow in these cross sections from the cooling lake to the wetland west of the lake. Andrews (1976) modeled flow in these cross sections and obtained average annual flow rates of $4.5 \text{ m}^2/\text{day}$ (m^3/day per meter width of the dike and $3.5 \text{ m}^2/\text{day}$, respectively. By using the trial-and-error procedure described in this appendix, values of $5.2 \text{ m}^2/\text{day}$ and $4.3 \text{ m}^2/\text{day}$ were obtained for flow in these two cross sections, respectively. An error criterion of 0.05 m was used in step 1. Thermal conductivities were set equal to values obtained in the laboratory. Longitudinal dispersivity was set to 20 cm, and transverse dispersivity was set to 5 cm on the basis of intro-element homogeneity considerations.

Temperatures in the Marsh on October 7, 1977

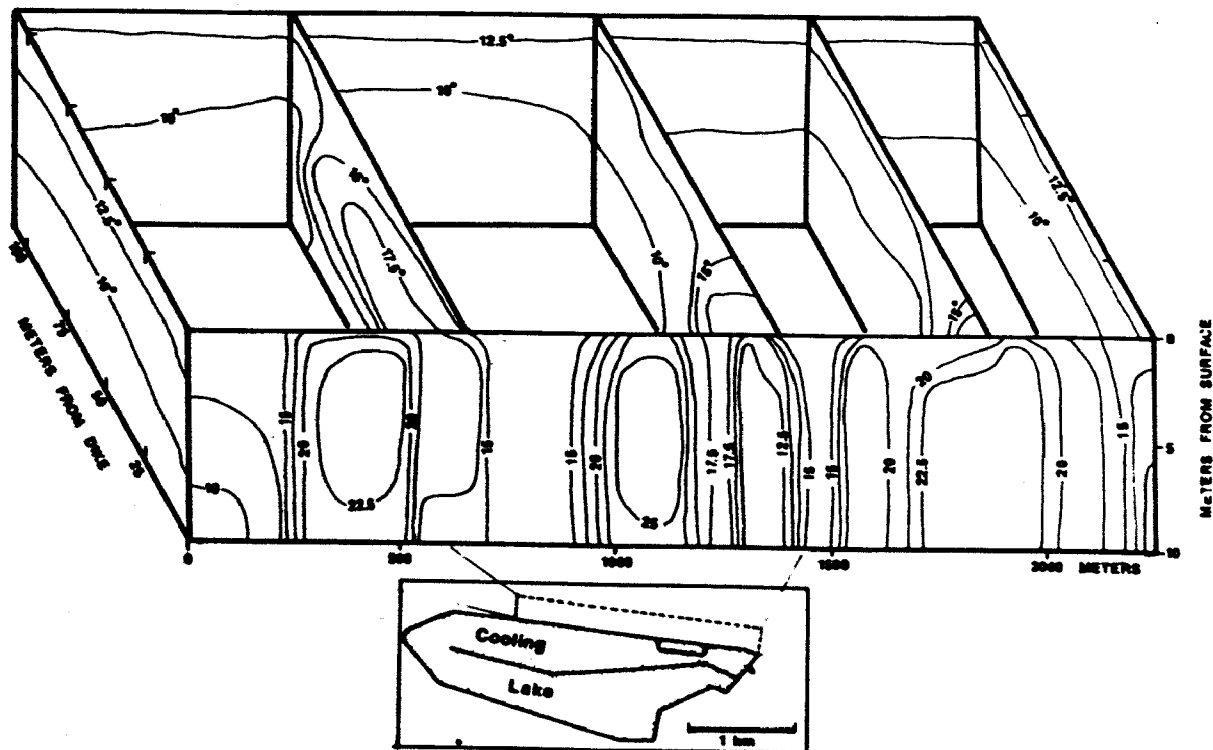


Figure D-1. Temperatures ($^{\circ}\text{C}$) in a section of the marsh adjacent to the cooling lake at the Columbia Generating Station site on 7 October 1977. The three-dimensional diagram depicts temperatures in a 2,500-m section along the dike which extends outward from the dike for a distance of 110 m and to a depth of 10 m.

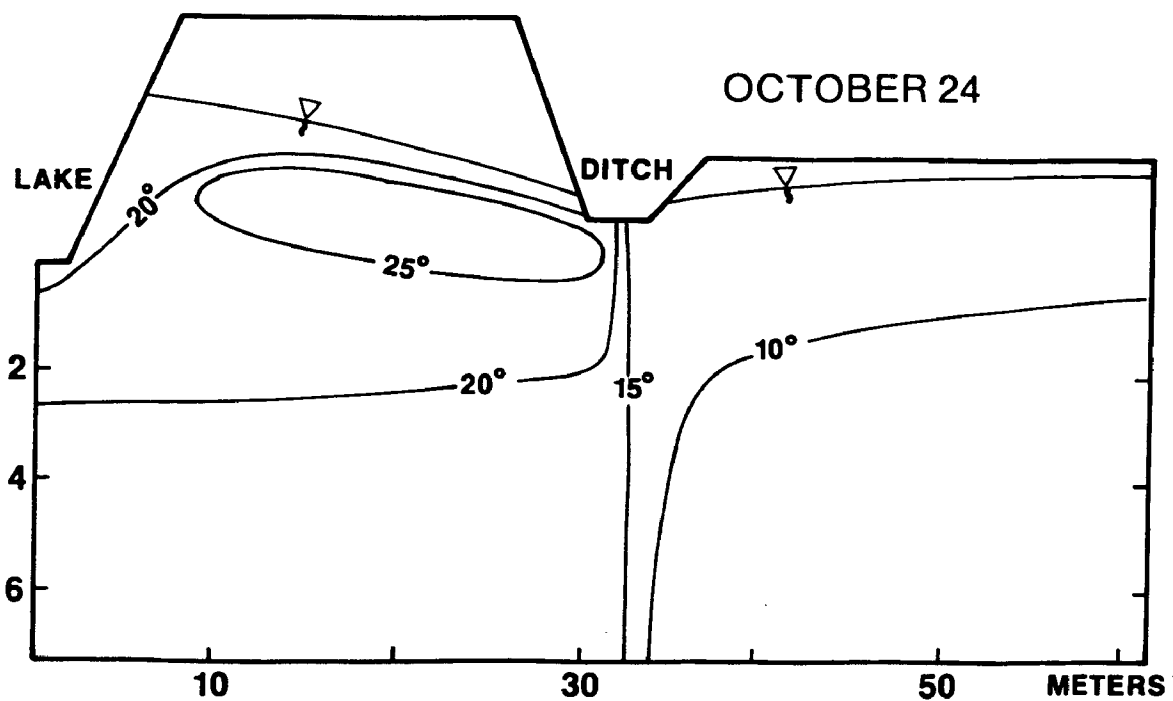
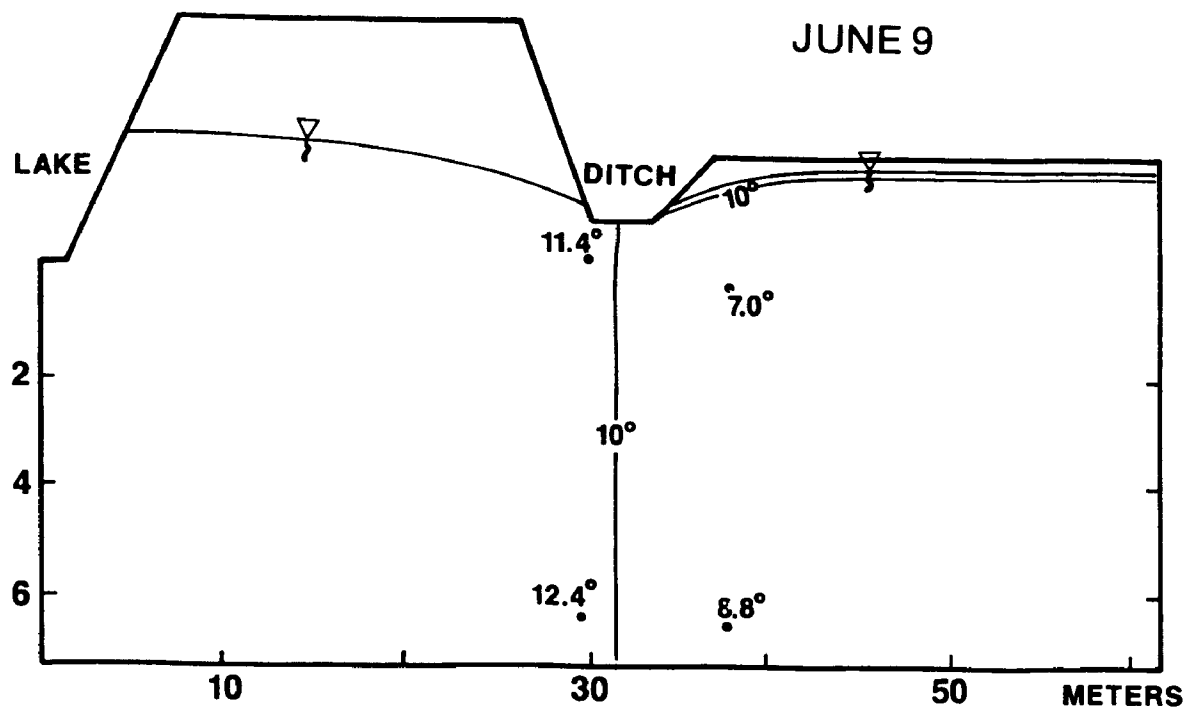


Figure D-2. Temperatures in a 60-m portion of cross-section B-B' of Figure 6 adjacent to the drainage ditch east of the cooling lake on 9 June 1977 and 24 October 1977.

The hydraulic conductivity distribution that best reproduced the observed temperature data was not sensitive to changes in the thermal conductivities or dispersivities within reasonable limits. Adjusting the thermal conductivities and the dispersivities did, however, reduce the residuals between the observed and the simulated temperatures. The changes in simulated temperature that resulted when dispersivities were changed are described in section 5.

This trial-and-error procedure does not lend itself to estimation of the standard error of the parameters in the best fit mode. It is only an intuitive observation that the standard error of the estimated hydraulic conductivities are reduced by using this technique rather than stopping at step 1 in the parameter estimation.

The temperature data were also used to attempt to determine flow rates in five other cross sections (Figure 15) at the Columbia Generating Station site. In all these cross sections only limited potential data were available, and several hydraulic conductivity distributions could be found that would reproduce the known potential distribution equally well. Since the temperature data were also limited, several hydraulic conductivity distributions which represented widely varying flow rates could reproduce the observed data equally well. Only in the simulated cross section located near the intake of the cooling lake were the results satisfactory. (Of the five cross sections, the best temperature and potential data were available for this cross section.) In this cross section the flow rates into the wetland were estimated to average $7.4 \text{ m}^2/\text{day}$.

CONCLUSIONS

Unfortunately, the information in Figure (D-1) was not sufficient to estimate flow rates from the cooling lake into the wetland along the dike. Figure (D-1) does illustrate vividly the complexity of ground-water flow patterns and hydraulic conductivity distributions near the dike. Although flow rates from the cooling lake to the wetland in the area shown in Figure (D-1) are most likely all within the range of $3.5\text{--}7.5 \text{ m}^2/\text{day}$, the temperature contrasts are dramatic. Small changes in peat thickness or the presence or absence of a clay lens can cause very different temperature patterns even though flows are approximately the same. Keys and Brown (1978) reached a similar conclusion. The temperature data, although indicating that flows are much greater in some areas than others, are not sufficient for determining hydraulic conductivity distributions.

TECHNICAL REPORT DATA <i>(Please read Instructions on the reverse before completing)</i>		
1. REPORT NO. EPA-600/3-80-079	2.	3. RECIPIENT'S ACCESSION NO.
4. TITLE AND SUBTITLE Impacts of Coal-Fired Power Plants on Local Ground-Water Systems Wisconsin Power Plant Impact Study	5. REPORT DATE August 1980 Issuing Date.	6. PERFORMING ORGANIZATION CODE
	8. PERFORMING ORGANIZATION REPORT NO.	
7. AUTHOR(S) Charles B. Andrews Mary P. Anderson	10. PROGRAM ELEMENT NO. 1BA820	
9. PERFORMING ORGANIZATION NAME AND ADDRESS Institute for Environmental Studies Environmental Monitoring and Data Acquisition Group University of Wisconsin-Madison Madison, Wisconsin 53706	11. CONTRACT/GRANT NO. R803971	
	13. TYPE OF REPORT AND PERIOD COVERED Final 7/75 - 6/78	
12. SPONSORING AGENCY NAME AND ADDRESS Environmental Research Laboratory Office of Research and Development U.S. Environmental Protection Agency Duluth, Minnesota 55804	14. SPONSORING AGENCY CODE EPA/600/03	
	15. SUPPLEMENTARY NOTES	
16. ABSTRACT Quantitative techniques for simulating the impacts of a coal-fired power plant on the ground-water system of a river flood-plain wetland were developed and tested. Effects related to the construction and operation of the cooling lake and ash-pit had the greatest impact. Ground-water flow system models were used to simulate ground-water flows before and after the cooling lake and ashpit were filled. The simulations and field data indicate that the cooling lake and ashpit altered local flow systems and increased ground-water discharge. Chemical changes in the ground-water system were minor. Contaminated ground water was confined to a small area near the ashpit. Thermal changes in the ground water are a major impact of the cooling lake. Changes in water temperature and levels have altered the vegetation of the wetland, a major ground-water discharge area. Ground-water temperatures near the cooling lake were monitored. A model was used to simulate the response of subsurface temperatures to seasonal changes in a lake and air temperatures. Long-term substrate temperature changes expected in the wetland were predicted. Using ground-water temperatures to estimate flow rates was investigated. Simulated temperature patterns agreed with field data, but were sensitive to the distribution of subsurface lithologies. It is predicted that by 1987 ground-water temperatures will be increased, resulting in an increase in ground-water flow.		
17. KEY WORDS AND DOCUMENT ANALYSIS		
a. DESCRIPTORS	b. IDENTIFIERS/OPEN ENDED TERMS	c. COSATI Field/Group
Ground water models, cooling lakes, temperature monitoring, river flood-plain wetlands, coal fired power plants, ash pit, flow rates, vegetation	Wisconsin Power Plant Study, Impacts on Biota Flow measurement, terrain models, artesian water, cooling water	06-F, T 08- D, F, H, M 10-C 13-B, M 14-B
18. DISTRIBUTION STATEMENT Release to the public	19. SECURITY CLASS (This Report) unclassified	21. NO. OF PAGES 215
	20. SECURITY CLASS (This page) unclassified	22. PRICE